MASS SPECTROMETRIC INVESTIGATIONS OF MOSQUITO ATTRACTION TO HUMAN SKIN EMANATIONS

By

ULRICH R. BERNIER

A DISSERTATION PRESENTED TO THE GRADUATE SCHOOL
OF THE UNIVERSITY OF FLORIDA IN PARTIAL FULFILLMENT
OF THE REQUIREMENTS FOR THE DEGREE OF
DOCTOR OF PHILOSOPHY

UNIVERSITY OF FLORIDA
1995

UNIVERSITY OF FLORIDA LIBRARIES

ACKNOWLEDGMENTS

I wish to express sincere appreciation and gratitude to my graduate research supervisor, Dr. Richard A. Yost, for his guidance, patience, and insightful discussions throughout the course of my graduate studies. I would like to also thank the members of my committee, Dr. James D. Winefordner, Dr. David H. Powell, Dr. J. Eric Enholm, and Dr. Daniel L. Kline, for their assistance during the course of these studies.

I am indebted to Dr. Jodie V. Johnson and Dr. Anthony P. Annacchino, Jr. for their instructions and guidance in the operation of the TSQ70 triple quadrupole mass spectrometer. I wish to thank Mr. Carl E. Schreck, Dr. Daniel L. Kline, and Dr. Donald R. Barnard for their assistance and open communication, over the last three years, with respect to the entomological aspects of this research. I also wish to thank soon-to-be Dr. Matthew Booth for spending many hours analyzing samples for me (above and beyond the call of duty) on a purge and trap GC/MS. Dr. Brad Coopersmith deserves thanks for assistance with reaction mechanisms during the course of this work. One final thanks with respect to colleagues goes out to all former and present group members for their friendship and assistance throughout the time I spent at the University of Florida.

Special thanks go to Pamela Cannon for her love, patience, and assistance over the last year. Pam did an extraordinary job of typing in tables for hours at a time as I sifted through data looking for additional compounds to insert into those tables. I wish to also thank Jesse Cannon for spending hours learning the elements of the periodic table, including exact masses, during his summer vacation. I probably had more fun quizzing him than he did learning. Finally, my greatest thanks are extended to my mother, who has stood by me through everything I have done in my life. She always encouraged me to obtain more education; I am certainly appreciative of her effort, especially now that I am near the completion of this degree.

TABLE OF CONTENTS

ACKNOWLEDGMENTS ii

Abstract viii

CHAPTER PAGE

1 INTRODUCTION 1

Research Objectives 1
Entomological Overview 2
Mosquito Physiology 3
Characteristics of gender and species 3
Mosquito sensilla 4
Mosquito vision 6
Mosquito Repellents 7
Mosquito Attractants 8
Nature of concern for attractant identification 9
Vision 11
Heat 11
Moisture 12
Carbon dioxide 12
Sound 13
Chemical attractants 14
Relation to Semiochemical Studies 16
Overview of Analytical Methods and Detection 18
Overview of Mass Spectrometry 18
Sample introduction 19
Sample ionization 21
Triple quadrupole mass spectrometry 22
Analysis of Complex Environmental and Biological Samples . . 28
Organization of Dissertation 29

CHAPTER PAGE

2 SAMPLING METHODS 31

Introduction 31
Sampling Considerations 31
Entomological Sampling 32
Olfactometer 32
Field studies 36
Mass Spectrometric Methods of Sample Introduction 36
Experimental 39
Thermal Desorption from a Single Bead 39
Thermal Desorption from Multiple Beads 40
Thermal Desorption from Multiple Beads/Cryo-focused GC Separation 45
Purge and Trap/GC Separation 47
Results and Discussion 49
Thermal Desorption from a Single Bead 49
Thermal Desorption from Multiple Beads 64
Thermal Desorption from Multiple Beads/Cryo-focused GC Separation 72
Purge and Trap/GC Separation 82
Conclusions 87

3 STUDIES INVOLVING ATTRACTION 89

Introduction 89
Lactic Acid as a Model Compound 89
Reaction Studies 89
Altering Attraction 90
Analysis of Methanolic Perspiration Solution 91
Experimental 91
Reactions of Lactic Acid 91
Altering Attraction 94
Analysis of Methanolic Perspiration Solution 97
Results and Discussion 97
Reactions of Lactic Acid 97
Characteristic fragmentations 98
Oligomerization and attachment reactions 108
Altering Attraction 130
Addition of acid or base to lactic acid 131
Addition of acid or base to esters 142
Analysis of Methanolic Perspiration Solution 142

Phase differences 149
Implication to attractant origin 152
Conclusions 153
Lactic Acid Reactions 153
Altering Attraction 154
Origin of Attraction 154

4 APPLICATIONS OF TANDEM MASS SPECTROMETRY 156

Introduction 156
Analysis of Multiple Beads Without GC Separation 157
Daughter Library 157
Compound Class Screening 158
Experimental 159
Daughter Library 160
Compound Class Screening 162
Results and Discussion 163
Analysis of Multiple Beads Without GC Separation 163
Daughter Library 176
Compound Class Screening 187
Conclusions 202

5 IDENTIFICATION OF SKIN EMANATIONS 205

Introduction 205
Sample Introduction and Separation 205
Cryo-focusing GC 208
Purge and trap GC 208
Mass Spectrometry 209
PCI theory 209
NCI theory 212
Characteristic ion fragmentations 217
Experimental 220
Identification of Emanations by CI and EI MS 220
Cryo-focusing GC/MS 220
Purge and trap GC/MS 223
Case Study Comparison of Emanations between Subjects 224
Case Study Comparison of Bio-assay to GC/MS Assay 226
Cryo-focusing GC/MS 226
Olfactometer 227
Results and Discussion 228
Identification of Emanations by CI and EI MS 228

CHAPTER PAGE

Cryo-focusing GC/MS 240
Purge and trap GC/MS 260
Case Study Comparison of Emanations between Subjects 270
Case Study Comparison of Bio-assay to GC/MS Assay 278
Conclusions 283
Identified Emanations 283
GC/MS Assay of Subjects with Different Attraction Levels . . 283
Bio-assay versus GC/MS Assay 284

6 CONCLUSIONS AND FUTURE WORK 285

Conclusions 285
Future Work 288

APPENDIX
CARBON DIOXIDE AS A CI REAGENT GAS 294

Introduction 294
High Pressure Charge Exchange Mass Spectrometry 295
Electron Capture Negative Ion Chemical Ionization 297
ECNCI with Carbon Dioxide 298
Instrument Optimization and Background Ions 299
Selected Examples 314
Summary 324

REFERENCE LIST 325

BIOGRAPHICAL SKETCH 333

Abstract of Dissertation Presented to the Graduate School
of the University of Florida in Partial Fulfillment of the
Requirements for the Degree of Doctor of Philosophy

MASS SPECTROMETRIC INVESTIGATIONS OF MOSQUITO ATTRACTION TO HUMAN SKIN EMANATIONS

By

Ulrich R. Bernier

December, 1995

Chairperson: Richard A. Yost
Major Department: Chemistry

Volatile compounds emanating from the host are the basis for chemical attraction of mosquitoes. This work is centered upon the identification of volatile emanations from the skin. The goal of this work is to provide the foundation for predicting relative host attraction by comparison of components and their relative abundance in samples. Altering the attraction of hosts (by changing the matrix conditions on the skin) may assist in understanding the factors which produce differences in attraction.

The underlying premise to this work is that chemical analysis (conducted by mass spectrometry) should allow for sample detection in a fashion similar to that which mosquitoes encounter: a volatile sample in the gas phase. Therefore, the sampling methods studied in this dissertation reflect that criterion. Direct thermal

desorption of volatiles from handled glass beads placed in the injection port of a gas chromatograph (GC) followed by cryo-focusing/GC analysis was determined to be the best sampling method with respect to sensitivity and selectivity.

Other than carbon dioxide, lactic acid is the only previously known chemical attractant for the *Aedes aegypti* species of mosquito. The acid/base effects on attraction to lactic acid, esters of lactic acid, and methyl isovalerate were studied. The addition of acid enhanced attraction for all tested compounds, while the addition of base decreased attraction. Perspiration was analyzed to determine the skin gland origin of attractants.

The major volatiles desorbed from handled glass beads have been identified through the use of positive and negative ion chemical ionization in conjunction with electron ionization. Mass spectrometric assays of two human subjects, differing markedly in their attraction to mosquitoes, have been conducted to determine differences in components present. Direct comparison of mass spectrometric assays to bio-assays over a five day period has been carried out and is presented herein. Additional identification of minor components present in skin emanations was accomplished by purge and trap GC/mass spectrometry (GC/MS). The utility of tandem mass spectrometry (MS/MS) as a tool for compound class screening is presented in the context of this work.

CHAPTER 1
INTRODUCTION

Research Objectives

The primary goal of this work is to provide a better understanding of the chemical basis for the attraction of mosquitoes to human hosts. Novel studies and approaches were conducted in three areas to meet this goal. The first objective is to determine the best method of sample introduction for analysis. The decision involves balancing sensitivity, resolution, as well as selectivity. Here, selectivity implies sampling in a manner similar to that in which mosquitoes are exposed, i.e. a volatile sample in the gas phase. The second objective of this work is to determine methods to alter attraction. Studies involving changing the matrix conditions of a sample and the effect on attraction will be addressed. The third objective is to determine compounds which emanate from the skin. This objective is closely linked to sampling in that the sampling method ultimately determines how many and which compounds are detected. An important component of this objective is to differentiate between unattractive and attractive components which emanate from the skin. This has been approached by case studies involving the comparison of skin emanations between hosts who differ in attraction to mosquitoes and by monitoring

mass spectrometric assays concurrently with samples analyzed for mosquito attraction.

Entomological Overview

Mosquitoes are a vector for the transmission of more than 250 million new cases of viral diseases each year; these diseases include malaria, encephalitis, and filariasis [1,2]. One method to control the spread of disease is alteration of mosquito capability to carry diseases. The yellow fever mosquito, *Aedes aegypti*, is responsible for the transmission of both yellow fever and dengue fever [3]. This species has shown reduced disease-spreading ability by gene alteration [1]. This approach ultimately requires mapping of the genome for this species and each new species examined. Thus, this method is tedious and may require some time until a useful strategy can be implemented.

A second approach to control the spread of disease is to develop and employ repellents; this is probably the standard approach to reducing biting from mosquitoes. A third approach, consistent with the work of this dissertation, is to develop an understanding of the basis of attraction. This would allow the development of strategies to reduce or counteract the attraction of human hosts. This knowledge would then allow for manufactured traps, possibly containing both insecticides and attractants. The difficulty with this approach is that it requires a suitable knowledge of attractants for a variety of species. As will be discussed in the following text, many species exhibit marked differences in terms of responses to cues.

These differences most likely result from the differences in sensilla. For example, species which are more dependent on olfactory cues will contain a greater proportion of chemosensilla versus mechanosensilla than for a species dependent primarily on physical cues. Understanding mosquito attraction necessitates an understanding of the physiological function of mosquito sensory organs.

Mosquito Physiology

Much research has been conducted on mosquitoes with the primary focus affixed upon characterizing the finding and selection of hosts. The use of scanning and transmission electron microscopy as well as electrophysiology has greatly expanded the understanding of mosquito sensory physiology [4]. The mosquito nervous system consists of three systems: the central nervous system (CNS) (brain, ventral nerve cord, ganglia), the stomodaeal nervous system (various ganglia and nerves), and the peripheral nervous system (PNS) (motor and sensory neurons, sense organs). The system most directly pertaining to host attractant/repellent stimuli responses is the PNS; the fundamental components of the PNS are examined in the following sections.

Characteristics of gender and species

The gender differences between male and female mosquitoes, for most species, lie in the host-seeking behavior of females. Generally only females take blood-meals, which are necessary for egg production. Both genders will feed on nectar. Males will respond to wingbeat frequency of females to orient towards the

females for mating. Additionally, differences exist among species as to preference of hosts for blood-meals. *Culex*, spp., generally prefer avian hosts while *Anopheles*, spp., feed on mammalian hosts (e.g. man) [5]. Therefore, there are some innate differences in the genetic make-up of different species. This difference will result in different preferences for various cues (attractants) as well as differences in sensilla between species.

Mosquito sensilla

Sensilla, or sense organs, are constituents of the PNS. The function of a sensillum is to transform a response from a stimulus into a viable means of response the mosquito can process, such as a nervous impulse [4]. There are a range of sensilla which can function to detect variations of thermal, chemical, mechanical, or visual stimuli, as well as changes in humidity. Visual detection will be addressed under its own section separate from this discussion of other sensilla.

There are five types of chemosensilla found on the antennae of *Ae. aegypti* and one type of chemosensillum on the palps (capitate pegs) [4,5]. The capitate pegs function in the detection of carbon dioxide. Grooved pegs, found on the antennae flagellar segments, respond to airborne vapors. These vapors may be water vapor or other airborne volatiles such as lactic acid, fatty acids, and essential oils in the case of *Ae. aegypti* [6]. The detection by grooved pegs and palps is processed by the CNS (see pg. 8); i.e., detection by each of these sensilla is specific and independent for different cues [7]. Anophelines contain large sensilla coeloconica which are thought to be similar to grooved pegs. The detection purpose of these sensilla is still

unknown, although they are presumed to provide information similar to that of the grooved pegs. Small sensilla coeloconica are at the tips of the antennae and respond to changes in air temperature. There are two sets of neural cells comprising the small coeloconica. One is activated by a temperature increase, whereas the second is inhibited by it. This allows a mosquito (i.e. *Ae. aegypti*) to sense temperature changes at short-range (within one meter of the host) [6]. The sensilla ampullaceae on the antennae are only suspected to function in temperature and humidity detection; no experiments as of yet confirm this. Sensilla trichodea are the most numerous sensilla found on the antennae. Fewer of these sensilla are present on male antennae compared to female antennae (for the same species). The responses of these sensilla vary widely in terms of olfactory detection, e.g. fatty acids, essential oils, oviposition compounds, and repellents. None has been found to give a response to lactic acid [6].

Sensilla found on the mosquito antennae may not be the sole location for chemical reception of odor cues. The mouth may also contribute some ability for chemical reception of odors and has been postulated to function in infrared detection [4]. The various setae found on the mosquito body are generally mechanosensilla, as are the chordotonal organs. In contrast to setae, chordotonal organs found in the cuticle provide information as to the position of mosquito body parts.

Sound detection in mosquitoes involves frequency detection by the Johnston's organ in antennae [4]. Experiments involving antennae removal or impedance of the Johnston's organ resulted in a lack of response of mosquitoes to sound stimuli [8].

The antennae of male mosquitoes is such that resonant vibration occurs with female wingbeat frequency; the shaft of the antennae transmit the vibration to the Johnston's organs. Directional information is most likely acquired from sound due to a triangulation method with the antennae. Depending on the phase offset of vibrations on each antennae, it is postulated that mosquitoes can determine whether the sound is originating within or outside of a 30 degree arc of their flight path line [4]. Thus, their approach to a stimulus follows a zig-zag pattern [9]. Additionally, mosquitoes fly at approximately one meter per second when in a controlled flight toward a host and up to eight meters per second maximum [2,9].

One final note on the sensory capacity of the PNS: in a study of *Toxorhynchites brevipalpis*, there were 622 neurons forming the PNS, not including photoreceptors. Mechanoreceptors attributed for 526 of the neurons, and chemoreceptors made up the final 96 neurons. Most of the mechanosensilla (500 of 526) were body setae.

Mosquito vision

The discussion in this section will focus mainly upon the eyes as sensilla pertaining to *Ae. aegypti*. In the larval stage, two types of eyes are present, the lateral ocelli and the developing adult compound eyes [4]. The ocelli are separated into two dorsal ocelli, a central ocellus, and a ventral ocellus. The ocelli contain cells to gather light and transmit the visual information to the brain via photosensitive nerve cells. Rhodopsin is the visual pigment in mosquito vision; the λ_{max} for absorption is 515 nm. This corresponds to a visual range of 323-631 nm with

a maximum spectral sensitivity at 520 nm obtained from electroretinograms with *Ae. aegypti* [4,10].

In adults, the lateral ocelli degenerate and compound eyes are present. The dorsal ocelli are absent. The compound eyes consist of ommatidia. Each ommatidium consists of a diotropic apparatus (cornea, lens, and four cone cells for light collection) and a retinal cell layer [4]. For *Ae. aegypti*, the interommatidial angle is 6.2°; this angle is much greater than, for example, for houseflies. Due to the greater angle, the *Ae. aegypti* has relatively poor visual resolution and poor acuity [10]. However, mosquito vision does exhibit a high overall sensitivity to light [9,10].

Mosquito Repellents

Almost all compounds found to be chemical attractants (kairomones) for a specific species of mosquito are chemical repellents (allomones) for other specific species. Work conducted using 1-octen-3-ol (see section on Emanations from animals including man) has shown that this is a very promising attractant. Octenol, in combination with carbon dioxide, attracted some of the 35 species in a field study by Kline [11]. However, this compound acted as an allomone in the case of *Culiseta melanura*.

The grooved pegs on *Ae. aegypti* respond to lactic acid and are inhibited by the popular repellent diethyl-meta-toluamide (deet) [3,6,12]. Although oxalic acid itself is not an attractant (i.e. the lactic acid excitatory neuron does not respond), it does interfere or inhibit lactic acid response [12]. This interference is also the basis

for the action of deet; it too inhibits the response of the lactic acid excitatory neuron. It has been observed that mosquitoes exhibit slower flight rates upon exposure to repellent; turn angles are greatly increased and the number of turn readjustments taken is also increased. Therefore, deet does not repel; rather, it inhibits favorable response to mosquito attractant(s).

Mosquito Attractants

The mechanism of attraction or repulsion from a potential host involves a behavioral response by the mosquito to one or more stimuli. This overall response has been characterized as a four-step process: detection of stimuli by the PNS, interpretation of the stimuli by the CNS, activation of the appropriate response to the stimuli, and mosquito response [4]. This response can be in the form of attraction, repulsion, or can be anosmic towards the source of the stimuli.

Sound attracts male mosquitoes via the Johnston's organs in the antennae; however, this connotation is more specific for attraction of males to females, via wingbeat frequency, for purposes of procreation. The stimuli used by mosquitoes for host location are visual cues [4-6,9,10,13-15], moisture [4-6,16], heat [4-6,16], carbon dioxide [4-7,9,11,13,15-24], and chemical (olfactory) attractants [4-6,9,11,13,16,18-24]. Pheromones are long or short range olfactory attractants among members of the same species for purposes of mating. In *Ae. aegypti*, the male tarsal chemosensilla has been found to detect a female contact pheromone. Attraction to bacteria has been examined [17]; although the results demonstrated some attraction resulting

from bacterial emanations, it should be noted that carbon dioxide is excreted during bacterial growth.

Females are attracted to a host at a greater distance than males; this is likely due to the greater number of olfactory sensilla found in females [4]. In species where the female does partake in blood meals, the difference between the number of chemosensilla between male and females is much greater than for species where the female does not blood-feed from hosts [4,5].

Nature of concern for attractant identification

One of the primary reasons for searching for mosquito attractants is the increasing number of restrictions placed upon suitable insecticides. This is attributable to increased costs incurred from Environmental Protection Agency registration (under the Federal Insecticide, Fungicide, and Rodenticide Act), greater costs to produce insecticides for a smaller market demand, and pressure from environmental groups [25,26]. In searching for a natural attractant, the risk of an airborne hazardous insecticide is alleviated. This would then allow for contained traps to be lined or filled with insecticide while minimizing contamination of the environment with the insecticide.

Current state of mosquito research. Research in the area of attractants continues with attractants/repellents and with the physiology of the mosquito. Research methods which have been successful for other species of pests are being adapted and used to aid in understanding the behavior of mosquitoes. Takken summarized the state of mosquito research in his 1991 review [5, p.293]:

> In the light of recent developments in tsetse ecology, where a range of kairomones has been found, it is surprising that to-date only one chemical (lactic acid) has been demonstrated to be a mosquito kairomone, while several studies indicate that other human emanations are also attractive to mosquitoes. Most studies used *Ae. aegypti* as a target insect and much remains to be done on host-oriented behavior of medically important groups such as the anophelines. . . .

It should be noted that studies in the last few years involving 1-octen-3-ol as an attractant for *Ae. taeniorhynchus*, among other species, have shown great promise since the review by Takken. Attraction of mosquitoes to 1-octen-3-ol will be addressed later in this chapter in the section covering emanations from animals including man.

Trapping of mosquitoes. Mosquitoes generally fly less than 2.5 m above the ground with the 1.2 to 1.8 m range having the greatest number of mosquitoes collected [14]. Some studies show that 0.6 m is the average height for appetitive flight [2]. Additional concerns in trapping focus on shapes of the target as well as construction material. For example, attraction was found to be more prevalent for rectangular traps compared to pyramidal traps and most species were attracted to projecting parts of these traps [14]. Color is also of concern in trapping and will be addressed in the section on visual cues as attractants.

Short- versus long-range attractants. The physiological state of the mosquito and the proportions of sensilla play a role in determining which stimuli will be employed by a species for long-range and short-range cues. Vision is generally employed for long-range attraction with respect to orientation for upwind flight, location of nectar, and location of oviposition sites [5]. Carbon dioxide also tends

to alert and/or attract from long-range as well as olfactory attractants [5,14]. Experiments with carbon dioxide show that near a source of carbon dioxide, mosquitoes behave abnormally; this may be due to lack of other stimuli for short-range attraction, or due to a tonic response of sensilla from non-intermittent release of carbon dioxide [7]. These airborne attractants are detected as odor plumes. Short-range attraction may be accomplished by visual cues, as by changes in temperature or humidity [5,7]. Additionally, sound or wingbeat frequency is used at short-range for mate location.

Vision

Visual patterns on the ground generally control appetitive flight. Mosquitoes will respond to dark shapes, movement, and colors preferably as visual cues; these will alter the mosquito flight path [9]. Darker colors attract to a greater extent that lighter colors [14]. One theory attributes vision to be used in orienting upwind flight. This theory describes mosquito ability to judge windspeed by measuring its own movement at specific heights [2]. For shelter-seeking mosquitoes, vision is the means of site location. Visual cues also tend to be preferred over olfactory cues for nectar and oviposition site location in mosquitoes. This implies a long-range use of vision for these conditions, and that olfactory cues are employed for short-range with respect to nectar feeding and oviposition [9].

Heat

The thermal neurosensory response can be tonic (continuous) to ambient temperature or phasic (intermittent) during rapid temperature changes [4].

Temperature changes of 0.05°C can be detected, allowing a 2 kg animal to be detected from a distance of 2 m, provided the change in temperature is rapid [12]. Mosquito activity has been found to be greatly reduced for temperatures below 52-56°F [14,15].

Moisture

Humidity may play a role in determination of suitable locations for oviposition by the female [4]. In contradiction to this is a theory that the reception may just be a reception of temperature changes rather than water vapor [16]. It has been established that mosquitoes are attracted preferentially to humid, warm air rather than dry, cold air. The attraction of mosquitoes to warm and damp areas may be explained by humid conditions carrying temperature information better than dry conditions [12]. The attraction to humidity alone is much less than attraction to volatile chemical attractants. Experiments show dry emanations attracted 48% of caged female *Anopheles quadrimaculatus* versus 3% attraction to damp air alone [16].

Carbon dioxide

A component of exhaled breath is carbon dioxide. Carbon dioxide is a stimulus for almost all species studied by Kline and others [3,7,11,12,15-18,20-24]. The actual role of carbon dioxide still remains a mystery as to whether or not it provides a cue for mosquitoes to alight [5]. Experiments have shown carbon dioxide to bring mosquitoes to within two meters of a wood trap; however, they turn away before being collected into this trap. Greater numbers were captured with plexiglass traps; therefore, vision most likely plays a range in short range attraction in this case

[15]. It is certain, however, that carbon dioxide activates flight in mosquitoes [7,17]. Experiments involving removal of carbon dioxide from exhaled breath showed reduction in mosquito attraction to a host; however, it is not certain that carbon dioxide was the only volatile compound removed in such a study [7]. The range of effectiveness of carbon dioxide has been shown to extend beyond 60 ft, possibly up to 120 ft [15].

Studies involving *Ae. aegypti* palpal sensilla showed logarithmic phasic response to carbon dioxide from 0.01% to approximately 0.5% and that these sensilla can detect changes in concentration of 0.01% carbon dioxide. Saturation occurs above 0.5%, with little or no additional response at higher carbon dioxide concentrations. Exhaled human breath contains approximately 4.5% carbon dioxide compared to 0.01-0.10% found in the surrounding air [7]. Therefore, detection of carbon dioxide plumes by the mosquito is possible after a two order-of-magnitude dilution of carbon dioxide in exhaled breath. An additional note is that upon palpectomy, mosquitoes showed little or no response to carbon dioxide at any concentration level [4,7,16].

Sound

Sound (wingbeat frequency) is a short-range attractant for orientation of males to females for purposes of mating [4,8,27]. The males of almost all species of mosquito have a wingbeat frequency which is approximately double that of the female [8,27]. The few species not employing sound as a short-range cue have approximately equivalent wingbeat frequencies for both genders. Sound level is also

important, as loud sounds tend to repel mosquitoes in flight and will not activate mosquito flight. The benefit of sound attraction is that it can attract many male mosquitoes in a relatively short period of time. For example, 80% of caged male *Ae. aegypti* were attracted within 5 s [8]. Doppler frequency shifts have been shown to have little effect upon attraction.

Chemical attractants

The search for attractants may identify single attractants for specific species; however, a universal mixture to attract a wide range of species is sought. Certain combinations of chemicals may synergistically attract species more than others [5,20-23]. As with heat, some evidence exists that responses to volatile attractants and carbon dioxide may be tonic or phasic. In a constant (tonic) emission of attractants and/or carbon dioxide, mosquito response was found to decrease within minutes [7,17].

Airborne chemical attractants are carried by wind producing a series of plumes of host odor [9]. These plumes are neither uniform in size or distribution, thus eliciting a phasic rather than tonic response by mosquitoes. As previously mentioned, mosquitoes fly upwind in a zig-zag pattern, constantly adjusting to fly upstream into the plumes. The turning readjustment increases as mosquitoes near the host or source due to increased plume rate as well as decreased plume size. Odor plumes alert mosquitoes; however, visual cues provide better means for long-range attraction.

Emanations from animals including man. The use of 1-octen-3-ol and its effect on some species of mosquito has been examined [11,20-24]. Octenol is present in ox breath and has been found to be an attractant for the tsetse fly. Although the response to octenol alone is not as great as the response to carbon dioxide, synergism is present when both are employed for attraction in some species of mosquitoes [20-24]. Lactic acid and octenol provided an additive effect for *Ae. taeniorhynchus* [11]. An interesting note is that Kline suspects that octenol will not activate flight, nor directionally alight the mosquito to the host at short range; instead, octenol is suggested to play a role in upwind flight, involving odor plumes, towards the host [11].

Lactic acid, obtained from acetone washings of human skin, was first identified as a chemical attractant to *Ae. aegypti* by Acree et al. in 1968 [28]. Studies of structurally similar compounds to lactic acid have produced mixed results [19]; to-date, lactic acid is the only widely accepted attractant for *Ae. aegypti*. In females, the response to lactic acid has been found to elicit response from the grooved peg sensilla [12]. Attributed to the grooved pegs are neurons which either give an excitatory or an inhibitory response to lactic acid. Studies comparing mosquito attraction between host-seeking and non-host-seeking mosquitoes have demonstrated differing sensitivities to lactic acid. After a blood meal, a mosquito which is non-host-seeking has a suppressed excitatory neuron response [12].

Emanations from plants. Almost all mosquito species examined take sugar meals [13]. Nectar feeding is necessary for survival in both sexes. If any differences

exist in sugar meals taken, males may feed more often but in less amount per feeding, regardless of age. Location of plant nectar is accomplished possibly by visual and most likely by olfactory cues. It has been suggested that nectar feeding occurs more often than blood feeding in females; nectar feeding may occur as often as once per night [13]. In terms of priority, however, blood meals most likely take precedence over nectar sugar (from studies involving *Ae. aegypti* and *Ae. albopictus*).

Flower odors play a role in alighting a mosquito onto a plant. The nectar sugar itself is not an airborne cue; however, contact sensilla most likely detect the presence of sugar. Fruits, honey, milkweed and rose extracts attract mosquitoes; strawberry and lilac extracts are suggested repellents [13]. Male *Ae. aegypti* have been found to be attracted to honey odors. Honey fragrance consists of methylphenylacetate and ethylphenylacetate and these were found to attract *Ae. aegypti*. Ethyl lactate and methyl propionate function in finding suitable oviposition sites [4]. Synthetic fragrances, specifically apple and cherry, were found to be attractive for *Ae. aegypti* [13].

Relation to Semiochemical Studies

Analysis of body secretions and excretions, particularly those focused on perspiration, yields knowledge of compounds present on the skin. Perspiration is a dilute solution of compounds containing salts and other involatile compounds as well as volatiles. Combined liquid chromatography/mass spectrometry (LC/MS) analysis has detected the presence of lactic acid (lactate is a by-product of exercise), urea,

and various amino acids (phenylalanine, leucine, valine, and alanine) [29]. Amino acids, e.g. alanine, are believed to have too low of a vapor pressure to be present at detectable levels by mosquito chemosensilla [12].

Direct analysis of perspiration differs from work conducted for purposes of identification of mosquito attractants in that direct analysis detects both involatiles and volatiles. A necessity for mosquito attraction is that the attractant is suitably volatile such that long-range detection by mosquito chemosensilla can occur. Analysis of human body odors satisfies the criterion of examining volatiles which emanate from the skin.

Odor analyses are typically conducted with GC separation. The detection can be accomplished by mass spectrometry, or another suitable detector, such as a flame ionization detector (FID). Determination of odiferous compounds can be done by using GC/MS in conjunction with GC/organoleptic evaluation by humans [30,31]. This is analogous to the use of GC/MS and an olfactometer in the work of this dissertation; the olfactometer performs the function of determining attraction level analogous to the use of the human nose to determine fragrance. Performing GC/MS and olfactomer studies on-line was not feasible at this time due to the complexity involved in the relocation of either the mass spectrometer or olfactometer. Additionally, mosquitoes typically require time to re-settle after detection of an attractive odor stimulus. Work involving GC separation with electrophysiological responses from antennae would obviate the need for re-settling time. Combined GC-

electroantennograms (GC/EAG) would be a valuable extension to the work reported in this dissertation; this topic will be readdressed in Chapter 6.

Overview of Analytical Methods and Detection

The majority of the work in this dissertation consists of sample introduction methods and detection of compounds by mass spectrometry. This section will provide fundamental information about the techniques referred to throughout this dissertation. This initial overview is intended to be very general in scope. More specific consideration of sample introduction methods, ionization methods, and tandem mass spectrometry will be addressed appropriately in subsequent chapters.

Overview of Mass Spectrometry

The first reports of mass spectrometry, as recounted by Nier, occurred in 1918-1919 from the work of Aston and Dempster [32]. Mass spectrometry allows for the determination of abundances of specific masses (specifically mass-to-charge ratios) [33]. It is arguably one of the most powerful tools for identification and quantitation of compounds. Identification of compounds by GC/MS trace detection is likely the most common information derived from mass spectrometric detection. This dissertation employs GC/MS; however, the introduction method employed to sample components is modified and will be addressed later. The fundamental ionization process of mass spectrometry is that of electron ionization. This mode as well as chemical ionization will be addressed from a historical view in this chapter

and a practical view in Chapter 5. The combination of successive stages of mass spectrometry (MS/MS) allows for analysis of more complex mixtures with less need of prior clean-up of sample and matrix [33]. Reaction studies, compound class screening, and elimination of chemical noise via selection of the parent ion of interest are some of the advantages attributable to MS/MS.

Sample introduction

The sampling methods examined for this work were, for the most part, chosen according to a specific criterion, to allow for sample detection in a fashion similar to that which mosquitoes encounter, i.e. a volatilized sample in the gas phase. Handled glass beads allows attractants present on the skin to be transferred to the glass surface; volatile attractants can then be desorbed by heating the glass.

Thermal desorption methods. Direct thermal desorption methods, without additional separation or processing, are simple and quick with respect to detection of compounds. The direct insertion probe (or solids probe) allows for samples to be placed through a vacuum lock, directly into the ion source of the mass spectrometer. Normally, a sample is placed in a crucible designed to fit in the end of this probe. For studies in this dissertation, a glass bead fitted onto a glass stem was placed onto the end of the probe. The probe, inserted into the mass spectrometer ion source, is heated to assist in volatilization of compounds off of the bead.

The idea of heating a single glass bead was extended to multiple beads. Since it is not possible to insert multiple beads directly into the ion source, an alternate method of transferring desorbed volatiles was required. Two to two hundred

handled beads were placed in an enclosed glass container which was placed inside the GC oven; helium passed over the beads transferred sample to the ion source via a deactivated fused silica column (transfer line). This technique will be discussed in greater detail in Chapter 2.

Separation methods. Complexity of the sample may dictate that a method of separation is necessary in order to adequately resolve compounds whose thermal desorption profiles overlap. The focus of this work is on volatiles; therefore, gas chromatographic separation was chosen. The initial phases of this work employed short columns for faster analyses. However, due to the number of components desorbed, longer columns were employed for identification and case studies in the final stages of this work.

Volatiles desorbed from the glass beads have wide desorption profiles; thus, some method of reducing bandwidth before chromatographic separation can significantly improve chromatographic resolution. This was accomplished either by cryo-focusing or by purge and trap. Cryo-focusing involves immersing a portion of the column, just after the column exits the injection port, into liquid nitrogen to collect volatiles and focus them into a narrow band [33]. After focusing, the column is removed from the liquid nitrogen and GC separation is conducted. Purge and trap is slightly more complex in that it typically contains an additional trap [33]. Prior to GC analysis, the sample is collected onto a suitable trap (e.g. Tenax) to perform the focusing operation. The trap is then heated to desorb volatiles which are then focused onto a cyro-trap.

Sample ionization

Mass spectrometric analysis requires that compounds of interest form gas-phase ions. Ionization can be accomplished in a number of ways. For the work in this dissertation, ionization of volatiles (already in the gas phase) is accomplished either by electron ionization (EI) or chemical ionization (CI).

Electron ionization (EI). The first EI source is credited to work in 1921 by Dempster; however, the precursor to the modern EI source was pioneered by Nier in 1947 [33]. Electron ionization involves direct ionization and fragmentation of volatile sample molecules in an electron beam. The fragmentation pattern provides structural information about the original sample molecules.

Chemical ionization (CI). The technique of chemical ionization (positive chemical ionization or PCI) is credited to Munson and Field; a series of papers from 1956-1966, including the work of Franklin and Lampe, cover the development of this technique [34-53]. Chemical ionization is accomplished via a reagent gas of choice. This reagent gas is in greater abundance in the ion source than the sample, and at a pressure high enough (approximately 1 torr) to favor ion-molecule reactions. The reagent gas is ionized by electron ionization; the resultant reagent ions ionize the sample molecules via ion-molecule reactions, typically this is by proton transfer. The result is that less fragmentation of the sample molecule will occur due to the transfer of less energy from ionized reagent ions than from electrons given off by the filament. The greater abundance of intact molecular species relative to fragmentation allows for molecular weight determination. In addition to positive ion

CI, negative ion chemical ionization (NCI) provides additional molecular weight information, and in some cases structural information. The concept of CI will be addressed in Chapter 5; informative structural information derived from NCI is examined in Chapter 3.

Triple quadrupole mass spectrometry

The first report of a triple quadrupole mass spectrometer for chemical analysis occurred in 1978 by Yost and Enke [54]. Figure 1-1 depicts a schematic of a triple quadrupole system. This figure is representative of the Finnigan MAT TSQ70 utilized throughout this dissertation. Although this instrument is still called a triple quadrupole, the second quadrupole (Q2) has been replaced by an RF-only octopole for better transmission of ions.

The ion source allows for passage of an electron beam from the filament to the collector. The electron beam is orthogonal to the vacuum-lock entrance (allowing for probe insertion) and to the GC transfer line. The TSQ70 ion source contains removable ion volumes which can be chosen to give either CI or EI operating conditions. Ions generated in the source are extracted into the first quadrupole mass filter (Q1) by a set of three lenses. The collision cell (Q2) is housed in an assembly such that a suitable inert gas can be leaked into it. The inert gas functions to fragment ions via collision-induced dissociation. Resultant ions are then passed into the second quadrupole mass filter (Q3). Subsequently, detection is accomplished via a conversion dynode (biased for either positive or negative ions) prior to amplification by the electron multiplier.

Figure 1-1 Schematic diagram of a Finnigan MAT TSQ70 triple quadrupole mass spectrometer.

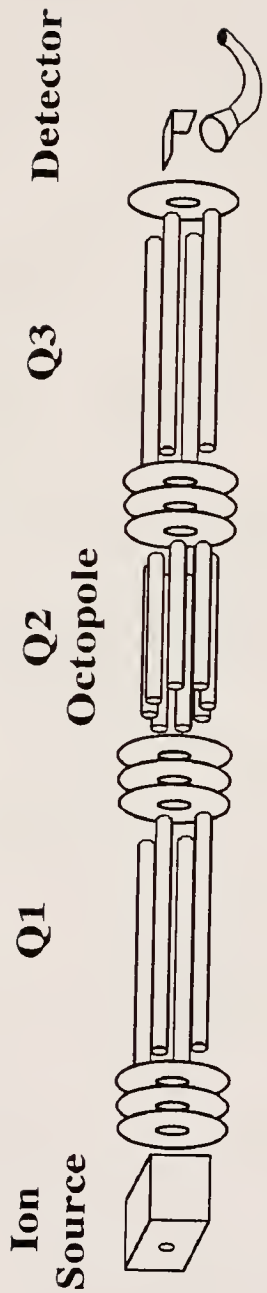
Ion Source
Q1
Q2 Octopole
Q3
Detector

Single-stage detection. The triple quadrupole mass spectrometer can be used for single-stage mass spectrometric analyses [55]. The corresponding modes and operation of the quadrupoles for single-stage operation are presented in figure 1-2. A full mass spectrum can be acquired by either of two modes. The first quadrupole can be scanned, acting as the mass filter, while Q2 and Q3 are held in RF-only mode to pass all ions (figure 1-2(a)). Alternatively, Q1 and Q2 can be held in RF-only mode while scanning Q3, as shown in figure 1-2(b). Selected ion monitoring (SIM), shown in figure 1-2(c), is a single-stage mode allowing passage of only selected m/z values through the mass filter; it can be performed with either Q1 or Q3. The advantage to SIM is the sensitivity gained by scanning the quadrupole over only one or a few m/z values of interest [33].

MS/MS scan modes. The benefits of tandem mass spectrometry lie in the use of various modes of operation derived from the two successive stages of mass filtering [56]. The four modes available for MS/MS operation are shown in figure 1-3. A daughter scan (figure 1-3(a)) consists of setting Q1 to a specific m/z value. This selected parent ion is then fragmented in Q2, the collision cell, via the presence of an inert gas for collision-induced dissociation. The third quadrupole (Q3) then scans the resultant daughter ions. Figure 1-3(b) depicts a parent scan; in this mode, Q3 is set to pass a specific m/z value of daughter ion produced by collisions in Q2. As Q1 scans and sequentially passes each m/z ion over the scan range, the data system records the intensity of the daughter ion and correlates back to the parent m/z value that was passed through Q1. If Q1 and Q3 are both scanned with

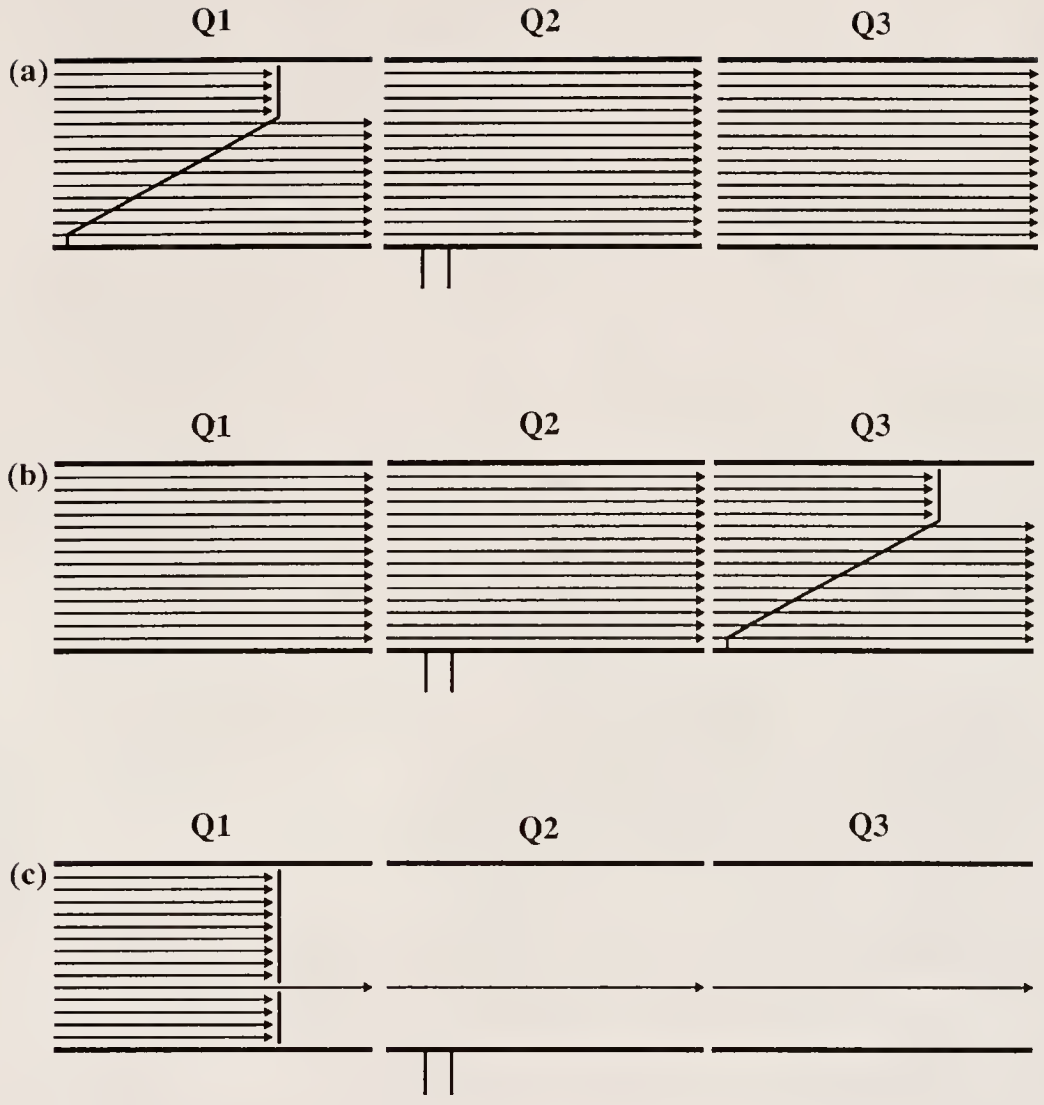

Figure 1-2 Single-stage scan modes with a tandem quadrupole mass spectrometer set for (a) Q1 full mass spectrum, (b) Q3 full mass spectrum, and (c) selected ion monitoring using Q1.

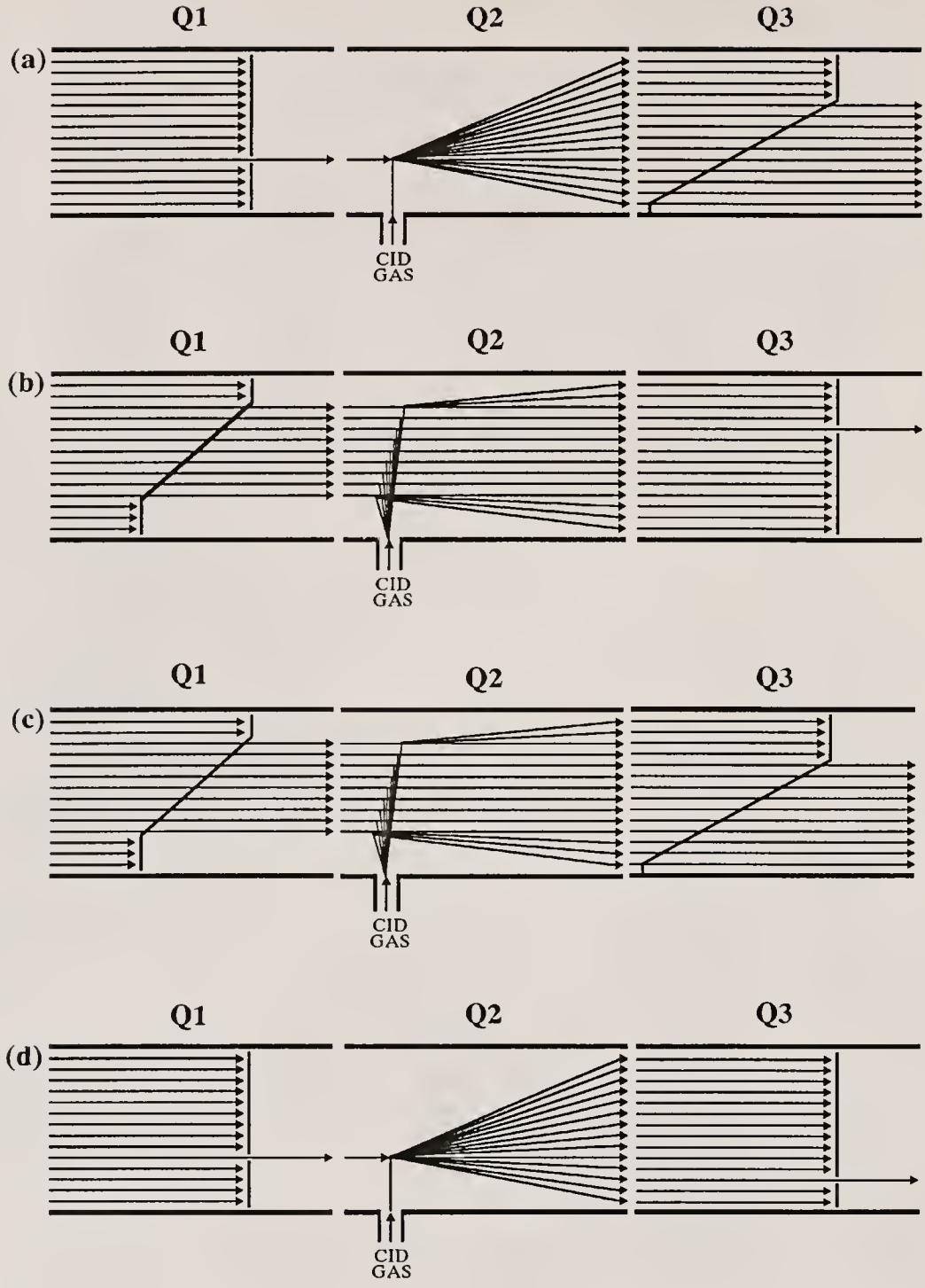

Figure 1-3 MS/MS scan modes of a triple quadrupole mass spectrometer set for (a) daughter mass spectrum, (b) parent mass spectrum, (c) neutral loss spectrum, and (d) selected reaction monitoring.

a fixed mass offset, a neutral loss spectrum can be generated (figure 1-3(c)). The scan m/z value, for each ion passed through Q1, is offset lower in Q3 by the mass of the neutral loss sought. The final scan mode, shown in figure 1-3(d), is selected reaction monitoring (SRM). The first quadrupole mass filter is set to a selected parent ion and the second mass filter is set to a selected daughter ion instead of scanning the full mass range. Several such reactions can be monitored sequentially.

Analysis of Complex Environmental and Biological Samples

The nature of the work found in this dissertation is similar to some issues in the analysis of environmental and biological samples. The approach involving identification of components is similar to methods used for environmental analyses. Modern environmental mass spectrometry is predominantly conducted by GC/MS, with ionization usually accomplished by EI and PCI [57,58]. Although the use of PCI can yield molecular weight information, the use of pulsed positive ion negative ion chemical ionization (PPINICI) allows for greater certainty in identification of the molecular weight of a particular compound [59]. Much of the identification of compounds emanating from human skin reported in this dissertation has involved the use of PPINICI and EI.

Screening of selected metabolites in a biological matrix, such as urine or blood, provides a rapid method to diagnose disorders in patients [60-62]. Compounds of interest include pesticides, steroids, or drug metabolites [63-66]. The use of MS/MS in the screening process allows for rapid determination with less

sample preparation and/or in some cases little or no prior separation [65,66]. It would be beneficial to have in place a rapid screening method for the identification of mosquito attractants. The work in this dissertation is the beginning stage to the development of a screening method for the analysis of human attraction to mosquitoes.

Organization of Dissertation

This dissertation is comprised of six chapters; the overall emphasis is on a combinatorial approach, involving both chemistry and entomology, to better understand the basis of chemical attraction of mosquitoes to hosts. The first chapter has presented the objectives of this work, an introductory overview of entomological fundamentals concerning the mosquito, the relation of this work to semiochemical studies, and an overview of the analytical methods of sampling and detection by mass spectrometry employed in this dissertation. Various methods of sampling emanations are possible; a comparison of techniques tested for this work is summarized in Chapter 2. Chapter 3 focuses on altering attraction with lactic acid as the model compound. Reactions with lactic acid are examined and analysis of solution-based perspiration is described with respect to origin of attractants from the skin. Chapter 4 focuses on the utility of MS/MS to this project and addresses compound class screening. The identification of compounds present on the skin is addressed in Chapter 5. This chapter contains studies comparing two subjects of differing attraction to mosquitoes as well as comparing subject bio-assay attraction to mass

spectrometric assay results. The conclusions and suggested future experiments are contained in the sixth and final chapter of this dissertation. The appendix to this dissertation is located after Chapter 6; this appendix covers preliminary work conducted with carbon dioxide as a reagent gas for chemical ionization.

CHAPTER 2
SAMPLING METHODS

Introduction

This chapter is an overview of methods of sampling and sample introduction. It will introduce the rationale for the sampling criteria and illustratively examine the various methods of sampling for the identification of volatile emanations from the skin.

Sampling Considerations

Ideally, the end result of this work would be to achieve a sampling method which maintains the integrity of the sample. Little chemical modification of the skin emanations is desired such that detection of volatiles is as comparable as possible to that of the mosquito sensilla. The mosquito chemosensilla show response to airborne components which specifically cause activation.

The components on the skin which are attractive to mosquitoes can be transferred to glass via handling the glass object. Glass petri dishes handled by humans are attractive in olfactometer experiments and indeed retain their attraction for up to 6 hours [67]. Furthermore, differences in attraction between human subjects are reflected in the attraction of the petri dishes handled by these subjects.

The glass can then attract mosquitoes due to desorption of volatiles from the surface. The mass spectrometric detection is then desired to sample in this manner.

Storage of samples and duration of the attraction once the sample is deposited on glass are also concerns. Some experiments involved collection of samples at a remote site with subsequent cooling in an acetone/dry ice bath to minimize premature desorption of volatiles. Volatile skin emanations, containing compounds which are attractive to mosquitoes, are amenable to cold-trapping. Experiments involving cold-trapping of emanations in an air stream provided, after reconstitution of the sample, approximately 60% attraction compared to direct introduction of emanations into an olfactometer [16].

Entomological Sampling

Entomological work consists of determining the response of mosquitoes to various cues. Samples may be pure compounds, mixtures, or skin emanations transferred to a specific surface. The surface used for these experiments is glass due to the ability to transfer attractants to it and subsequently desorb these attractants. Experiments of this nature can be done in a laboratory controlled setting via the use of an olfactometer or directly in the field.

Olfactometer

The olfactometer used for measuring attraction is shown in figure 2-1 [67]. The olfactometer used in these studies consists of three pairs of ports for sample introduction; the figure represents only one pair of these. Each pair of ports

Figure 2-1 Diagram of an olfactometer for determination of mosquito attraction to suspected attractants relative to a control sample.

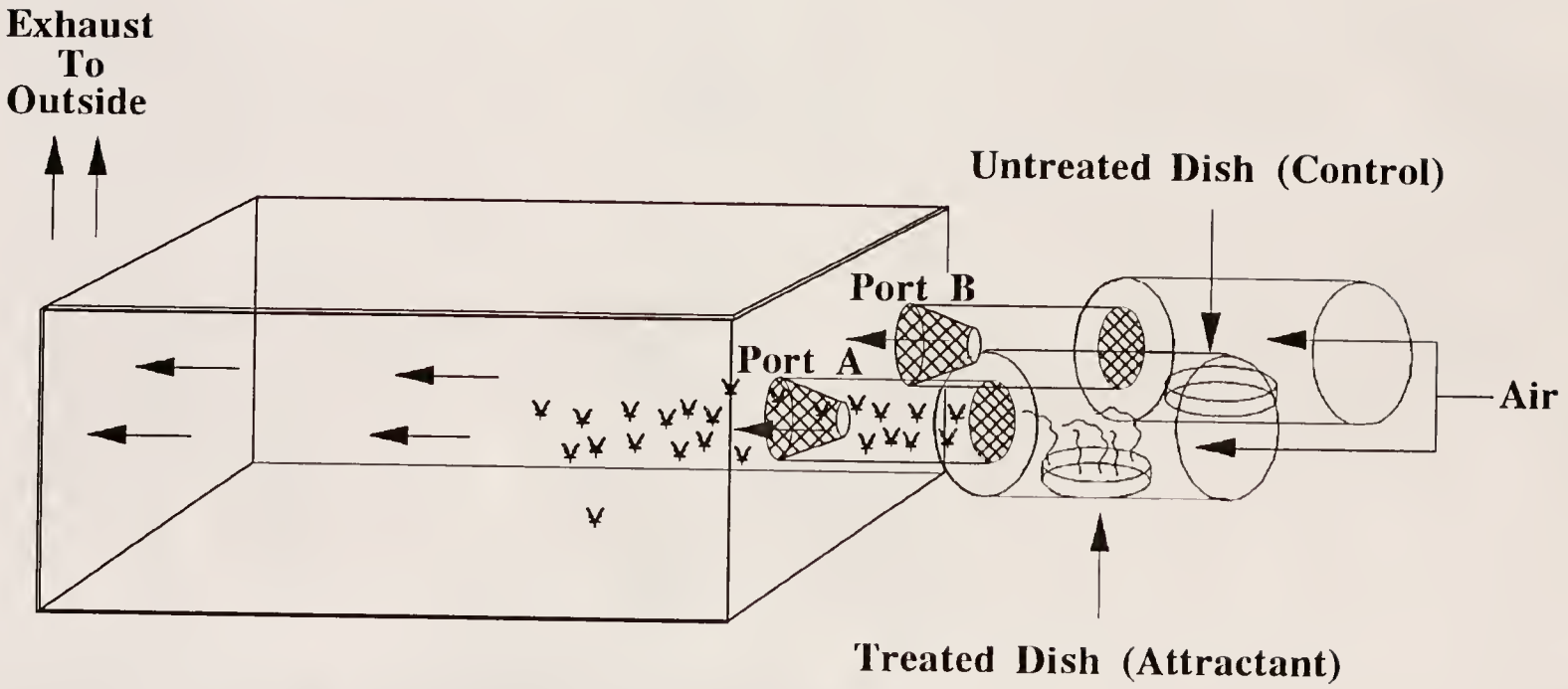
Exhaust
To
Outside
Untreated Dish (Control)
Port B
Port A
Air
Treated Dish (Attractant)

consists of one port (port A) for introduction of the sample and the second port (port B) for the introduction of the control or a second comparative sample. The sample sizes or media of introduction are limited only by the volume of the ports; in this figure, petri dishes are shown. In port A, the petri dish has either been inserted after handling or inserted after deposition of a sample consisting of a sole compound or mixture of compounds. The dish in port B is a cleaned untreated petri dish used as a control. A humidity-controlled stream of air, pure gas, or mixture of gases is passed through the ports, over the samples. Any volatiles desorbed from the sample will be carried via the gas stream through a trap on each port. The outlet of the trap then opens into a enclosed chamber where the mosquitoes are held. The enclosed chamber also contains an exhaust to enhance the airstream effect through the olfactometer.

Mosquitoes used in these tests are typically female *Ae. aegypti*, although not limited to this species or gender. Mosquitoes are usually not fed for a period of time in order to enhance the response to any attractive compounds. If the volatiles are odor cues for the mosquitoes, the mosquitoes will be activated to flight and follow upstream into the appropriate trap. Should mosquitoes not be able to directionally locate the source of the odor with accuracy but do alight upstream, they will be collected in the control port trap. After a specified period (typically 3-5 minutes), the experiment is ended and the mosquitoes trapped in each port counted. This allows for the percentage of mosquitoes attracted to a specific stimulus to be calculated.

Field studies

Studies in the field are less precise in determining the actual percentage attracted to a sample. Sampling in the field also involves careful consideration in the design of traps, the release rates of samples, the location of samples, and the influence of parameters in the outdoors. Some of these parameters are wind speed, wind direction, humidity, and temperature. Additional concerns are manifested in the actual population of mosquitoes during the test, i.e. whether or not they are in close proximity to the test region such that odors could be detected. Trapped mosquitoes are separated and counted according to species. The information obtained from these experiments consists of a net capture rate relative to other species and/or a control. Estimating the total population of unattracted mosquitoes is not possible via field tests of this nature.

Mass Spectrometric Methods of Sample Introduction

The sampling for this dissertation was conducted numerous ways; a chart representing this is portrayed in Figure 2-2. The sample in this diagram refers to emanations or sweat found on human skin. These emanations were either deposited on glass beads via handling the beads, washing the beads with solvent after handling the beads, or directly dissolving perspiration into methanol.

Methods of direct analysis of glass beads consisted of either using a single bead fitted on the end of a solids probe stem or placing multiple beads in an enclosed glass sample container or "vial". The term "vial" is used to describe any of

Figure 2-2 Overview of sampling methods examined for the work in this dissertation.

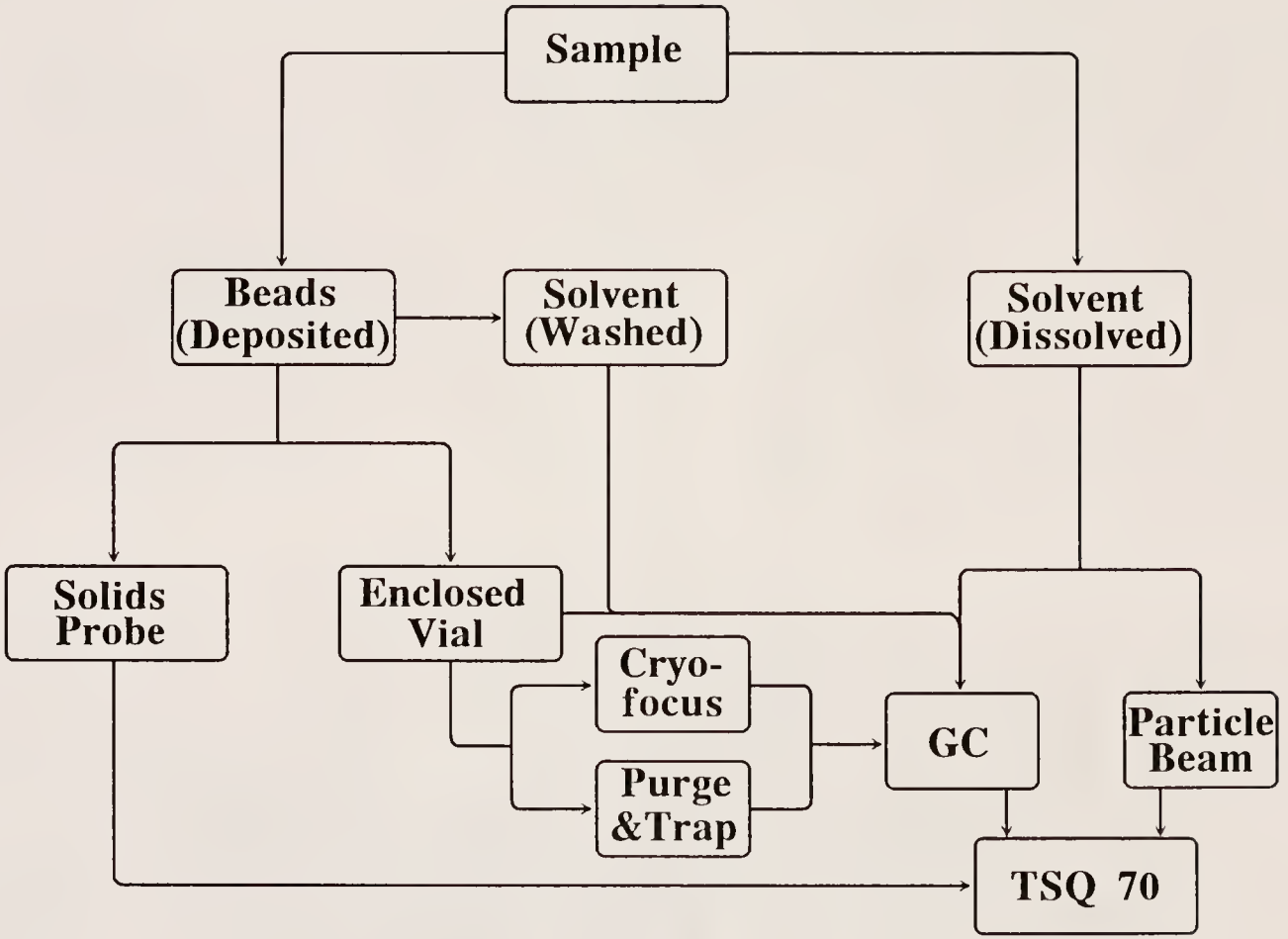
Sample
Beads (Deposited)
Solvent (Washed)
Solvent (Dissolved)
Solids Probe
Enclosed Vial
Cryo-focus
Purge &Trap
GC
Particle Beam
TSQ 70

a number of various shapes and volumes of glass sample containers. The enclosed vials allowed for heating of the beads for subsequent analysis, usually by cryo-focusing or trapping. Cryo-focusing and trapping methods are covered in greater detail in Chapter 5.

Additional experiments conducted with glass beads involved solvent washing of the handled beads with methanol. Methanolic solutions were also employed for the direct analysis of perspiration via GC and for particle beam/liquid chromatography (PB/LC). Work involving solutions is covered in Chapter 3.

Experimental

Thermal Desorption from a Single Bead

Single bead thermal desorption was employed to produce the chromatograms and spectra found in some of the figures in this chapter. The 0.115" (2.9 mm) glass bead was fitted (glass-blown) to a glass stem for insertion into the mass spectrometer ion source. The dimensions of the stem (5 mm long x 1.4 mm diameter) were chosen to fit in the direct insertion probe in place of the typical aluminum crucible. The bead (attached to the stem) was handled for 3-10 min prior to analysis. Handling consisted of rubbing in the palms of the hands only. Subjects for these analyses included the author of this dissertation, Mr. Dan Smith of the USDA, and Dr. Anthony Annacchino, Jr., a former member of this research group.

Prior to analyses of a handled bead, a blank bead was analyzed to determine the background components. The experimenter who handled the bead then placed

the bead onto the solids probe for analysis. The solids probe containing the bead was inserted into the mass spectrometer ion source. The probe ramp consisted of increasing the temperature from 50°C to 300°C over a six minute period.

The mass spectrometer was a Finnigan MAT TSQ70 triple quadrupole mass spectrometer equipped with a Varian 3400 gas chromatograph. This modified instrument contains an octopole for Q2 and a 20 kV dynode. The instrument was employed only for single-stage (MS) detection. The filament emission current was set to 200 μA in all cases. The electron energy was 70 eV for EI analyses and 100 eV for CI analyses. The manifold temperature was set to 70°C while the ion source temperature was set to 150°C for CI and 170°C for EI. The mass ranges scanned were m/z 10-650 for EI and m/z 60-650 for CI. The reagent gas for CI analyses was methane; the indicated pressure of methane in the ion source was 1650 mtorr. The electron multiplier was set between -1000 and -1200 V and the conversion dynode set at -5 kV. Prior to data acquisition, the instrument was tuned for maximum transmission of characteristic ions from perfluorotributylamine (PFTBA).

Thermal Desorption from Multiple Beads

The sampling of multiple beads is not amenable to solids probe introduction via insertion through the probe lock of the mass spectrometer. Initial sampling of multiple beads was accomplished by the apparatus shown in figure 2-3. The beads were placed in a round bottom flask; a 100 mL or 250 mL round bottom flask modified for use with this apparatus. The modification consisted of removing the

Figure 2-3 Apparatus constructed for the delivery, via transfer by a deactivated FSOT column, of desorbed skin emanations from glass beads contained in the round bottom flask.

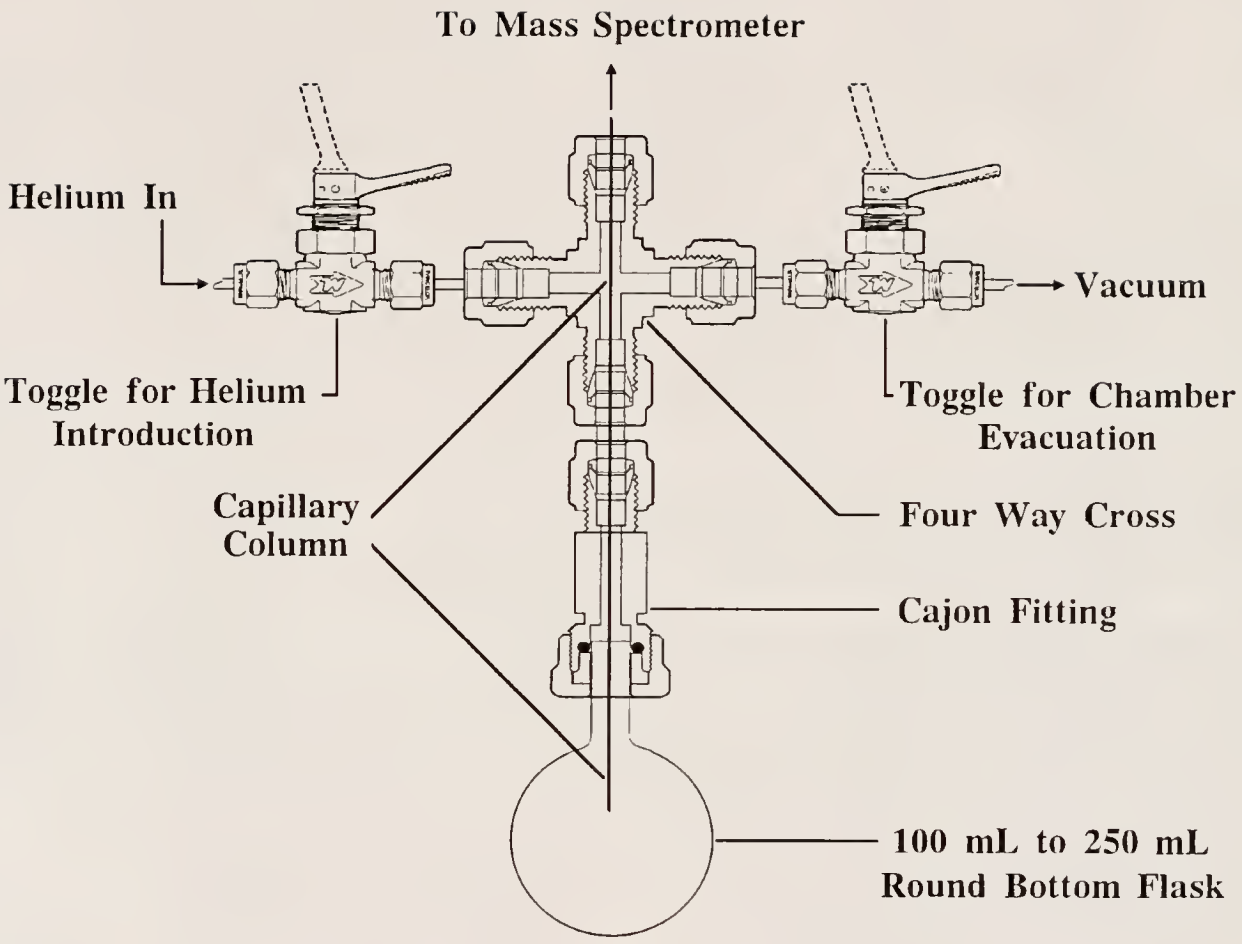
To Mass Spectrometer
Helium In
Vacuum
Toggle for Helium Introduction
Toggle for Chamber Evacuation
Capillary Column
Four Way Cross
Cajon Fitting
100 mL to 250 mL Round Bottom Flask

original stem and replacing it with a 1/2" diameter glass tube. This allowed the round bottom flask to be inserted into a Cajon fitting connected to a four-way 1/4" Swagelok cross via 1/4" tubing. The four-way Swagelok cross was attached to two toggle valves. One allowed for evacuation of air in the chamber prior to analysis; the other allowed for helium to be passed into the chamber, mixing with desorbed volatiles from the beads. The Whitey toggle valves were connected via a 1/4" to 1/8" reducer to the 1/8" Swagelok fitting. The vacuum line was connected to the TSQ70 pumping system via a Swagelok fitting normally used to evacuate the calibration gas probe. The high purity helium was delivered to the apparatus by diverting the helium line out of the pressure regulator on the Varian 3400 GC and interfacing it with the toggle for helium introduction. The final port on the four-way cross consisted of reducing the 1/4" fitting to 1/16" and employing a 0.4 mm i.d. vespel ferrule (SIS, GVF16-004) for insertion of a 1.0 to 1.5 m x 0.10 to 0.25 i.d. deactivated fused silica open tubular (FSOT) column. One end of the column extended down into the round bottom flask, above the layer of beads. The other end of the column was interfaced to the ion source of the TSQ70 via the GC transfer line.

The operation and sampling for the apparatus shown in figure 2-3 consisted of placing it in the Varian 3400 GC oven. The round bottom flask was removed from the Cajon fitting just prior to the transfer of glass beads into it. The flask was then re-inserted into the Cajon fitting. For some studies, the round bottom flask and Cajon fitting were replaced by a 3" x 1/4" o.d. glass tube swaged to the cross with a

1/4" glass filled teflon ferrule. The tube had an inner diameter slightly larger than the bead diameter (approximately 1/8").

Once the sample was placed in the apparatus contained in the GC oven, evacuation is conducted by opening the toggle to vacuum. After 2-3 s of evacuation, the toggle was closed and the second toggle, supplying helium, is opened. The helium pressure was set to 8 psig via the regulator normally used to control injection port pressure on the Varian 3400 GC. Data acquisition was started at this point via instrument automated control through an ICL program.

The GC column was a 1.0 to 1.5 m x 0.10 to 0.25 mm i.d. deactivated FSOT column. The heating parameters consisted of a GC oven ramp and a transfer line ramp. The GC oven ramp consisted of a 0.5 to 1.0 min hold at 25 to 30°C followed by a 10-15°C/min ramp up to a final temperature of 190-210°C and a final hold of 2.0 to 5.0 min. The transfer line was initially set to 50°C and ramped immediately at 20°/min up to 200-210°C and held at that temperature for the duration of the experiment.

The NCI experiments were conducted with 1650 mtorr methane as the electron moderating gas. The scan times were 0.5 to 3.0 s; scanning over Q3 (i.e. Q3MS) was employed with a mass range of m/z 10-650. The electron multiplier was set at -900 V, the conversion dynode at +5kV, and the filament emission current set at 200 μA with 100 eV electron energy. The ion source temperature was set at 150°C and the manifold set at 70°C. Prior to analysis, the mass spectrometer was

tuned for Q3MS NCI mode via maximizing transmission of characteristic negative ions from PFTBA.

Thermal Desorption from Multiple Beads/Cryo-focused GC Separation

Heating of beads to desorb volatiles for cryo-focusing was accomplished by loading the beads into the GC injection port. A Varian 3400 GC fritted glass injection insert was inserted reversed into the injection port. This allowed for up to 12 beads to be placed between the frit (located approximately halfway down the insert) and the GC septum sealing the injection port. The frit kept the beads from dropping down onto the column entrance and provided a means for volatile emanations to be loaded onto the column; the column entrance extends up into the injector insert just below the frit. Operating the injection port in a entirely splitless mode (i.e. it was not necessary to open the split valve due to the absence of solvent in samples) for the duration of the experiment provides essentially only one exit for volatiles, through the column.

Beads were rubbed for 5 min prior to being placed into the injector insert. Experiments were typically performed with 5 to 12 beads. After loading the beads into the insert, the insert was placed into the injection port held at 25°C to minimize sample loss from evaporation. Repetitive analyses required a method of cooling the glass insert prior to subsequent analyses; Dust-Off (difluoroethane) was used for this purpose. The cap, septum, and needle guide were replaced. Throughout the loading process the head pressure of helium was set to 0 psig to allow for proper alignment

of the septum and to prevent premature migration of volatiles past the intended point of cryo-focusing on the column.

Before increasing the helium head pressure, liquid nitrogen was placed in a 12 oz. styrofoam cup. The cup was placed in the oven such that approximately 8 cm of column could be looped in the cup about 15 cm below the point where the column passes from injection port to oven. The helium pressure was then increased to 20 psig and the initial desorption phase started. This entailed loading a program to ramp the injection port from 25°C to 250°C over 7.5 min and holding at 250°C for 2.5 min. Throughout the cryo-focusing phase, the GC oven was set at 25°C and the transfer line set 40°C. Liquid nitrogen was added to the cup as necessary during this 10 min cryo-focusing phase.

Subsequent to the completion of the cryo-focusing, a new program was loaded from the TSQ70 to the Varian 3400 GC. Prior to running this program and concurrently acquiring data, the cup containing liquid nitrogen was removed. The GC oven ramp consisted of an initial 1.0 min hold at 25°C, a 12 min ramp at 15°C/min up to 210°C, and then a hold at 210°C for 5.0 min. The transfer line was concurrently ramped, after a 1.0 min hold at 40°C, up to 225°C at 15°C/min, and held 5.0 min at 225°C. Experiments were performed with either an 18 m x 0.18 mm i.d. DB-5 column (d_f=0.25 μm) or a 20 m x 0.25 mm i.d. Carbowax column (d_f=0.25 μm).

The mass spectrometer was operated in NCI mode, positive and negative ion mode (PPINICI), or EI mode. For NCI and PPINICI experiments the reagent gas

was methane at 1650 mtorr and 1660 mtorr (indicated) pressures, respectively. The ion source and manifold temperatures were 150°C and 70°C, respectively, for CI and 170°C and 70°C, respectively, for EI. The electron energy for CI experiments was 100 eV and for EI, 70 eV. The third quadrupole (Q3) was scanned with a scan time of 2 s for figures in this section. The filament emission current was set at 200 μA. The conversion dynode was set at +5 kV for positive ion CI and EI, and -5 kV for negative ion CI. The electron multiplier was set at -1000 V to -1200 V. Prior to analysis the instrument was tuned with PFTBA as previously mentioned and blanks (appropriate number of beads without sample) were analyzed.

Purge and Trap/GC Separation

Some analyses were performed using a microscale purge & trap system. The sampling difference between figures shown in this section of the chapter was the method of collection of skin emanations. Some experiments involved handling 200-250 glass beads 10 min. The beads were then transferred to the same 100 mL round bottom flask discussed previously. The round bottom flask was attached to the purge and trap system via a 1/2" Cajon fitting to 1/4" Swagelok, further reduced to a 1/8" Swagelok fitting. Skin emanations were also sampled by placing the left hand in a Tedlar bag and fastening the bag around the wrist with a rubber band. The Tedlar bag was attached to the purge and trap system by a 1/8" Swagelok fitting. The flask or bag was attached to a port on an ELA2010 canister manifold (Entech Laboratory Automation).

The canister manifold allowed for 70-100 mL of volatiles and residual air to be sampled by the ELA2000 concentrator. The concentrator consisted of three stages. The first stage employed a dryer with a gradient of large to small glass beads through the dryer. This served to remove most of the water in the sample. During concentration, this stage is set to -160°C for three minutes and heats up to -16°C as sample is transferred to the second stage. The second stage in these experiments was a Tenax trap. During concentration, the trap was set to -20°C and then heated to 156°C for desorption of trapped volatiles onto the focusing trap. The cryo-focusing trap was set a -160°C for concentration and was heated ballistically (approximately 10 seconds) to 150°C to purge volatiles onto the head of the GC column.

The GC employed was an HP5890 series I with a 30 m x 0.25 mm i.d. DB-1 column (d_f=1 μm). For analyses involving glass beads, the column was initially cryo-cooled at -35°C and held for 3.0 min. Subsequently, the column was ramped at 12°C/min up to 180°C, then ramped at 25°C/min from 180°C to 225°C and held for 5.0 min at 225°C. For analyses from the Tedlar bag, the column was held 6.0 min at -35°C then ramped at 6°C/min to 180°C and 12°C/min from 180°C to 225°C, and held for 10.0 min at 225°C.

The mass spectrometer used for these studies was a Finnigan MAT Incos 50 single-stage quadrupole. The scan rate employed was 0.75 s per scan. The filament emission current was set at 750 μA with an electron energy of 100 eV. The electron multiplier was set to -1200 V. The ion source temperature was set at 180°C; there

is no heater for the manifold. Prior to analysis, the instrument was tuned with PFTBA.

Results and Discussion

Thermal Desorption from a Single Bead

The initial crucial phase of the work in this dissertation was demonstrating the ability of mass spectrometry to detect emanations found on the skin. This problem was approached by employing the knowledge gained from olfactometer experiments that glass which has been handled retains attraction to mosquitoes. Shown in figure 2-4 is the total ion current versus time trace for a single handled glass bead. This trace is typically called a reconstructed ion chromatogram (RIC), even though no chromatography is being performed. This figure represents one of the experiments from this beginning series where the single glass bead was introduced into the mass spectrometer ion source via the direct insertion (solids probe). It is evident from the shape of the RIC that separation from distillation off of the probe is minimal and more sophisticated analyses would be required to discern the components hidden below these peaks. This figure clearly illustrates the drawback to this probe method, i.e. that temporal resolution, although satisfactory for simple samples, is not capable of providing efficient resolution from so complex a sample as skin emanations.

Matters are further complicated when searching for trace components. One such example, for cholesterol (cholest-5-en-3-ol), is presented in figure 2-5. Displayed in this figure are the mass chromatograms for m/z 386, the characteristic

Figure 2-4 Reconstructed ion current trace from the PCI analysis, via the direct insertion probe, of thermally desorbed skin emanations from a single glass bead rubbed in the palms of the hands for 10 min by the author of this dissertation. Data were acquired in Q3MS mode with a scan time of 1 s per scan. The probe was ramped from 50°C to 300°C over 6 min (360 scans).

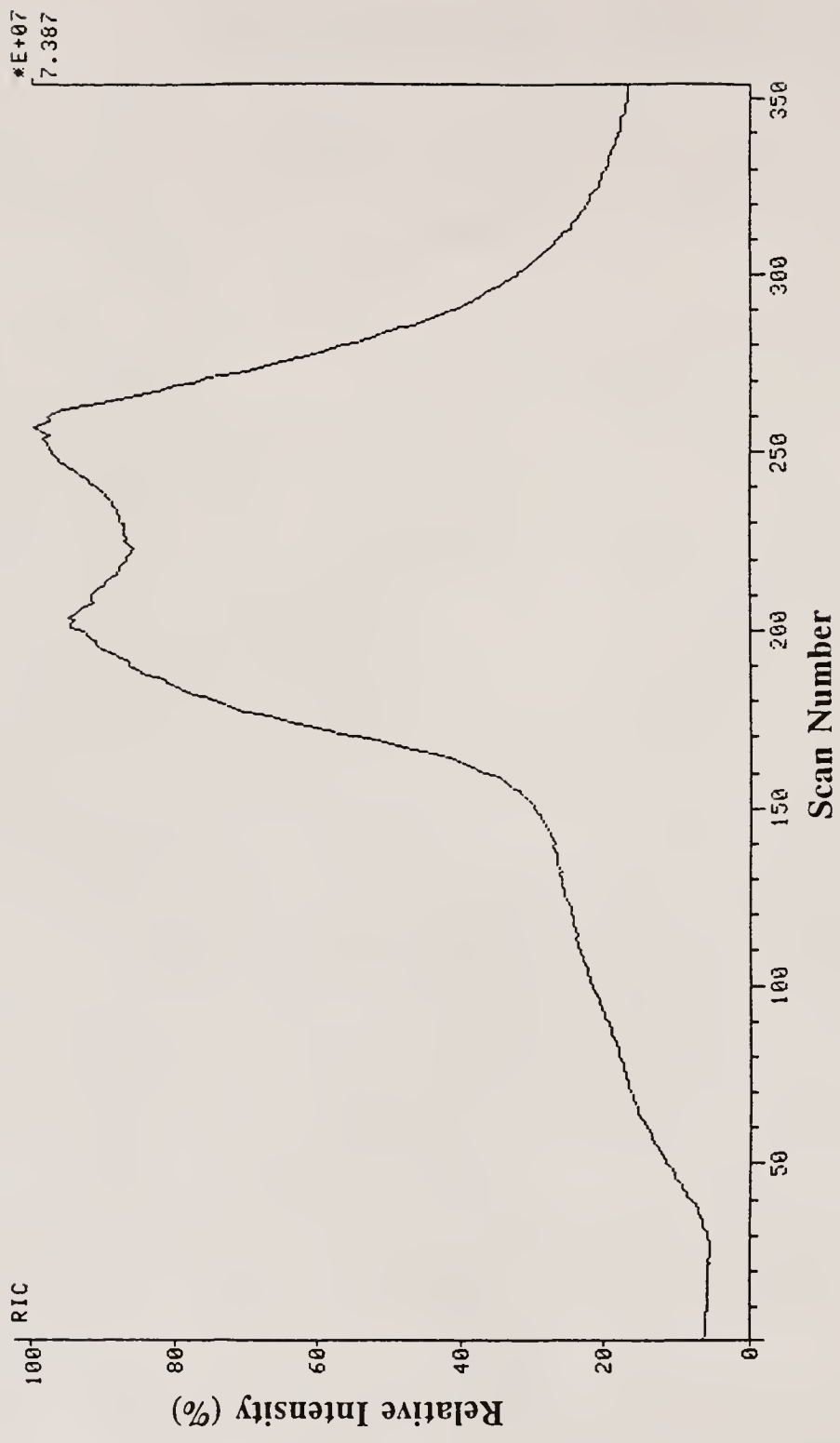
RIC
*E+07
7.387
100
80
60
40
20
0
50
100
150
200
250
300
350
Relative Intensity (%)
Scan Number

Figure 2-5 Mass chromatograms of m/z 386 and m/z 387 from the EI analysis, via the direct insertion probe, of thermally desorbed skin emanations from a single glass bead rubbed in the palms of the hands for 3 min by the author of this dissertation. Data were acquired in Q3MS mode with a scan time of 1 s per scan. The probe was ramped from 50°C to 300°C over 6 min (360 scans).

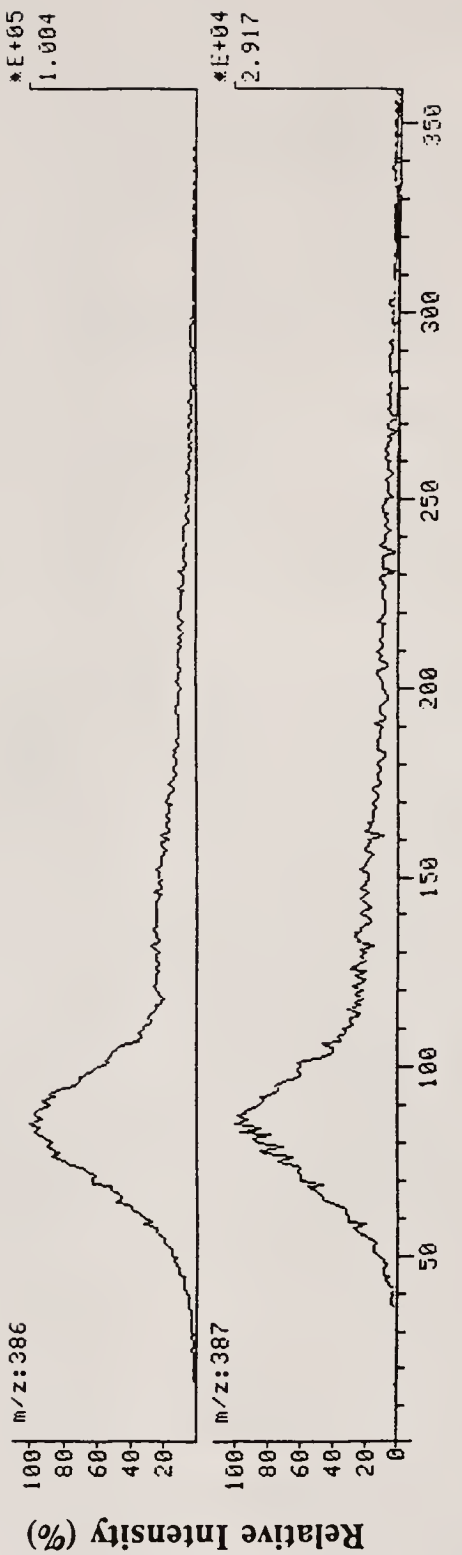
*E+05
1.004
m/z:386
100
80
60
40
20
*E+04
2.917
m/z:387
100
80
60
40
20
0
50
100
150
200
250
300
350
Relative Intensity (%)
Scan Number

molecular ion ($M^{+\bullet}$) of cholesterol and m/z 387, the carbon-13 isotope of the molecular ion. Positive identification of cholesterol during this initial phase was difficult to obtain due to the abundance of fragment ions from other species found in the mass spectrum over the selected peak; background subtraction was not able to fully remove the interferant masses due to the width of the desorption profiles.

Trace components of lower m/z become increasingly difficult to identify due to overlapping profiles of fragment ions when examining the mass chromatograms for particular m/z values (see discussion of figure 2-8). Additionally, re-examination of each mass over the entire scan range, or sections of the RIC devoid of discernible peaks, makes identification a tedious process. The positive identification of cholesterol was achieved in the work of Chapter 5.

During this first series of experiments with a single bead, different subjects were involved in handling the beads. Figure 2-6 is the RIC from the mass spectrometric analysis of a single bead rubbed by Mr. Dan Smith; this individual has been consistently found to be the most attractive person to mosquitoes in USDA tests conducted with the olfactometer. Comparing figure 2-6 to figure 2-4 (the RIC of a bead rubbed by the author of this dissertation) it is evident that the traces are very similar. This comparison also demonstrates that examination of this nature is insufficient to ascertain differences among people in terms of relating what components and what abundance of components is present on the skin causing the differentiation.

Figure 2-6 Reconstructed ion current trace from the PCI analysis, via the direct insertion probe, of thermally desorbed skin emanations from a single glass bead rubbed in the palms of the hands for 10 min by Mr. Dan Smith of the USDA. Data were acquired in Q3MS mode with a scan time of 1 s per scan. The probe was ramped from 50°C to 300°C over 6 min (360 scans).

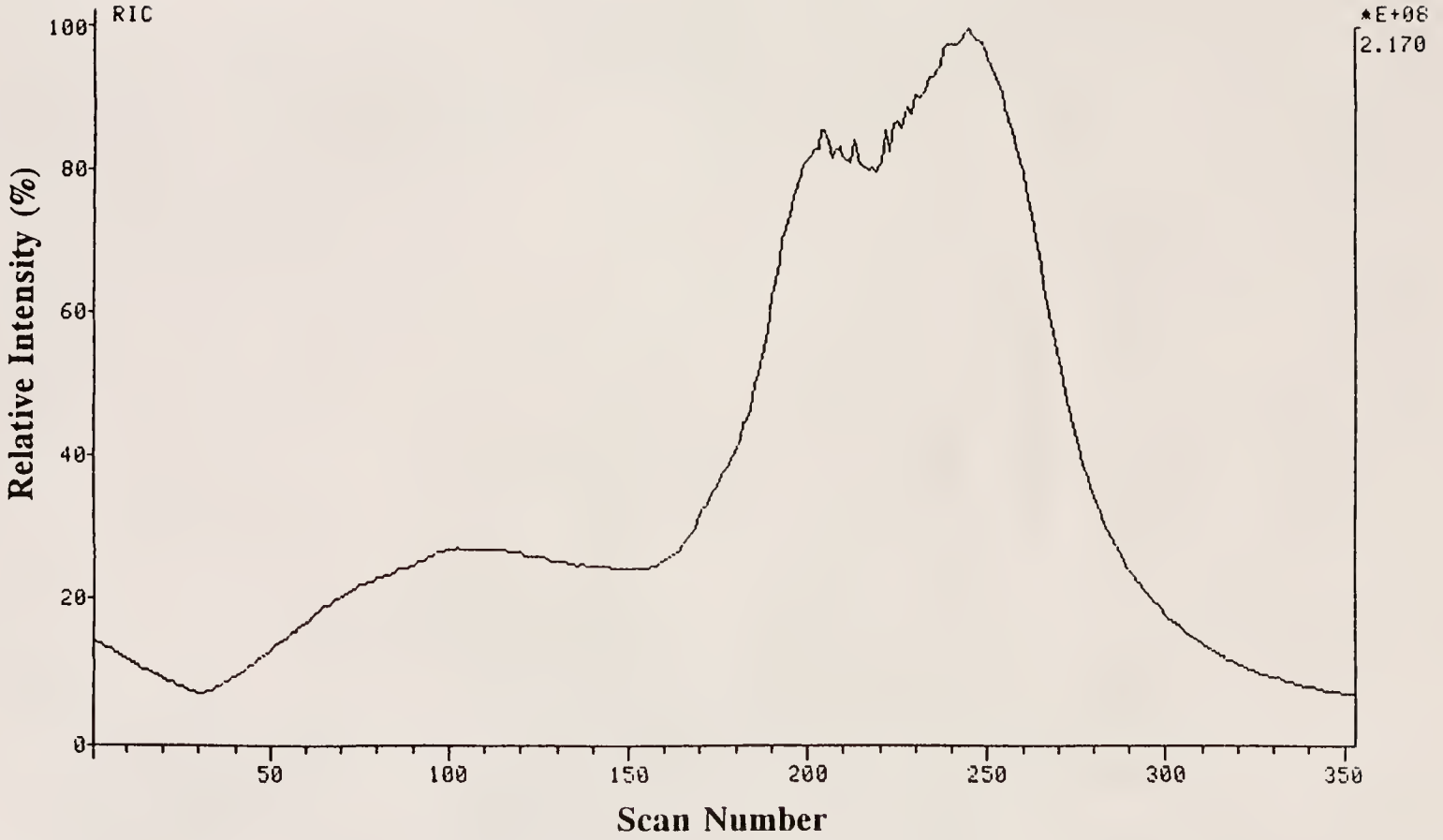
RIC
*E+08
2.170
100
80
60
40
20
0
Relative Intensity (%)
50
100
150
200
250
300
350
Scan Number

Figure 2-7 is the RIC of a second bead rubbed by Dan Smith of the USDA. This experiment was run 30 min after the experiment which produced the RIC in figure 2-6. The differences in peak heights between these figures show that significant variations may exist between analyses from the same person. This difference could very well be a difference in the substances deposited on the beads, i.e. some substances may be retained on the skin more efficiently than others; the difference between figures 2-6 and 2-7 could reflect this. The difference between these two figures may also indicate the irreproducibility of this method of sample introduction. Analysis of repeated samples taken over an extended period of time will be addressed in Chapter 5 of this dissertation.

Figure 2-8 shows mass chromatograms obtained from the analysis giving the RIC trace in figure 2-7. The ions shown are m/z values for the protonated aliphatic fatty acids. Specifically these are the $[M+H]^+$ ions for tetradecanoic acid (m/z 229), pentadecanoic acid (m/z 243), hexadecanoic acid (m/z 257), and octadecanoic acid (m/z 285). The profiles found below scan number 150 are clearly offset and depict the trend of this series of acids; however, without the knowledge acquired later in this work, the results would still be lacking in terms of identifying the full series. With this knowledge, some of the earlier mass spectra, such as the spectrum presented in figure 2-9, can be examined. Figure 2-9 is a mass spectrum from scans 151-200 for a single bead rubbed by Dr. Anthony Annacchino. Clearly shown is the molecular ion for cholesterol (m/z 386) and the loss of water from cholesterol (m/z 368). Although, the ions at m/z 200, 228, 256, and 284 correspond to the molecular

Figure 2-7 Reconstructed ion current trace from the second PCI analysis (acquired 30 min after that of figure 2-6), via the direct insertion probe, of thermally desorbed skin emanations from a single glass bead rubbed in the palms of the hands for 10 min by Mr. Dan Smith of the USDA. Data were acquired in Q3MS mode with a scan time of 1 s per scan. The probe was ramped from 50°C to 300°C over 6 min (360 scans).

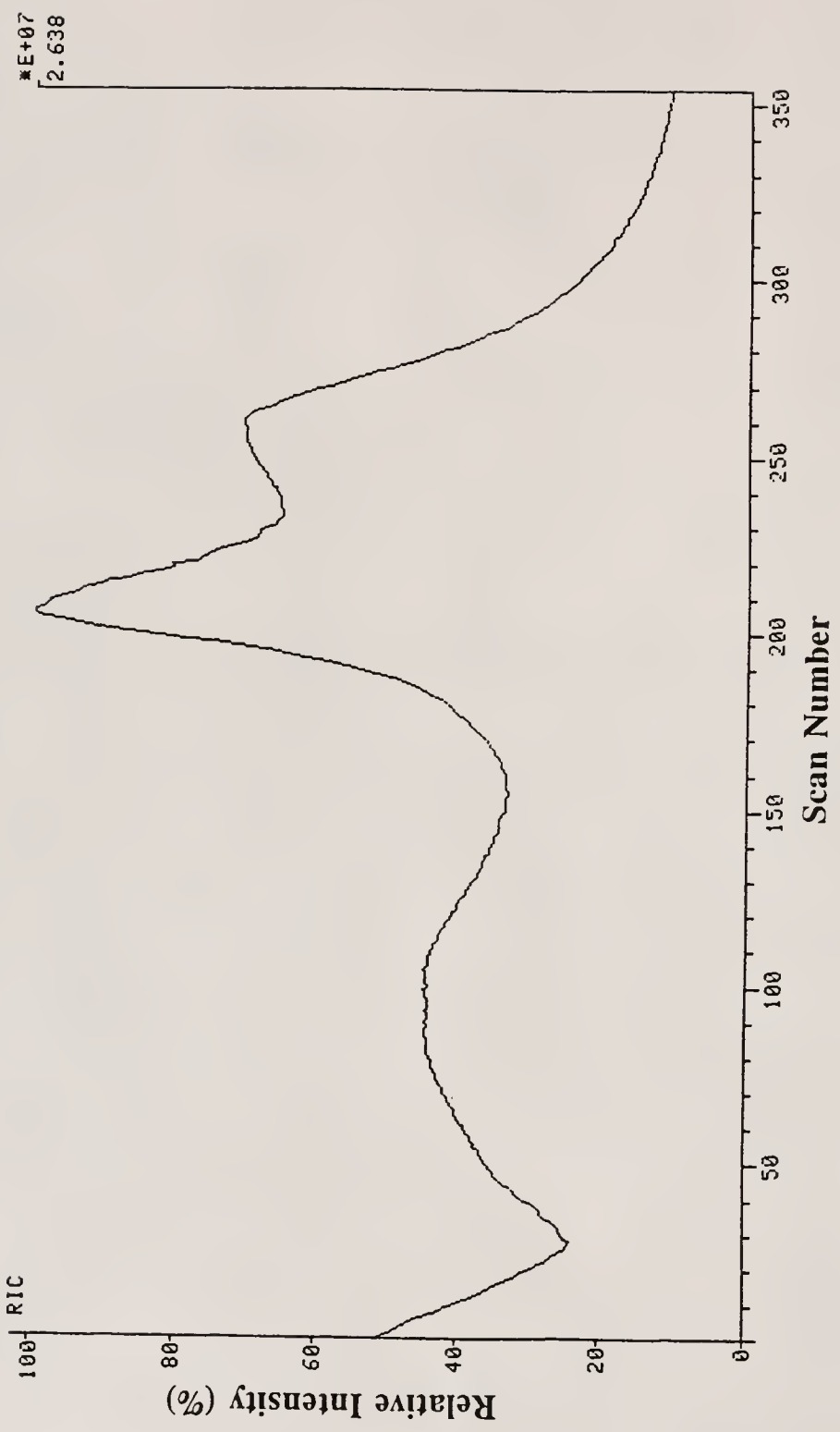
RIC
*E+07
2.638
100
80
60
40
20
0
50
100
150
200
250
300
350
Relative Intensity (%)
Scan Number

Figure 2-8 Mass chromatograms of m/z 229, 243, 257, and 285, with the RIC for PCI analysis, via the direct insertion probe, of thermally desorbed skin emanations from a single glass bead rubbed in the palms of the hands for 10 min by Mr. Dan Smith of the USDA. Data were acquired in Q3MS mode with a scan time of 1 s per scan.

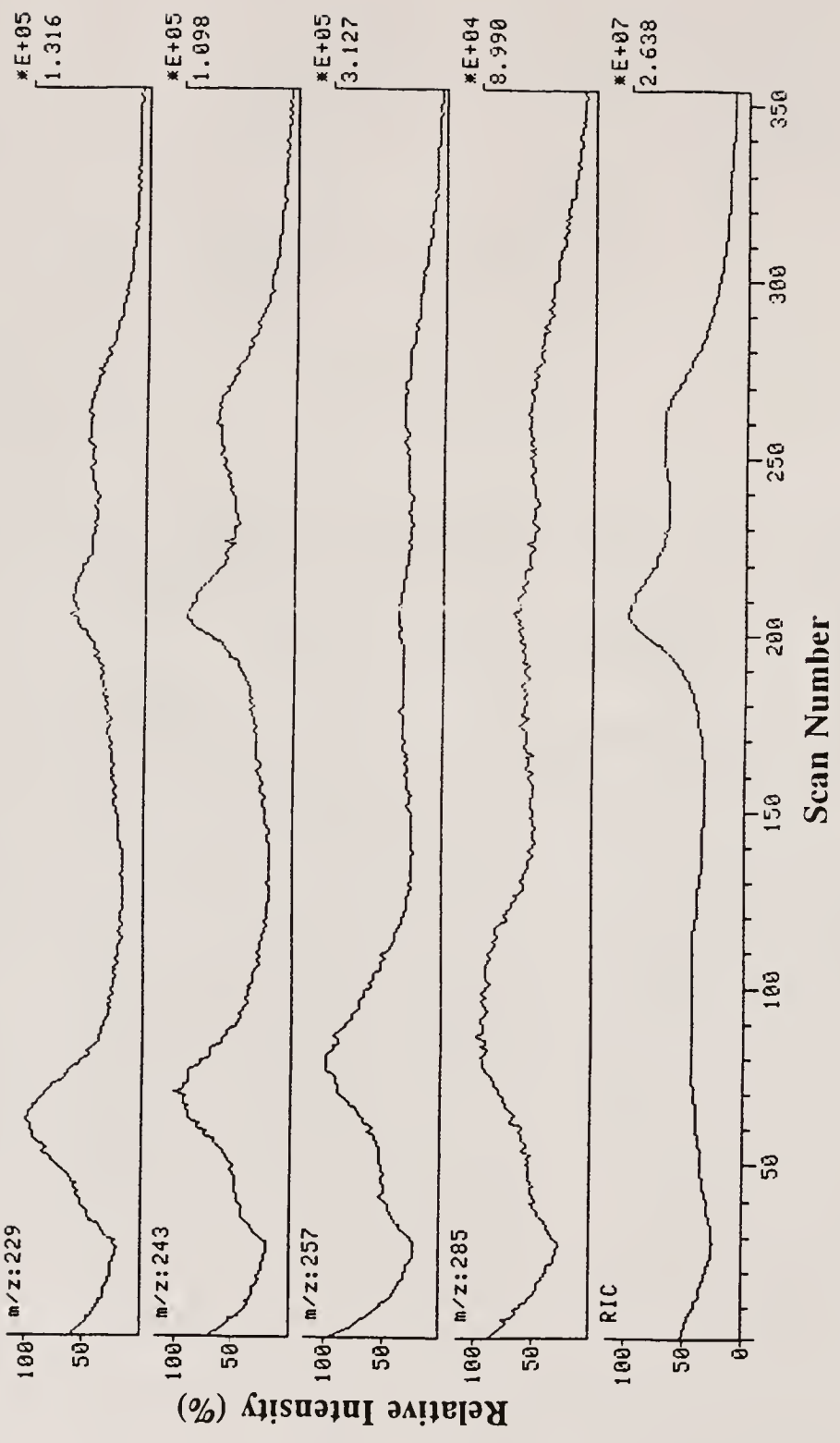
*E+05
1.316
m/z:229
*E+05
1.098
m/z:243
*E+05
3.127
m/z:257
*E+04
8.990
m/z:285
*E+07
2.638
RIC
100
50
0
50
100
150
200
250
300
350
Relative Intensity (%)
Scan Number

Figure 2-9 Mass spectrum acquired for scans 151-200 for EI analysis, via the direct insertion probe, of thermally desorbed skin emanations from a single glass bead rubbed in the palms of the hands for 8 min by Dr. Anthony Annacchino. Data were acquired in Q1MS mode with a scan time of 1 s per scan. Intensities of peaks have been blown up by a factor of 10 for m/z 100 to 260 and by a factor of 100 for m/z 260 to 612.

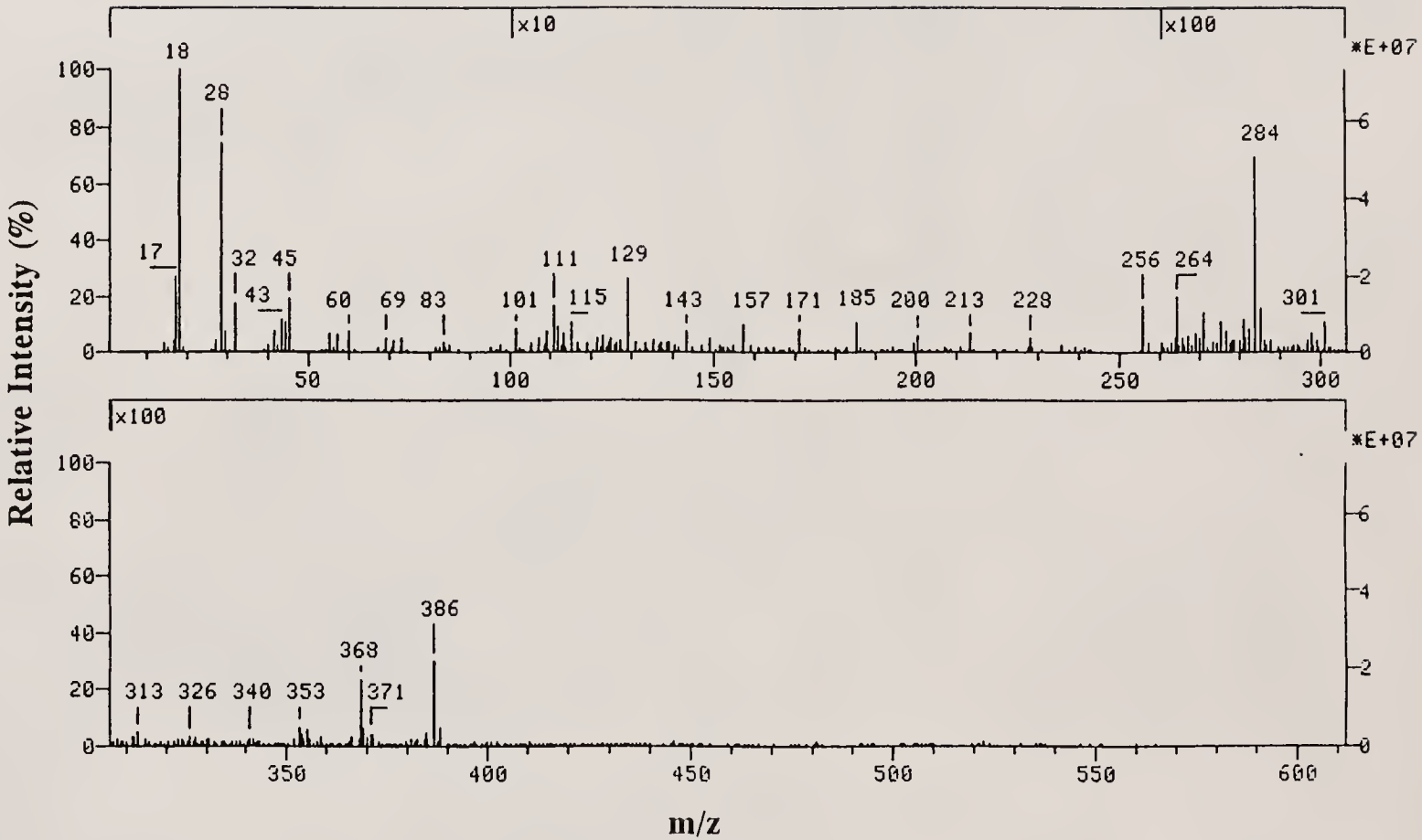
Relative Intensity (%)
m/z
x10
x100
*E+07
18
28
17
32
43
45
60
69
83
101
111
115
129
143
157
171
185
200
213
228
256
264
284
301
313
326
340
353
368
371
386

ions ($M^{+\bullet}$) of aliphatic fatty acids, some of these ions may be due to fragment ions from higher molecular weight compounds (e.g. longer chain fatty acids in the same series).

Thermal Desorption from Multiple Beads

The first approach to improving identification of components was to develop methods of increased sample size to obtain greater ion signal for the identification of trace components. The apparatus initially constructed for this purpose was described in the experimental section and depicted in figure 2-3. Figure 2-10 is an illustration of the NCI results of thermal desorption from multiple beads in a round bottom flask. In this case, the 100 handled beads were spiked with additional lactic acid prior to heating and analysis of the beads. There is an erratic response of the RIC past scan number 1100. This problem was characteristic for the analysis of a large number of beads. This may arise from saturation of the electron-capture/NCI process in the ion source due to the increased abundance of sample components from the large number of beads. Alternatively, this problem could arise from the desorption of volatiles from the surface of the beads, where non-uniform heating produces warm spots and "burping" occurs from volatiles escaping around the beads.

The problems associated with the analysis of a large number of beads were rectified by reducing the number of beads and size of the sample container used to hold the sample in the GC oven. The RIC in figure 2-11, obtained by using 5 rubbed beads in a small tube, demonstrates that the erratic fluctuations in the RIC

Figure 2-10 Reconstructed ion chromatogram from the NCI analysis, via transfer by a deactivated 1.5 m x 0.18 mm i.d. FSOT column from the apparatus described in figure 2-3. One hundred glass beads rubbed in the palms of the hands for 3 min by the author of this dissertation and placed in the flask. A spike of 600 ng of lactic acid in methanol (2 μL of a 300 ng/μL solution) was added to the beads prior to analysis. Data were acquired in Q3MS mode with a scan time of 0.5 s per scan. The GC run time was 18.5 min.

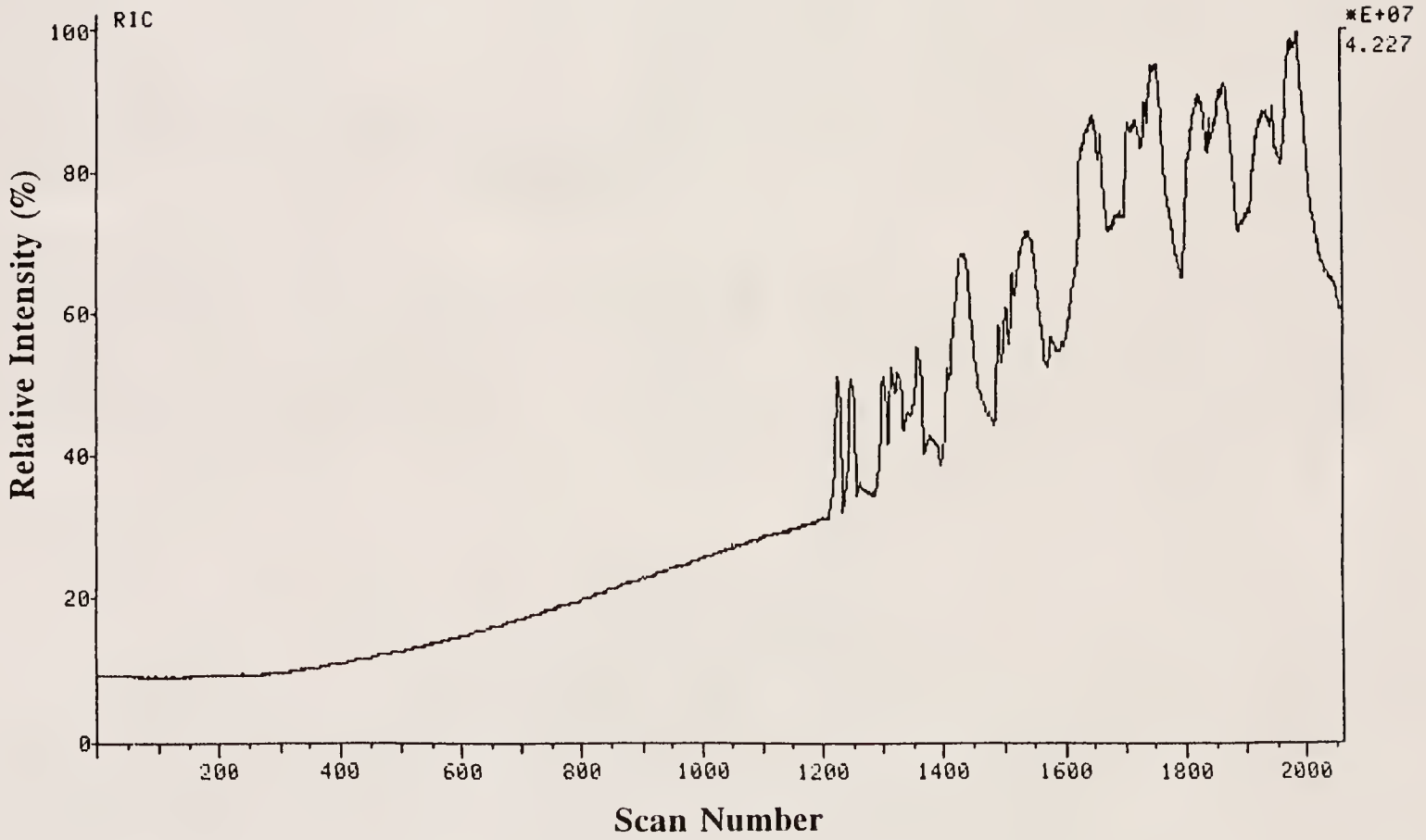
RIC
*E+07
4.227
100
80
60
40
20
0
Relative Intensity (%)
200
400
600
800
1000
1200
1400
1600
1800
2000
Scan Number

Figure 2-11 Reconstructed ion chromatogram from the NCI analysis, via transfer by a deactivated FSOT column from an enclosed 3" by 1/4" o.d tube in the GC oven. Five glass beads rubbed in the palms of the hands for 5 min by the author of this dissertation were sampled. Data were acquired in Q3MS mode with a scan time of 3 s per scan.

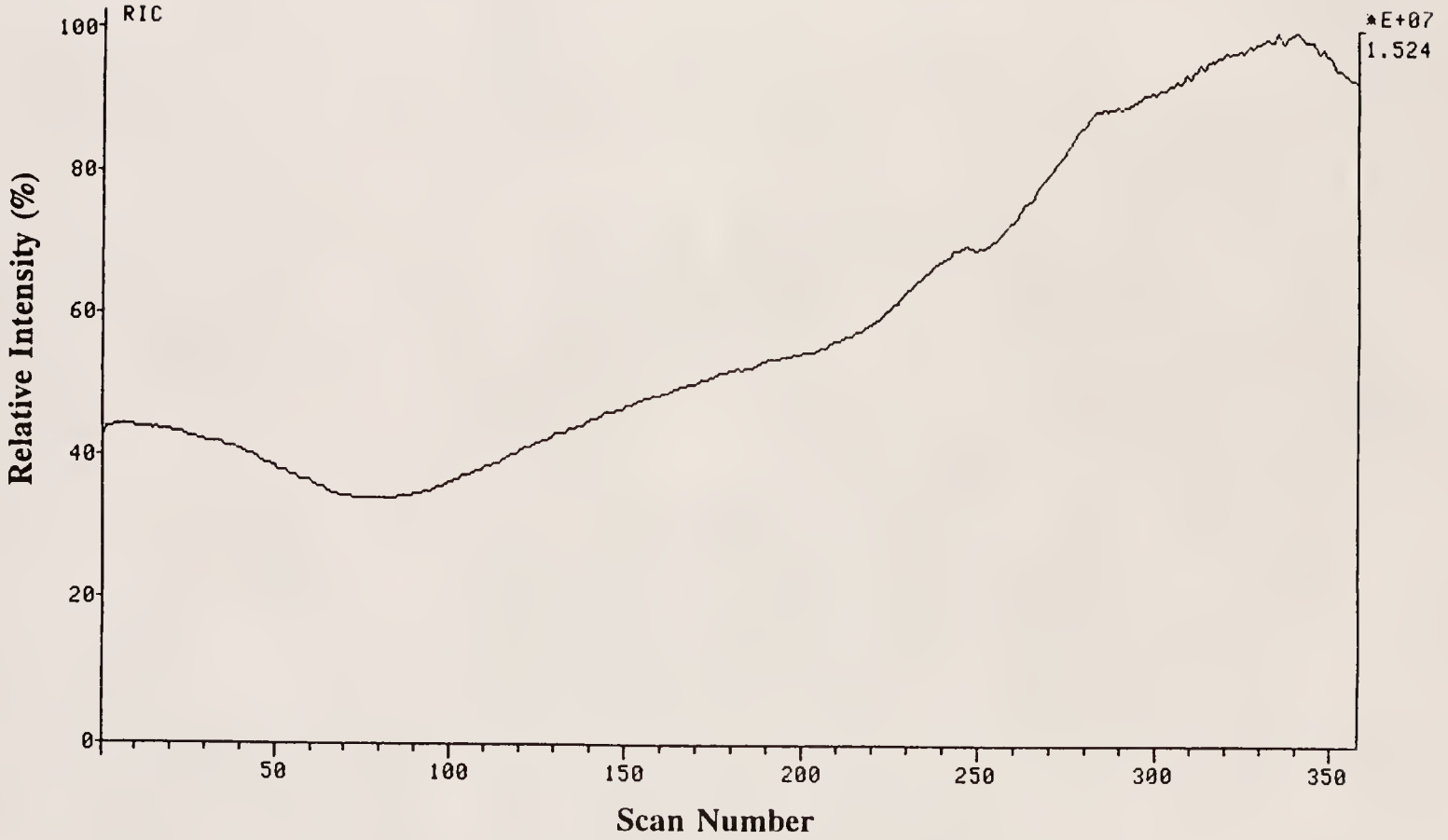
RIC
*E+07
1.524
100
80
60
40
20
0
Relative Intensity (%)
50
100
150
200
250
300
350
Scan Number

are not present. However, this figure also illustrates that the thermal desorption profile is still less distinct than from the solids probe. In contrast to the solids probe, where volatiles are desorbed directly into the ion source, the enclosed sample container permits greater head space above the sample. This space allows for volatiles to be desorbed and remain in the enclosed sample container, mixing with additional desorbed volatiles as the temperature increases. Furthermore, the beads in the vial are probably not at a uniform temperature. As a result, the distinction between desorption profiles for different compounds appears simply as differences in the initial appearance of masses, similar in appearance to frontal chromatography. This point is illustrated in figure 2-12.

Figure 2-12 depicts the mass chromatograms for four ions associated with lactic acid. These representative ions shown are the loss of H_2 from the $[M-H]^-$ ion at m/z 87, which may also correspond to the $[M-H]^-$ ion of pyruvic acid, the $[M-H]^-$ ion of lactic acid at m/z 89, the $[M_2-H]^-$ lactic acid dimer ion at m/z 179, and the $[M_4-3H]^-$ lactic acid tetramer ion at m/z 357. The profiles of these ions are clearly disbursed over most of the run once the temperature is sufficient for the desorption of lactic acid. The wide profile makes identification of molecular and fragment ions with identical m/z values virtually impossible without a reduction in the profile width by either more efficient loading of desorbed species onto the column or by re-focusing the sample bands either prior to or directly on the column.

Figure 2-12 Mass chromatograms of m/z 87, 89, 179, and 357, the characteristic ions formed by lactic acid in NCI analysis. The transfer line was a deactivated 1.5 m x 018 mm i.d. FSOT column leading from an enclosed 3" x 1/4" o.d. tube in the GC oven to the mass spectrometer ion source. Five glass beads rubbed in the palms of the hands for 5 min by the author of this dissertation were sampled. Data were acquired in Q3MS mode with a scan time of 3 s per scan.

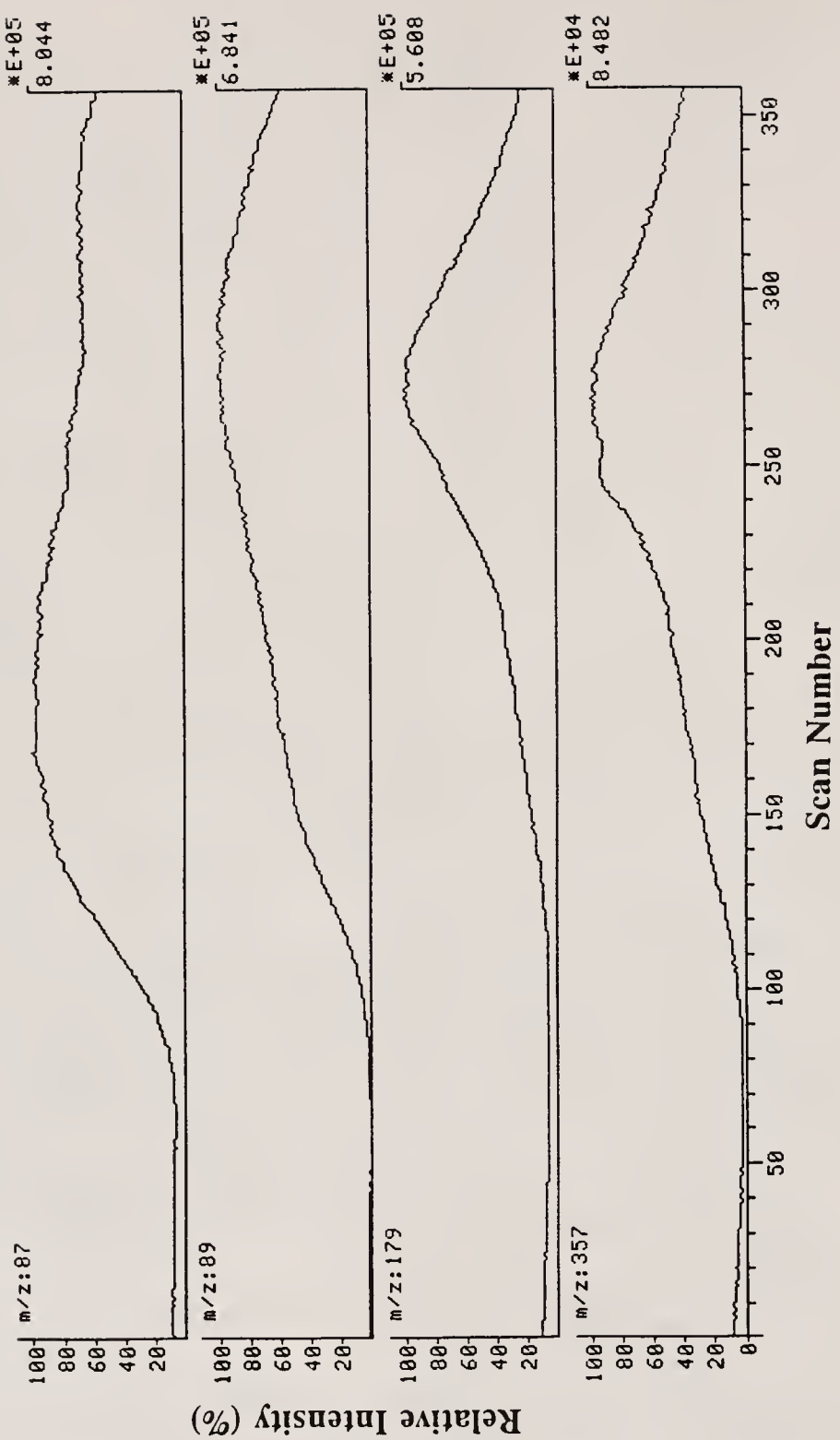
*E+05
8.044
m/z:87
*E+05
6.841
m/z:89
*E+05
5.608
m/z:179
*E+04
8.482
m/z:357
100
80
60
40
20
0
50
100
150
200
250
300
350
Scan Number
Relative Intensity (%)

Thermal Desorption from Multiple Beads/Cryo-focused GC Separation

Cryo-focusing GC/MS has been previously used in the detection of volatile emanations from humans [68]. The collection and desorption of human emanations was achieved by the use of charcoal, and re-focusing accomplished via the use of three successively colder traps. Most of the experiments reported in this dissertation employed a single stage of cold-trapping. The use of on-column cryo-focusing solved the problem of wide desorption profiles due to inefficient compound removal from the headspace above the beads in the previous series of experiments. Due to the similarity in size of the 3" x 1/4" glass tube (use for multiple bead studies above) and the glass injector insert in the GC injection port, experiments were conducted using the insert as the sample holder. By reversing the injection insert, beads could be placed into the insert. Using an insert with a glass frit allowed the beads to be supported above the column entrance and more importantly, allowed free passage of volatiles past the beads. Additionally the design of the injection port allows for a directional sweep of helium over the beads and out of the injector through the column entrance; the enclosed vials for multiple beads have less directional flow. The additional advantage of using the injection port to initially desorb volatiles is that the column could then be held at ambient room temperature with a section of it cryo-focused while the beads were heated external to the GC oven.

The injection insert, when inserted reversed, held up to 12 beads. Figure 2-13 is the RIC for the first such experiment involving the maximum number of beads (12). Two points are evident when examining this figure. First, this was by far the

Figure 2-13 Reconstructed ion chromatogram from the NCI analysis, via cryo-focusing prior to temperature programmed separation on a 18 m x 0.18 mm i.d. DB-5 FSOT column (d_f=0.25 μm). Twelve glass beads were analyzed after being rubbed in the palms of the hands for 5 min by the author of this dissertation. Data were acquired in Q3MS mode with a scan time of 2 s per scan. The electron multiplier was set at -1000 V.

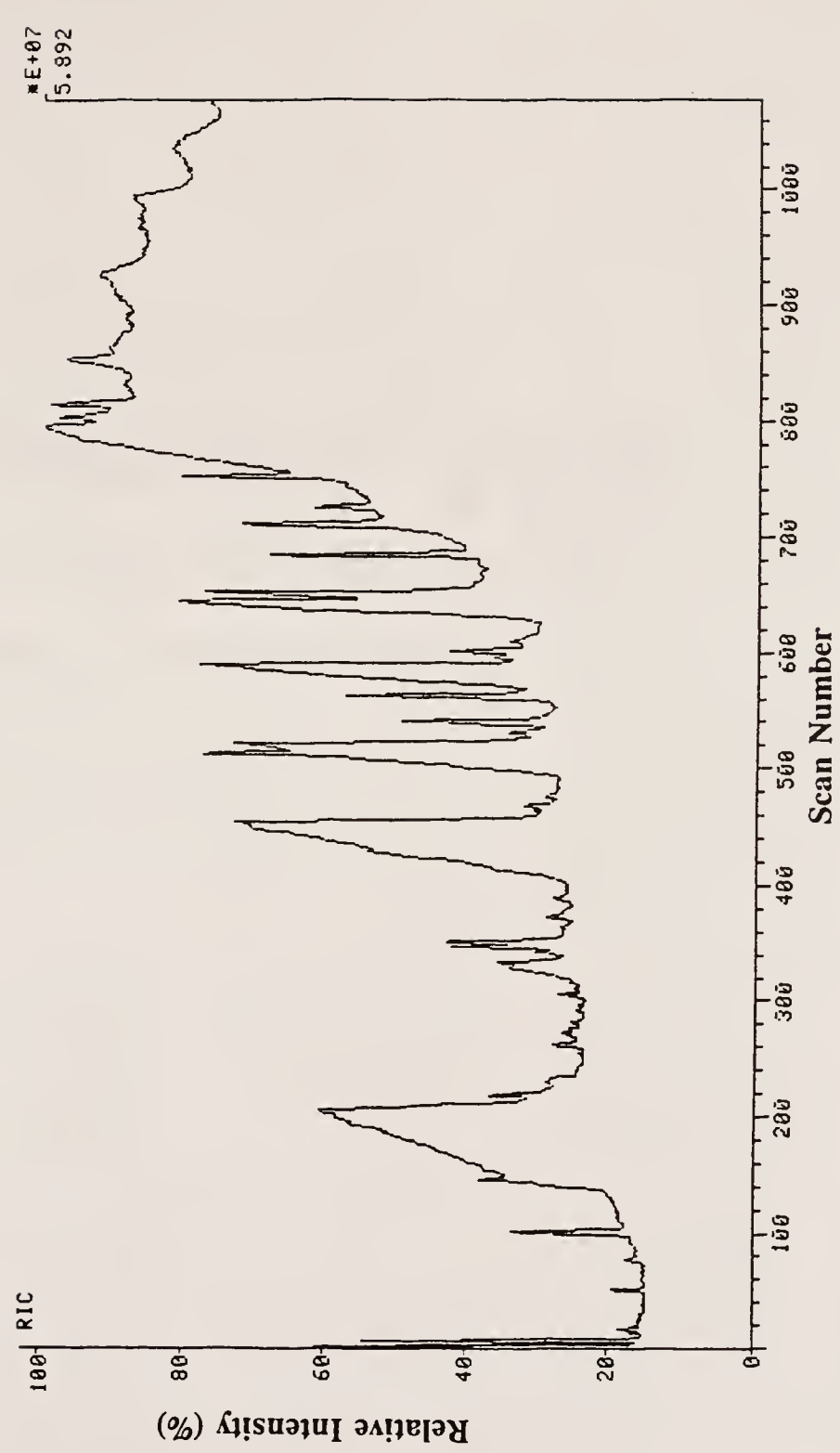
RIC
*E+07
5.892
100
80
60
40
20
0
100
200
300
400
500
600
700
800
900
1000
Relative Intensity (%)
Scan Number

best separation achieved at the time for the analysis of beads, greatly improved over direct thermal desorption. The second point is that the peak shapes demonstrate that the column is overloaded and that a reduction in the number of beads analyzed is necessary for better chromatographic peak shapes. The components found in lesser abundance in the sample show less fronting, i.e. evidence of more abundant components overloading the column sample capacity.

Figure 2-14 demonstrates this point by the examination of characteristic cholesterol ions. These ions are the $[M-H]^-$ ion at m/z 385, the $M^{-\bullet}$ ion at m/z 386 and the carbon-13 isotope of the $M^{-\bullet}$ ion at m/z 387. The peak shape near scan number 800 is a significant improvement over previous experiments where cholesterol was detected (including the thermal desorption profiles shown in figure 2-5).

Reducing the number of beads to from 12 to 5 and employing a slightly longer polar (Carbowax) column further improved peak shape, as can be seen in figure 2-15. A Carbowax column was effectively used previously for thermal desorption and sniffing mass spectrometric fruit odor analysis [69]. This figure demonstrates an analysis employing PPINICI, to allow for detection of both positive and negative ions via alternating scans between positive and negative ions [70]. The complementary EI analysis of 8 rubbed beads is found in figure 2-16. The data in this figure was acquired with a slightly slower temperature ramp of the GC oven. Comparison between the positive and negative ion CI RICs in figure 2-15 and the RIC for the EI analysis in figure 2-16 shows that peaks can be clearly correlated between the two

Figure 2-14 Mass chromatograms of m/z 385, m/z 386, and m/z 387 from the NCI analysis, via cryo-focusing prior to temperature programmed separation on a 18 m x 0.18 mm i.d. DB-5 FSOT column (d_f=0.25 μm), of thermally desorbed skin emanations from 12 glass beads rubbed in the palms of the hands for 5 min by the author of this dissertation. Data were acquired in Q3MS mode with a scan time of 2 s per scan. The electron multiplier set at -1000 V.

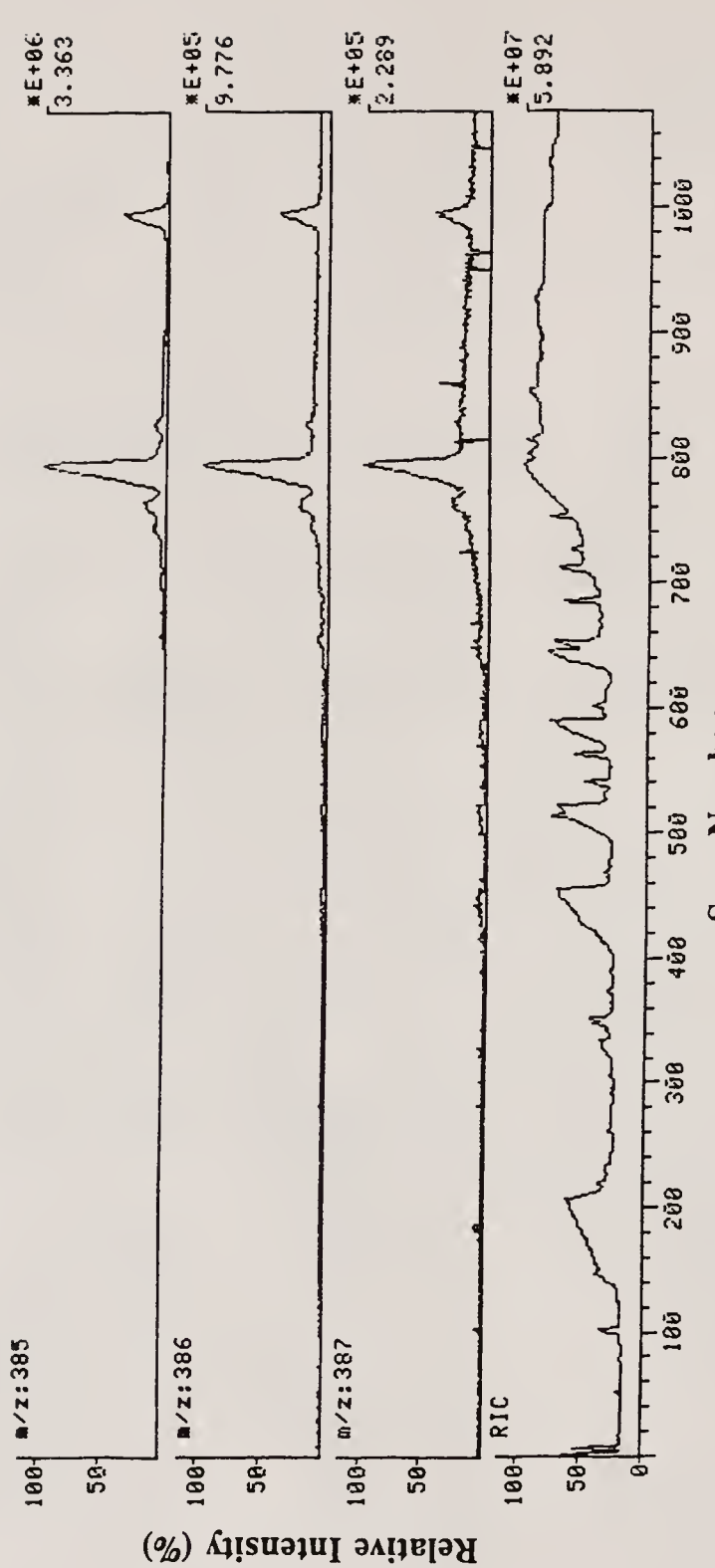
Relative Intensity (%)
m/z:385
m/z:386
m/z:387
RIC
*E+06
3.363
*E+05
9.776
*E+05
2.269
*E+07
5.892
100
50
0
100
200
300
400
500
600
700
800
900
1000
Scan Number

Figure 2-15 Reconstructed ion chromatograms from PPINICI analysis, via cryo-focusing prior to temperature programmed separation on a 20 m x 0.25 mm i.d. Carbowax FSOT column (d_f=0.25 μm), of thermally desorbed skin emanations from 5 glass beads rubbed in the palms of the hands for 5 min by the author of this dissertation. The Q3 scan time was 2 s per scan. The electron multiplier set at -1100 V. The trace for negative ions (NCI) is shown in the top portion; the trace for positive ions (PCI) is show in the bottom portion.

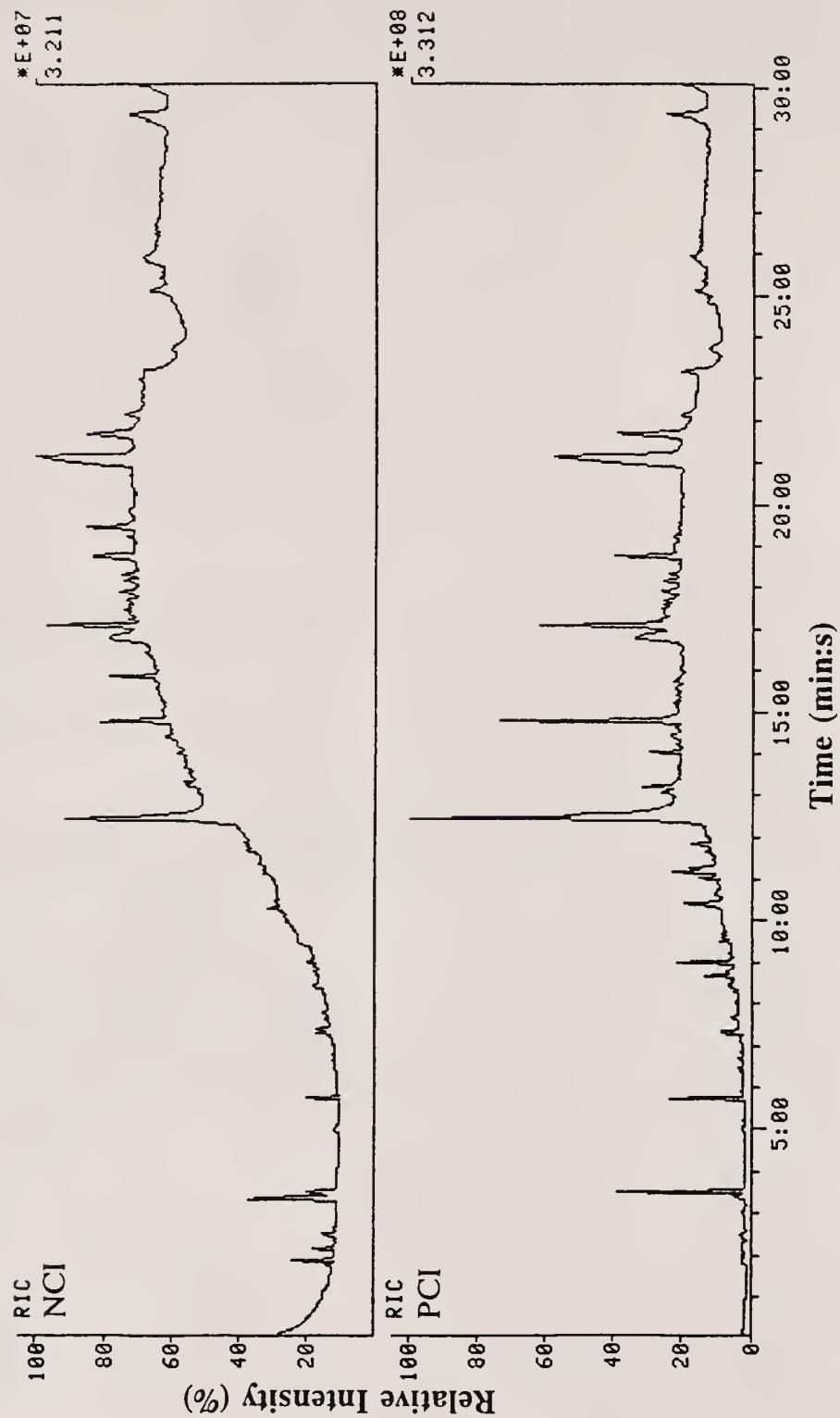
RIC
NCI
*E+07
3.211
RIC
PCI
*E+08
3.312
Relative Intensity (%)
100
80
60
40
20
0
5:00
10:00
15:00
20:00
25:00
30:00
Time (mins)

Figure 2-16 Mass chromatogram of m/z 386 (top) and the reconstructed ion chromatogram (bottom) from EI analysis, via cryo-focusing prior to temperature programmed separation on a 20 m x 0.25 mm i.d. Carbowax FSOT column (d_f=0.25 μm), of thermally desorbed skin emanations from 8 glass beads rubbed in the palms of the hands for 5 min by the author of this dissertation. Data were acquired in Q3MS mode with a scan time of 2 s per scan. The electron multiplier was set at -1200 V.

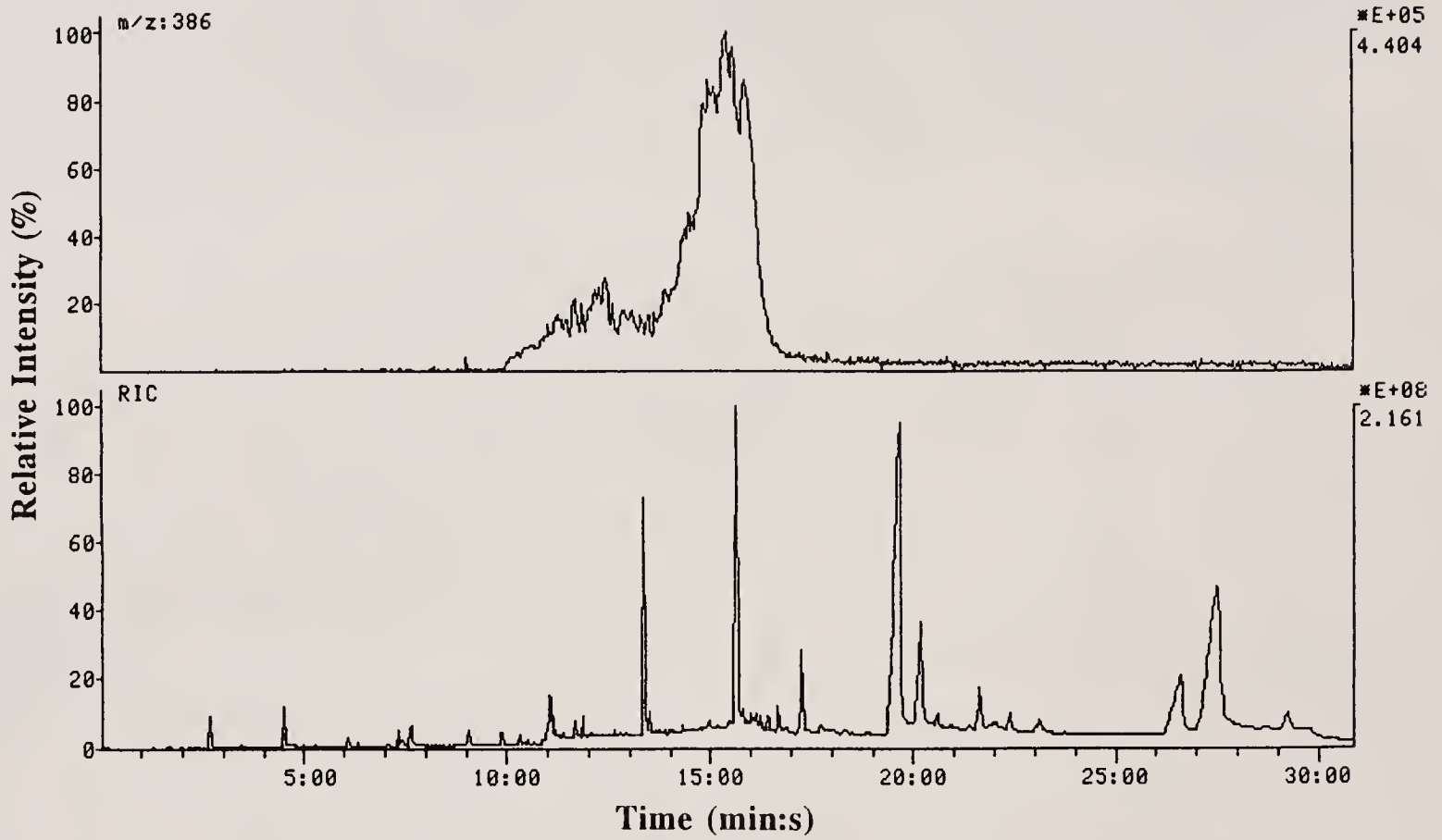
m/z:386
*E+05
4.404
RIC
*E+08
2.161
Relative Intensity (%)
100
80
60
40
20
0
5:00
10:00
15:00
20:00
25:00
30:00
Time (min:s)

experiments. Additionally, the top trace on figure 2-16 is that of the molecular ion of cholesterol at m/z 386. The major peaks found in the RIC of these figures are aliphatic fatty acids; the examination of the cholesterol molecular ion demonstrates the ability to detect trace components. The quality of figures 2-15 and 2-16 are similar (although slightly lower) to that of the subsequent cryo-focused analyses found for studies in Chapter 5.

Purge and Trap/GC Separation

Thermal desorption/purge and trap has been used previously for studies such as identification of fruit fragrances and analysis of volatiles from smoke [69,71]. However, purge and trap was initially avoided in this study due to the possibility of sample discrimination by the trap, i.e. being unable to desorb some volatiles back off of the trap for analysis. However, upon analysis via a three-stage microscale purge and trap GC/MS system, it was found that a great number of trace components could be concentrated and identified, as readily seen in the RIC traces for figures 2-17 and 2-18. Data for figure 2-17 were acquired from rubbed beads and data for figure 2-18 (using a heating rate approximately half of that for figure 2-17) were acquired from direct introduction of volatiles from the skin by sampling a Tedlar bag with the hand contained therein.

The microscale purge and trap system does not allow for detection of the acids and other polar compounds; they are lost somewhere in the system, possibly in the nickel-plated lines or perhaps in the first drying trap. The removal of the

Figure 2-17 Reconstructed ion chromatogram from EI analysis, via purge and trap prior to temperature programmed separation on a 30 m x 0.25 mm i.d. DB-1 FSOT column (d_f=1 μm), of thermally desorbed skin emanations from 200-250 glass beads rubbed in the palms of the hands for 10 min by the author of this dissertation.

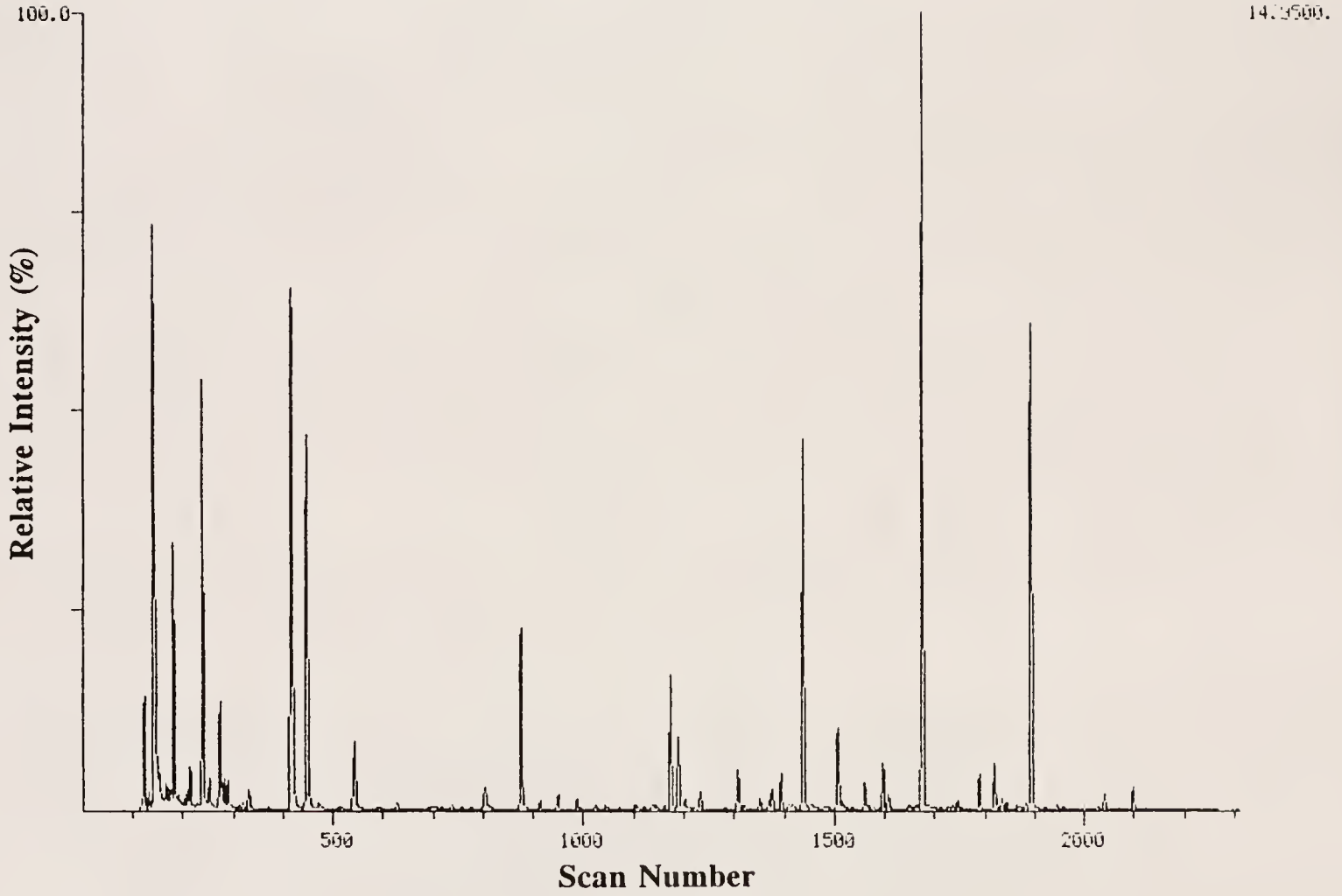
100.0
Relative Intensity (%)
500
1000
1500
2000
Scan Number

Figure 2-18 Reconstructed ion chromatogram from EI analysis, via purge and trap prior to temperature programmed separation on a 30 m x 0.25 mm i.d. DB-1 FSOT column (d_f=1 μm), of thermally desorbed skin emanations collected via placing the hand of the author of this dissertation in a Tedlar bag during the concentration/collection stage.

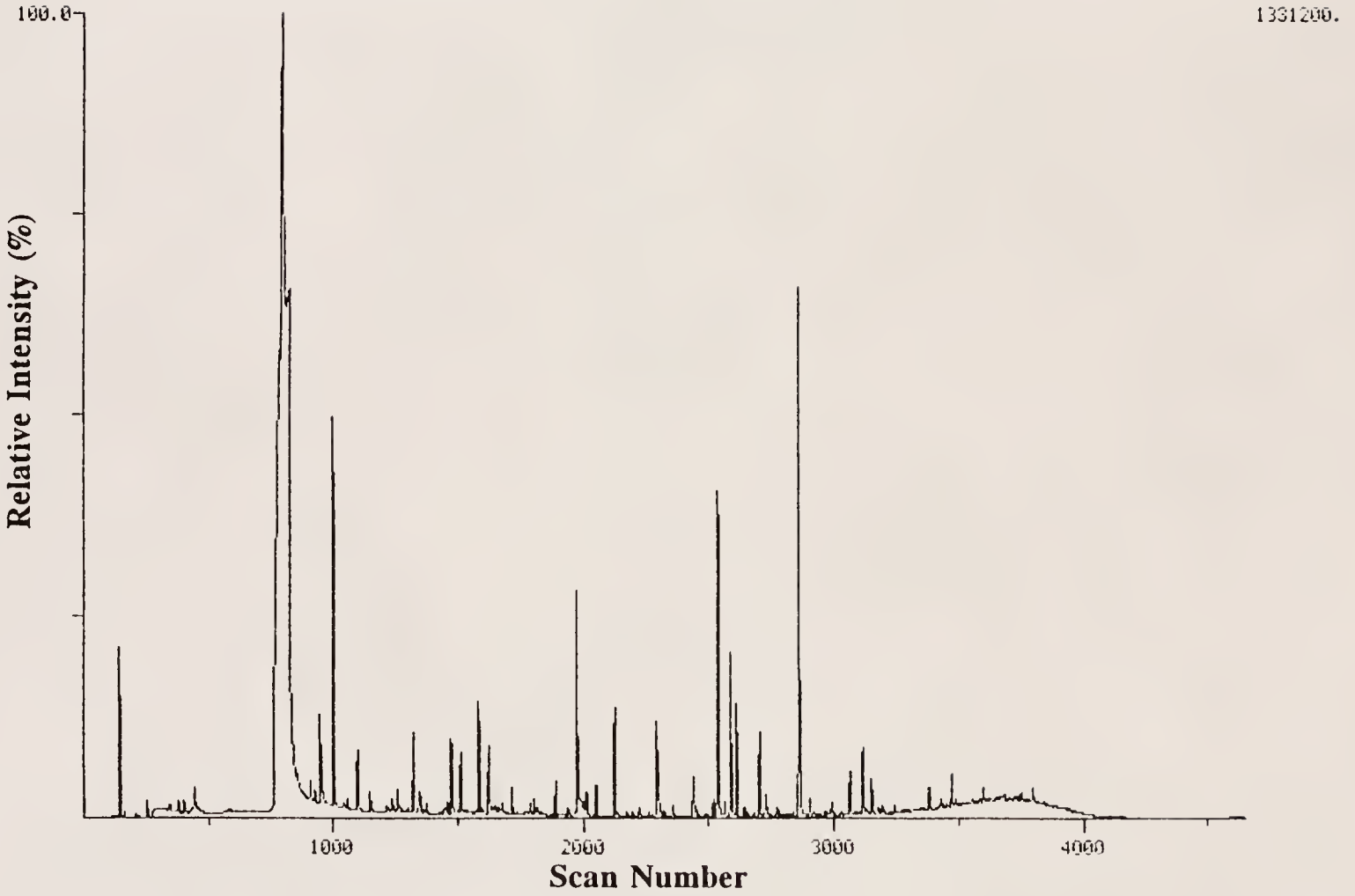
100.0
1331200.
Relative Intensity (%)
1000
2000
3000
4000
Scan Number

acids was a benefit rather than a hinderance in this case. Based on the thermal desorption/cryo-focusing GC results, the aliphatic fatty acids are the most abundant components in emanations; their removal permits the analysis of trace level components constituting other compound classes.

Conclusions

All sampling methods in this section satisfy the initial criterion of sampling volatile emanations in a manner similar to that which mosquitoes encounter. Specifically, this refers to sampling a chemically unmodified sample volatilized into the gas-phase. Direct analysis of a single bead with thermal desorption via the use of a direct insertion probe was found to be inadequate in terms of temporal resolution and the ability to detect trace level components. The use of multiple beads in an enclosed glass sample container increased the sample size for the purpose of detecting trace level components; however, the temporal resolution was even worse than the single bead method due to the headspace volume of the sample container which had to be heated and swept by helium to transfer volatilized compounds onto the column. The problem with poor temporal resolution was resolved via the use of on-column cryo-focusing. This method is used for much of the identification of compounds in Chapter 5. Purge and trap introduction was employed as an alternative method to detect volatile components; furthermore, it discriminates against fatty acids, which are predominant in cryo-focused analyses. This allows for detection of some trace components (low to nonpolar) not readily

detected in the cryo-focused analyses. Additionally, purge and trap analyses involving the sampling of the hand enclosed in a Tedlar bag provided the most accurate sampling introduction method with respect to analyzing airborne volatiles emanated from the skin.

CHAPTER 3
STUDIES INVOLVING ATTRACTION

Introduction

Lactic Acid as a Model Compound

At the inception of the work for this dissertation, lactic acid was the only widely recognized mosquito attractant [5]. This compound only attracts the *Ae. aegypti* species of mosquito. Due to this aforementioned attribute and due to the abundance of lactic acid on the skin, it is the most studied compound in this dissertation. The studies reported in this chapter are arranged in three sections, as described below.

Reaction Studies

The identification of lactic acid can be achieved through knowledge of its characteristic fragmentations and associative reactions in the mass spectrometer; therefore, these reactions will be examined. The extent of these reactions and the abundance of ions is dependent upon operating parameters and sample conditions [72,73]. Additionally, mass spectrometer ion sources have slightly different designs; therefore, some differences in relative abundances are inherent to the mass spectrometer. These studies are beneficial to studies involving identification of lactic

acid in complex samples due to the lack of a molecular ion ($M^{+\bullet}$) formed by EI of lactic acid and due to the presence of additional ions, characteristic of instrument parameters, which contribute to the difficulty in identifying this compound by library searching of EI spectra.

Altering Attraction

Previous work with altering attraction via acidification consisted of the addition of sulfuric acid to solutions of carboxylic acid salts in acetone. The purpose of the sulfuric acid addition was to increase the concentration of the free acid versus the sodium salt rather than to examine possible enhancement of attraction [19]. Mosquitoes responded to these acidified solutions by exhibiting a greater activation to flight; however, there was little increase in directional attraction.

The increase in attraction effected by the acidification of lactic acid solutions had not been examined. Logically, addition of acid should increase the proportion of free acid (volatile) relative to the dissociated form (involatile). This should increase attraction; addition of base should produce the opposite effect. The utility of mass spectrometry in this case was in its application to the examination of possible solution-phase reactions involving lactic acid and the methanol solvent. Specifically, this is an examination for products of acid-catalyzed or base-catalyzed esterification.

Analysis of Methanolic Perspiration Solution

The final study in this chapter involves the direct dissolution of components in perspiration into methanol. This work is aimed at determining the residence of lactic acid in the matrix on the skin. By examination of each phase for lactic acid, insight was gained into the abundance and distribution of lactic acid in perspiration.

Experimental

Reactions of Lactic Acid

Most of the lactic acid mass spectra found in this section were acquired from direct thermal desorption of handled glass beads. The sample was desorbed from 5 beads which had been rubbed in the palms of the hands for 5 min by the author of this dissertation. The beads were placed in a 1/4" o.d. glass tube (maximum 25 beads) which was inserted into the apparatus described in chapter two (figure 2-3). Helium, at 8 psig was passed over the beads and used as the carrier gas through a 1.0 m x 0.10 mm i.d. deactivated FSOT column. The GC oven temperature was ramped via initially holding the column at 28°C for 1.0 min followed by a 12 min ramp at 15°C/min to 207°C, with a 5 min hold at that temperature. The transfer line was concurrently ramped from 50°C to 210°C at 20°C/min once the run was started, and held at 210°C for the final 10 min of the analysis. Ionization was effected by isobutane CI at an indicated source pressure of 1647 mtorr. The ion source temperature was set at 150°C and the manifold temperature at 70°C. The electron

energy was set at 100 eV for CI conditions and the filament emission current set at 200 μA. The collision gas was nitrogen with an indicated pressure of 1.97 mtorr in the collision cell; the collision energy was typically 9 eV. The electron multiplier setting was -1200 V with the dynode set at +5 kV. Data were collected employing various MS/MS scan modes, indicated in the figure captions, with a scan time of 3 s per scan.

Some experiments in this section employed cryo-focused GC/MS analysis of 5 beads; the beads were rubbed for 5 min in the palms of the hands by the author of this dissertation. The beads were placed in a reversed GC injection insert, as described in Chapter 2. The injection port was ramped from 25°C to 250°C over 7.5 min and held at that temperature for an additional 2.5 min. Compounds desorbed from the beads were cryo-focused in the first 40 cm of column in the GC oven throughout the injection port heating period. Prior to beginning the oven ramp for analysis, the cup of liquid nitrogen was removed. The ramp consisted of a 1.0 min hold at 25°C, a 12 min ramp at 15°C/min up to 210°C, and a final hold at 210°C for 5.0 min. The transfer line was concurrently ramped, after a 1.0 min hold at 40°C, up to 225°C at 15°C/min, and held at 225°C for 5.0 min. The separation was effected on a 20 m x 0.25 mm i.d. Carbowax column (d_f=0.25 μm). Positive and negative ion data were acquired with methane at 1660 mtorr (indicated) using PPINICI. The ion source and manifold temperatures were 150°C and 70°C, respectively. The electron energy was 100 eV with the filament set at 200 μA. The Q3 scan time was 2 s per

scan. The conversion dynode alternated between positive and negative 5 kV for the detection of both positive and negative ions with the electron multiplier at -1100 V.

Solution-based analyses of methanolic lactic acid were also performed. A 100 mL methanol stock solution containing 1.206g of (85% w/w L-lactic acid in water) was prepared. This 12 μg/μL L-lactic acid solution was then diluted by a factor of 100 to give a 120 ng/μL L-lactic acid solution in methanol, allowing for GC/MS analysis without overloading the sample capacity of the GC column. An 0.5 μL injection of this solution was made onto a 10.5 m x 0.178 mm i.d. DB-5 column (d_f=0.4 μm). The GC injection port and transfer line were operated isothermally at 250°C and 190°C, respectively. The column was initially held at 30°C for 0.25 min, then ramped at 30°C/min for 4.0 min to 180°C and held at that temperature for 0.25 min. Samples were ionized by CI using methane reagent gas at an indicated pressure of 1600 mtorr. Daughter ion spectra were acquired using nitrogen as the collision gas (2.00 mtorr) with collision energies of 2 eV or 0 eV. The ion source and manifold temperatures were 150°C and 70°C, respectively. The filament emission current was set at 200 μA with and electron energy of 100 eV. The electron multiplier was at -1300 V with the dynode at +5 kV. Data were collected in the daughter ion mode by scanning Q3 at 0.5 s per scan.

Some experiments were performed using the apparatus described in figure 2-3. One hundred glass beads were handled for 3 min and then transferred to a 100 mL round bottom flask with a specially fitted stem (described in Chapter 2). The beads were spiked with 2 μL of a 300 ng/μL L-lactic acid solution prior to heating.

The heating ramp consisted of a 0.5 min hold at 30°C followed by a 10°C/min ramp up to 190°C and a final hold of 2.0 min. The transfer line was initially set to 50°C and ramped immediately at 20°C/min to 200°C and held at the temperature for the remainder of the experiment. A deactivated 1.5 m x 0.10 mm i.d. FSOT column was used to transfer the sample to the ion source of the mass spectrometer. These experiments employed methane (1650 mtorr indicated) as the moderating gas for negative ion CI. The ion source and manifold temperatures were 150°C and 70°C, respectively. The filament emission current was set at 200 μA with 100 eV as the electron energy. The scan time was 0.5 s. The electron multiplier voltage was -900 V with the conversion dynode at +5 kV.

Altering Attraction

Data were acquired by examining mosquitoes collected over a three minute interval of exposure to sampled compounds. These experiments were conducted at the USDA laboratories. Prior to sampling, seventy-five mosquitoes are acclimated in the holding tank for approximately one hour. Once a sample was tested, a new batch of mosquitoes were allowed to acclimate in the tank. The samples examined were methanolic lactic acid solutions. A stock solution of 12 μg/μL L-lactic acid in methanol was prepared. The stock solution was split into 20 mL aliquots and spiked with either acid or base, leaving one solution unspiked as the control. The pH was measured relative to a glass electrode to give an approximate value of the acid or base content of the solution. The pH measurements, from methanolic solutions, do

not represent a true reflection of the [H^+] ion or [OH^-] ion concentration. The indicated pH, amount of acid or base added, and concentration of acid or base to a 20 mL aliquot of 12 μg/μL methanolic L-lactic acid were: pH 0.45 from addition of 50 μL 12M HCl, pH 3.05 from the unadjusted control, pH 7.10 from addition of 200 μL of 10N NaOH, pH 11.80 from addition of 250 μL 10N NaOH, and pH 13.10 from addition of 1 mL 10N NaOH. It was observed that a white precipitate was present in the most basic solution. A 100 μL aliquot from each of the 20 mL stock solutions were placed on petri dishes and dried. The sample-containing petri dishes were then tested for attraction versus a control petri dish in the olfactometer.

Esters were tested in the olfactometer in the same fashion as the L-lactic acid solutions; however, the sample preparation differed. Sampling consisted of 100 μL each of lactic acid, methyl lactate, ethyl lactate, and ethyl isovalerate dried on separate petri dishes. A second series of experiments was conducted in which a 100 μL spike of 10% HCl was mixed with 100 μL of each sample and allowed to dry on the petri dish prior to analysis.

Methanolic L-lactic acid solutions and methyl lactate solutions were analyzed mass spectrometrically. Solutions consisting of 205 ng/μL L-lactic acid plus 400 ng/μL NaOH, methanolic 120 ng/μL L-lactic acid solutions (spiked with 12M HCl and 10N NaOH to give indicated pH values of 3.05 and 11.80, respectively), and a 214 ng/μL standard methyl lactate solution in methanol were analyzed. Injections of 0.5 μL of each of these solutions were employed; however, the GC conditions differed. Solutions containing 205 ng/μL L-lactic acid (with 400 ng/μL NaOH) and

solutions containing 214 ng/μL methyl lactate were analyzed on a 25 m x 0.2 mm i.d. HP-5 FSOT column (d_f=0.33 μm). The transfer line and injection port temperature were both set to be isothermal at 200°C and 220°C, respectively. The GC oven was initially held at 40°C for 1.0 min after injection, then ramped at 20°C/min for 8 min up to 200°C and held at that temperature for 1.0 min. The GC was run in splitless mode, with the split valve opening after 0.5 min. The column carrier gas was helium at a head pressure of 20 psig. Methanolic 120 ng/μL L-lactic acid solutions spiked with acid or base were analyzed on a 10.5 m x 0.178 mm i.d. DB-5 FSOT column (d_f=0.4 μm). The transfer line and injection port temperature were both set to be isothermal at 250°C and 200°C, respectively. The GC oven was initially held at 30°C for 0.25 min after injection, then ramped at 30°C/min for 4.0 min up to 150°C and held for 0.25 min. The GC was run in splitless mode, with the split valve opening after 0.2 min. The column carrier gas was helium at a head pressure of 5 psig.

The ion source temperature was set at 170°C for EI analyses and 150°C for CI analyses; the manifold temperature was set at 70°C. Data acquired using PPINICI employed methane at 1650 mtorr. Data were acquired in single mode operation (NCI or PCI) with methane reagent gas at an indicated pressure of 1610 mtorr. The filament emission current was set to 200 μA with an electron energy of either 100 eV for CI or 70 eV for EI operation. Scanning at 0.5 s scan over Q3 was used to obtain all data. The conversion dynode was set at +5 kV or -5 kV depending upon the desired collection of negative or positive ions. The electron multiplier was set at -800 V to -1000 V for experiments in this section.

Analysis of Methanolic Perspiration Solution

The perspiration samples were analyzed by dissolving approximately 150 μL of forehead perspiration (from the author of this dissertation) in 3 mL of methanol. The mixture separated into two phases after allowing it to sit overnight. One μL of each phase was injected onto a 10.5 m x 0.178 mm i.d. DB-5 FSOT column (d_f=0.4 μm). The injection port temperature and transfer line temperature were set isothermal at 250°C and 200°C, respectively. The GC oven was held at 30°C for 0.25 min after injection, then ramped at 30°C/min for 4.0 min up to 150°C and held for 0.25 min. The GC was run in splitless mode, with the split valve opening after 0.2 min. The column carrier gas was helium at a head pressure of 8 psig. The ion source temperature was set at 150°C and the manifold temperature was set at 70°C. NCI was accomplished with methane at an indicated source pressure of 1695 mtorr. The filament emission current was set to 200 μA with an electron energy of 100 eV. Scanning with a 0.5 s scan time over Q1 was used to obtain all data. The conversion dynode was set at +5 kV for the collection of negative ions. The electron multiplier was set to -1000 V.

Results and Discussion

Reactions of Lactic Acid

Negative chemical ionization with methane as the reagent gas leads to the formation of negative ions by two main processes [33,72,74]. The formation of a

$M^{-\bullet}$ ion by electron capture utilizes methane as a moderating gas for the production of thermal electrons. Thermal electrons can then be captured by species with a sufficient electron affinity. Carboxylic acids such as lactic acid have not been found to successfully undergo electron capture without derivatization [74]. Lactic acid analyzed under the conditions employed for this work typically exhibits an odd-electron $M^{-\bullet}$ (formed via electron capture) abundance which is <0.5% of the even-electron deprotonated molecular species $[M-H]^-$ intensity. The process which forms the deprotonated molecular species involves abstraction of a proton from lactic acid by ionic species formed via ion-neutral reactions with methane reagent gas in the ion source. Examination of negative ions for structurally informative fragments is not as prevalent as the use of EI or positive CI for structure elucidation. Examination of negative ions with lactic acid was found to be not only informative but facile due to the presence of the carboxyl function group.

Characteristic fragmentations

The deprotonated molecular species, $[M-H]^-$, of lactic acid is formed via the loss of the hydrogen on the carboxyl group, leaving the species with a net negative charge. This species is generally the base peak in NCI mass spectra of lactic acid, provided the sample concentration in the ion source is adequately low to prevent additional reactions with neutral lactic acid (this is addressed later in this chapter).

Selection of the $[M-H]^-$ followed by fragmentation via CID produces the daughter spectrum in figure 3-1. It should be noted that this daughter spectrum was acquired using a collision energy of 9 eV and an indicated pressure of 1.97 mtorr N_2.

Figure 3-1 Negative ion daughter mass spectrum of m/z 89, the $[M-H]^-$ ion of lactic acid. Five beads were sampled after being handled in the palms of the hands for 5 min. The beads were placed in a 1/4" o.d. glass tube (maximum 25 beads) which was inserted in the apparatus described in figure 2-3. Isobutane was employed (indicated pressure of 1647 mtorr) as the reagent gas. The CID gas was N_2 at 1.97 mtorr (indicated) in the collision cell. The collision energy was 9 eV. The scan time was 3 s per scan. The m/z scale is split into two sections. The vertical scale for certain regions of this figure are expanded to better observe the fragment ions.

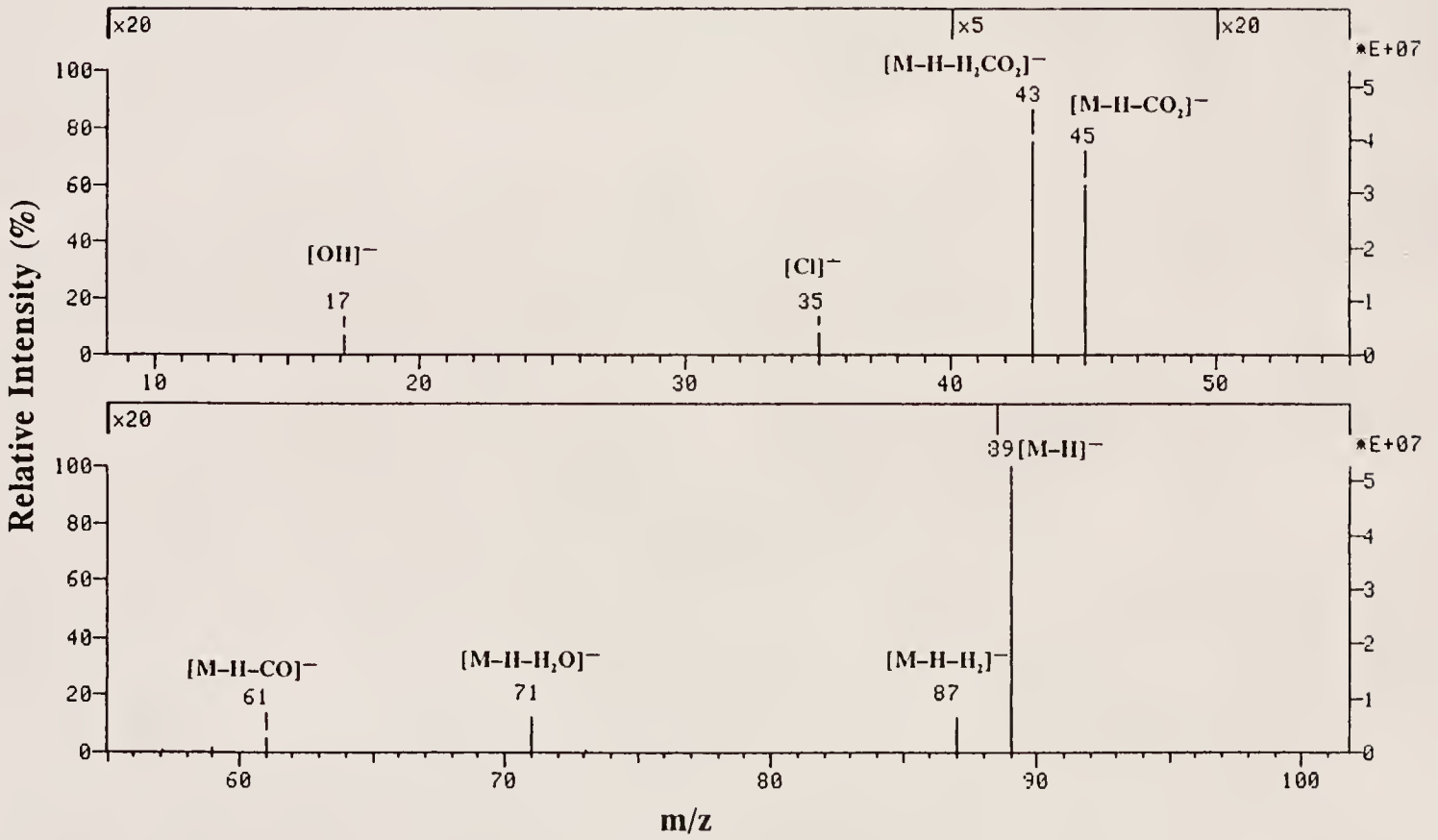
x20
x5
x20
*E+07
[M-H-H2CO2]−
43
[M-H-CO2]−
45
[OH]−
17
[Cl]−
35
Relative Intensity (%)
100
80
60
40
20
0
10
20
30
40
50
x20
39 [M-H]−
*E+07
[M-H-CO]−
61
[M-H-H2O]−
71
[M-H-H2]−
87
60
70
80
90
100
m/z

Use of a greater collision energy enhanced the abundance of fragments relative to the parent $[M-H]^-$ ion; although the relative intensities among fragment (daughter) ions were not altered. The daughter ions are formed by neutral losses of small molecules. The most abundant daughters are due to the loss of formic acid (46 Da) and carbon dioxide (44 Da) to produce ions at m/z 43 and m/z 45, respectively. The process by which these losses can occur will be described later in the discussion of a later figure. Additional neutral losses found in the daughter spectrum include losses of carbon monoxide (28 Da) and water (18 Da) to form the ions at m/z 61 and m/z 71, respectively; there is a low abundance of m/z 59, corresponding to loss of formaldehyde (30 Da). The ion at m/z 87 is formed by the elimination of H_2 (2 Da) from deprotonated lactic acid.

The daughters of the m/z 87 ion, obtained under identical conditions (to that for daughters of m/z 89), are presented in figure 3-2. It is interesting to note the similarity in fragmentation patterns found in daughter spectra of this ion and the $[M-H]^-$ ion in figure 3-1. The labeling of masses in figure 3-2 remains consistent with the representation of lactic acid as the neutral parent of all these species. Therefore, the parent ion for daughter analysis in this case is the $[M-H-H_2]^-$ ion of lactic acid at m/z 87. The most abundant fragment ion is now the species corresponding to a neutral loss of CO_2 (at m/z 43) from the parent ion. Although still present, the loss of formic acid producing the ion at m/z 41 is significantly decreased, as are the ions at m/z 57 and m/z 59, corresponding to losses of formaldehyde and carbon monoxide

Figure 3-2 Negative ion daughter mass spectrum of m/z 87, the $[M\text{-}H\text{-}H_2]^-$ ion of lactic acid. Five beads were sampled after being handled in the palms of the hands for 5 min. The beads were placed in a 1/4" o.d. glass tube (maximum 25 beads) which was inserted the apparatus described in figure 2-3. Isobutane was employed (indicated pressure of 1647 mtorr)as the reagent gas. The CID gas was N_2 at 1.97 mtorr (indicated) in the collision cell. The collision energy was 9 eV. The scan time was 3 s per scan.

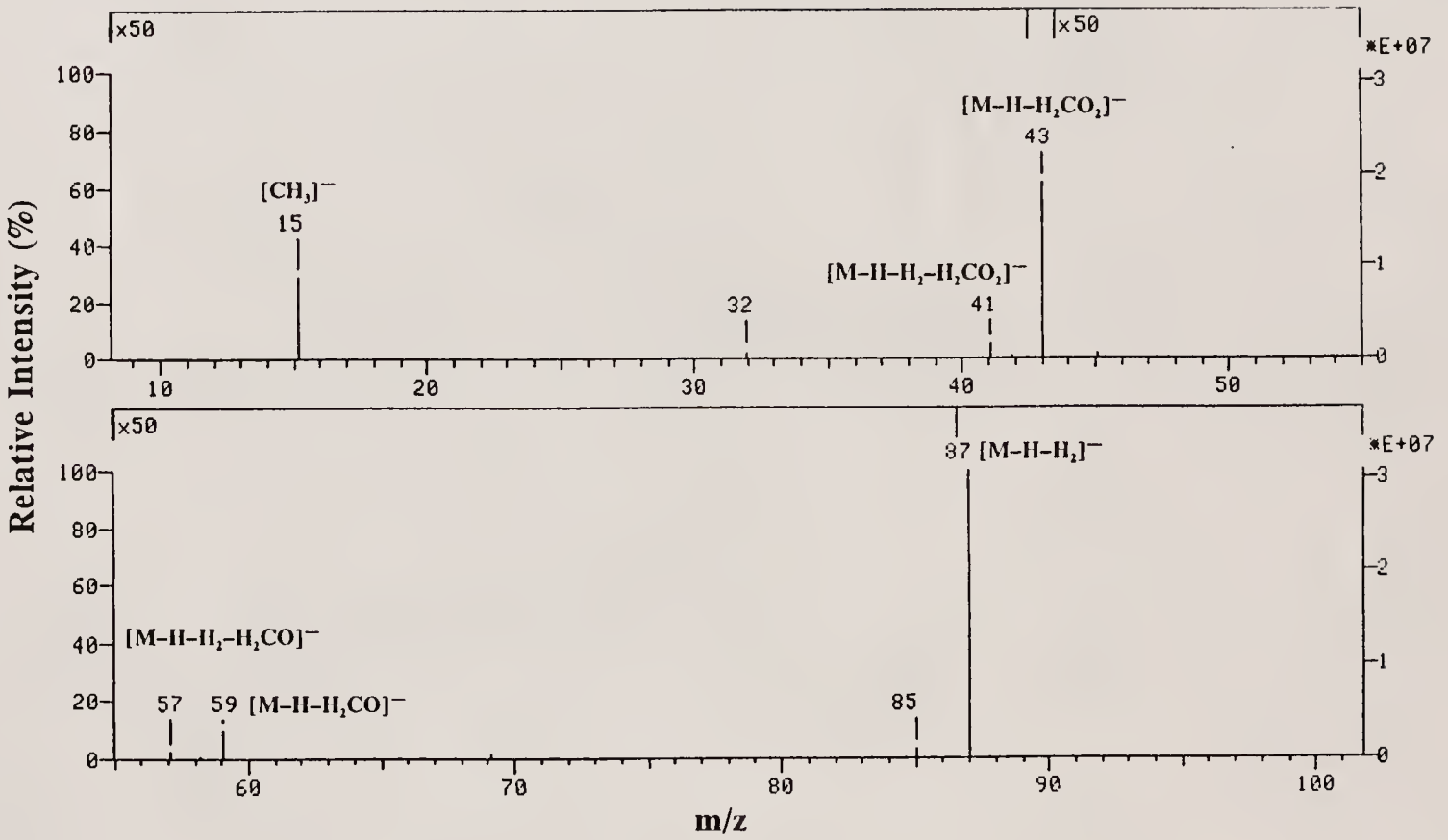

Relative Intensity (%)
x50
x50
*E+07
[CH3]−
15
32
[M-H-H2-H2CO2]−
41
[M-H-H2CO2]−
43
x50
*E+07
[M-H-H2-H2CO]−
57
59 [M-H-H2CO]−
85
87 [M-H-H2]−
m/z

from m/z 87, respectively. Additionally, there is presence of an ion at m/z 85 from the neutral loss of H_2.

A summary of the fragmentation pathways for negative ions of lactic acid examined by NCI MS/MS is presented in figure 3-3. There are two points about this figure which warrant mentioning. The first is that ions shown in the figure represent a selection according to threshold conditions for these experiments. This chosen threshold was that the abundance of these ions be greater than or equal to 1% of the base peak intensity in each daughter spectrum. The second point concerning figure 3-3 is that the structures listed are postulated from losses and reasonable fragmentations and rearrangements [75-78]. Additional measures, such as the use of high resolution mass spectrometry and isotopic labeling, were not employed to confirm these structures.

The trend via losses of H_2 is apparent; this loss most likely occurs by cleavage of the hydrogen from the α-hydroxy group and a γ-hydrogen from the terminal methyl group. This process occurs through a four-centered intermediate ring state [79]. This same cleavage most likely produces the species at m/z 85 from the m/z 87 ion. Due to the absence of sufficient hydrogens, the m/z 85 species does not undergo a further neutral loss of H_2. The availability of hydrogens limit the possible fragments resulting from precursors in other cases. Examination of the loss of water from the m/z 89 and m/z 87 species reinforce this. Both these ions will undergo a neutral loss of water, while m/z 85 will not. The fragments formed (m/z 71 and m/z 69) show this trend.

Figure 3-3 Diagram of significant negative ion fragmentation pathways, postulated neutral losses and fragment ions of the deprotonated molecular species of lactic acid.

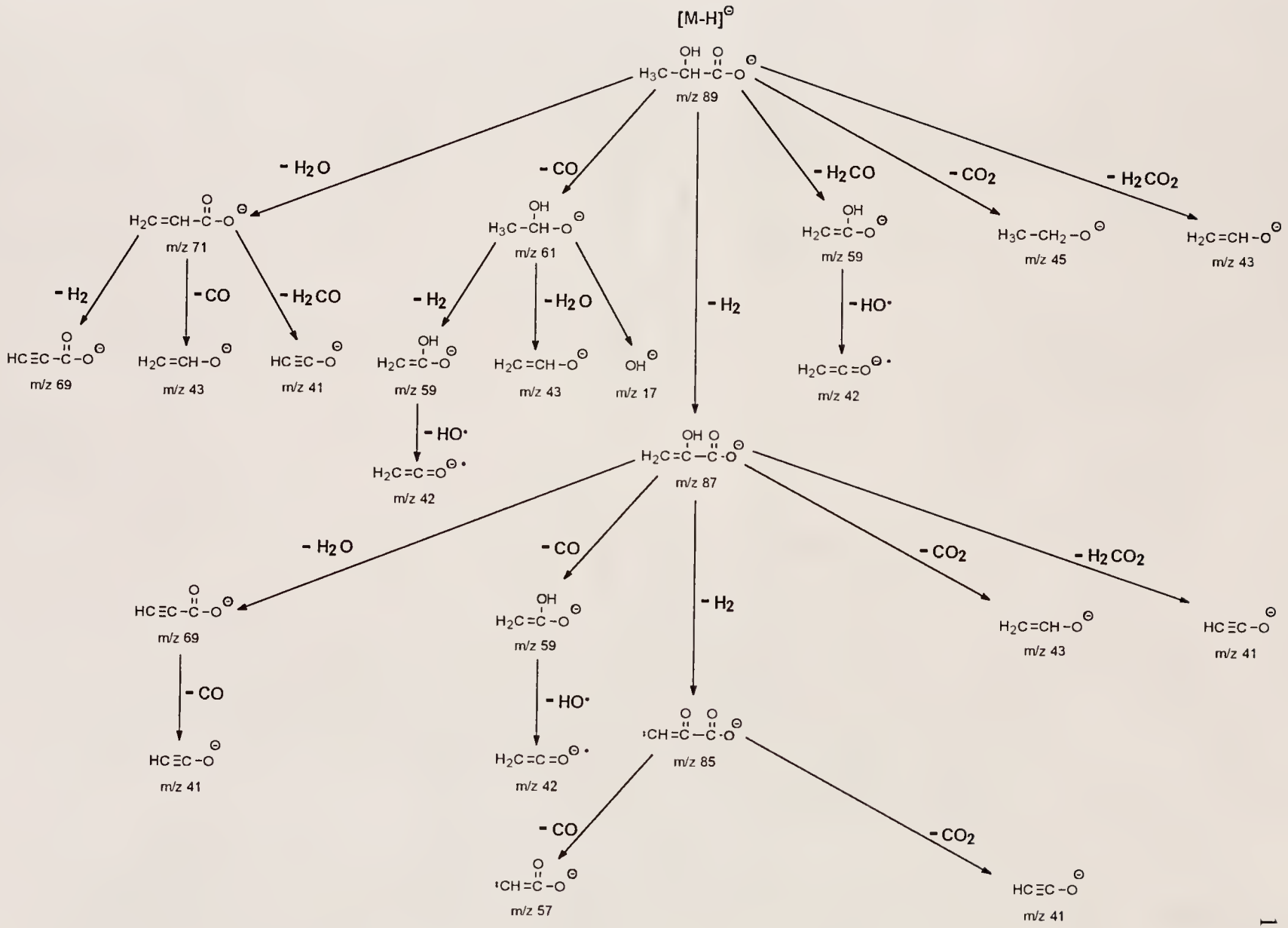
[M-H]⊖
m/z 89
- H2O
- CO
- H2CO
- CO2
- H2CO2
- H2
m/z 71
m/z 61
m/z 59
m/z 45
m/z 43
m/z 69
m/z 43
m/z 41
m/z 59
m/z 43
m/z 17
m/z 42
- HO•
m/z 42
m/z 87
m/z 69
m/z 41
m/z 59
m/z 42
m/z 43
m/z 41
m/z 85
m/z 57
m/z 41

The species at m/z 71 will undergo a subsequent loss of H_2 via elimination resulting in the formation of a triple bond at the methyl terminal to produce the ion at m/z 69; this is identical to the fragment occurring from loss of H_2O from the m/z 87 species. In addition, m/z 71 undergoes additional losses of CO and H_2CO, whereas the m/z 69 ion can only further lose CO. The direct neutral losses of CO from m/z 89 and m/z 87 are similar. However, again, the m/z 61 ion formed from m/z 89 can undergo losses of H_2, and H_2O, whereas the ion at m/z 59 cannot. It is interesting to note that the m/z 59 ion will undergo homolytic cleavage to form an odd-electron ion at m/z 42, via the loss of a $HO^{\bullet}$ radical. This is relatively uncommon and unfavorable for an even-electron precursor [79]. Since the charge is retained on the odd-electron species, this fragment arises from cleavage of a single bond, i.e. between the hydroxyl group and the carboxyl carbon. A fragmentation involving cleavage of two bonds would necessitate charge migration for production of an odd-electron fragment.

The only cases where a direct loss of formaldehyde occurs are from m/z 89 directly, or from m/z 71, which resulted via the loss of H_2O from the m/z 89 species. In contrast to this, the loss of CO_2 occurs from all three major species (m/z 89, m/z 87, and m/z 85). In each case the products formed depict losses of hydrogens characteristic of the precursor species. If an additional two hydrogens are lost via loss of formic acid, then the required number of hydrogens to constitute these losses are only present when losses come from the m/z 89 and m/z 87 species.

Oligomerization and attachment reactions

Lactic acid in the gas phase is also susceptible to oligomer formation as well as other associative ion-molecule reactions. Examining mass chromatograms (figure 3-4) for oligomer and attachment ions produced from lactic acid demonstrates the presence of a dimer ion at m/z 179, a trimer at m/z 268, and a tetramer at m/z 357, all of the form $[M_n\text{-}H]^-$. The time correlation of the peaks indicate that these ions are related. The formation of oligomers is most prevalent at high concentrations of neutral species in the ion source. Therefore, the oligomeric peaks have narrower peak widths than their precursor ion. The presence of oligomers or at least dimerization is predictable from knowledge of the solution-phase chemistry. Lactic acid is an α-hydroxy acid. Due to the inability of this species to form a lactone ring which is stable, it undergoes oligomerization and self-esterification [80]. Further examination of oligomeric ions will be addressed later in this section.

Two additional ions yield peaks which correlate to lactic acid. These peaks at m/z 125 and m/z 127 arise from chloride ion attachment to a neutral lactic acid molecule. Verification of this is presented in the daughter spectrum in figure 3-5. The m/z 125 ion was mass-selected and fragmented by CID to yield fragment ions at m/z 35 and m/z 89. The m/z 35 ion is clearly the $^{35}Cl^-$ ion. By virtue of MS/MS, this ion could only have arisen from the m/z 125 ion rather than being attributable to background. The ion at m/z 89 is the deprotonated molecular species of lactic acid (i.e. the lactate ion). This fragment is formed via the neutral loss of HCl from

Figure 3-4 Negative ion mass chromatograms of species associated with lactic acid. Shown are the $[M-H]^-$ ion of lactic acid, the chloride attachment ions, and ions resulting from gas-phase oligomerization. Five beads were sampled after being handled in the palms of the hands for 5 min. The beads were placed in a reversed injection insert and volatiles were cryo-focused with LN_2 prior to GC separation. Methane was employed as the reagent gas. The CID gas was N_2 at 2.00 mtorr (indicated) pressure in the collision cell. The collision energy was 9 eV. The scan time was 2 s per scan.

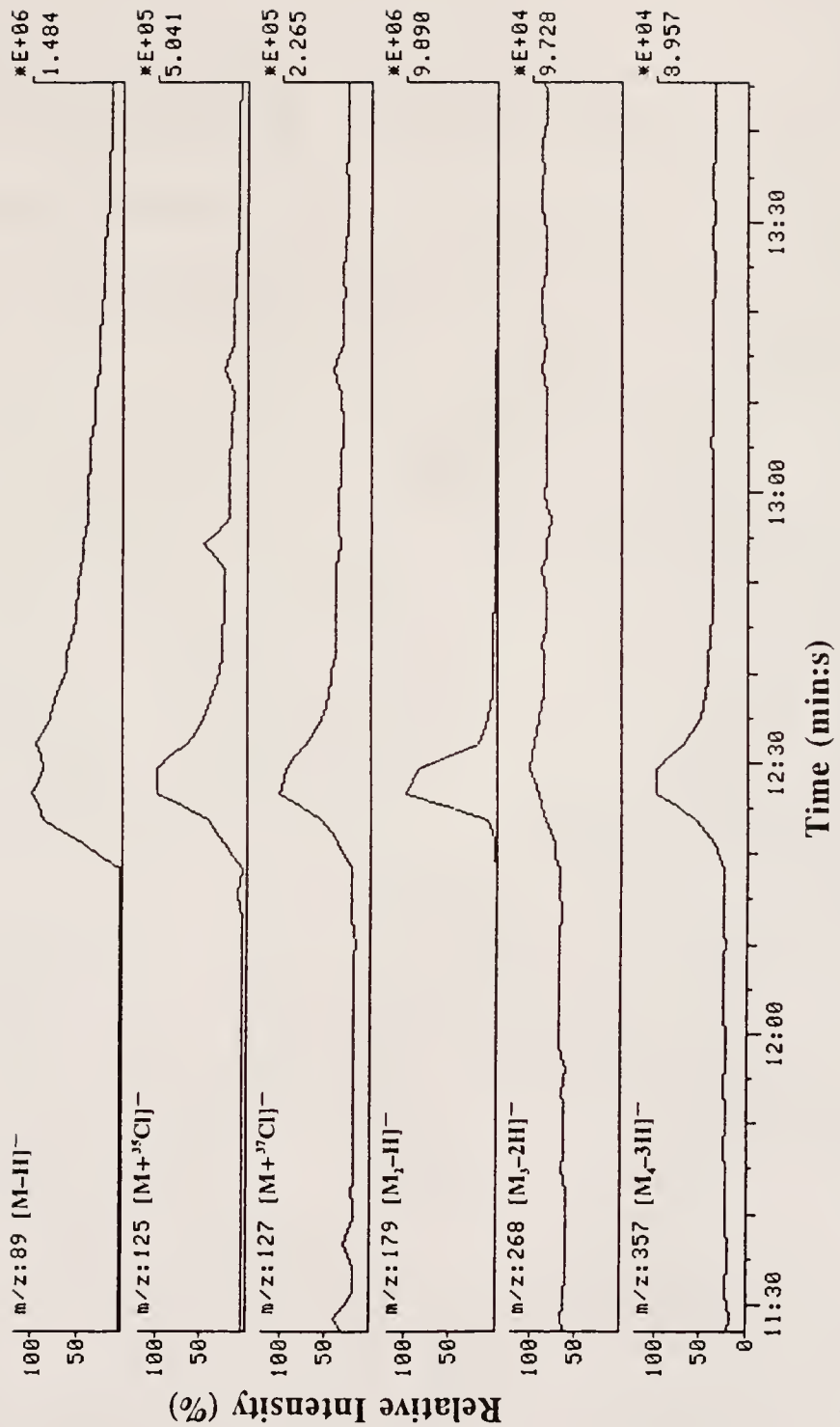
Relative Intensity (%)
m/z:89 [M-H]⁻
m/z:125 [M+³⁵Cl]⁻
m/z:127 [M+³⁷Cl]⁻
m/z:179 [M₂-H]⁻
m/z:268 [M₃-2H]⁻
m/z:357 [M₄-3H]⁻
*E+06
1.484
*E+05
5.041
*E+05
2.265
*E+06
9.890
*E+04
9.728
*E+04
8.957
100
50
0
11:30
12:00
12:30
13:00
13:30
Time (min:s)

Figure 3-5 Negative ion daughter spectrum of m/z 125, the chloride attachment ion of lactic acid. A 0.5 μL injection of a 12 ng/μL methanolic L-lactic acid solution was analyzed. Methane CI was employed at an indicated pressure of 1600 mtorr. The CID gas was N_2 at an indicated pressure of 2.00 mtorr. The Q2 collision energy was set at 2 eV. The scan time was 0.5 s per scan.

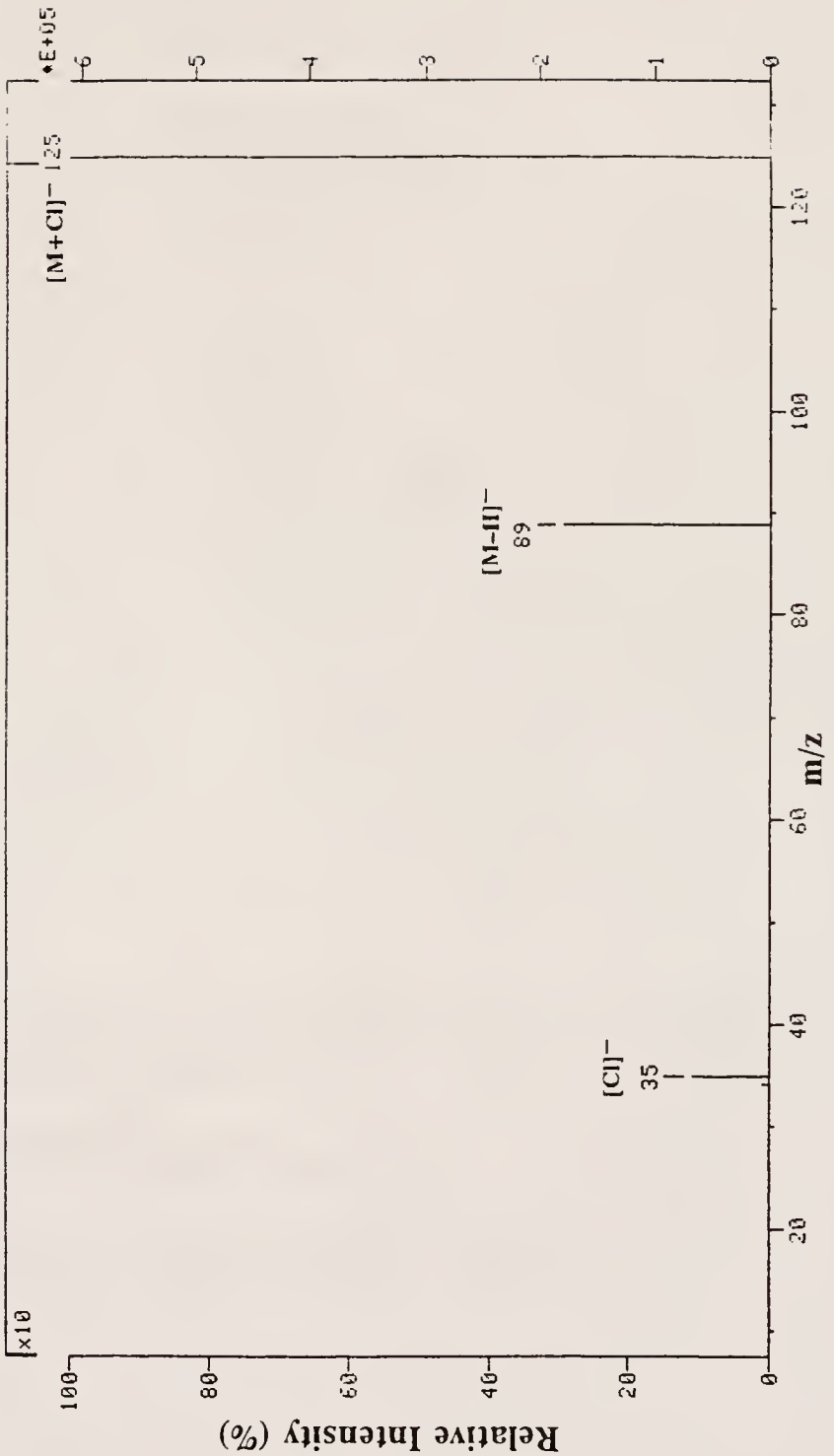
Relative Intensity (%)
m/z
[Cl]⁻
35
[M-H]⁻
89
[M+Cl]⁻ 125
x10
E+05

the m/z 125 parent ion. The daughter spectrum of m/z 127 consisted of the expected daughter ions at m/z 37 and 89.

Chloride ion attachment spectra are useful for applications involving detection of organic compounds with acidic protons [81]. This attachment is somewhat selective for specific classes of compounds which meet this criteria. Typically, methylene chloride is used as the reagent gas to effect the attachment in the ion source. In the instrument employed for this work, residual chloride ions are always present in the negative ion background and, as demonstrated, can undergo ion-molecule reactions even in the presence of additional reagent gas. This reaction itself is of secondary importance in the work for this dissertation rather than a primary mode of identification.

Negative ions which undergo a neutral loss of 90 Da (i.e. lactic acid) are presented in figure 3-6. The chloride attachment ion at m/z 125 was previously shown (figure 3-5) to undergo a neutral loss of 90 Da. The other ions found in this neutral loss spectrum are at m/z 179 and m/z 177. The lactic acid-lactate dimer ion at m/z 179 was pointed out in figure 3-4. Additionally, dimer formation can result from the combination of a neutral lactic acid molecule and the hydrogen-eliminated lactate ion (m/z 87) to produce a dimer at m/z 177. Experimental data not shown indicate that the m/z 177 dimer can also undergo losses of 88 Da and 92 Da to form ions at m/z 89 and m/z 85, respectively. Additional data will be presented later in this chapter (figure 3-10).

Figure 3-6 Negative ion neutral loss spectrum acquired with a selected neutral loss of 90 Da, the relative molecular mass of lactic acid. Five beads were sampled after being handled in the palms of the hands for 5 min. The beads were placed in a 1/4" o.d. glass tube (maximum 25 beads) which was inserted in the apparatus described in figure 2-3. Isobutane was employed (indicated pressure of 1647 mtorr) as the reagent gas. The CID gas was N_2 at 1.97 mtorr (indicated) pressure in the collision cell. The collision energy was 9 eV. The scan time was 3 s per scan.

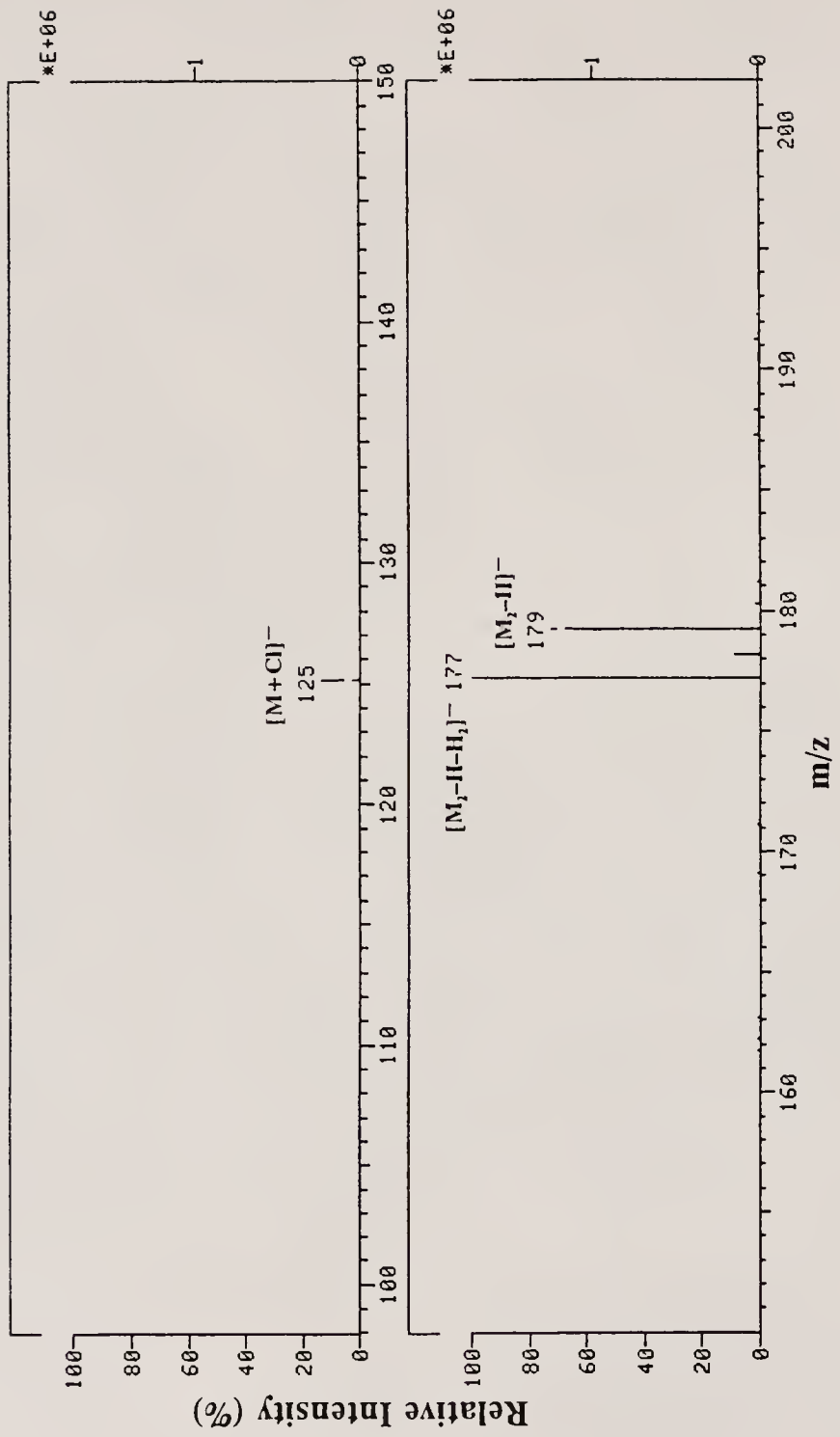
*E+06
[M+Cl]⁻
125
[M₂-H-H₂]⁻ 177
[M₂-H]⁻
179
Relative Intensity (%)
m/z

If the dimer ion at m/z 179 is selected as the parent ion and fragmented by CID (figure 3-7), it exhibits similar neutral losses as the $[M-H]^-$ at m/z 89, i.e. loss of H_2O to form m/z 161, loss of CO to form m/z 151, loss of CO_2 to form m/z 135, as well as the presence of m/z 87. The similarity in neutral losses indicate that identical cleavages occur from the negatively charged carboxyl terminal site. The formation of m/z 87 from the dimer ion at m/z 179 occurs via a loss of 92 Da, as was mentioned for the m/z 177 dimer ion.

This can be confirmed by examining the parents of the $[M-H-H_2]^-$ species at m/z 87 (figure 3-8). Both m/z 179 and m/z 177 dimer ions will produce this daughter ion; however, the m/z 175 dimer ion can also lose 88 Da (neutral lactic acid molecule which has undergone H_2 elimination) to form the m/z 87 ion. An ion at m/z 133 is also present; this is formed via the neutral loss of CO_2 from the m/z 177 ion analogous to the formation of m/z 135 from the m/z 179 dimer ion (figure 3-7).

These dimer ions and fragment ions discussed thus far are present in NCI mass spectra as well as MS/MS daughter spectra produced by CID, provided there is sufficient collision energy. An example of the variability of CID daughter spectra is evident by comparing figure 3-9, acquired with nominally 0 eV collision energy, to figure 3-7. Figure 3-9 displays only the mass-selected parent ion at m/z 179 and the daughter ion at m/z 89. This implies that the neutral loss of lactic acid from the dimer ion to regenerate the lactate ion is a lower energy process than fragmentations associated with lactate.

Figure 3-7 Negative ion daughter spectrum of m/z 179, the $[M_2\text{-}H]^-$ dimer ion of lactic acid. The Q2 collision energy was set at 9 eV. Five beads were sampled after being handled in the palms of the hands for 5 min. The beads were placed in a 1/4" o.d. glass tube (maximum 25 beads) which was inserted in the apparatus described in figure 2-3. Isobutane was employed (indicated pressure of 1647 mtorr) as the reagent gas. The CID gas was N_2 at 1.97 mtorr (indicated) pressure in the collision cell. The collision energy was 9 eV. The scan time was 3 s per scan.

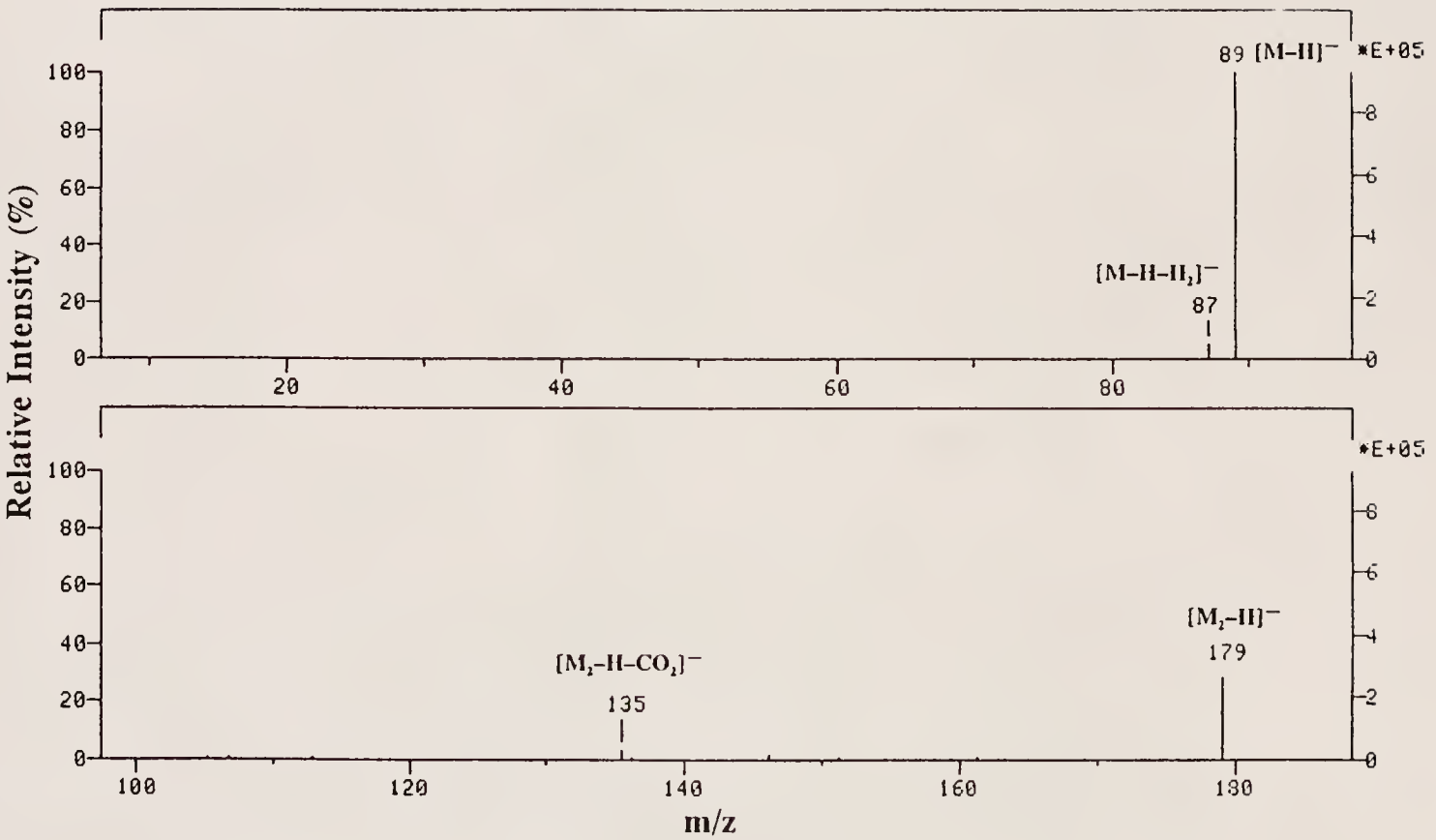
Relative Intensity (%)
89 [M–H]⁻
*E+05
[M–H–H₂]⁻
87
[M₂–H–CO₂]⁻
135
[M₂–H]⁻
179
m/z

Figure 3-8 Negative ion parent spectrum of m/z 87, the $[M\text{-}H\text{-}H_2]^-$ ion of lactic acid. Five beads were sampled after being handled in the palms of the hands for 5 min. The beads were placed in a 1/4" o.d. glass tube (maximum 25 beads) which was inserted in the apparatus described in figure 2-3. Isobutane was employed (indicated pressure of 1647 mtorr) as the reagent gas. The CID gas was N_2 at 1.97 mtorr (indicated) pressure in the collision cell. The collision energy was 9 eV. The scan time was 3 s per scan.

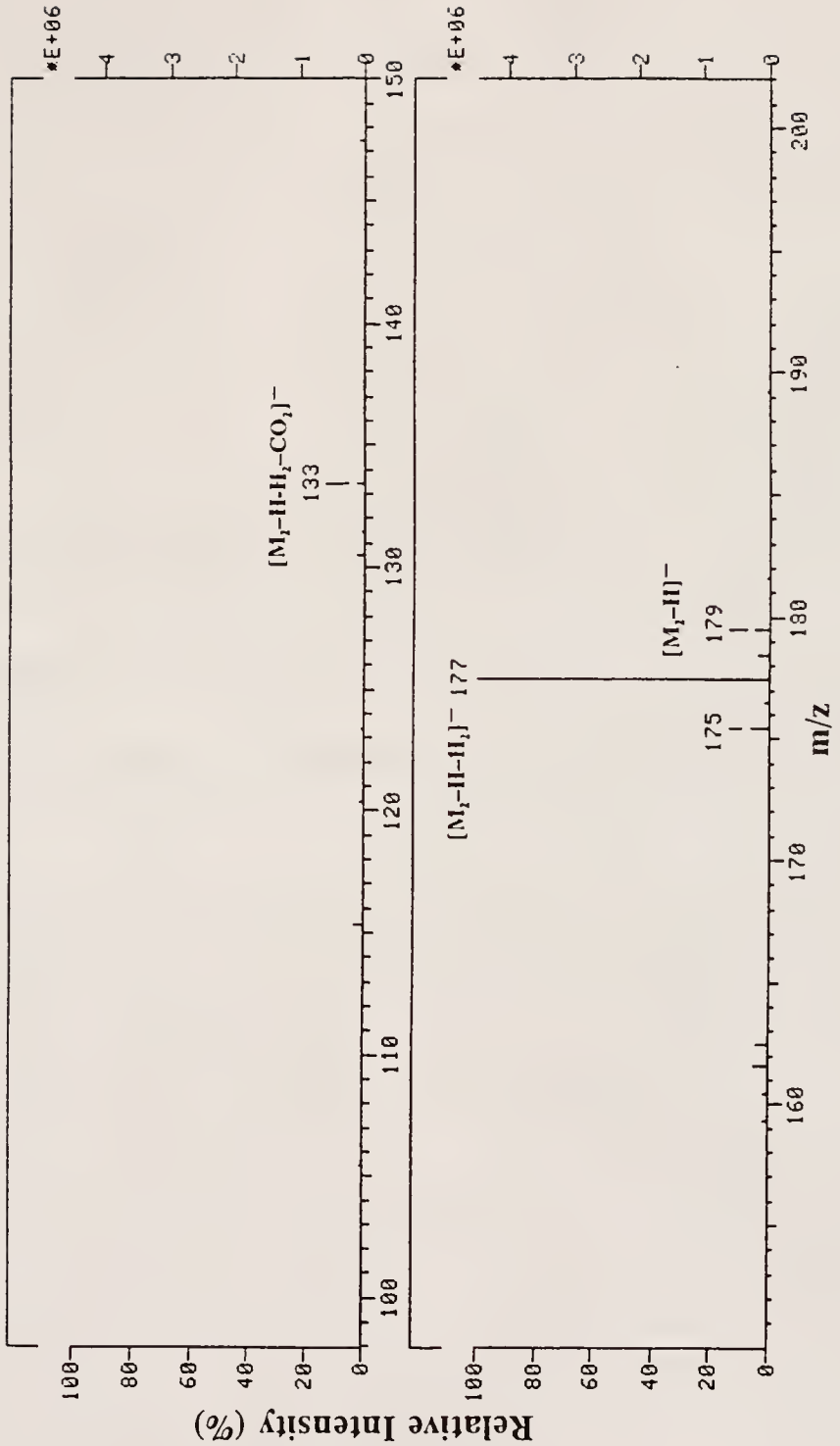
Relative Intensity (%)
m/z
[M1–H–H2–CO2]− 133
[M1–H–H2]− 177
[M1–H]− 179
175
*E+06

Figure 3-9 Negative ion daughter spectrum of m/z 179, the $[M_2\text{-}H]^-$ dimer ion of lactic acid. A 0.5 μL injection of a 12 ng/μL methanolic L-lactic acid solution was analyzed. Methane CI was employed at an indicated pressure of 1600 mtorr. The CID gas was N_2 at an indicated pressure of 2.00 mtorr. The Q2 collision energy was set at 0 eV. The scan time was 0.5 s per scan.

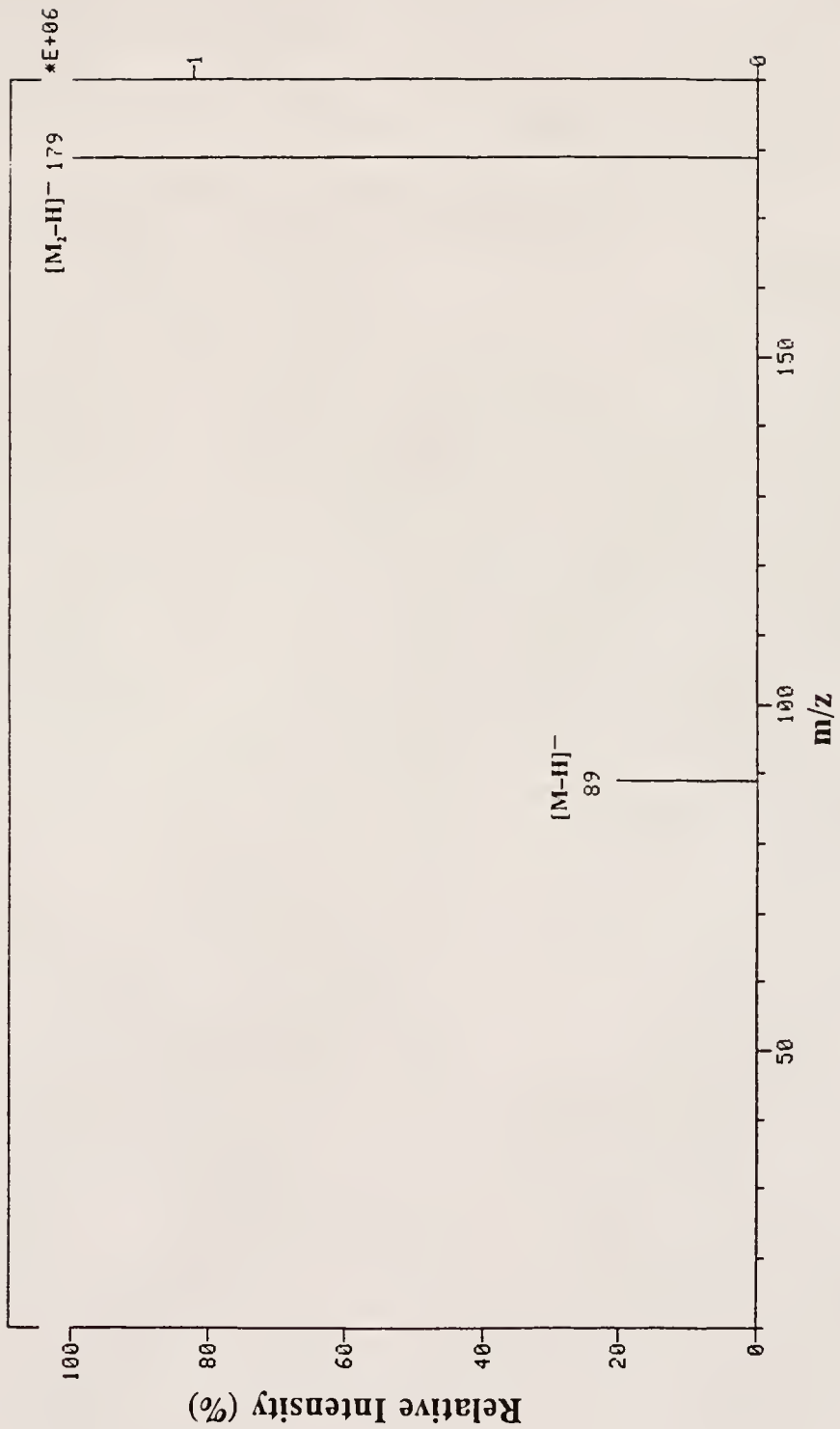
Relative Intensity (%)
100
80
60
40
20
0
50
100
150
m/z
[M-H]⁻
89
[M₂-H]⁻ 179
*E+06
-1
0

A summary of selected major fragmentations of dimers and associated attachments is presented in figure 3-10. This figure is arranged such that reactions involving lactate, or the lactate-lactic acid dimer are found towards the top left corner of the diagram; those involving the H_2-eliminated analogs of these species are found towards the bottom right corner.

The similarity in fragmentations of m/z 179 and m/z 177 is clearly evident. Both species undergo neutral losses of CO_2 to form ions which can then cleave the remainder of the neutral lactic acid molecule to form ions at m/z 89 and m/z 87 depending on the initial dimeric species. Both the m/z 179 and m/z 177 dimer can form ions at m/z 89 and m/z 87. Additionally, both neutral lactic acid (90 Da) and the H_2-eliminated lactic acid neutral (88 Da) can form chloride attachment ions.

Differences are found in the fragments of the dimer ions. The m/z 179 dimer ion can undergo a neutral loss of CO and a neutral loss of H_2O. The intensities of fragment ions formed by identical losses from the m/z 177 dimer ion fall below the threshold percentage (1% base peak) chosen for presentation. An additional dimer ion at m/z 175 formed from the association of H_2-eliminated lactate and lactic acid fragments to yield only m/z 87; this is also not presented in the figure. The only significant fragment ion arising from the m/z 177 dimer (with exception of m/z 89 and m/z 87) is due to the neutral loss of CO_2, forming the m/z 133 ion.

Lastly the issue of dimer formation in the NCI mass spectrum of lactic acid just prior to and after saturation of the ion source can be addressed and illustrated by examining figures 3-11 and 3-12. Figure 3-11 depicts the m/z 87 ion in greater

Figure 3-10 Diagram of significant negative ion attachments, dimers, and fragmentations resultant from the NCI analysis of lactic acid.

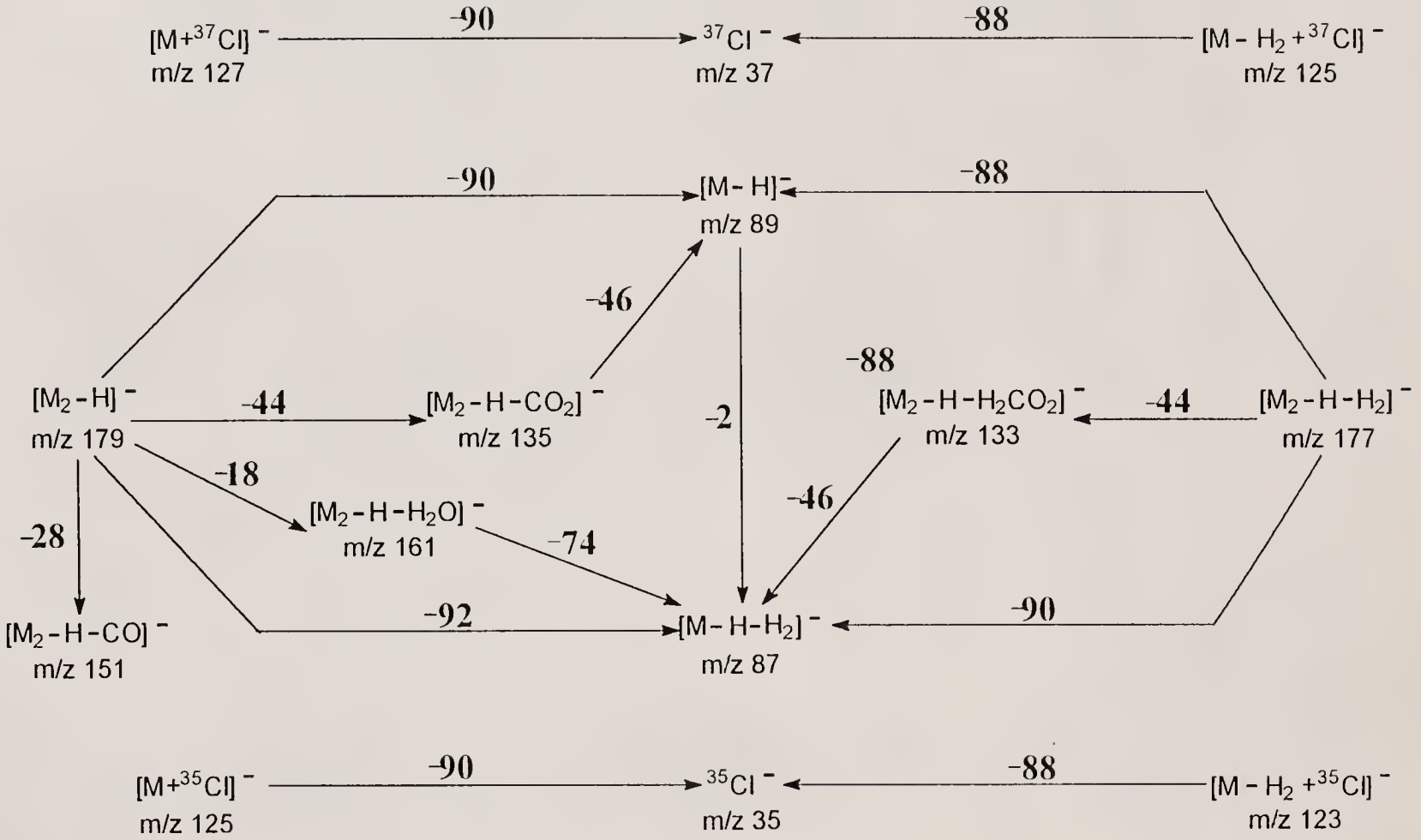
[M+37Cl] -
m/z 127
-90
37Cl -
m/z 37
-88
[M - H2 +37Cl] -
m/z 125
-90
[M - H] -
m/z 89
-88
-46
[M2 - H] -
m/z 179
-44
[M2 - H - CO2] -
m/z 135
-2
-88
[M2 - H - H2CO2] -
m/z 133
-44
[M2 - H - H2] -
m/z 177
-18
[M2 - H - H2O] -
m/z 161
-46
-28
-74
[M2 - H - CO] -
m/z 151
-92
[M - H - H2] -
m/z 87
-90
[M+35Cl] -
m/z 125
-90
35Cl -
m/z 35
-88
[M - H2 +35Cl] -
m/z 123

Figure 3-11 NCI mass spectrum of lactic acid during the initial elution of lactic acid off of the column. This mass spectrum depicts ions prior to saturation of the ion source. One hundred glass beads were sampled after being handled in the palms of the hands for 3 min. The beads were placed in a 100 mL round bottom flask which was inserted in the apparatus described in figure 2-3. The beads were spiked with an additional 2 μL of a 300 ng/μL methanolic L-lactic acid solution. Methane was employed (indicated pressure of 1650 mtorr) as the reagent gas. The CID gas was N_2 at an indicated pressure of 1.97 mtorr in the collision cell. The collision energy was 9 eV. The scan time was 0.5 s per scan.

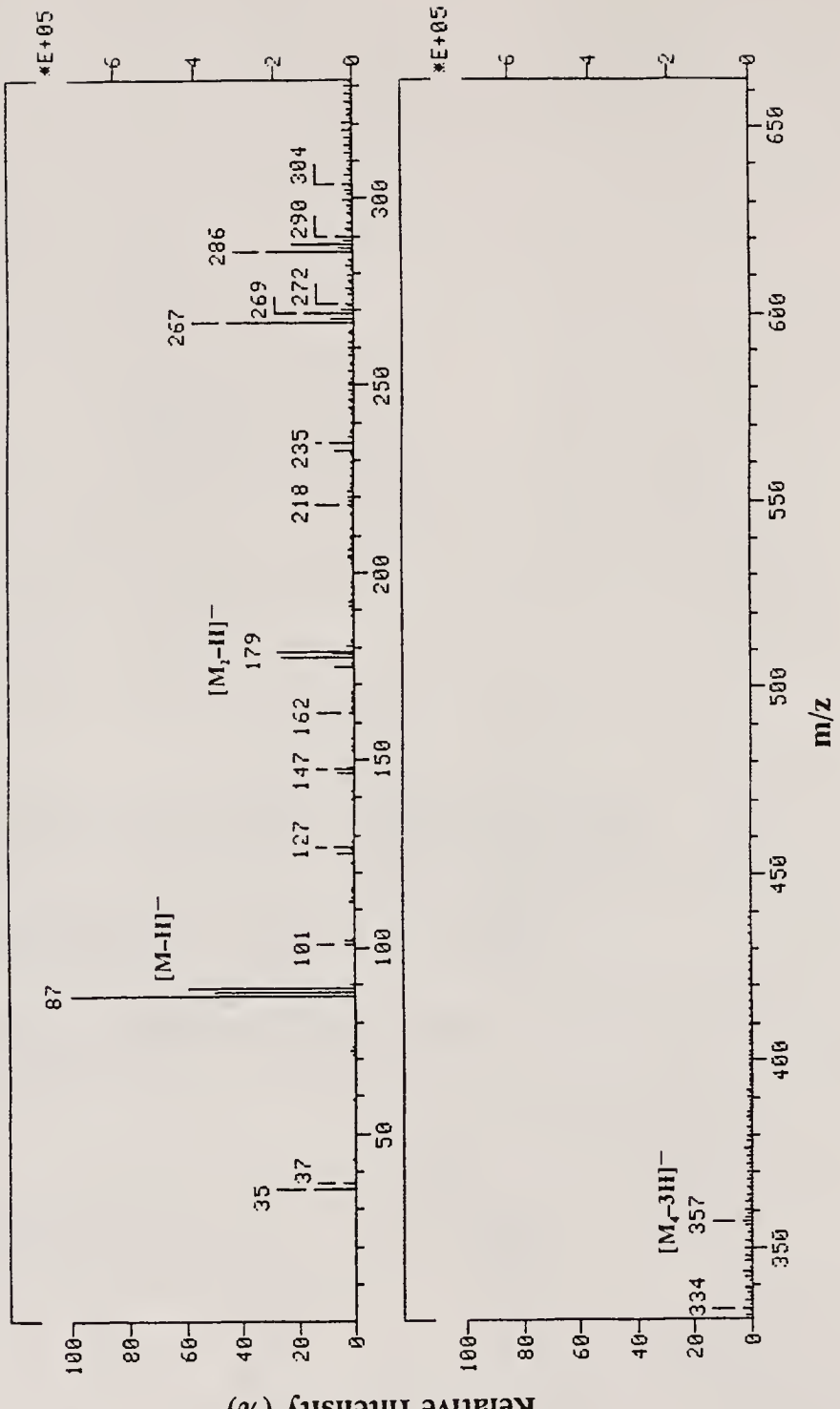
Relative Intensity (%)
m/z
[M-H]⁻
[M₂-H]⁻
[M₄-3H]⁻
87
35
37
101
127
147
162
179
218
235
267
269
272
286
290
304
334
357
*E+05
*E+05

Figure 3-12 NCI mass spectrum of lactic acid while eluting off of the column. This mass spectrum depicts ion present in the ion source after saturation has occurred. One hundred glass beads were sampled after being handled in the palms of the hands for 3 min. The beads were placed in a 100 mL round bottom flask which was inserted in the apparatus described in figure 2-3. The beads were spiked with an additional 2 μL of a 300 ng/μL methanolic L-lactic acid solution. Methane was employed (indicated pressure of 1650 mtorr) as the reagent gas. The CID gas was N_2 at an indicated pressure of 1.97 mtorr in the collision cell. The collision energy was 9 eV. The scan time was 0.5 s per scan.

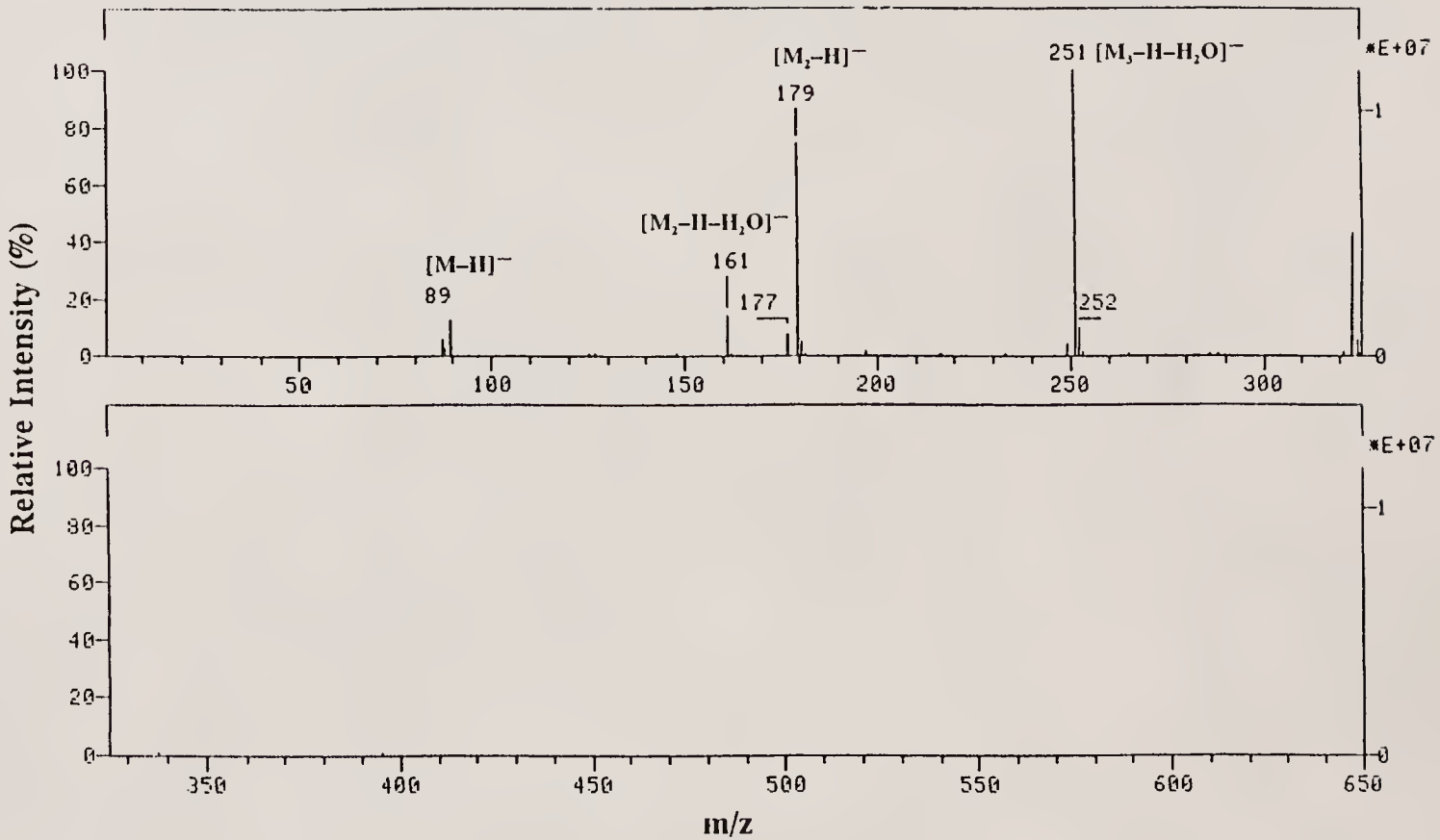
Relative Intensity (%)
m/z
[M–H]⁻
89
[M₂–H–H₂O]⁻
161
177
[M₂–H]⁻
179
251 [M₃–H–H₂O]⁻
252
*E+07
*E+07

abundance than m/z 89 ion. The m/z 177 dimer ion abundance is approximately equal to that of the m/z 179 dimer ion. The presence of the trimer and tetramer ions at m/z 268 and 357 can also be seen. Although the source is not yet fully saturated, the increased pressure leads to oligomerization reactions from lactic acid.

Examination of NCI mass spectrum of lactic acid after saturation has occurred (figure 3-12) shows increased m/z 179 relative to m/z 89, as well as loss of H_2O (m/z 161) from esterification. The relative abundance of m/z 177 is increased with respect to m/z 179. Also, the trimer ions now include both oligomerization ions and esterification ions due to a single loss of H_2O; the tetramer ion at m/z 323 corresponds to the loss of two molecules of water, $[M_4\text{-}H\text{-}2H_2O]^-$. As expected, dimer ion formation is more prevalent at higher pressures. Additionally, the ions formed indicate that esterification becomes more prominent with respect to oligomerization as the source pressure is increased due to greater abundance of neutral lactic acid. The oligomerization and esterification reactions are similar to solution-phase reactions addressed earlier in this section.

Altering Attraction

Experiments in this section involve analysis of methanolic lactic acid solutions modified by the addition of acid or base. Samples were initially examined by an olfactometer to determine the attraction of *Ae. aegypti* to these solutions. Mass spectrometric analysis was employed as a complementary technique for the identification of species present in these solutions. The mass spectrometric results

led to additional testing of compounds. The entomological data and selected mass spectrometric data will be presented.

Addition of acid or base to lactic acid

The experiments in this section were conceived from the knowledge that lactic acid is a known attractant for *Ae. aegypti* and the hypothesis that differences in human skin pH may affect attraction. Perspiration on the skin is typically near pH 5.5 in value. This value may seem slightly acidic due to the popular notion that perspiration should be slightly basic either from the use of basic soaps or from bacterial action which produces an ammonia odor when perspiration is collected and held at room temperature in open air for an extended period of time.

Five stock solutions of lactic acid in methanol were prepared; spikes of acid or base were added to four of the solutions, leaving the fifth unmodified. The preparation of these solutions was previously discussed in the experimental section. It is important to reiterate that the measured pH values for the solutions serve only as a reference scale. The unmodified solution yielded a pH 3.1 reading.

The percentage of *Ae. aegypti* attracted to each of the five solutions is presented in figure 3-13. The acidified solution is shown to have slightly less attraction than the unmodified solution; however, the trend for solutions with increasing base added is more apparent; the successive addition of base decreases the attraction.

The reactions from the previous section as well as a chemical explanation for the results depicted in figure 3-13 are illustrated in figure 3-14. Experiments

Figure 3-13 Effect of pH on attraction. Percentage of mosquitoes attracted versus measured pH value of methanolic lactic acid solutions with added acid or base. The unmodified solution containing no additional acid or base measures pH 3.1 with a glass electrode.

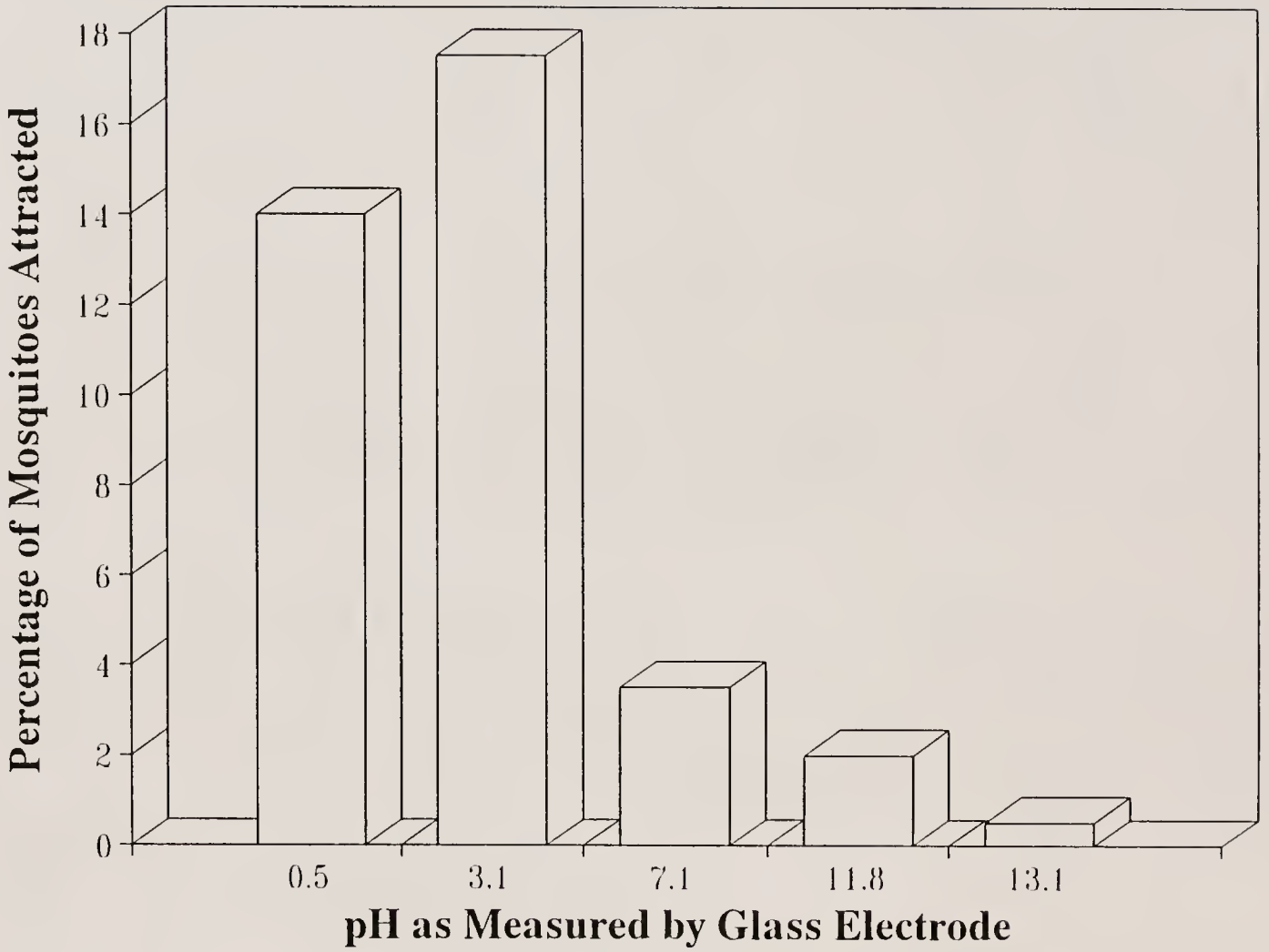
Percentage of Mosquitoes Attracted
18
16
14
12
10
8
6
4
2
0
0.5
3.1
7.1
11.8
13.1
pH as Measured by Glass Electrode

Figure 3-14 Equilibria which are associated with lactic acid (HA) and have been examined thus far in this work. The acid dissociation equilibrium explains the effects noted upon addition of acid or base to methanolic lactic acid solutions.

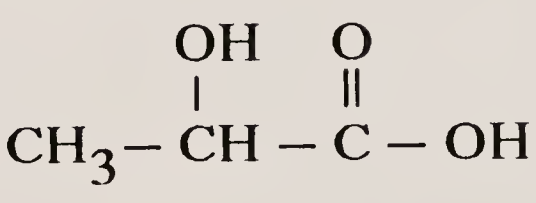

Lactic Acid

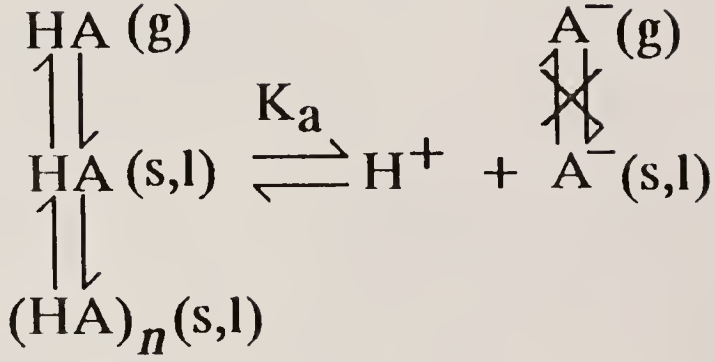

involved the volatilization of lactic acid to the gas phase via desorption. This is a necessity for subsequent mass spectrometric analysis, as well as for mosquito detection of lactic acid which has evaporated off of the skin. This is the equilibrium represented by the double arrow between the aqueous and gaseous forms of lactic acid. Addition of heat to this system favors the volatilization of lactic acid.

Oligomerization reactions of lactic acid in the gas phase were discussed previously. This process can also occur in the condensed phase as represented by the double arrow leading from lactic acid to $(HA)_n$ (s,l). This process occurs at high concentrations of sample in the ion source.

There is an acid dissociation equilibrium in the condensed phase governed by this K_a between the associated lactic acid and the dissociated form (free hydrogen ion and lactate ion). In the dissociated form, the lactate ion is not susceptible to volatilization; thus, detection of lactate by mosquitoes via olfaction cannot exist. Recalling LeChatlier's principle, this system can be affected by the hydrogen ion concentration, $[H^+]$. Upon acidification, the system will move towards formation of associated lactic acid, increasing volatility. The removal of free $[H^+]$ via addition of base shifts the equilibrium towards the production of dissociated lactate. This will decrease the free acid available for volatilization, thereby decreasing attraction via mosquito olfactory cues.

There was an additional condensed-phase concern besides implications of acid/base effects on mosquito attraction. This was the possibility of additional species produced by reactions occurring in the condensed phase. The possibility of

reaction between lactic acid and methanol via acid-catalyzed or base-catalyzed esterification was examined by mass spectrometry. There are two purposes behind the selection of mass chromatograms displayed in figure 3-15. The first purpose is the verification that masses corresponding to the protonated molecular species of lactic acid and methyl lactate are indeed present (in this case, under basic conditions). The additional mass chromatogram (m/z 73) displayed in the figure explains additional peaks found in the RIC which are not attributable to either lactic acid or methyl lactate. A fragment ion at m/z 73 is characteristic of siloxanes from GC analysis.

The second purpose behind selecting these data was to illustrate a phenomenon which can occur for these compounds. The data were acquired under EI conditions; however, a significant abundance of the protonated molecular species occurs rather than the molecular ion. It was previously mentioned that lactic acid does not form a molecular ion under EI conditions; however, the formation of $[M+H]^+$ is relatively facile by self-induced chemical ionization due to high ion source concentrations and pressure. Reactions of similar compounds at high ion source pressure under EI conditions support this supposition [82].

Verification that the peak found at scan number 320 is indeed lactic acid can be found in figure 3-16. The data for this figure were acquired under NCI conditions; this clearly depicts the characteristic chloride ion attachment and oligomer ions formed by lactic acid. Confirmation of the presence of methyl lactate by NCI is not possible since it does not readily form an $[M-H]^-$ ion.

Figure 3-15 Mass chromatograms of m/z 73 (characteristic of siloxanes), m/z 91 (protonated molecular species of lactic acid), and m/z 105 (protonated molecular species of methyl lactate). Data were acquired under EI conditions; however, m/z 91 and m/z 105 are due to self-CI reactions attributable to high ion source pressure. A 0.5 μL injection was made of a methanolic 205 ng/μL and 400 ng/μL NaOH in methanol.

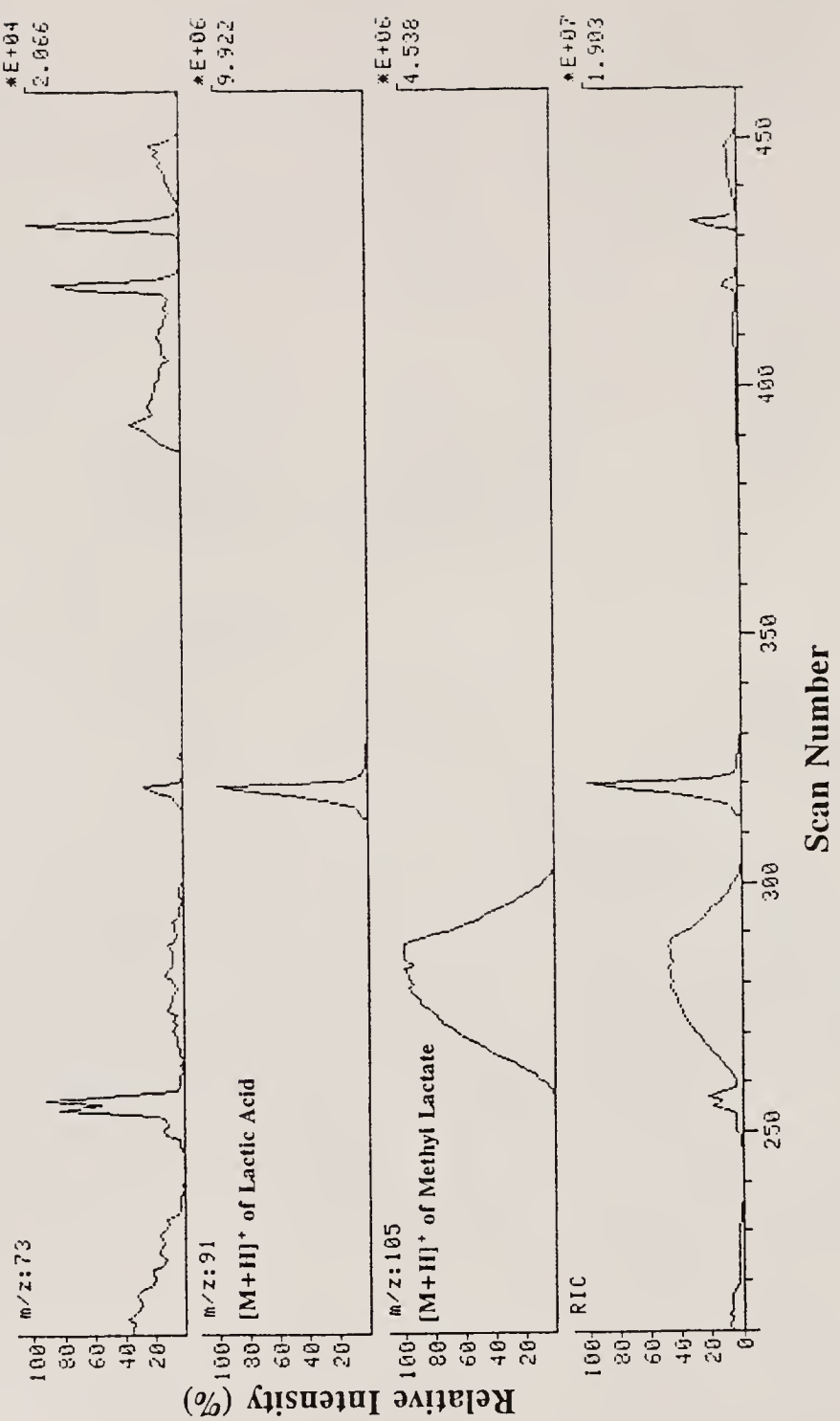
m/z:73
*E+04
2.066
m/z:91
[M+H]+ of Lactic Acid
*E+06
9.922
m/z:105
[M+H]+ of Methyl Lactate
*E+06
4.538
RIC
*E+07
1.903
Relative Intensity (%)
Scan Number
100
80
60
40
20
0
250
300
350
400
450

Figure 3-16 NCI mass spectrum of the peak corresponding to scans centered around scan number 320. Ions observed in the mass spectrum confirm the presence of lactic acid. A 0.5 μL injection was made of a methanolic 120 ng/μL L-lactic acid solution spiked with 12M HCl to give and indicated pH value of 3.05.

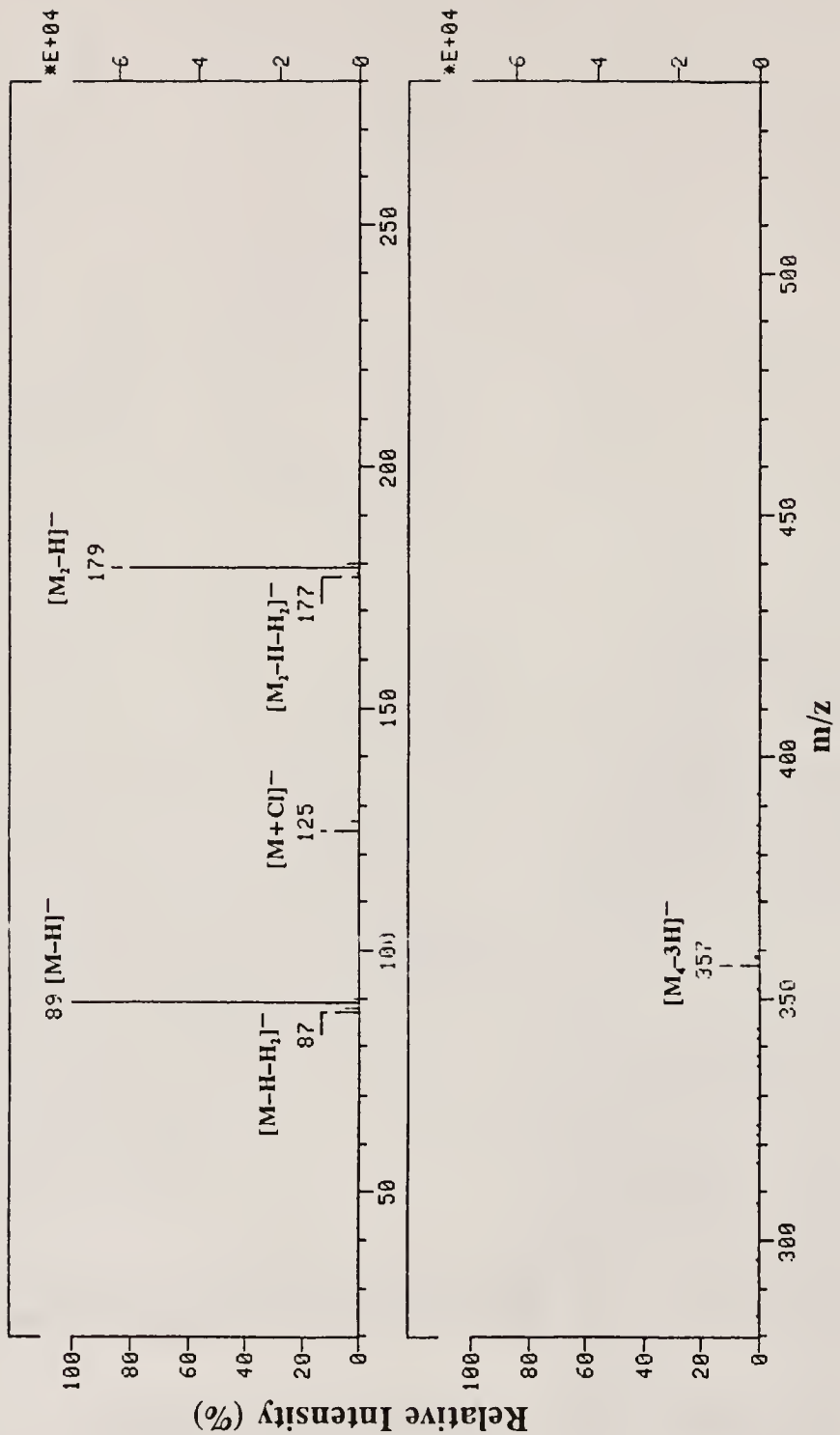
Relative Intensity (%)
m/z
89 [M-H]⁻
87
[M-H-H₂]⁻
[M+Cl]⁻
125
[M₂-H]⁻
179
[M₂-H-H₂]⁻
177
[M₄-3H]⁻
357
*E+04
*E+04

Analysis by methane PCI of the peak suspected to be methyl lactate provided the mass spectrum found in figure 3-17. The ions at m/z 105 and m/z 77 correspond to the $[M+H]^+$ and $[M+H-CO]^+$ CI ions, indicating a possible relative molecular mass of 104 Da (that of methyl lactate). For comparison, figure 3-18 shows the methane PCI mass spectrum of standard methyl lactate in methanol.

Addition of acid or base to esters

The confirmation of the presence of methyl lactate in lactic acid solutions prompted the testing of methyl lactate and two additional esters for attraction. The previous knowledge gained from acidification of solutions was also incorporated into the experiment; the results are displayed in figure 3-19. There are two evident trends. The first is that as esters increasingly differ structurally from lactic acid, the attraction decreases. The second trend is that upon addition of acid, all solutions increase in attraction. Acidification of lactic acid was addressed in the previous section. Acidification of ethyl lactate and methyl lactate may lead to partial hydrolysis of the esters, producing lactic acid, thus enhancing attraction. Note that isovalerate exhibits no response until acidified. Partial hydrolysis of the ester to form isovaleric acid may be the reason for the increased attraction of *Ae. aegypti*.

Analysis of Methanolic Perspiration Solution

This final section is focused upon a brief extension of condensed-phase work to human emanations. Previous olfactometer studies have shown little attraction when attractants are dissolved in solution. The attraction was only found to be

Figure 3-17 PCI mass spectrum of peak centered around scan number 280. The ions present suggest that the this compound has a relative molecular mass of 104 Da. A 0.5 μL injection was made of a methanolic 120 ng/μL L-lactic acid solution spiked with 10N NaOH to give and indicated pH value of 11.80.

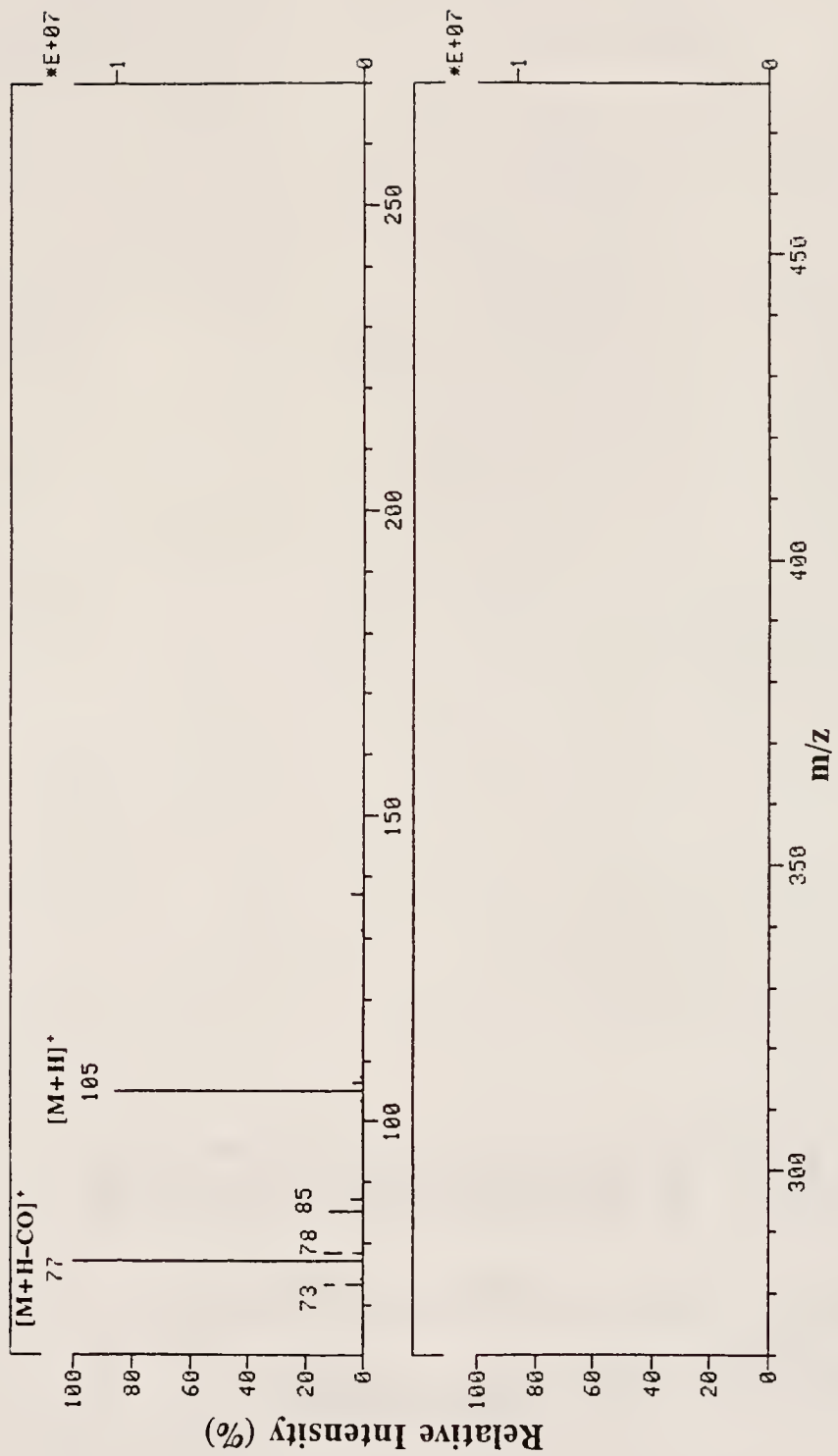
[M+H-CO]+
77
73
78
85
[M+H]+
105
*E+07
*E+07
Relative Intensity (%)
m/z

Figure 3-18 PCI mass spectrum of standard methyl lactate in methanol. A 0.5 μL injection of a 214 ng/μL methanolic methyl lactate solution was analyzed.

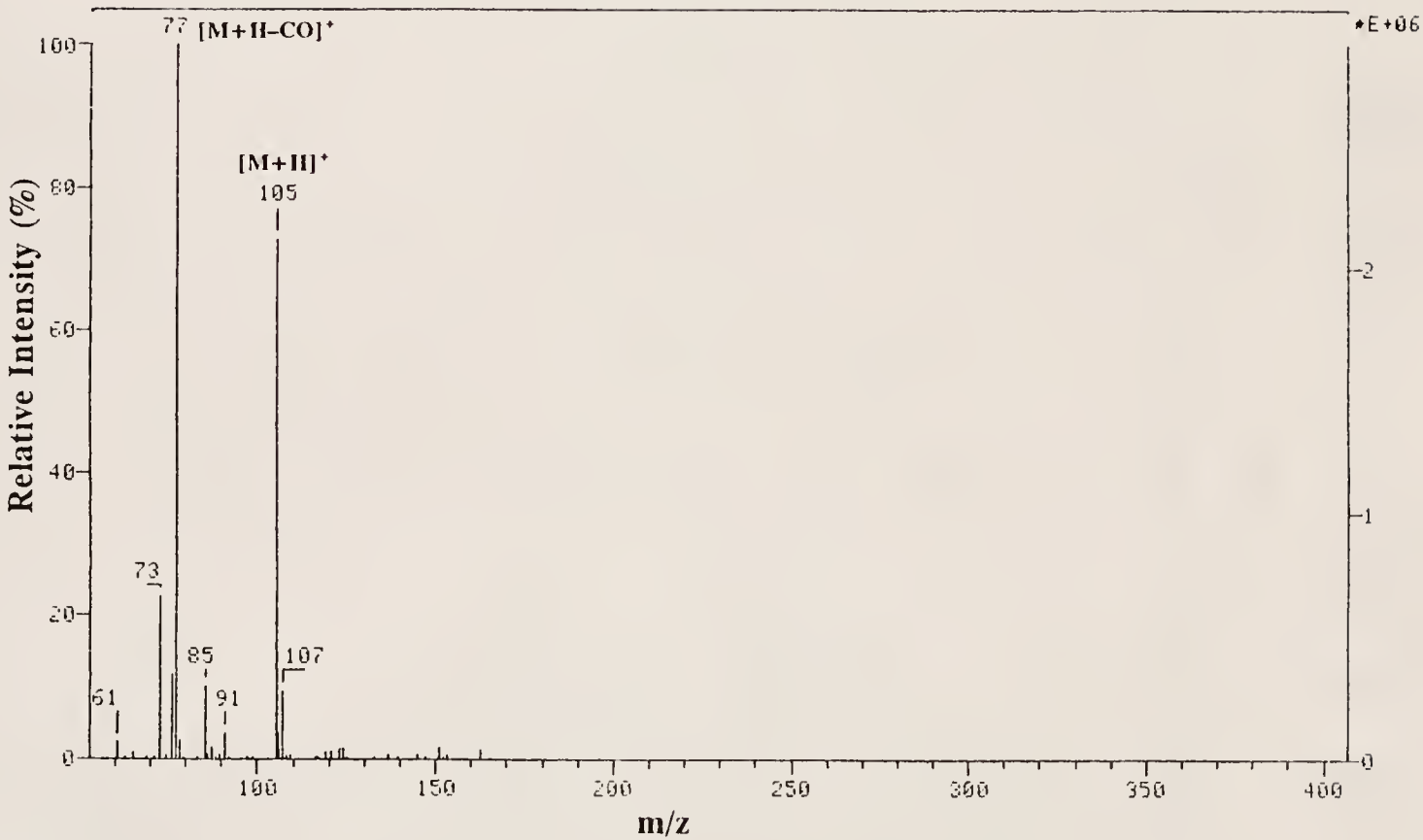

Relative Intensity (%)
m/z
[M+H-CO]+
[M+H]+
77
105
73
85
91
107
61
*E+06
100
80
60
40
20
0
100
150
200
250
300
350
400
2
1
0

Figure 3-19 Effect of acidity on attraction. Percentage of mosquitoes attracted to unmodified and acidified methanolic solutions of lactic acid and related esters.

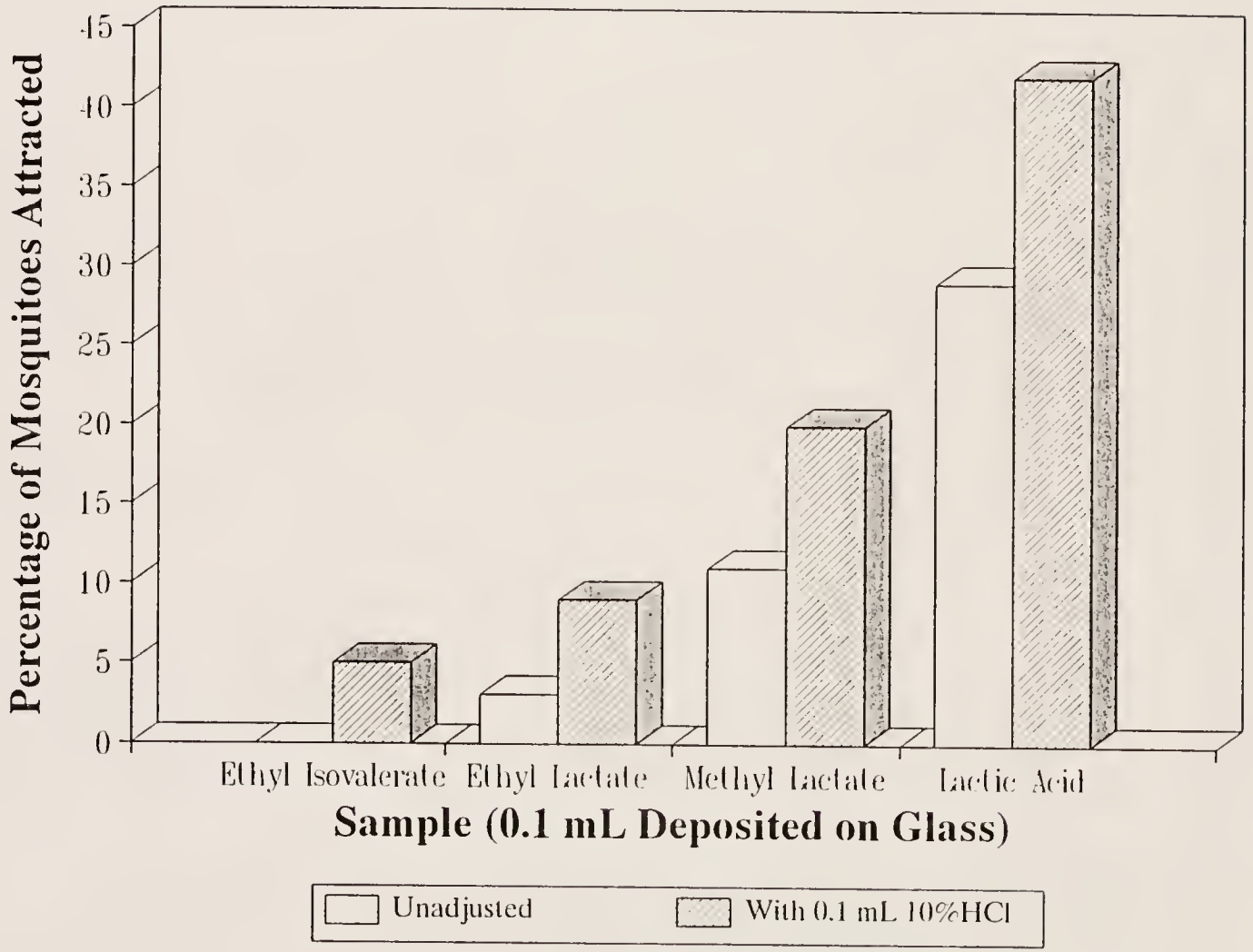
Percentage of Mosquitoes Attracted
45
40
35
30
25
20
15
10
5
0
Ethyl Isovalerate
Ethyl Lactate
Methyl Lactate
Lactic Acid
Sample (0.1 mL Deposited on Glass)
Unadjusted
With 0.1 mL 10%HCl

present in the oily or waxy phase rather than the aqueous phase when these phases were tested in an olfactometer. The general thought is that excess perspiration masks the attractants. The emphasis of this section is to provide additional insight as to why attraction is diminished with respect to emanation of attractants (e.g. lactic acid) from the skin.

Phase differences

Dissolution of perspiration directly in methanol was expected to produce relatively abundant ions in the mass spectra due to the relatively large amount of perspiration (approximately 150 mg) dissolved. This can be compared to the amount of emanations transferred to beads by handling. One hundred glass beads were weighed prior to and after being handled for 10 minutes. A negligible weight difference was measured (i.e. < 0.1 mg). Since the minute quantities deposited on beads was adequate to produce the spectra shown here, it was expected that approximately 150 mg (0.15 mL dissolved in 3 mL of methanol) of perspiration would contain more than an adequate amount of emanations.

The perspiration solution existed as a cloudy white mixture. After allowing this mixture to settle overnight, two distinct phases were present. The aqueous (methanolic) phase was separated from the oily phase containing the white residue. The aqueous phase was analyzed by GC/NCI/MS; characteristic ions seen from the analysis of beads were noticeably absent. Lactic acid was not observed in this fraction of the sample either (see top mass chromatogram in figure 3-20). Analysis of the oily phase revealed the presence of fatty acids and lactic acid; although, these

Figure 3-20 NCI mass chromatograms of m/z 89 (the $[M-H]^-$ ion of lactic acid) from perspiration sample phases. Top mass chromatograms portrays the absence of lactic acid in the methanolic aqueous phase. The bottom mass chromatogram shows lactic acid to be present in the oily/waxy phase.

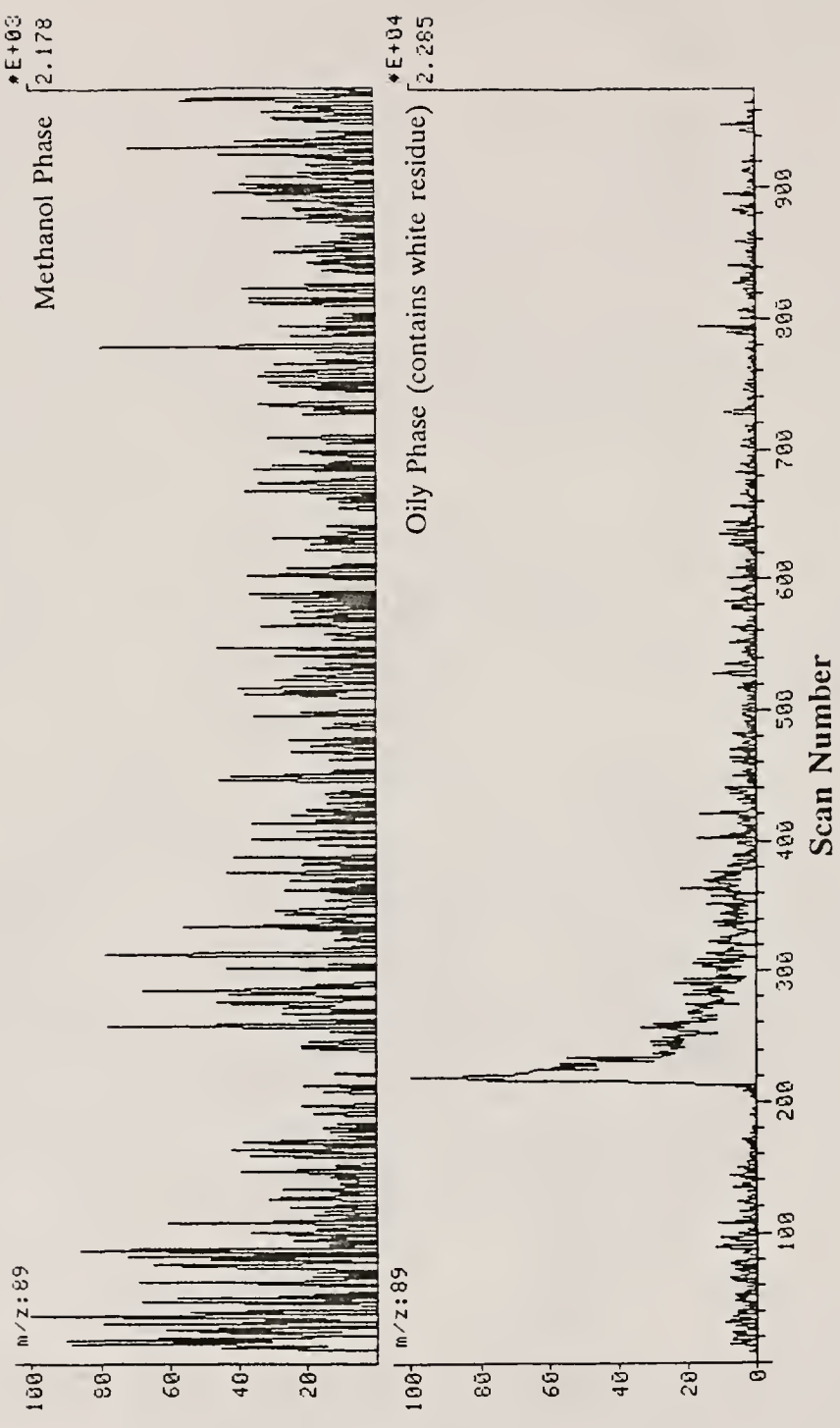
Methanol Phase
Oily Phase (contains white residue)
m/z:89
m/z:89
Relative Intensity (%)
Scan Number

ions which normally dominate the RIC trace were significantly reduced in intensity. Shown in the bottom mass chromatogram is the trace for the m/z 89 $[M-H]^-$ ion of lactic acid. It is evident that the intensity of the lactate ion is reduced when compared to mass chromatogram of m/z 89 analyzed from rubbed beads.

Implication to attractant origin

The relation of this work to semiochemical studies was discussed in the first chapter. The work with methanolic solutions of perspiration directly overlaps with analysis of perspiration for odor determination. Analyses for odors focus upon emanations from three types of glands found on the human body, the sebaceous glands, the eccrine glands, and the apocrine glands [30].

Sebaceous glands are mainly found on the face and scalp. These glands excrete sebum, which contains cholesterol, alcohol esters, and fatty acids [5]. Eccrine glands are located over most of the human body and are most concentrated on the forehead, the palms, and the soles of feet. Apocrine glands are found mainly in the armpits and in the genital area. Eccrine and apocrine excretions are sudoriferous in nature. These excretions are mainly water and sodium chloride. Traces of metabolites from blood plasma may also be present in this solution [5].

Excreted sudor initially has no odor; it is the interaction with bacteria on the skin which produces the acidic odor. The main contributor to this odor has been identified as isovaleric acid [30]. Additionally, two steroids (17-oxo-5α-androstan-3α-yl sulfate and 17-oxo-5α-androsten-3β-yl sulfate) as well as 2-18 carbon aliphatic acids were found to be present [30,31]. It should be noted that these results were

obtained with sample concentration, whereas analyses in this dissertation were conducted without sample concentration.

The existence of lactic acid in the oily phase implies that it preferentially resides in this phase. Handling glass beads appears to favor the deposition of oily or waxy emanations over aqueous perspiration. Perspiration on the skin tends to be very dilute [29]. It also exists above the layer of sebaceous excretions in order to readily evaporate. The absence of lactic acid in this phase supports the assertion that excess perspiration may mask lactic acid attraction. Additional attractants may also be masked by excess perspiration, implying that they also exist in the oily phase on the skin. The origin of most oily excretions are sebaceous glands. Therefore, the deduction from this work is that attractants, whether sebaceous in origin or not, tend to preferentially reside in the sebaceous phase rather than aqueous perspiration phase.

Conclusions

Lactic Acid Reactions

The negative ion fragmentations, attachments, and oligomerization were examined and rationalized. Analysis of negative ions from lactic acid provided informative fragments allowing for quick identification of the presence of this compound in a sample; lactic acid is difficult to identify by EI library searching. The oligomerization reactions in the gas phase were found to be similar to solution-phase reactions. The formation of these oligomers (in the form of dimers, trimers,

tetramers, and esterification products) produce ions which allow complementary confirmation of lactic acid presence. Additionally, the chloride attachment ions can be used for confirmation of lactic acid.

Altering Attraction

The addition of acid or base to lactic acid solutions was found to alter the attraction of *Ae. aegypti* to the sample. These effects presumably occur through the acid dissociation equilibrium. Addition of acid shifts the equilibrium towards the formation of the volatile associated acid form. Addition of base shifts this equilibrium towards the involatile dissociated lactate anion. Examination of similar solutions to those employed in the acid/base lactic acid study revealed that methyl lactate was formed while in methanolic solution. Subsequent testing of lactic acid esters and a similar ester revealed that lactic acid provides greater attraction than the esters. It was also found that addition of acid enhanced mosquito attraction in all cases.

Origin of Attraction

The data presented support the view that excess perspiration masks attraction by hindering volatility off the skin of lactic acid and other possible attractants. These data also show that the lactic acid signal from direct dissolution of perspiration in methanol is diminished compared to analyses with one or more glass beads. This confirms the very dilute nature of perspiration, and that handling glass transfers a

greater amount of components of interest in this study. Lactic acid preferentially resides in the oily sebaceous phase. This supports the assertion that other attractants, also susceptible to masking by excess perspiration, reside in this phase.

CHAPTER 4
APPLICATIONS OF TANDEM MASS SPECTROMETRY

Introduction

Tandem mass spectrometers contain a second mass analyzer not found in conventional single-stage instruments. This extra stage adds an additional dimension to the selectivity of analysis via fragmentation by collision-induced dissociation (CID) [33,56,83]. Tandem mass spectrometry has been demonstrated as an effective tool in the determination of moth pheromones as well as shown to be beneficial in the continuous monitoring of volatiles via the use of a membrane inlet system [84,85]. These examples utilize the capability of the tandem mass spectrometer to perform selected reaction monitoring (SRM). The work in this dissertation differs from these in that MS/MS is applied for compound identification rather than monitoring specific compounds. Additionally, the volatile compounds to be identified are relatively low in relative molecular mass and thus are more amenable to CID than high molecular weight compounds [86].

The applications of MS/MS to this project have been categorized into three sections. The first section addresses the use of daughter spectra for compound identification, both by spectral interpretation and by comparison to standards analyzed under similar conditions. The second part concerns the formulation of a

daughter library to aid in spectral interpretation and in screening for compound classes via examination of specific neutral losses. The final section examines the use of selected neutral losses for rapid screening for compound classes present in the emanations of a human subject.

Analysis of Multiple Beads Without GC Separation

Tandem mass spectrometry was initially employed in this work for the identification of compounds desorbed from multiple beads in a glass chamber. The lack of GC separation and poor temporal resolution achieved by simple desorption of volatiles off of glass beads necessitated the use of some means of additional selectivity (see Chapter 2). The use of a second stage of mass spectrometry provided the means for mass analysis of one selected mass of interest; however, similar compounds which fragment to yield the selected mass, or compounds with identical parent mass to the selected ion, complicated the mass spectral interpretation. This made GC separation attractive for further identification of components emanated from the skin.

Daughter Library

The focus of the second part of this chapter is the compilation of a daughter library under a set of conditions chosen to be constant throughout this work. The collision cell offset, collision gas, and collision gas pressure affect the degree of fragmentation via collision energies, collision processes, and numbers of collisions

[83,87,88]. Therefore, the set of conditions for the daughter library and subsequent analyses need to remain constant throughout to obtain reproducible daughter spectra. The daughter library allowed for determining the specific daughters and neutral losses for particular compounds and compound classes. This information provided the basis for additional spectral interpretation of daughter spectra as well as provided the information on specific neutral losses associated with compound classes. An additional note of interest is the extensive examination of negative ion fragmentations, as well as those of more typical positive ions, used in this dissertation. Analysis of compound classes by positive ions remains more prevalent than the use of negative ions [89-91]. There are some cases, e.g. for ethers and carboxylic acids, where negative ion analysis yields better results than positive ion analysis [92-95].

Compound Class Screening

The final part of this chapter is focused on applying the information on neutral losses obtained from the daughter library for rapid compound class screening of samples of human skin emanations which have been desorbed off of handled glass beads. The actual screening employs cryo-focusing of desorbed volatiles and GC separation. The sample introduction used for MS/MS screening by neutral losses is also employed for almost all work pertaining to compound identification by GC/MS (addressed in Chapter 5).

Experimental

Analysis of Multiple Beads Without GC Separation

Five beads handled 5 minutes by the author of this dissertation were placed in a 1/4" glass tube (maximum 25 beads), which was inserted into the apparatus described in Chapter 2 (figure 2-3). Helium, at 6-8 psig, was passed over the beads and used as the carrier gas through a 1.0 m x 0.10 mm i.d. deactivated FSOT column. The GC oven (holding the glass tube) was held initially at 28-30°C for 1.0 min, followed by a 12 min ramp at 15°C/min to 207-210°C, with a 5 min hold at the final temperature. The transfer line was concurrently ramped from 50°C to 210-215°C at 20°C/min once the run was started.

Sample ionization was effected by positive ion CI or negative ion CI with methane reagent gas at an indicated source pressure of 1687-1700 mtorr. The ion source and manifold temperatures were set at 150°C and 70°C, respectively. The electron energy was set at 100 eV with the filament emission current at 200 μA. The parent ion was selected to be passed by Q1 to the collision cell for fragmentation and subsequent daughter spectrum analysis. The collision gas was argon at an indicated pressure of 1.4-1.5 mtorr for positive ions and nitrogen at 1.97 mtorr for negative ions; the collision energy was set at 15 eV for positive ions and 9 eV for negative ions. The electron multiplier setting was -1200 V with the conversion dynode at -5 kV for positive ions and +5 kV for negative ions. Data were acquired with Q3 scanning at one s per scan for positive ions and 3 s per scan for negative ions.

A standard of ethylene glycol (250 μL) was diluted to 100 mL with methanol. A 0.5 μL injection of the solution was made onto a 10.5 m x 0.178 mm i.d. DB-5 FSOT column (d_f=0.4 μm). The GC injection port temperature was set at 250°C; the helium carrier gas head pressure was set to 4 psig. The column oven was ramped after an initial 1.0 min hold at 30°C, up to 210°C at 15°C/min, then held at 210°C for 5 min. The transfer line was concurrently ramped from 50°C to 215°C at 20°C/min once the run had been started, and held at 215°C for the remainder of the analysis.

Sample ionization was effected by PCI with methane reagent gas at an indicated source pressure of 1700 mtorr. The ion source temperature was set at 150°C and the manifold temperature set at 70°C. The electron energy was 100 eV and the filament emission current was set at 200 μA. The collision gas was argon at an indicated pressure of 1.5 mtorr in the collision cell; the collision energy was 15 eV. The electron multiplier setting was -1200 V with the conversion dynode at -5 kV. The daughter spectrum was acquired at a scan rate of 1 s per scan.

Daughter Library

The data comprising the daughter library consist of data tabulated from analyses of 40 standard compounds. The compounds differed in functional groups (some containing more than one functional group) as well as including isomers for comparison within a specific class. For solid-phase standards, approximately 50 mg of the standard compound was dissolved in methanol in a 100 mL volumetric flask.

For liquid-phase standards, approximately 250 μL was diluted in methanol in a 100 mL volumetric flask. The standards employed were acrolein, acetone, acetic acid, ethylene glycol, pyruvic acid (sodium salt), DL-α-alanine, oxalic acid, glycerol, benzaldehyde, anisole, malonic acid, acetophenone, sec-butylamine, 2-butenal, 1,3-butanediol, 1,4-butanediol, benzoic acid, cyanoacetic acid, benzyl alcohol, benzonitrile, benzamide, 1-butanol, 1-decene, diethylene glycol, *n*-decane, dodecane, L-leucine, diethylamine, glycine, tetradecanoic acid, 2-butanone, phenol, styrene, 1-pentanol, 2-pentanone, vinyl acetate, sebacic acid, octadecanoic acid, tartaric acid, and toluene.

Each standard solution was injected (0.5 μL) onto a 10.5 m x 0.178 mm i.d. DB-5 FSOT column (d_f=0.4 μm). The GC injection port was set at 250°C and the helium carrier gas head pressure was set at 4 psig. The column oven was ramped, after an initial 1.0 min hold at 30°C, up to 210°C at 15°C/min, then held at 210°C for 5 min. The transfer line was concurrently ramped from 50°C to 215°C at 20°C/min once the run was started, and held at 215°C for the remainder of the analysis.

Sample ionization was effected by PCI and NCI with methane reagent gas at an indicated source pressure of 1700 mtorr. The ion source was set at 150°C and the manifold set at 70°C. The electron energy was set at 100 eV and the filament emission current at 200 μA. The collision gas was argon at an indicated pressure of 1.5 mtorr; the collision energy was 15 eV. The electron multiplier was set at -1200 V and the conversion dynode set at +5 kV for negative ion detection and -5 kV for positive ion detection. Daughter spectra were acquired at the rate of 1 s per scan.

Each standard was injected and analyzed three times in order to obtain daughter spectra for the $[M+H]^+$ and $[M-H]^+$ ions in positive ion mode, and the $[M-H]^-$ ion in the negative ion mode.

Compound Class Screening

Volatiles desorbed from 8 glass beads rubbed in the palms of the hands for 5 minutes by the author of this dissertation were analyzed by cryo-focused GC/MS. The beads were placed in a reversed fritted injection port liner and replaced into the GC injection port (set at 25°C). The cap, septum, and needle guide were replaced on the injection port. Liquid nitrogen in a 12 oz. styrofoam cup was placed in the column oven and approximately 8 cm of column (starting approximately 15 cm into the oven) was placed into the cup, as described in the experimental section on cryo-focusing in Chapter 2. The helium pressure was increased from 0 to 20 psig before initiating the cryo-focusing of desorbed volatiles. The cryo-focusing consisted of a 20 min injection port ramping program downloaded from the TSQ70. The program consisted of a ramping the injection port from 25°C to 250°C over 7.5 min and then holding at 250°C for 12.5 min. Throughout cryo-focusing, the GC oven was set at 25°C and the transfer line was set at 40°C. Liquid nitrogen was added to the cup as needed to compensate for evaporation.

After the cryo-focusing stage was completed, a new program was downloaded to the GC. The cup containing the liquid nitrogen was removed and the analysis started. The GC program consisted of an initial 1.0 min hold at 40°C, an 18 min

ramp at 10°C/min up to 220°C, and then a 16.0 min hold at 220°C. The transfer line was concurrently ramped, at the onset of the program, from 50°C to 220°C at 20°C/min for 8.5 min, then held at 220°C for the remaining 27.0 min of the analysis.

The experiments were conducted with by PCI and NCI with methane reagent gas at an indicated pressure of 1680 mtorr. The column employed was a 25 m x 0.20 mm i.d. (d_f=0.33 μm) HP-FFAP FSOT column. The scan rate for all neutral loss scans was 0.5 s per scan over m/z 50-650. Each analysis consisted of examining three different neutral losses, controlled by a program written in ICL language on the TSQ70. The program allowed for incrementing the neutral loss data acquired with each scan such that a specific neutral loss was sampled every 1.5 s. The electron multiplier was set at -1400 V. The filament emission current was 200 μA with 100 eV electron energy. The ion source temperature was set at 150°C and the manifold temperature was set at 70°C. The instrument was tuned, at the beginning of each day, to optimize the transmission of daughter ions, in both the positive and negative mode, produced from the m/z 69, 219, 264, and 414 ions of PFTBA. Positive ion daughter spectra were acquired with -5 kV on the conversion dynode. Negative ion daughter spectra were acquired with +5 kV on the conversion dynode.

Results and Discussion

Analysis of Multiple Beads Without GC Separation

The analysis of handled glass beads requires the analysis of a complex sample. It is estimated that there are typically over 350 distinct component peaks visible in

the cryo-focused GC analyses of 5-8 glass beads (as discussed in Chapter 5). The technique of simple thermal desorption both from a single glass bead mounted on a probe tip and desorption from multiple glass beads heated in a container in the GC oven was discussed in Chapter 2. The RIC profiles of components desorbed from multiple beads in the apparatus (figure 2-3) depict the leading edge of a selected m/z value when it appears; if the compound is volatile enough, the tailing side of the component peak can also be observed within the time frame of the experiment. The "peaks" appear similar to those observed in frontal chromatography; however, chromatographic separation is not employed for these analyses. Clearly, analysis in this manner will only allow for the possible identification of the more volatile components. The spectra of components desorbed at higher temperatures will include ions from components previously desorbed due to inefficient removal of compounds from the apparatus.

The use of tandem mass spectrometry was necessary to isolate a particular mass for further fragmentation. The first example using this method is that of ethylene glycol (figure 4-1). Ethylene glycol desorbs off of the glass beads early in the analysis to produce an ion at m/z 63, the $[M+H]^+$ ion, under PCI conditions in the ion source of the mass spectrometer. Positive identification of this compound was achieved by comparison of the daughter spectrum from handled glass beads (top of figure 4-1) to the daughter spectrum produced by a standard solution of ethylene glycol (bottom of figure 4-1) acquired under identical conditions.

Figure 4-1 Comparison of daughter spectra from the $[M+H]^+$ (m/z 63) ion of ethylene glycol obtained from five handled glass beads (top mass spectrum) and standard ethylene glycol (bottom mass spectrum). Methane reagent gas was used for CI (at an indicated source pressure of 1700 mtorr). The CID gas was argon at an indicated pressure of 1.4-1.5 mtorr. The collision energy was 15 eV.

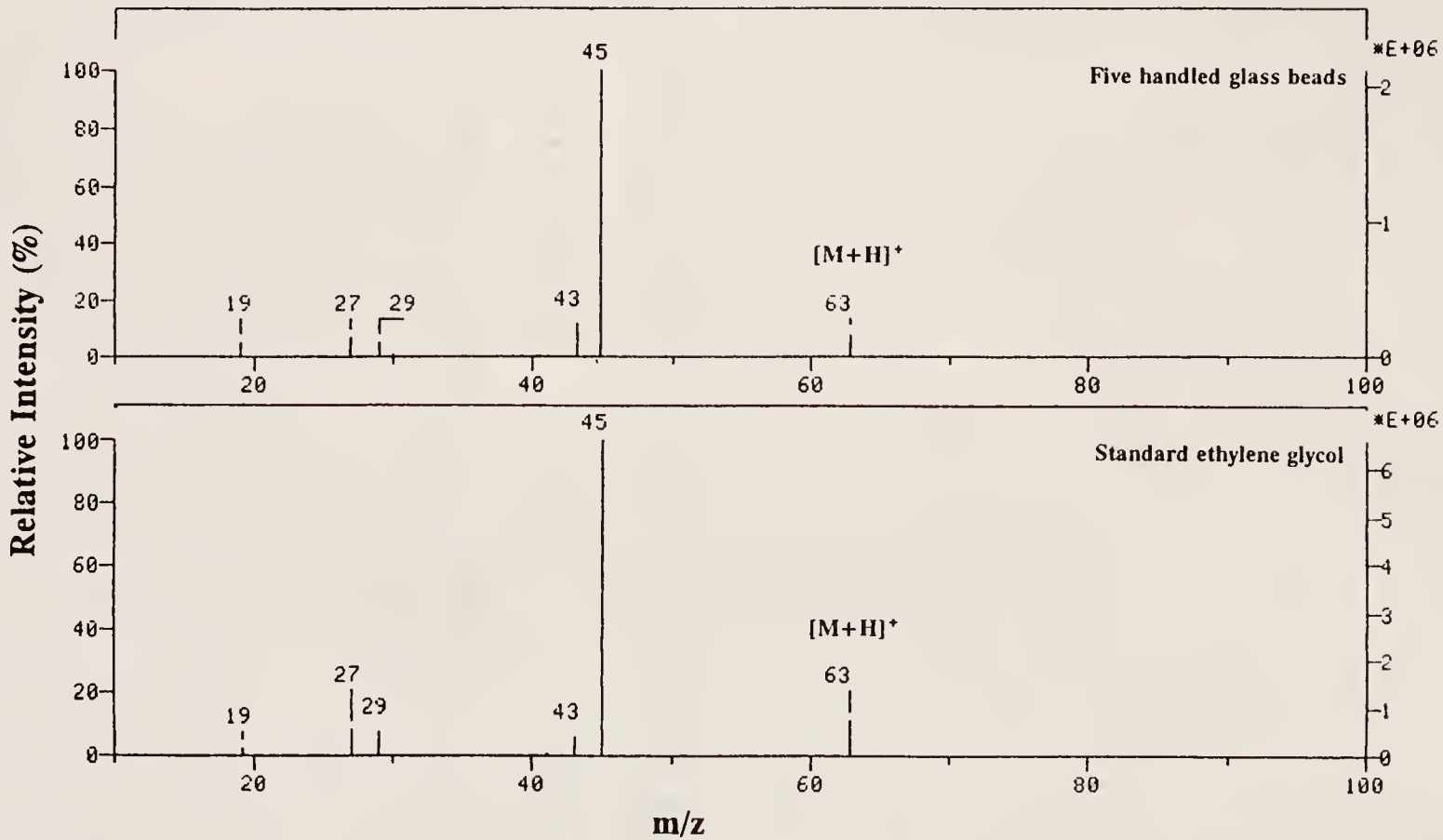
Relative Intensity (%)
Five handled glass beads
Standard ethylene glycol
[M+H]+
[M+H]+
*E+06
*E+06
45
45
19
27
29
43
63
19
27
29
43
63
m/z

This approach provided positive compound identification; however, it should be noted that analyses in this manner are tedious. Daughter spectra, once acquired, need to be interpreted to determine the suspected identity of the compound. To confirm the identity by comparison to standard, the standard which may not be readily available is necessary. Once the comparison is conducted, the daughter spectra may not match, leading to further examination and interpretation with subsequent comparisons to additional standards.

Another disadvantage to this method of compound identification, as stated earlier, is the presence of multiple compounds at any point in the desorption. It is therefore possible that a particular parent ion m/z may correspond to ions from more than one component (just as two or more components may coelute during GC operation). An example where the daughter spectrum includes ions from the parent ions of two components is shown in figure 4-2. Selection of negative ion at m/z 72 by Q1 and CID fragmentation produced a daughter spectrum revealing the presence of $^{35}Cl^-$ and $^{37}Cl^-$ isotope peaks, as well as losses of 30 Da, 28 Da, and 1 Da. The parent ion at m/z 72 thus includes both Cl_2^- and one (or more) other compounds.

There are some cases where spectral interpretation alone was used to identify compounds; the presence of most of these compounds was later confirmed by the GC/MS data contained in Chapter 5. The presence of propanoic acid (figure 4-3) and propenoic acid (figure 4-4) is easily determined. The $[M-H]^-$ ions of both compounds undergo a neutral loss of CO_2 (44 Da), which is characteristic of carboxylic acids (characteristic neutral losses will be discussed further in the next

Figure 4-2 Daughter spectrum of m/z 72. Fragmentation observed is from $^{35}Cl^{37}Cl^-$ and an additional compound. Methane reagent gas was used for CI (at an indicated source pressure of 1647 mtorr). The CID gas was Nitrogen at an indicated pressure of 1.97 mtorr. The collision energy was 9 eV.

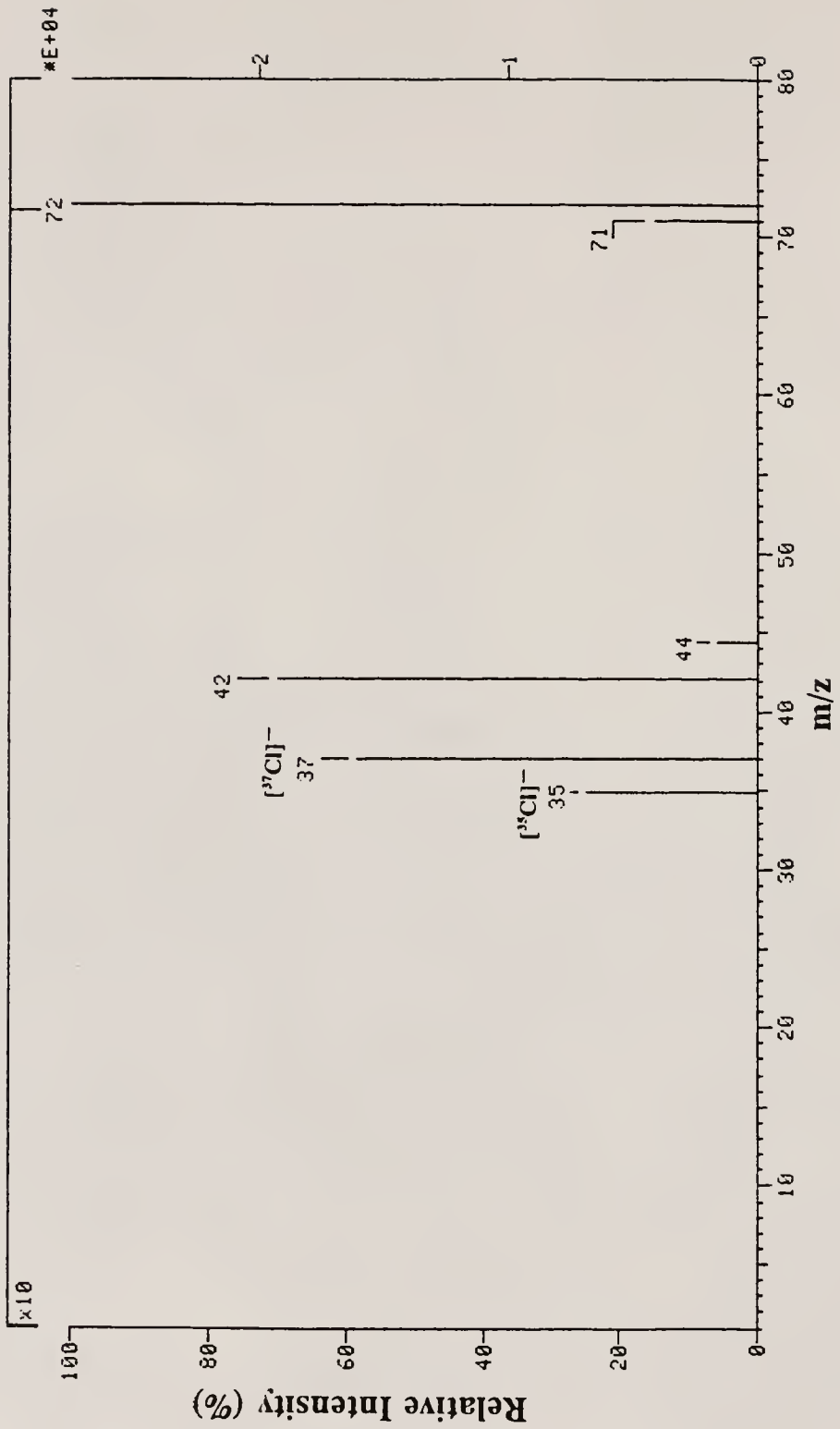
Relative Intensity (%)
m/z
[35Cl]−
35
[37Cl]−
37
42
44
71
72
×10
*E+04

Figure 4-3 Daughter spectrum of m/z 73, interpreted to be the $[M+H]^+$ ion of propanoic acid. Methane reagent gas was used for CI (at an indicated source pressure of 1647 mtorr). The CID gas was Nitrogen at an indicated pressure of 1.97 mtorr. The collision energy was 9 eV.

Relative Intensity (%)
m/z
[M-H]⁻
[M-H-CO]⁻
45
[M-H-CO₂]⁻
29
[M-H-H₂CO]⁻
[M-H-H₂O]⁻
55
100
80
60
40
20
0
10
30
40
50
60

Figure 4-4 Daughter spectrum of m/z 71, interpreted to be the $[M+H]^+$ ion of propenoic acid. Methane reagent gas was used for CI (at an indicated source pressure of 1647 mtorr). The CID gas was Nitrogen at an indicated pressure of 1.97 mtorr. The collision energy was 9 eV.

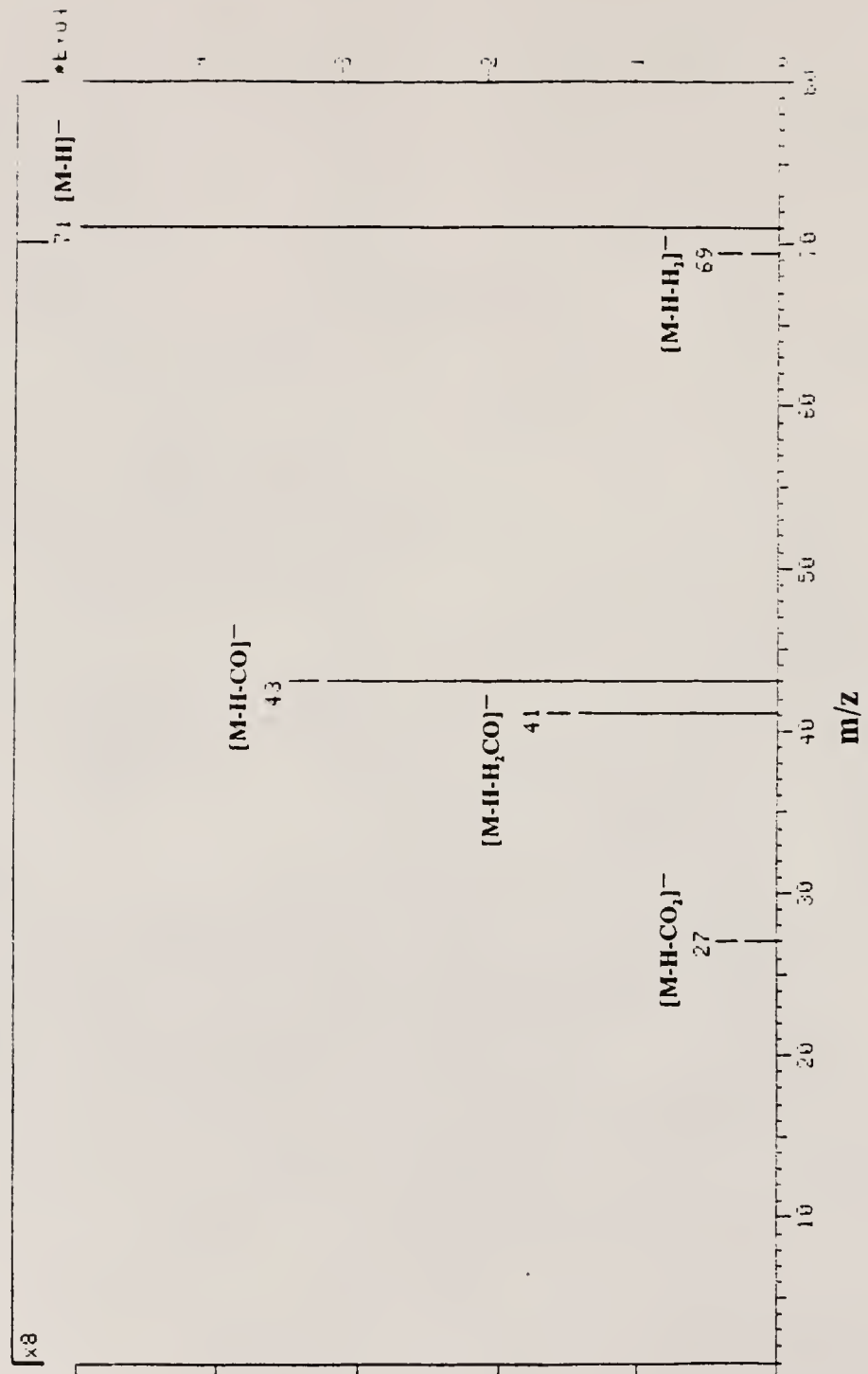
Relative Intensity (%)
m/z
[M-H]⁻
[M-H-CO]⁻
43
[M-H-H₂CO]⁻
41
[M-H-CO₂]⁻
27
[M-H-H₂]⁻
69
x8

section). Additionally, both compounds undergo neutral losses of CO (28 Da) and H_2CO (30 Da), further confirming the presence of a carboxylic acid functional group for both species.

Compounds identified or suspected by tandem mass spectrometric analysis are listed in table 4-1. Most of the compounds found to be present by analysis of daughter spectra were carboxylic acids. The saturated and unsaturated acids are well known to be present on the skin [30,31]. These compounds were readily identifiable; the most abundant species found when desorbed skin emanations are sampled from glass beads are carboxylic acids as shown in this chapter and Chapters 2 and 5. Due to the presence of methane CI adduct ions from lower carbon-number carboxylic acids continually being transferred to the ion source, interpretation of daughter spectra of the $[M+H]^+$ ions of carboxylic acids consisting of ten or greater carbons was ambiguous and speculative.

In addition, substituted acids, such as lactic acid, were found to be present. Lactic acid was the most abundant compound found in these analyses. Pyruvic acid was also suspected to be present. In negative ion analyses (NCI), the $[M-H]^-$ ion of lactic acid will undergo elimination of H_2 to form an ion at m/z 87, identical in m/z value to the pyruvate ion, the $[M-H]^-$ ion of pyruvic acid. Inspection of mass chromatograms from NCI with single stage detection clearly showed that the thermal desorption profile of m/z 87 contained the profile of the m/z 87 ion produced from the lactic acid deprotonated molecule (m/z 89) as well as a profile depicting m/z 87 resulting from an additional source. Analysis of this region by NCI combined

Table 4-1 Compounds suspected or identified as emanating from the skin. Analysis by MS/MS without prior separation, as described in the text, was used to compile this list; confirmation by other experiments in this dissertation and published reports is indicated.

Compound	Confirmation source
Ethylene glycol	Chapter 5
Phenol	Reference 30, Chapter 5
Cholesterol	Chapter 5
Butanoic acid	Reference 30, Chapter 5
Pentanoic acid	References 30 and 31, Chapter 5
Propanoic acid	Reference 30, Chapter 5
Propenoic acid	Chapter 5
Hexanoic acid	References 30 and 31, Chapter 5
Hexenoic acid	References 30 and 31, Chapter 5
Heptanoic acid	References 30 and 31, Chapter 5
Heptenoic acid	References 30 and 31, Chapter 5
Decanoic acid	References 30 and 31, Chapter 5
Lactic acid	Reference 5, Chapters 2 and 5
Oxalic acid	Chapter 5 (Table 5-1)
Tartaric acid	Chapter 5 (Table 5-1)
Pyruvic acid	Chapter 5 (Table 5-1)

with CID yielded a daughter spectrum that can be interpreted as the $[M-H]^-$ ion of pyruvic acid due to the similarity of fragmentation to that of the $[M-H]^-$ ion of lactic acid.

The remainder of the compounds identified by this technique contain an alcohol moiety. Phenol and ethylene glycol were identified by comparison of daughter spectra from skin emanations to daughter spectra of $[M-H]^-$ ions of the pure standards acquired under identical conditions. The presence of cholesterol was suspected mainly due to the presence of m/z 385 under NCI conditions, and the neutral loss of 18 Da from CID of the m/z 387 $[M+H]^+$ parent ion.

Daughter Library

The initial driving force behind compiling a library of daughter spectra was to aid in the determination of compounds by MS/MS. The library itself is made up of numerous classes of compounds, some multi-class, and some containing two or more functional groups of the same class. Compilation of an extensive library for work in this dissertation was not necessary due to the nature in which the library was ultimately used. The information derived from the tabulated library data was used to aid in rapid screening by MS/MS rather than, as originally planned, extensive identification of compounds by MS/MS.

The MS/MS trends observed for the positive and negative ion CI parent ions of the compounds tested are listed in Table 4-2; some of these observations will be discussed in the text following this paragraph. This table contains fragmentation and

Table 4-2 Characteristics of compound classes under MS/MS conditions of 15 eV collision energy and 1.5 mtorr argon in the collision cell. Table consists of MS/MS data from 40 compounds containing functional groups listed in the table. Parent ions formed by methane CI and selected for fragmentation were the $[M+H]^+$ protonated molecular species, the $[M-H]^-$ hydride abstracted molecular species, and the $[M-H]^-$ proton abstracted molecular species.

Compound Class	Parent Ion	MS/MS Characteristics
Alkenes (10 or more carbons)	$[M+H]^+$	Intensity of the remaining parent ion is less than 1% relative abundance (RA) Base peak usually at m/z 57 Absence of small neutral losses less than 12 Da Series of successive neutral losses of 14±1 Da
	$[M-H]^+$	Base peaks usually at m/z 55 Absence of small neutral losses less than 12 Da Series of successive neutral losses of 14±1 Da
	$[M-H]^-$	No $[M-H]^-$ ion formed by NCI
Alkanes (10 or more carbons)	$[M+H]^+$	Intensity of the remaining parent ion is less than 1% RA Base peak usually at m/z 57 Absence of small neutral losses less than 12 Da or when present less than 1% RA Series of successive neutral losses of 14±1 Da
	$[M-H]^+$	Intensity of the parent ion is less than 1% RA Base peak usually at m/z 57 Absence of small neutral losses less than 12 Da or when present less than 1% RA Series of successive neutral losses of 14±1 Da Variation from 14 Da is more prevalent for lower m/z fragments
	$[M-H]^-$	No $[M-H]^-$ ion formed by NCI
Aldehydes	$[M+H]^+$	Small neutral loss of 2 Da at less than 2% RA from the parent ion Neutral losses of 26-30 Da produce the most abundant daughter ions Presence of daughter ions at m/z 39 and m/z 19 in most cases Presence of m/z 31 daughter ion at 90-100% RA

Table 4-2 continued

Compound Class	Parent Ion	MS/MS Characteristics
Aldehydes	$[M-H]^+$	Small neutral loss of 1 Da from the parent ion at less than 2% RA Neutral losses of 26-30 Da produce the most abundant daughter ions Similar daughter ions produced from $[M-H]^+$ are lower in RA to those produced from $[M+H]^+$ Presence of daughter ions at m/z 39 and m/z 19 in most cases
	$[M-H]^-$	Base peak is the parent ion except when attached to a phenyl (base peak is m/z 77) Neutral loss of 28 Da (CO) produces a daughter ion at 50-100% RA Presence of daughter ion at m/z 17 may be observed
Ketones	$[M+H]^+$	Base peak appears at lower m/z as substitution or chain length is increased Neutral loss of 42 Da produces a daughter ion at 5-100% RA, the RA increases with increased branching Neutral loss of 30 Da (H_2CO) produces a daughter ion at 1-60% RA Neutral loss of 28 Da (CO) produces a daughter ion at 10-100% RA Neutral loss of 18 Da (H_2O) produces a daughter ion at 10-100% RA Presence of daughter ion at m/z 33 in most cases
	$[M-H]^+$	Base peak is at m/z 43 except for the case of acetone Neutral loss of 42 Da produces a daughter ion at 5-100% RA, the RA with increases with increased substitution Neutral loss of 30 Da (H_2CO) produces a daughter ion at 1-60% RA Neutral loss of 28 Da (CO) produces a daughter ion at 10-100% RA Neutral loss of 18 Da (H_2O) produces a daughter ion at 10-100% RA Presence of daughter ion at m/z 31 in most cases
	$[M-H]^-$	Base peak is the parent ion for less substituted ketones, and decreases in RA as substitution or chain length increases Small neutral loss of 1 Da from the parent ion at less than 2% RA Presence of m/z 41 daughter ion at 20-70% RA

Table 4-2 continued

Compound Class	Parent Ion	MS/MS Characteristics
Carboxylic Acids	$[M+H]^+$	For acids of 10 or more carbons, base peak is located between m/z 57 and m/z 121, with intense daughter ions (greater than 10% RA) at m/z 121,103,97,95,85,83,81, 71,69,57, and 43 in most cases Neutral loss of 46 Da frequently observed Neutral losses of 1-2 Da (1% RA) from acids and di-acids of four or less carbons Presence of a daughter ion at m/z 43 at 10-50% RA
	$[M-H]^+$	For acids of 10 or more carbons, base peak is located between m/z 43 and m/z 121, with intense daughter ions (greater than 10% RA) at m/z 121,101,97,95,83,81, 69,67,57,55, and 43 in most cases Neutral loss of 18 Da at up to 35% RA, more prevalent in longer chain di-acids Neutral losses of 1-2 Da (1% RA) from acids and di-acids of four or less carbons Presence of m/z 43 daughter ion at 10-50% RA
	$[M-H]^-$	Base peak is usually either the parent ion or the daughter ion from the neutral loss of 44 Da Neutral loss of 44 Da is less predominant as the relative molecular mass increases Neutral losses of 1-2 Da (1% RA) from acids and di-acids of four or less carbons
Alcohols	$[M+H]^+$	Intensity of parent ion is at 5-20% RA Significant neutral loss of 18 Da, frequently forms the base peak Base peak for diols and triols is produced from the neutral loss of 36 Da Presence of daughter ion at m/z 19 ion frequently observed
	$[M-H]^+$	Intensity of parent ion is at 5-20% RA Significant neutral loss of 18 Da, frequently forms the base peak Base peak for diols and triols is produced from the neutral loss of 36 Da Presence of daughter ion at m/z 19 ion frequently observed

Table 4-2 continued

Compound Class	Parent Ion	MS/MS Characteristics
Alcohols	$[M-H]^-$	Intensity of parent ion is 5-20% RA, except for phenol where the parent ion is the base peak Neutral loss of 2 Da produces the base peak for straight chain alcohols Presence of daughter ion at m/z 17 ion frequently observed
Amines	$[M+H]^+$	Intensity of parent ion is at 15-100% RA Neutral loss of 17 Da from parent ions frequently yields the base peak Presence of m/z 33 ion at 1-25% RA Presence of m/z 18 daughter ion at 10-20% RA
	$[M-H]^+$	Intensity of parent ion is at 15-100% RA Neutral loss of 17 Da from parent ions frequently yields the base peak Presence of m/z 33 daughter ion at 1-25% RA
	$[M-H]^-$	Intensity of parent ion is at 15-100% RA
Amino Acids	$[M+H]^+$	Neutral loss of 46 Da produces the base peak
	$[M-H]^+$	Neutral loss of 46 Da usually produces the base peak
	$[M-H]^-$	Base peak is the parent ion Presence of m/z 17 daughter ion seen frequently at less than 5% RA
Aromatics	$[M+H]^+$	Base peak is either at m/z 77 or m/z 79 except for acetophenone (m/z 43) and benzamide (m/z 105) Neutral loss of 78 Da is typically seen resulting in a fragment at 1-10% RA Small neutral losses of 1-2 Da from are frequently seen at less than 2% RA Aromatic pattern of daughter ions, eg. m/z 65 and m/z 51 at less than 10% RA

Table 4-2 continued

Compound Class	Parent Ion	MS/MS Characteristics
Aromatics	$[M-H]^+$	Base peak is either m/z 77, m/z 79, or m/z 91 Small neutral losses of 1-2 Da from are frequently seen at less than 2% RA Aromatic pattern of daughter ions, eg. m/z 65 and m/z 51 at less than 10% RA
	$[M-H]^-$	Daughter ions at m/z 77 or m/z 75 yield the base peak except for amide attachment where m/z 77 is present but the base peak is due to the amide group
Nitriles/ Cyanides	$[M+H]^+$	No observable characteristics from samples examined
	$[M-H]^+$	Neutral loss of 26 Da at approximately 50% RA Neutral loss of 27 Da at approximately 20% RA
	$[M-H]^-$	No observable characteristics from samples examined

neutral loss data from selected parent ions; the parent ions surveyed are the methane CI produced $[M+H]^+$, $[M-H]^+$, and $[M-H]^-$ ions of each tested compound. The inclusion of information in the table is by no means a statement that all compounds within a class will exhibit the same trend. Additionally, the trends observed here were determined for a specific set of CID conditions. Exclusion of trends from the table for a parent ion of a class of compounds is due to the inability to find an observable trend and/or due to insufficient data from the analyses. The purpose of this table is to provide a foundation for screening different classes within a sample. Identification of compounds can then be carried out by GC/MS employing CI and EI analysis with the screening information aiding as a preview of classes present.

The first two classes listed in table 4-2 are the alkanes and alkenes. The information for their inclusion in the table was derived from the MS/MS analyses of straight chain aliphatics as well as compounds containing an alkyl chain attached to a functional group. One of the more significant indications of the presence of these classes is the existence of the $[M+H]^+$ ion under PCI and the inability to form the deprotonated $[M-H]^-$ ion under NCI conditions. Simple alkanes and alkenes are not easily deprotonated, even by the strongest reagent bases, due to their weakly acidic nature [74,96]. In these experiments, proton abstraction from simple alkanes did not occur with methane reagent gas. An additional characteristic is the successive neutral losses of approximately 14 Da. This trend is also observed for alkyl chains attached to various functional groups. There are mass spectrometric methods for

determining double bond positions and differentiating isomers [97-101]. These, however, were not used in these studies.

The PCI parent ions of the examined aldehydes fragmented predominantly by even neutral losses of 26, 28, and 30 Da. These losses have been attributed to losses of ethene, carbon monoxide, and formaldehyde, respectively. Additionally, fragment ions were observed at m/z 39 ($C_3H_3^+$) and m/z 19 (H_3O^+). Daughter spectra produced from the selected $[M+H]^+$ ion contained an intense ion at m/z 31 (CH_3O^+). Analysis of daughter spectra of the $[M-H]^-$ ion revealed, in most cases, the base peak as the selected parent ion, except in the case of benzaldehyde. A neutral loss of 28 Da (CO) from the $[M-H]^-$ ion occurs and the OH^- ion, at m/z 17, may be present.

The $[M+H]^+$ and $[M-H]^+$ ions of the ketones (all methyl ketones in this study) fragmented by even neutral losses of 42, 30, 28, and 18 Da. These neutral losses are similar to those of the aldehydes; therefore, differentiation between these classes may not be possible using the rules from these analyses. An ion at m/z 33, most likely protonated methanol, was produced from the $[M+H]^+$ ion in most cases; an ion at m/z 31, most likely deprotonated methanol, was produced from the $[M-H]^+$ ion in most cases (as was also the case for the aldehydes). The negative ion fragmentations were also similar to those of the aldehydes, except for the presence of an ion at m/z 41 ($CHCO^-$).

The most studied class in the library and table are the carboxylic acids; this stems from earlier analyses demonstrating the abundance and frequency of acids on

the skin. In the PCI mode, a neutral loss of 46 Da (formic acid) from the $[M+H]^+$ ion is commonly observed. There are small neutral losses of 1-2 Da observed from both selected parents produced by PCI, as well as the $[M-H]^-$ parent ion, produced by NCI. The most indicative evidence for the presence of a carboxylic acid comes from the analysis of negative ions. A neutral loss of 44 Da (CO_2) is very common and abundant. This neutral loss often produces the base peak in the negative ion daughter spectrum. Unfortunately, as the relative molecular mass of the acid increases, the fragment ion resulting from this neutral loss is less prominent. The presence of ions at m/z 60 and m/z 73 (McLafferty rearrangement ions) in EI mode and m/z 74 from PCI with single stage detection can then be used to indicate the presence of acids; this is examined in Chapter 5.

The alcohols, in positive ion mode, exhibit a significant neutral loss of 18 Da (H_2O), which may be the base peak in daughter spectra. The base peak of PCI daughter spectra from diol and triol parent ions was the fragment ion which resulted from the neutral loss of 36 Da (two water molecules). The presence of a daughter ion at m/z 19 $(H_3O)^+$ was also observed in almost all PCI produced daughter spectra. An indicator of straight chain alcohols in the negative ion mode is the presence of the base peak formed by a neutral loss of 2 Da (H_2). Additionally, a fragment ion at m/z 17 (OH^-) is commonly observed.

The examined amines demonstrated an odd neutral loss of 17 Da (NH_3) in the positive ion mode. This loss commonly formed the base peak of the daughter spectra. Additionally, an ion at m/z 18 (NH_4^+) may be present in the PCI daughter

spectra. The cyanides/nitriles located at the end of the table also exhibit an odd neutral loss of 27 Da, as well as an even neutral loss of 26 Da from the hydride abstracted $[M-H]^+$ parent ion. Both of these classes, which contain a nitrogen in the functional group, did not reveal an observable trend from the $[M-H]^-$ parent ions. The amino acids did, however, provide information in the negative ion mode due to the presence of the carboxylic functional group. The OH^- daughter ion at m/z 17 was from the $[M-H]^-$ parent ion; a neutral loss of 46 Da (formic acid) occurred from the $[M+H]^+$ and $[M-H]^+$ parent ions.

The final class to be addressed in the table is the aromatics (i.e. monosubstituted benzenes) for these studies. The base peak in almost all cases was due to the phenyl group. A neutral loss of 78 Da (benzene) was typically seen in daughter spectra produced from the $[M+H]^+$ ion. Additionally, in positive ion mode, the daughter spectra exhibit the fragmentation pattern of benzene commonly seen in EI mass spectra.

The information addressed above and found in table 4-2 can now be applied to screening a complex sample. A summary of characteristic neutral losses, derived from the information in table 4-2, appears in table 4-3. The neutral losses are listed (in order of increasing mass) as well as the classes found to be associated with these neutral losses. There is some ambiguity associated with most neutral losses, i.e. more than one functional group may produce a particular neutral loss. It should be reiterated that not all compounds within a given class may exhibit these neutral losses. Additionally, trace components may be difficult to detect with this screening

Table 4-3 Characteristic neutral losses of compound classes.

Neutral loss (Da)	PCI produced parent ion	NCI produced parent ion
1	aldehydes, carboxylic acids, aromatics	ketones, carboxylic acids
2	aldehydes, carboxylic acids, aromatics	carboxylic acids, alcohols
14	alkanes, alkenes, alkyl chains	
17	amines	
18	ketones, carboxylic acids, alcohols	
26	aldehydes, cyanides/nitriles	
27	cyanides/nitriles	
28	aldehydes, ketones, carboxylic acids	aldehydes
30	aldehydes, ketones, carboxylic acids	
36	alcohols (diols, triols)	
42	ketones	
44		carboxylic acids
46	carboxylic acids, amino acids	
78	aromatics	

method, given the lack of chromatographic separation as well as the transmission losses through an additional mass-filtering quadrupole and the less-than-unit efficiency of CID.

Compound Class Screening

An example of the information obtained by GC/MS/MS neutral loss scans for screening a complex sample (8 handled glass beads) is shown in figure 4-5. Depicted are the reconstructed ion chromatograms for the neutral losses of 46 Da (top), 30 Da (middle), and 18 Da (bottom) from positive ions. The neutral loss of 46 is indicative of carboxylic acid presence. The RIC traces for neutral losses of 30 Da and 18 Da confirm that these peaks found in the top trace are acids. There are some additional GC peaks found in the neutral loss of 30 Da and neutral loss of 18 Da chromatograms which do not match up to the peaks found in the top chromatogram. These peaks, according to the table 4-3, are most likely due to aldehydes and/or ketones for a neutral loss of 30 Da; the additional GC peaks in the neutral loss of 18 Da chromatogram arise from the presence of ketones and/or alcohols. A final note pertaining to these chromatograms is that the major peaks are those of acids (confirmed in Chapter 5). The pattern of peaks is similar to that seen in the GC/MS analyses conducted in Chapter 5 due to the abundance of carboxylic fatty acids in the sample.

The most abundant GC peak in figure 4-5 is centered approximately at scan 1675. The neutral loss mass spectrum for a neutral loss of 18 Da of this peak is

Figure 4-5 RIC traces for positive ion neutral losses of 46 Da, 30 Da, and 18 Da from 8 handled glass beads.

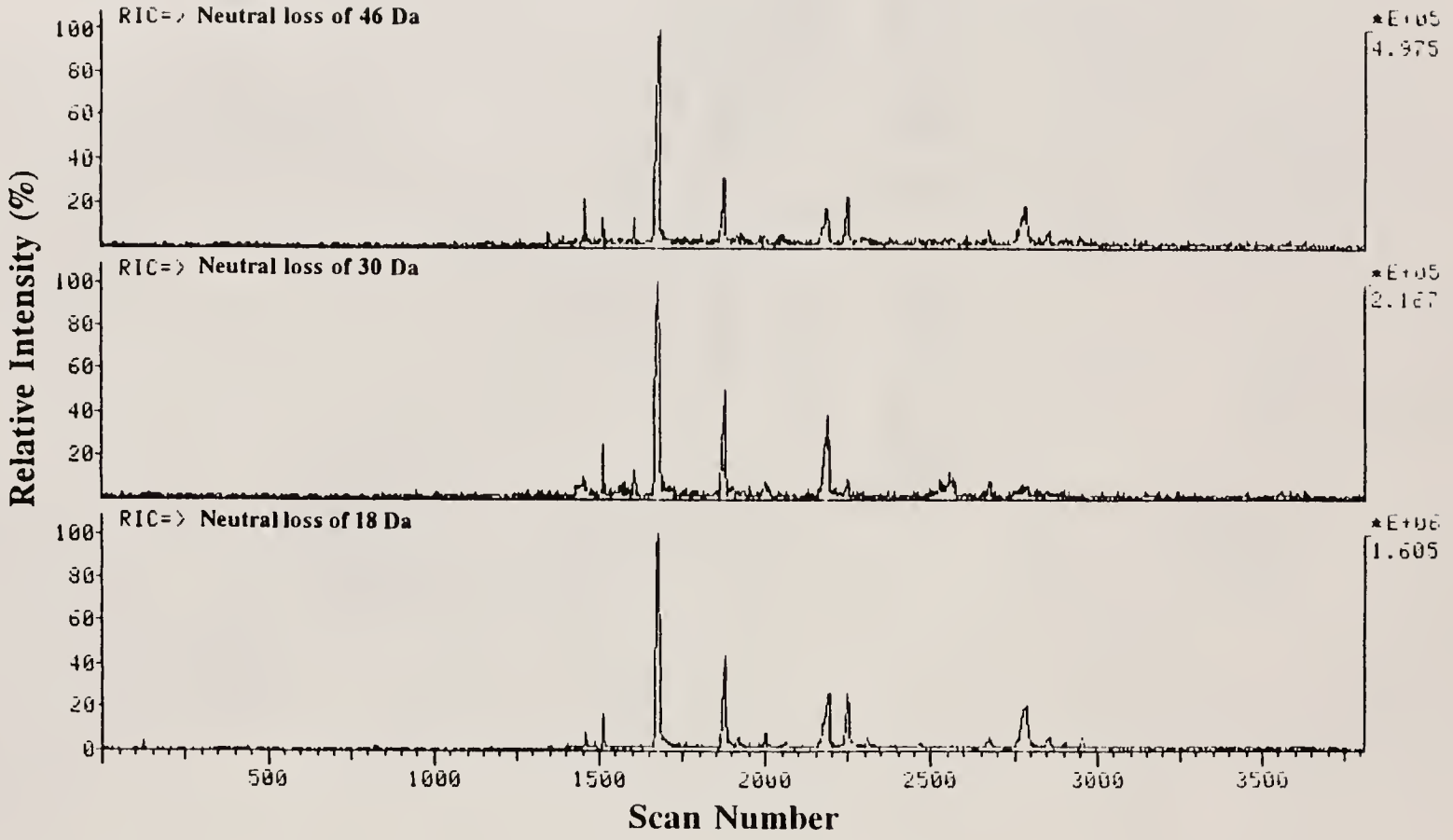
RIC=> Neutral loss of 46 Da
*E+05
4.975
RIC=> Neutral loss of 30 Da
*E+05
2.167
RIC=> Neutral loss of 18 Da
*E+06
1.605
Relative Intensity (%)
100
80
60
40
20
0
500
1000
1500
2000
2500
3000
3500
Scan Number

displayed in figure 4-6. The mass spectrum contains the m/z of ions passed by Q1 into Q2, which fragmented by collision-induced dissociation to form ions detected by Q3 as 18 Da lower in mass than the ions transmitted by Q1. The actual assignment of the m/z 199 to be the $[M-H]^+$ ion of dodecanoic acid could only be speculated at the time these experiments were conducted. The confirmation, both by GC retention time and by PCI and EI spectra is located in Chapter 5. Note that in addition to the $[M-H]^+$ ion, PCI of dodecanoic acid produces a number of other ions which undergo a neutral loss of H_2O, including the $[M+H]^+$, $[M-H-(CH_2)_n]^-$, $[M-H-H_2O]^-$, and $[M-H-H_2O-(CH_2)_n]^-$ ions at m/z 201, the series of m/z 185,171,157, . . ., the m/z 181 ion, and the series of m/z 167, 153, 139, 125, . . ., respectively.

The last peak in the neutral loss of 18 Da chromatogram (scan number 2780) is also presented in this chapter as figure 4-7. As with the previous case, knowledge of retention time as well as information from Chapter 5 aids in drawing the conclusion that this peak is due to octadecanoic acid. This is the last visible peak in the chromatogram; therefore, additional acids of higher m/z in this series are either absent or are at a trace level not detectable by these experiments.

The identification of the peak corresponding to lactic acid was straightforward, even without confirmation from GC/MS. Lactic acid has been used throughout this dissertation as the model or target compound for various applications due mainly to its characteristic being the only previously known attractant to *Aedes aegypti*. Additionally, it is typically the most abundant compound found emanating from the skin throughout the work for this dissertation. The neutral loss spectra examined in

Figure 4-6 Examination of the largest GC peak in figure 4-5 which undergoes a neutral loss of 18 Da (approximately scan number 1675). The m/z 199 ion is attributed to the $[M-H]^+$ ion of dodecanoic acid.

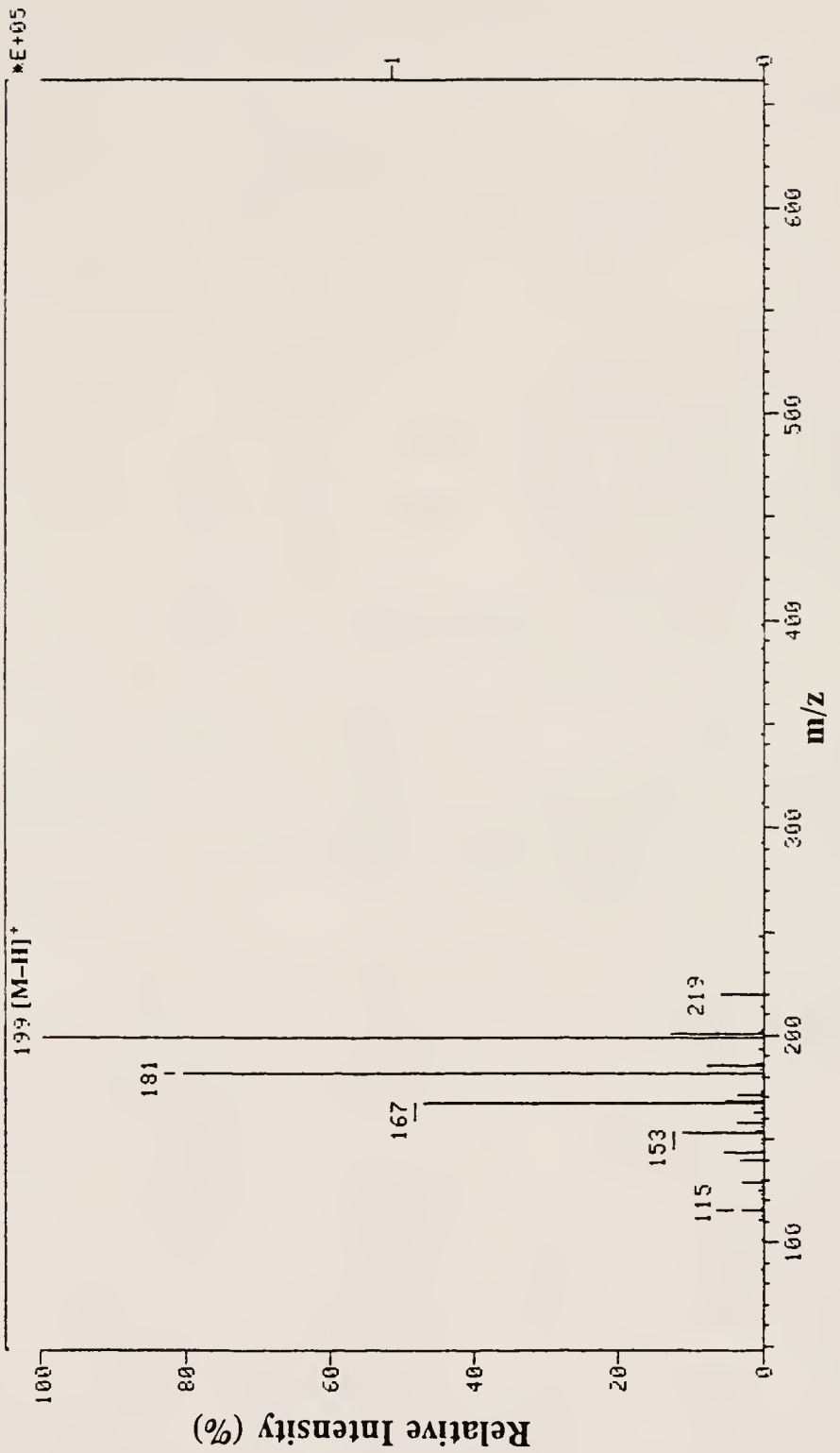
Relative Intensity (%)
m/z
199 [M-H]+
181
167
153
115
219
*E+05
100
80
60
40
20
0
100
200
300
400
500
600

Figure 4-7 Examination of the peak at approximate scan number 2780 in figure 4-5. The examined mass spectrum is that of a neutral loss of 18 Da. The m/z 283 ion is attributed to the $[M-H]^+$ ion of octadecanoic acid.

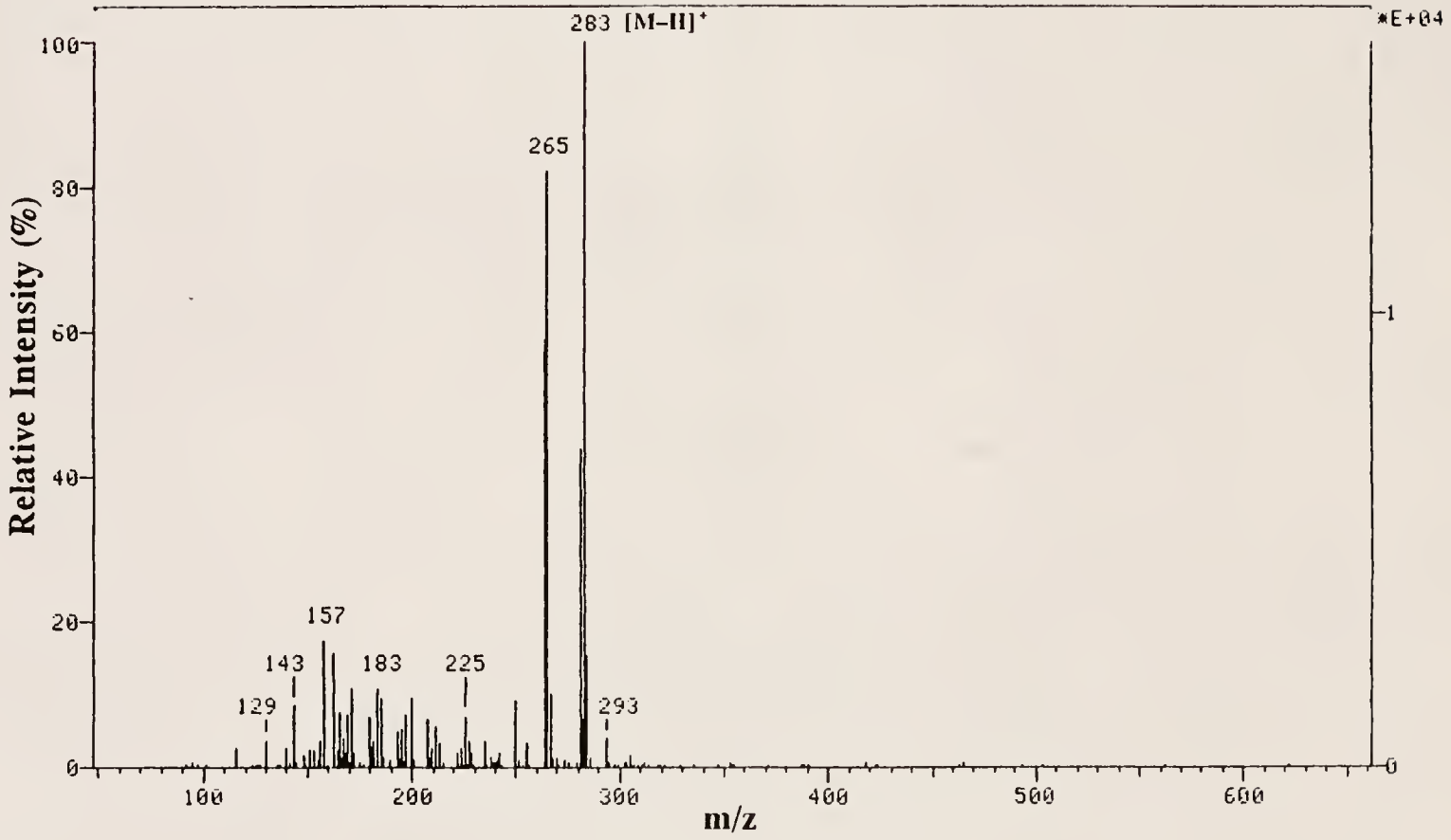
283 [M-H]+
*E+04
100
80
60
40
20
0
Relative Intensity (%)
265
157
143
183
225
129
293
1
0
100
200
300
400
500
600
m/z

this section exhibit the most abundant peaks to be those of fatty acids rather than lactic acid. It is known from previous work in Chapter 3 that lactic acid will undergo a neutral loss of 18 Da (H_2O) from the $[M+H]^+$ ion. Therefore, the presence of an ion at m/z 91 in the neutral loss (of 18 Da) spectra from these analyses should be readily be observed. Figure 4-8 reveals the location of what is suspected to be lactic acid in these experiments. This can be confirmed by comparing the retention times to those acquired under the same GC conditions in Chapter 5. It is interesting to note (from the RIC trace in figure 4-8), that lactic acid appears to be less abundant than the fatty acids. The experiments for figures 4-5 through 4-7 were conducted in December, a relatively cold month. Therefore, lactic acid may not be as prevalent on the skin as it would be were the temperature warmer.

These experiments were repeated a month later under warmer weather conditions as well as after physical exertion to produce a greater amount of perspiration on the skin for subsequent sampling. Comparing the RIC for a neutral loss of 18 Da in figure 4-9 (bottom trace) to that of figure 4-8 (bottom trace), it is quite evident that lactic acid is the most abundant compound in this second sample. Included at the top of figure 4-9 is the chromatogram for the neutral loss of 28 Da (CO) from the m/z 91 ion, additionally providing confirmation that this is lactic acid. The final figure (4-10) confirms this; this is the neutral loss of 44 Da mass spectrum in the negative ion mode from the peak centered around scan 1480. Present are the $[M-H]^-$ ion of lactic acid at m/z 89, which loses CO_2 to form m/z 45, as well as the

Figure 4-8 RIC traces of the neutral loss of 18 Da corresponding to the lactic acid $[M+H]^+$ ion (m/z 91) (top trace) and the RIC of the sample (bottom trace).

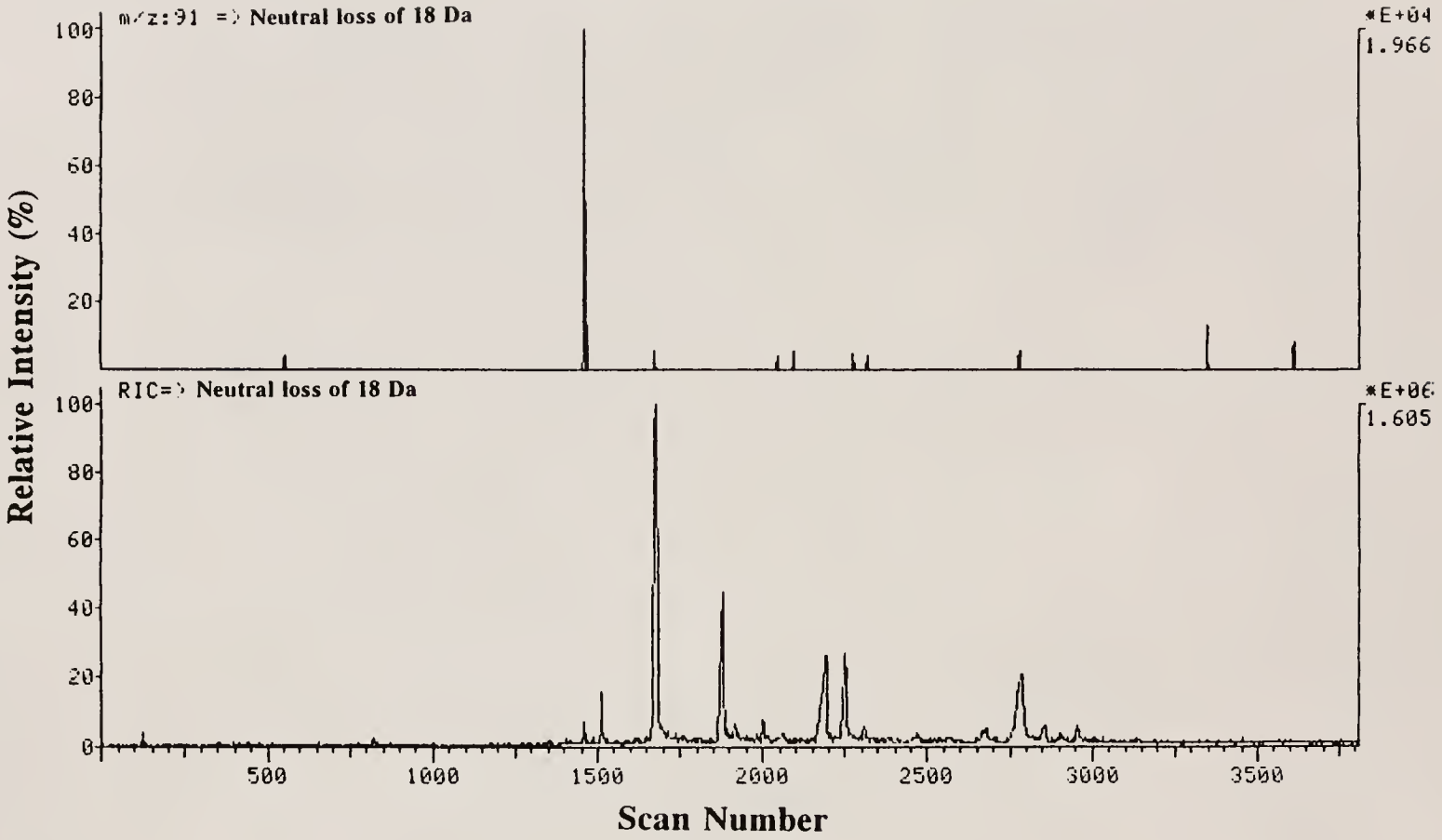
m/z:91 => Neutral loss of 18 Da
*E+04
1.966
RIC=> Neutral loss of 18 Da
*E+06
1.605
Relative Intensity (%)
100
80
60
40
20
0
500
1000
1500
2000
2500
3000
3500
Scan Number

Figure 4-9 Examination of the lactic acid peak via the neutral loss of 28 Da from the $[M+H]^+$ (m/z 91) ion of lactic acid (top trace) and the RIC from the sample (bottom trace).

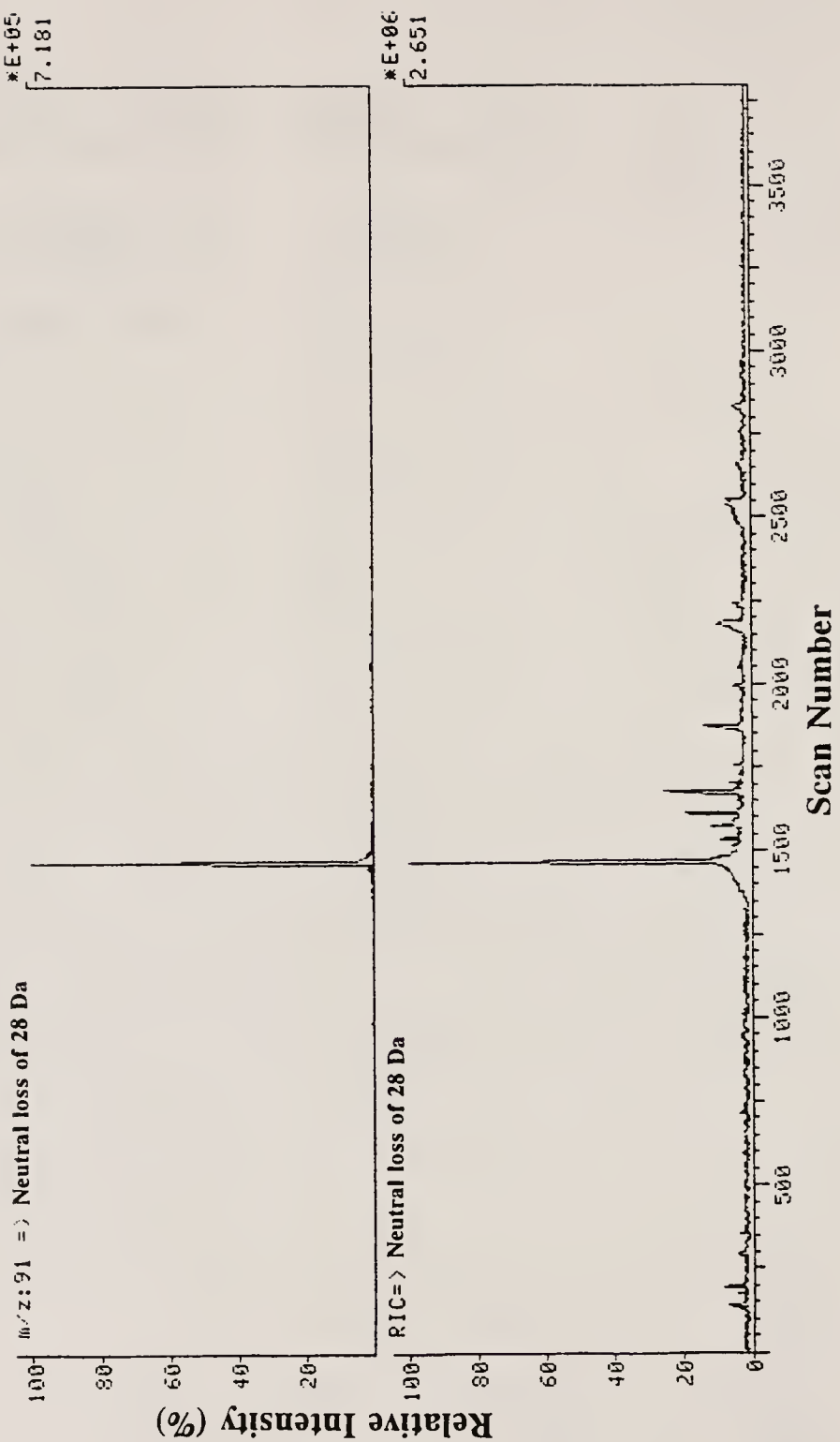
*E+05
7.181
m/z:91 => Neutral loss of 28 Da
*E+06
2.651
RIC=> Neutral loss of 28 Da
Relative Intensity (%)
Scan Number

Figure 4-10 Neutral loss spectrum of 44 Da, in negative ion mode, of the peak corresponding to the lactic acid $[M-H]^-$ at m/z 89.

Relative Intensity (%)
100
80
60
40
20
0
89 [M-H]-
194
100
200
300
400
500
600
m/z
1
E+04

m/z 87 ion corresponding to H_2 elimination from lactate with subsequent loss of CO_2 to form the m/z 43 ion.

The examples described in this section were successful in terms of determining the compounds present. The intended use of the MS/MS neutral loss scans is to provide information about compound classes present. The manner in which this will be presented for this dissertation is by determining the GC peaks observed for a particular neutral loss. The frequency of relatively intense GC peaks is reported; however, overlap exists between compound classes due to similar neutral losses for certain classes. The results are listed in table 4-4, arranged by frequency of GC peaks in each neutral loss spectrum, as well as attributing the loss to possible compound classes. If experiments were not conducted for a particular neutral loss, such is listed in the table.

Conclusions

The use of tandem mass spectrometry allowed for the identification, without GC separation, of highly volatile compounds desorbed from handled glass beads. This method did not allow for further identification of less volatile components due to poor temporal resolution from the sampling system as well as the inefficient removal of volatilized compounds from the sample apparatus. Sixteen compounds were identified using this method; most of these have been confirmed in the literature and/or by experiments in the next chapter.

Table 4-4 Frequency of observed GC peaks for particular neutral losses and possible compound classes which contribute to these observed neutral losses. The frequency corresponds only to those GC peaks which are directly observable in the chromatograms; therefore, the actual frequency may be higher at the trace level. The mode corresponds to analysis of positive ions (P) or negative ions (N).

Frequency	Neutral loss (mode)	Possible classes
21	1 (P)	carboxylic acids, aldehydes, ketones
20	28 (P)	carboxylic acids, aldehydes, ketones
16	18 (P)	carboxylic acids, ketones, alcohols
15	46 (P)	carboxylic acids, amino acids
12	30 (P)	carboxylic acids, aldehydes, ketones
12	1 (N)	carboxylic acids, ketones
11	2 (P)	carboxylic acids, aldehydes, aromatics
11	2 (N)	carboxylic acids, alcohols
9	44 (N)	carboxylic acids
8	14 (P)	alkanes, alkenes, alkyl chains
7	26 (P)	aldehydes, cyanides/nitriles
2	17 (P)	amines
2	78 (P)	aromatics
not tested	27 (P)	nitriles
not tested	36 (P)	diols, triols
not tested	42 (P)	ketones

Further use of tandem mass spectrometry for compound identification necessitated the compilation of a library of daughter spectra from CI produced parent ions of standard compounds. The library provided the trends for compound class screening used in the following section. The examples chosen for inclusion in this dissertation were straightforward with respect to identifying the compound present. In most cases, the identification of the compound present is not as straightforward; rather, the information obtained from screening proves most useful for identifying compound classes present. The complexity of the skin emanation samples, combined with the desire to identify unexpected (rather than targeted) compounds prompted further studies to emphasize GC/MS analyses, as summarized in Chapter 5.

CHAPTER 5
IDENTIFICATION OF SKIN EMANATIONS

Introduction

This chapter addresses issues concerning emanations from the skin. The practical aspects of CI and EI analyses, as they pertain to this work, will be presented in this section. The results cover the qualitative identification of components which are detectable via desorption from handled glass beads. Two case studies are presented involving human subjects. The first study compares differences in the mass spectra of two human subjects who differ significantly in their attraction of mosquitoes. The second case study will compare results obtained from the mass spectra of handled beads to the attraction reported by bio-assay in an olfactometer for samples collected on different days from the same human subject.

Sample Introduction and Separation

The concerns regarding sample introduction were partially addressed in Chapters 1 and 2. The most important criterion was detection with as little sample modification as possible, mimicking the response of mosquito chemosensilla to volatilized compounds. Due to this principle, methods involving dissolution of emanations into solvents were avoided; this limited the possibility of discriminating

against specific classes or components. Recent experiments comparing the collection of extracts with isopropyl alcohol from the fingers of adults and children were reported in the literature [102]. This method of collection was reported to provide more material than extraction of fingerprints from glass; however, the time delay regarding collection of prints from glass was not reported. Sampling from glass, as was done in this work, provides a discriminating benefit with respect to attractant analysis. It is known that attractive emanations will be transferred to glass, and from observed mosquito attraction to glass, these compounds will evaporate providing a directional attraction of mosquitoes to the glass surface. The use of glass beads allows for preferential concentration of oily/waxy material over that of aqueous perspiration. The work contained in Chapter 3 demonstrated the low amounts of components present in the aqueous phase of perspiration.

Desorption from multiple beads (in this method) involves heating these beads in a GC injection port. Three handled glass beads (2.9 mm diameter) provided enough sample to detect readily carboxylic acids, as well as many components of lower abundance in the sample. The use of five or more beads has saturated the ion source upon the elution of acids. The GC injection port provides a closed chamber for volatile samples to expand whether samples are injected or introduced as described in this work. The injection port is designed to rapidly move components onto the column via a carrier gas. The major difference between sampling beads in an injection port and in an olfactometer is the rapid heating of the beads in the GC

injection port rather than evaporation at ambient temperature in the olfactometer port.

In the initial stages of this project, the separation process employed relatively short column lengths (approximately 15 m). The stationary phases ranged from a highly nonpolar column (DB-5) to a polar column (Carbowax). The abundant acids in the sample were better chromatographed on the Carbowax column, i.e. the peak profiles were more Gaussian. The limitations of these analyses were two-fold. Although the 15 m columns did provide better separation than previously seen from simple thermal desorption, even better separation was desired. This required the use of longer columns to increase the number of theoretical plates. The second problem involved the instability of the Carbowax column at high temperatures. The stationary phase of the carbowax column is not stable at temperatures above 220°C. Analyses routinely involved approaching or holding the column at this temperature. These problems were rectified by employing longer columns (25 m) and using an HP-FFAP FSOT column in place of the Carbowax column. The maximum temperature of the HF-FFAP column is listed at 240°C.

The rapid heating of the beads with subsequent loading of volatilized components onto a column does not provide adequate temporal resolution for identification of compounds present. Therefore, cryo-focusing or microscale purge and trap was used prior to separation on the column.

Cryo-focusing GC

Cryo-focusing was employed for the majority of analyses in this chapter. The need for cryo-focusing to narrow sample component bands is due to the wide desorption profiles from simple thermal desorption of components. Liquid nitrogen (LN_2, b.p. -196°C) is used to prevent further migration of component bands beyond the section of column immersed in LN_2. In actuality, some of the higher boiling components may reside in the first 15 cm of column above the LN_2. The column oven is set at 25°C; therefore, the high boiling components may be focused in this section. These will, however, proceed through the column upon the ramping the oven. No apparent broadening of peaks due to this effect was observed. The advantage of using cryo-focusing is that it does not introduce discrimination of sample compound classes. Essentially, the observed compounds are those which were transferred to the glass beads and simply heated off without loss of particular compound classes. The drawback to this method are contaminant peaks. These possibly arise from the septum of from the breakdown of the stationary phase at the column entrance located in the injection port. These contaminants may be cryo-focused and detected along with the sample components. The high abundance of acids dominate the mass spectra and obscure some of the trace components, making identification of the trace components difficult.

Purge and trap GC

The use of microscale purge and trap discriminates against acids and other more polar compounds, but this is beneficial when used to complement information

obtained from analyses with cryo-focusing. The drawback of this technique is, as mentioned, discrimination against polar compounds in addition to the acids; however, these compounds are still readily detected with single-stage cryo-focusing.

Mass Spectrometry

The historical significance and a brief description of CI and EI modes of ionization were presented in chapter one. This section of Chapter 5 contains an introduction to the more practical aspects of these ionization modes. The reagent gases employed for CI throughout the course of this work have been methane, carbon dioxide, and in a few cases, isobutane. Some of the work involving carbon dioxide is presented in the appendix. Methane reagent gas was employed for all experiments in this chapter; therefore, the presentation of CI below will be primarily focused on methane as the reagent gas. The discussion of EI will be aimed at specific aids (i.e. characteristic peaks) in the mass spectra used to predict the compound class of peaks which may or may not have failed the library searching process.

PCI theory

The reagent gas for chemical ionization is present in the ion source at higher levels than the sample to be ionized by CI. Therefore, a greater probability exists that the reagent gas instead of the sample will undergo electron ionization. Electron ionization of methane produces the following ions [33,53,74]:

$$CH_4 \rightarrow CH_4^{+\bullet}, CH_3^+, CH_2^{+\bullet} \qquad 5\text{-}1$$

These ions further react with CH_4 neutrals in the ion source to produce CH_5^+, $C_2H_5^+$, and $C_3H_5^+$, which are formed via the ion/molecule reactions:

$$CH_4^{+\bullet} + CH_4 \rightarrow CH_5^+ + CH_3^{\bullet} \qquad 5\text{-}2$$

$$CH_3^+ + CH_4 \rightarrow C_2H_5^+ + H_2 \qquad 5\text{-}3$$

$$CH_2^{+\bullet} + CH_4 \rightarrow C_2H_3^+ + H_2 + H^{\bullet} \qquad 5\text{-}4$$

$$C_2H_3^+ + CH_4 \rightarrow C_3H_5^+ + H_2 \qquad 5\text{-}5$$

The major ions formed with methane reagent gas are discussed later in the text; the ion/molecule reactions available for CI are discussed below.

There are four categories of CI reactions which can occur between positive reagent ions, X^+ or XH^+, and sample molecules, M [33,74]. These are:

$$XH^+ + M \rightarrow MH^+ + X \qquad \text{proton transfer} \qquad 5\text{-}6$$

$$X^+ + M \rightarrow [M\text{-}H]^+ + XH \qquad \text{anion (hydride) abstraction} \qquad 5\text{-}7$$

$$X^+ + M \rightarrow MX^+ \qquad \text{adduct formation} \qquad 5\text{-}8$$

$$X^{+\bullet} + M \rightarrow M^{+\bullet} + X \qquad \text{charge exchange} \qquad 5\text{-}9$$

Proton transfer (Eq 5-6) involves the transfer of a proton from the reagent gas ion to the sample molecule. This will occur if the proton affinity (PA) of the sample molecule is greater than that of the conjugate base of the reagent ion. In this case, the conjugate base (CH_4) of the CH_5^+ reagent ion has a proton affinity of 552 kJ/mol [33,74]. Additionally, the conjugate base of the $C_2H_5^+$ ion has a PA of 682 kJ/mol, which is lower than that of isobutane and of water [33]. Therefore, the reagent ions formed from CH_4 will readily yield exothermic proton transfer reactions

with most components in the sample. The drawback to such exothermic reactions is the extensive fragmentation which results for compounds of much higher proton affinity than methane.

Hydride ion abstraction (Eq 5-7) can occur if the hydride ion affinity (HIA) of the reagent gas ion is greater than the corresponding HIA of the sample $[M-H]^+$ ion. The HIA values of CH_5^+ and $C_2H_5^+$ are 1127 kJ/mol and 1135 kJ/mol, respectively [74]. Hydride ion abstraction will occur with the $C_3H_5^+$ ion and possibly the $C_2H_5^+$ ion.

Adduct formation (Eq 5-8) typically occurs when the sample proton affinity is slightly less than that of the conjugate base of the reagent ion. This can occur for both the $C_2H_5^+$ ion and the $C_3H_5^+$ ion. Due to the much lower PA of the conjugate base of CH_5^+, this species would rather transfer a proton, as discussed previously, than form an adduct ion.

The final reaction (Eq 5-9), is charge exchange. This process occurs typically for reagent gases that do not have a hydrogen available for proton transfer reactions. Charge transfer can occur to produce the $M^{+\bullet}$ molecular ion of a compound. The fragmentation is EI-like with increased relative abundance of the molecular ion compared to that of conventional EI. The extent of fragmentation is dependent upon the internal energy of the sample ion formed, which is given by the difference of the recombination energy of the reagent gas ion and the ionization energy of the sample molecule (see appendix). The recombination energies of the CH_5^+ and $C_2H_5^+$ ions are 7.9 eV and 8.3 eV, respectively [74]. These energies are very low

compared to commonly employed charge exchange reagent gases, and thus, charge exchange is not expected to be an abundant process with methane reagent gas.

The analysis of PCI mass spectra consisted of determination of the relative molecular mass (r_M) by identifying specific ions. This information is complementary to the structural information obtained from EI. Therefore, the focus is mainly on determination of r_M for specific peaks rather than employing CI for structural elucidation. The first two ions examined for are the even-electron $[M+H]^+$ ion produced by proton transfer from CH_5^+ , $C_2H_5^+$, or the $[M-H]^+$ ion produced from from hydride abstraction with $C_2H_5^+$ and $C_3H_5^+$. These ions bracket the r_M of the compound of interest. Additional confirmation can be obtained from the presence of ions at $[M+29]^+$ and $[M+41]^+$, representing adduct formation of $C_2H_5^+$ and $C_3H_5^+$ to the sample molecule, respectively. Although not examined in the work, ions produced by CI may exhibit some informative rearrangements [103,104]. Due to the availability of EI mass spectra along with on-line libraries of EI data, fragmentation information was derived solely from this mode of ionization. It should be pointed out that the actual CI analysis consisted of acquisition by PPINICI, where the PCI and NCI data are acquired as consecutive scans into a single file [70]. This allows for using the negative ion data, specifically the $[M-H]^-$ ion, to aid in determination of the compound relative molecular mass.

NCI theory

When bombarded by electrons in the ion source, methane produces various positive reagent ions as discussed in the previous section. The collision of an

electron with a methane molecule to form a positive ion removes approximately 30 eV of the kinetic energy from the incident electron [105,106]. At high enough methane pressures, multiple collisions lead to a population of thermal electrons (e_{th}^-) for reaction with sample molecules by electron capture negative ion chemical ionization (ECNCI) [33,70,72,74,76,105,107,108]. The possible negative ion mode electron capture (EC) reactions are as follows:

$$e_{th}^- + MX \rightarrow MX^{-\bullet} \qquad \text{associative resonance capture} \qquad 5\text{-}10$$

$$e_{th}^- + MX \rightarrow M + X^{-\bullet} \qquad \text{dissociative resonance capture} \qquad 5\text{-}11$$

$$e_p^- + MX \rightarrow M^+ + X^{-\bullet} + e_p^- \qquad \text{ion-pair production} \qquad 5\text{-}12$$

The common denominator of these processes is the capture of an electron by a species (MX). Ion-pair production (Eq 5-12) is a special case and will be explained later. In order for electron capture to occur, the electron affinity (EA) of MX must be positive. Provided the species does not rapidly undergo autodetachment of an electron, it can proceed through one or more of the processes given in equations 5-10 through 5-12.

Associative resonance capture (Eq 5-10) involves the capture of a thermal electron, forming an excited species in which the excess energy can be distributed over the molecule without bond rupture [72]. Studies have shown associative resonance capture to be observed when electron energies are in the range of 0 to 2 eV [72,76,108].

Dissociative electron capture (Eq 5-11) occurs when the electron captured species contains sufficient excess internal energy to cause the rupture of one of more

bonds. This can result if the excited $MX^{-\bullet}$ species makes the transition to an attractive state (forming both $MX^{-\bullet}$ and $M+X^{-\bullet}$), or makes the transition to a repulsive state (forming $M+X^{-\bullet}$ only). The fragment retaining the negative charge in these equations is the fragment that has the greater EA. Dissociative electron capture is typically observed for electron energies of 2-15 eV. The extent of fragmentation for dissociative capture and ion-pair production (below) is dependent upon the internal energy of the ion and thus the incident electron energy. The internal energy can also be influenced by temperature; increased source temperature has been shown to produce an approximately linear increase in fragmentation [72,74].

Ion-pair production (Eq 5-12) occurs for electron energies greater than 15 eV. In this case, the intermediate is more often an excited molecule rather than an $MX^{-\bullet}$ species [72]. The primary electron (e_p^-) functions to excite MX to (MX^*) which then dissociates to form the ion pair.

In the absence of reagent gas, a conventional 70 eV electron beam yields approximately 1000 times more positive ions than negative ions [76]. Additionally, the negative ions are typically only low mass fragment ions or "molecular debris." [72]. Normally, the sensitivity with respect to detection of informative fragments of negative ions under these conditions is poor. In cases where an $MX^{-\bullet}$ is produced of sufficient intensity to be observed, it can be explained by the production of secondary thermal electrons. That is, the species captures the primary electron, undergoes autodetachment as well as releasing a low energy secondary electron of near-thermal energy to form and $M^{+\bullet}$ ion. The secondary near-thermal electron can

then react with a neutral sample molecule via associative or dissociative resonance capture. Therefore, it is necessary that a suitable reagent gas is used to produce thermal electrons for ECNCI to take place.

It is estimated that the rate of capture of electrons by compounds amenable to EC is approximately 400 times greater than for CI ion/molecule reactions; thus, enhanced sensitivity is observed for these compounds [72]. The compounds amenable to ECNCI are generally oxidizing or alkylating agents [107]. The molecular anions of these compounds were found to be stable if a "low-lying" unoccupied molecular orbital is available, or if the molecule can be stabilized through π-system resonance [72]. It is best stated that the more "molecular debris" and less $MX^{-\bullet}$ or $[M\text{-}H]^-$, the less resonance stabilization is available to the molecule. Generally, the best systems or molecules for EC are extended π-systems with strong electron withdrawing groups.

There are additional constraints as well as differences between the characteristics of negative ions and positive ions in the gas phase [72]. Each positive ion fragment can carry a charge, whereas the EA must be greater than zero for negative ion fragments to be present as an anion. The probability of anion formation is approximately a linear function of the EA of the neutral species. In positive ion analysis, the fact that the filament does not produce monoenergetic electrons nor does it significantly alter the fragmentation within the standard operation regime of filament electron energies (70 eV). The lack of monoenergetic electrons in the negative mode allows for multiple reaction processes to occur. The autodetachment

process competes with fragmentation in the negative ion mode; therefore, simple bond cleavages will be favored over more complex rearrangements. Due to autodetachment, only ions with low energy and relatively long lifetimes will be recorded [72,107]. Positive ions can retain this charge for longer times and can only lose a positive charge via abstraction of an electron or proton from collision with a neutral [107].

Despite these aforementioned limitations, ECNCI can still provide information complementary to or not accessible with PCI. The CI reagent gas can function in three ways for negative ion analyses [72]. It can produce thermal electrons for EC processes described above, produce charge transfer reactions (Eq 5-13) provided the EA of the sample molecule is greater than the EA of the reagent gas molecule, and it can allow for true CI reactions (Eq 5-14 and Eq 5-15) between the reagent ions and sample molecules to occur:

$$X^{-\bullet} + M \rightarrow M^{-\bullet} + X \qquad \text{charge transfer} \qquad 5\text{-}13$$

$$[X\text{-}H]^- + M \rightarrow [M\text{-}H]^- + X \qquad \text{proton abstraction} \qquad 5\text{-}14$$

$$X^- + M \rightarrow MX^- \qquad \text{adduct formation} \qquad 5\text{-}15$$

The term NCI is commonly used to indicate ion/molecule reactions between the reagent gas and sample. Electron capture reactions are usually referred to as ECNCI since these involve a different process than NCI ion/molecule reactions [76]. The problem with many reagent gases, including methane and isobutane, is that the spectra produced are difficult to classify as either ECNCI or NCI [76]. When using lower energy electrons, an $[M\text{-}H]^-$ ion is typically observed in place of $MX^{-\bullet}$. In

some cases, this can be explained by high EA of the resulting anions or high bond dissociation energies of the C-H and O-H bonds. In this dissertation, the distinction is not of particular importance. What is sought is the $MX^{-\bullet}$ ion or the $[M-H]^-$ ion in order to deduce the r_M of the compound.

The analysis of NCI spectra consisted of determining the m/z of either the $MX^{-\bullet}$ ion or the $[M-H]^-$ ion, regardless of whether generated by ECNCI or true NCI, in the mass spectrum to aid in the determination of relative molecular mass. Additional confirmation came from the presence of the following ions: $[M+CH_3^{\bullet}]^-$, $[M-H+CH_3]^-$, and $[M+C_2H_5]^-$ [76]. Additionally, manual inspection of mass spectra for compounds suspected of being esters or alcohols was conducted; esters fragment to yield the carboxylate ion while alcohols yield an $[M-H-H_2]^-$ ion [72].

Characteristic ion fragmentations (EI)

Electron ionization generally employs a distribution of electron energies centered around 70 eV emitted by the filament in a low-pressure ion source. These conditions maximize fragmentation and structural information. As described above, negative ions formed by EI are low molecular weight fragments of quite low intensity. In the positive ion mode, ions retain their charges longer and can distribute excess internal energy more efficiently, thus undergoing less fragmentation.

The purpose of this introduction to EI is not to provide a complete set of rules for EI fragmentation; these may be found elsewhere [79,109]. For the most part, EI mass spectra acquired in this dissertation were evaluated by library searching on the TSQ70 with a NBS library database of over 49,000 compounds. In some

cases, library searching failed to provide a reasonable compound choice for the unknown mass spectrum. When this occurred, r_M information obtained from CI analyses was relied upon to further restrict the search. If this still failed to produce a reasonable selection, the mass spectra were manually examined. This involved a quick inspection for characteristic compound class fragments or McLafferty rearrangement ions. This information was then employed and library re-searched with new constraints. Compounds which remained unidentified are not listed in the tables contained throughout this chapter, although speculative identifications are listed and noted. The remainder of this introduction will address the characteristic fragments and McLafferty rearrangement ions which were examined in the interpretation used in this dissertation.

Aliphatic acids show a characteristic McLafferty rearrangement ion at m/z 60. This rearrangement can occur for compounds with an available γ-hydrogen and unsubstituted α-carbon [79,109,110]. For EI GC/MS analysis, mass chromatograms for this ion were examined to determine the location of the carboxylic acid series from propenoic acid up to octadecanoic acid. Fragment ions corresponding to $[M-18]^+$, $[M-28]^+$, and $[M-45]^+$ were fairly common in these mass spectra. The possible presence of amines was determined by examining the mass chromatogram for an ion at m/z 58. Esters produce an m/z 74 ion when methyl substituted and an m/z 88 ion when ethyl substituted. Mass chromatograms for the m/z 58 and 74 ions were also examined in almost every case.

Other characteristic ions or fragments were not examined unless an unknown mass spectrum failed the library search. In general, examination of isotope peaks for halogen-containing compounds was not necessary due to the library database readily identifying the halogenated compounds. Mass spectra which the library targeted as sulfur-containing compounds were visually inspected for the presence of a loss of 34 Da (characteristic of thiols) as well as the presence of the series m/z 47, 61, 75, 89, ... Mass spectra of suspected aldehydes, ketones, or aliphatics were examined when needed for the presence of the series m/z 15, 29, 43, 57, . . . as well as for losses of 1, 18 and 28 Da from aldehydes. Mass chromatograms were examined for the McLafferty rearrangement ion for aldehydes at m/z 44, as well as for ions at m/z 58 and m/z 72, which could be indicative of a methyl and ethyl ketones, respectively; however, it should be noted that the m/z 58 ion also results from amines. Alcohols of five or more carbons display $[M-18]^+$ and $[M-46]^+$ ions; however, acids may yield these ions also. Instead, analysis of the corresponding peak in NCI for the presence of an $[M-H-H_2]^-$, as described in the NCI section, was employed for suspected alcohols. Mass chromatograms for the m/z 77 ion or cluster of ions within 2 mass units were examined to determine the presence of aromatics. Mass spectra were examined for an $[M-27]^+$ ion when an amine was suspected, as well as the even ion series of m/z 44, 58, 72, 86, . . . which is characteristic of amines.

Experimental

Identification of Emanations by CI and EI MS

Cryo-focusing GC/MS

The results from these analyses are tabulated later in this chapter. The list of components was derived from the analysis of cryo-focused volatiles from handled glass beads. The cryo-focusing process involved heating of beads in the GC injection port to desorb volatiles. A Varian 3400 GC fritted glass injection insert was inserted reversed into the injection port. This allowed for up to 12 beads to be placed between the frit (located approximately halfway down the insert) and the GC septum sealing the injection port. The frit kept the beads from dropping down onto the column entrance and provided a means for volatile emanations to be loaded onto the column; the column entrance extends up into the injector insert and is located below the frit. Additionally, the injection port was operated in an entirely splitless mode for the duration of the experiment providing essentially only one exit for volatiles, i.e. through the column.

Beads were rubbed for 5-15 min prior to placing into the injector insert. The initial experiments employed eight beads handled by the author of this dissertation; later experiments (discussed in the comparison sections) involved from two to five beads handled by Mr. Dan Smith, Mr. Carl Schreck, and Mr. Ken Posey, all of the USDA. After loading the beads into the insert, the insert was placed into the injection port held at 25°C to minimize sample loss from evaporation. The cap,

septum, and needle guide were replaced. Throughout the loading process the head pressure of helium was set to 0 psig to allow for proper alignment of the septum and prevent premature migration of volatiles past the intended point of cryo-focusing on the column.

Before increasing the helium head pressure, liquid nitrogen was placed in a 12 oz. styrofoam cup. The cup was placed in the oven such that the approximately 8 cm of column could be looped in the cup about 15 cm below the point where the column passes from injection port to oven. The helium pressure was then increased to 20 psig and the initial desorption phase started. This entailed loading a program to ramp the injection port from 25°C to 250°C over 7.5 min and holding at 250°C for 2.5 min. Throughout the cryo-focusing phase, the GC oven was set at 25°C and the transfer line set at 40°C. Liquid nitrogen was added to the cup as necessary during this 10 min cryo-focusing phase.

Subsequent to the completion of the cryo-focusing, a new program was loaded from the TSQ70 to the Varian 3400 GC. Prior to running this program and concurrently acquiring data, the cup containing liquid nitrogen was removed. There were four different ramp programs used. The initial experiments employed a GC oven ramp used for the analysis of 8 beads handled by the author of this dissertation. The ramp consisted of an initial 1.0 min hold at 25°C, a 12 min ramp at 15°C/min up to 210°C, and then a hold at 210°C for 5.0 min. The transfer line was concurrently ramped, after a 1.0 min hold at 40°C, up to 225°C at 15°C/min, and held 5.0 min at 225°C (18 min analysis time). Separation was effected by a 20 m x 0.25

mm i.d. Carbowax column (d_f=0.25 μm). Analyses involving the comparison of subjects were performed with two ramp programs, depending upon the column employed. The columns were a 25 m x 0.20 mm i.d. HP5 FSOT column (d_f=0.33 μm) or a HP-FFAP 25 m x 0.20 mm i.d. FSOT column (d_f=0.33 μm). For experiments conducted with the HP5 column (35 min run time), the GC ramp consisted of a-1.0 min hold at 40°C followed by a 11 min ramp at 17°C/min, and then a hold at 220°C for 23 min. The transfer line was concurrently ramped from 50°C to 220°C at 20°C/min over 8.5 min and held at 220°C for the remainder of the analysis. The ramp program for the FFAP column (45 min run time) consisted of a 1.0 min hold at 40°C followed by an 18 minute ramp at 11°C/min to 236°C, and then a hold for 26 min at this temperature. The transfer line was ramped from 50°C to 236°C at 23°C/min for 8 min and held at 236°C for the remaining 37 min. The final ramp which was used is described in the experimental section covering the five-day comparison of bio-assay to GC/MS.

Acquisition of PPINICI data employed methane reagent gas at 1660-1690 mtorr (indicated) pressure. The ion source and manifold temperatures were 150°C and 70°C, respectively for CI and 170°C and 70°C, respectively for EI. The electron energy for CI experiments was 100 eV and for EI, 70 eV. The third quadrupole was typically scanned with a scan time of 1 s per scan for PPINCI and 2 s per scan for EI data (except for the five-day comparison study). The filament emission current was set at 200 μA. The conversion dynode was set at +5 kV for positive ion CI and EI, and -5 kV for negative ion CI. The electron multiplier was set between -1000 V

and -1200 V. Prior to analysis the instrument was tuned with PFTBA as previously mentioned and blanks (appropriate number of beads without sample) were recorded.

Purge and trap GC/MS

These experiments involving microscale purge & trap mainly employ samples from the author of this dissertation; two samples, one from handled beads and one involving placing the left hand in a Tedlar bag, were collected from Mr. Matt Booth of Environmental Science & Engineering (ESE). The bead method involved handling 200-250 glass beads for 10 min, and transferring them to a 100 mL round bottom flask, as discussed previously (Chapter 2). The round bottom flask was attached to the system via a 1/2" Cajon fitting to 1/4" Swagelok, further reduced to a 1/8" Swagelok fitting. Alternatively, sampling was accomplished by placing the left hand in a Tedlar bag and fastening the bag around the wrist with a rubber band; the Tedlar bag was simply attached by a 1/8" Swagelok fitting. The 1/8" Swagelok was connected to a port on an ELA2010 canister manifold (Entech Laboratory Automation).

The canister manifold allowed for 70-100 mL of volatiles and residual air to be sampled by the ELA2000 concentrator. The concentrator consisted of three stages. The first stage employed a dryer with a gradient of large to small beads. This served to remove most of the water in the sample. During concentration, this stage is set to -160°C for three minutes and heats up to -16°C as sample is transferred to the second stage. The second stage in these experiments was a Tenax trap. During concentration, the trap was set to -20°C; it was then heated to 156°C

for desorption of trapped volatiles onto the cryo-focusing trap. The cryo-focusing trap was set a -160°C for concentration and heated ballistically (over 10 s) to 150°C to purge volatiles onto the head of the GC column.

The GC employed was an HP5890 series I with a 30 m x 0.25 mm i.d. DB-1 column (d_f=1 μm) for initial experiments. Experiments with the hand enclosed in a Tedlar bag were conducted on a 60 m x 0.25 mm i.d. DB-1 column (d_f=1 μm). The column was initially cryo-cooled at -35°C and held for 3.0 min. Subsequently, the column was either ramped at 12°/min up to 180°C, then ramped at 25°/min from 180°C to 225°C and held for 5.0 min at 225°C, or in later experiments, the column was held 6.0 min at -35°C then ramped at 6°/min to 180°C and 12°/min from 180°C to 225°C, and held for 10.0 min.

The mass spectrometer used for these studies was a Finnigan MAT Incos 50 single-stage quadrupole. The scan rate employed was 0.75 s per scan. The filament emission current was set at 750 μA with an electron energy of 100 eV. The electron multiplier was set to -1200 V. The ion source temperature was set at 180°C; there is no heater for the manifold. Prior to analysis, the instrument was tuned with PFTBA and the appropriate blanks were analyzed.

Case Study Comparison of Emanations between Subjects

A series of experiments were conducted comparing emanations desorbed off of beads handled by Mr. Carl Schreck and Mr. Dan Smith. Mr Schreck, in entomological assays via an olfactometer, consistently provides relatively low

attraction of mosquitoes to handled glass (c. 25%). Mr. Smith provides the highest attraction percentage on a consistent basis (c. 70%). Samples were analyzed in sets of two similar analyses, each involving beads handled by the two different subjects. In the morning session, five blank beads were analyzed prior to the arrival of the subjects. After arrival, 10-12 beads were handled by the first subject. A chosen number of beads, from 2-5 beads, were sampled immediately after handling. The number used remained consistent throughout the day. The remainder of the rubbed beads were placed in a 1/4" diameter tube at room temperature and open to ambient air. Fifteen minutes before the completion of the first analysis, the second subject handled 10-12 beads. Between 2 and 5 beads, consistent with the previous analysis, were sampled immediately; the remainder were stored in a second tube under the same conditions as previously described. The morning session involved either PPINCI or EI as the mode of ionization. The mode chosen to analyze at the beginning of the day was alternated for subsequent days.

The TSQ70 was switched over to the complementary mode for the afternoon session; i.e. if PPINICI data was acquired in the morning session, EI data were acquired in the afternoon session. An analysis of 5 blank beads was performed prior to the return of the subjects. The subjects repeated the handling procedures. The beads were sampled and stored as described above for the morning session. After these sessions, the acquired data consisted of PPINICI and EI analyses from each subject. The analyses were repeated in the evening, with the same ionization mode used in the afternoon session, but with beads handled in the morning session. This

allowed a 6-8 hour gap between handling time and analysis time. After each sample from the morning session was analyzed, the beads stored from the afternoon session were analyzed under the complementary ionization mode.

The GC parameters were dependent upon the column employed. The columns and corresponding GC parameters were discussed previously (in the cryo-focused GC/MS section of this chapter). The mass spectrometer was operated in EI and PPINICI modes as previously discussed and reported in this chapter. A blank was not analyzed in the evening for studies involving beads which had been stored in tubes (open to ambient air) for over 6 hr.

Case Study Comparison of Bio-assay to GC/MS Assay

Cryo-focusing GC/MS

Experiments were performed involving analyzing emanations collected from one subject, each day, for five consecutive days. The collection process was similar to that for the case study described for the comparison of subjects. In this case, Mr. Ken Posey of the USDA served as the test subject. On each of the five days, a blank was recorded in EI mode prior to analysis. The subject handled ten glass beads for 15 min; three beads were used for each analysis. The remaining beads were stored for analysis with the complementary ionization mode. The cryo-focusing stage for the first handled-bead analysis was initiated at approximately 8:40 am each day. Upon completion of the this analysis, the mass spectrometer ion volume was switched to allow for PPINICI. A blank was acquired and three beads were

analyzed. The time delay between rubbing and analysis of the beads in this mode was approximately 2 hr.

The cryo-focusing parameters were identical to those described previously in the experimental section of this chapter. The GC oven ramp, however, was conducted at a lower rate than previously used in studies. This was done to provide additional resolution for co-eluting peaks found in previous studies with ramp programs employing a steeper ramp. The GC oven ramp consisted of an initial 1.0 min hold at 40°C, a 27 min ramp at 6°C/min up to 200°C, and then a hold at 200°C for 12 min. The transfer line was concurrently ramped from 50°C up to 210°C at 10°/min for 16 min, and held for 24 min at 210°C. GC Separation was effected by a 25 m x 0.20 mm i.d. HP5 FSOT column (d_f=0.33 μm).

The mass spectrometer operation in EI and PPINCI modes is similar to that described previously in this chapter. Methane reagent gas at 1680 to 1700 mtorr (indicated) pressure was employed for PPINICI analyses. The third quadrupole was scanned at 0.5 s per scan for EI and PPINICI analyses. The conversion dynode was set at +5 kV for positive ion CI and EI, and -5 kV for negative ion CI. The electron multiplier was set to -1000 V for EI experiments and -1100 V for CI experiments. Prior to the analysis of blanks, the instrument was tuned with PFTBA.

Olfactometer

Bio-assays of a glass petri dish handled by Mr. Ken Posey of the USDA were conducted approximately one hour after sample collection for GC/MS analysis. These experiments were conducted at the USDA laboratories and involved analysis

in the olfactomer at that location. The petri dish was handled for 15 min prior to insertion into a port of the olfactometer. Testing typically occurred at approximately 10:00 a.m. for each of the days. The testing was conducted with 75 (six-to-eight-day-old) female *Ae. aegypti* mosquitoes. The relative humidity, air temperature, and gas flow were controlled throughout each analysis. Over the five day period, none of the 75 mosquitoes tested each day were collected in the control port. The lowest collection percentage (12%) occurred on the first day (Monday). The remainder of the week, from Tuesday through Friday, yielded collection percentages of 24%, 21%, 27%, and 20%, respectively.

Results and Discussion

Identification of Emanations by CI and EI MS

Prior to reporting compounds observed in the analyses of this dissertation, a compilation of compounds previously reported in the literature as being present on the skin are presented in table 5-1. Compounds not expected to be amenable to the manner in which analyses were conducted for this dissertation will be noted. Literature sources pertaining to skin emanations are relatively scarce [102]. The data compiled in table 5-1 are extracted from semiochemical work (odor analysis) and government studies (space exploration) concerning the identification of human dermal emanations [30,31,111]. Approximately 260 compounds, spanning a range of classes, are contained in this table. These classifications will remain as consistent as

Table 5-1 Compounds previously reported in the literature as species which emanate from human skin. Listed with the compounds are the corresponding molecular formula and relative molecular mass (r_M). Explanation of remarks follows this table.

Compound	Formula	Remarks	r_M
Acids/Carboxylic acids			
Formic acid	CH_2O_2		46
Acetic acid	$C_2H_4O_2$		60
Propenoic acid	$C_3H_4O_2$		72
Propanoic acid	$C_3H_6O_2$		74
Butanoic acid	$C_4H_8O_2$		88
Pentanoic acid	$C_5H_{10}O_2$		102
Hexenoic acid	$C_6H_{10}O_2$		114
Hexanoic acid	$C_6H_{12}O_2$		116
Heptenoic acid	$C_7H_{12}O_2$		128
Heptanoic acid	$C_7H_{14}O_2$		130
Octenoic acid	$C_8H_{14}O_2$		142
Octanoic acid	$C_8H_{16}O_2$		144
Nonenoic acid	$C_9H_{16}O_2$		156
Nonanoic acid	$C_9H_{18}O_2$		158
Decenoic acid	$C_{10}H_{18}O_2$		170
Decanoic acid	$C_{10}H_{20}O_2$		172
Undecenoic acid	$C_{11}H_{20}O_2$	D	184
Undecanoic acid	$C_{11}H_{22}O_2$		186
Dodecanoic acid	$C_{12}H_{24}O_2$		200
Hexadecanoic acid	$C_{16}H_{32}O_2$	C	256
Octadecanoic acid	$C_{18}H_{34}O_2$	C	284
Eicosanoic acid	$C_{20}H_{38}O_2$		312
Oxoacetic acid	$C_2H_2O_3$		74
Glycolic acid	$C_2H_4O_3$		76
Pyruvic acid	$C_3H_4O_3$		88
Lactic acid	$C_3H_6O_3$		90
Malic acid	$C_4H_6O_5$		134
Oxalic acid	$C_2H_2O_4$		90
Propanedioic acid	$C_3H_4O_4$		104
Butanedioic acid	$C_4H_6O_4$		118
Pentanedioic acid	$C_5H_8O_4$		132
Benzoic acid	$C_7H_6O_2$		122
Cinnamic acid	$C_9H_8O_2$		148
Isophthalic acid	$C_8H_6O_4$		166

Table 5-1 Continued

Compound	Formula	Remarks	r_M
Acids/Carboxylic acids (continued)			
Lithocholic acid	$C_{24}H_{40}O_3$		376
Deoxycholic acid	$C_{24}H_{40}O_4$		392
Cholic acid	$C_{24}H_{40}O_5$		408
Hydrocyanic acid	HCN	A	27
Hydrosulfuric acid	H_2S	A	34
Hydrochloric acid	HCl		36
Hydrobromic acid	HBr		80
Cyanic acid	CHNO		43
Isocyanic acid	CHNO		43
Carbonic acid	CH_2O_3	E	62
Chloroacetic acid	$C_2H_3O_2Cl$		94
Chlorocarbonic acid	CHO_3Cl	E	80
Acyl Halides/Related			
Formyl chloride	CHOCl		64
Acetyl chloride	C_2H_3OCl		78
Propanoyl chloride	C_3H_5OCl		92
Carbamoyl chloride	CH_2NOCl		79
Alcohols			
Methanol	CH_4O	A	32
Vinyl alcohol	C_2H_4O		44
Ethanol	C_2H_6O		46
1-propen-3-ol	C_3H_6O		58
Propanol	C_3H_8O		60
Isopropanol	C_3H_8O		60
Pentanol	$C_5H_{12}O$		88
Tetradecanol	$C_{14}H_{30}O$		214
Hexadecanol	$C_{16}H_{34}O$		242
Ethylene glycol	$C_2H_6O_2$		62
Glycerol	$C_3H_8O_3$		92
Phenol	C_6H_6O		94
Benzyl alcohol	C_7H_8O		108
1,2-dihydroxybenzene	$C_6H_6O_2$		110

Table 5-1 Continued

Compound	Formula	Remarks	r_M
Alcohols (continued)			
1,3-dihydroxybenzene	$C_6H_6O_2$		110
1,4-dihydroxybenzene	$C_6H_6O_2$		110
Inositol	$C_6H_{12}O_6$		180
Dehydrocholesterol	$C_{27}H_{44}O$		384
Cholesterol	$C_{27}H_{46}O$		386
Aldehydes			
Formaldehyde	CH_2O	A	30
Acetaldehyde	C_2H_4O		44
Propenal	C_3H_4O		56
Propanal	C_3H_6O		58
2-methylpropanal	C_4H_8O		72
Butanal	C_4H_8O		72
3-methylbutanal	$C_5H_{10}O$		86
Ethanedial	$C_2H_2O_2$		58
Glycolicaldehyde	$C_2H_4O_2$		60
Glyceraldehyde	$C_3H_6O_3$		90
Aliphatics/Aromatics			
Methane	CH_4	A	16
Acetylene	C_2H_2	A	26
Ethane	C_2H_6	A	30
Propyne	C_3H_4	A	40
Cyclopropane	C_3H_6		42
Propene	C_3H_6		42
2-methyl-1,3-butadiene	C_5H_8		68
2-methylnonane	$C_{10}H_{22}$		142
Squalene	$C_{30}H_{50}$		410
Benzene	C_6H_6		78
Toluene	C_7H_8		92
Amides			
Formamide	CH_3NO		45
Acetamide	C_2H_5NO		59

Table 5-1 Continued

Compound	Formula	Remarks	r_M
Amides (continued)			
Methylacetamide	C_3H_7NO		73
Propanamide	C_3H_7NO		73
Oxamide	$C_2H_4N_2O_2$	B	88
Cyanamide	CH_2N_2	A	42
Amino acids/Amines/Related			
Glycine	$C_2H_5NO_2$	B	75
Alanine	$C_3H_7NO_2$	B	89
Proline	$C_5H_9NO_2$	B	115
Valine	$C_5H_{11}NO_2$	B	117
Isoleucine	$C_6H_{13}NO_2$	B	131
Leucine	$C_6H_{13}NO_2$	B	131
Phenylalanine	$C_9H_{11}NO_2$	B	165
Serine	$C_3H_7NO_3$	B	105
Threonine	$C_4H_9NO_3$	B	119
Tyrosine	$C_9H_{11}NO_3$	B	182
Aspartic acid	$C_4H_7NO_4$	B	133
Glutamic acid	$C_5H_9NO_4$	B	147
Lysine	$C_6H_{14}N_2O_2$	B	146
Tryptophan	$C_{11}H_{12}N_2O_2$	B	204
Histidine	$C_6H_9N_3O_2$	B	155
Arginine	$C_6H_{14}N_4O_2$	B	174
Cysteine	$C_3H_7NO_2S$	B	122
Methionine	$C_5H_{11}NO_2S$	B	149
Cystine	$C_6H_{12}N_2O_4S_2$	B	240
Sarcosine	$C_3H_7NO_2$	B	89
Hydroxyproline	$C_5H_9NO_3$	B	131
Carbamic acid	CH_3NO_2		61
Aminobutanoic acid	$C_4H_9NO_2$		103
Aminoisobutanoic acid	$C_4H_9NO_2$		103
Aminobenzoic acid	$C_7H_7NO_2$		137
Ornithine	$C_5H_{12}N_2O_2$		132
Pantothenic acid	$C_9H_{17}NO_5$		219
Ammonia	H_3N	A	17
Methylamine	CH_5N	A	31
Dimethylamine	C_2H_7N		45

Table 5-1 Continued

Compound	Formula	Remarks	r_M
Amino acids/Related (continued)			
Ethylamine	C_2H_7N		45
Trimethylamine	C_2H_9N		59
2-aminopropane	C_2H_9N		59
Aniline	C_6H_7N		93
Benzylamine	C_7H_9N		107
2-aminotoluene	C_7H_9N		107
Diphenylamine	$C_{12}H_{11}N$		169
Aminophenol	C_6H_7NO		109
Ethylenediamine	$C_2H_8N_2$		60
Guanidine	CH_5N_3		59
Choline	$C_5H_{15}NO^+$	B	104
Acetylcholine	$C_7H_{17}NO_2^+$	B	146
Acid Anhydrides			
Formic anhydride	$C_2H_2O_3$		74
Acetic anhydride	$C_4H_6O_3$		102
DNA bases			
Adenine	$C_5H_5N_5$	B	135
Guanine	$C_5H_5N_5O$	B	151
Esters			
Formic acid, ethyl ester	$C_3H_6O_2$		74
Formic acid, propyl ester	$C_4H_8O_2$		88
Formic acid, butyl ester	$C_5H_{10}O_2$		102
Acetic acid, methyl ester	$C_3H_6O_2$		74
Acetic acid, ethyl ester	$C_4H_8O_2$		88
Acetic acid, isopropyl ester	$C_5H_{10}O_2$		102
Acetic acid, propyl ester	$C_5H_{10}O_2$		102
Acetic acid, pentyl ester	$C_7H_{14}O_2$		130
Acetic acid, phenyl ester	$C_8H_8O_2$		136
Propanoic acid, ethyl ester	$C_5H_{10}O_2$		102

Table 5-1 Continued

Compound	Formula	Remarks	r_M
Esters (continued)			
Butanoic acid, ethyl ester	$C_6H_{12}O_2$		116
Carbonic acid, methyl ester	$C_3H_6O_3$		90
Carbonic acid, ethyl ester	$C_5H_{10}O_3$		118
Ethers			
Dimethyl ether	C_2H_6O		46
Methyl vinyl ether	C_3H_6O		58
Methyl ethyl ether	C_3H_6O		60
Diethyl ether	$C_4H_{10}O$		74
Methyl propyl ether	$C_4H_{10}O$		74
Ethyl propyl ether	$C_5H_{12}O$		88
Dipropyl ether	$C_6H_{10}O$		102
Ethyl phenyl ether	$C_8H_{10}O$		122
Halides/Related			
Fluorine	F_2	A	38
Chlorine	Cl_2	A	70
Bromine	Br_2		158
Iodine	I_2		254
Methyl chloride	CH_3Cl		50
Methyl bromide	CH_3Br		94
Methyl iodide	CH_3I		142
Vinyl chloride	C_2H_3Cl		62
Ethyl chloride	C_2H_5Cl		64
Ethyl bromide	C_2H_5Br		108
Ethyl iodide	C_2H_5I		152
2-chloro-1,3-butadiene	C_4H_5Cl		88
Chlorobenzene	C_6H_5Cl		112
Benzyl chloride	C_7H_7Cl		126
Methylene chloride	CH_2Cl_2		84
Dichloroethylene	$C_2H_2Cl_2$		96

Table 5-1 Continued

Compound	Formula	Remarks	r_M
Heterocyclics			
Pyrrole	C_4H_5N		67
Pyridine	C_5H_5N		79
Nicotinic acid	$C_6H_5NO_2$		123
Pyridoxal	$C_8H_9NO_3$		167
Pyridoxine	$C_8H_{11}NO_3$	B	169
Creatinine	$C_4H_7N_3O$		113
Indole	C_8H_7N		117
Skatole	C_9H_9N		131
Purine	$C_5H_4N_4$		120
Ethylene oxide	C_2H_4O		44
Propylene oxide	C_3H_6O		58
Furan	C_4H_4O		68
Tetrahydropyran	$C_5H_{10}O$		86
Pyrone	$C_5H_4O_2$		96
Thiophene	C_4H_4S		84
Thiazole	C_3H_3NS		85
Ketones			
Acetone	C_3H_6O		58
2-butanone	C_4H_8O		72
3-pentanone	$C_5H_{10}O$		86
Acetophenone	C_8H_8O		120
Benzalacetone	$C_{10}H_{10}O$		146
1-chloro-2-propanone	C_3H_5OCl		92
2,3-butanedione	$C_4H_6O_2$		86
2,4-pentanedione	$C_5H_8O_2$		100
Nitrates/Nitro/Related			
Nitrogen	N_2	A	28
Nitrogen monoxide	NO	A	30
Nitrogen dioxide	NO_2	A	46
Nitrogen tetroxide	N_2O_4		92

Table 5-1 Continued

Compound	Formula	Remarks	r_M
Nitrates/Nitro/Related (continued)			
Nitrogen oxychloride	$NOCl$		65
Nitromethane	CH_3NO_2		61
Nitrobenzene	$C_6H_5NO_2$		123
Nitrophenol	$C_6H_5NO_3$		139
Ethyl nitrite	$C_2H_5NO_2$		75
Ethyl nitrate	$C_2H_5NO_3$		91
Acetyl nitrate	$C_2H_3NO_4$		105
Acetonitrile	CH_3CN		41
Diazomethane	CH_2N_2		42
Sugars/Related			
Arabinose	$C_5H_{10}O_5$	B	150
Ribose	$C_5H_{10}O_5$	B	150
Xylose	$C_5H_{10}O_5$	B	150
Deoxygalactose	$C_6H_{12}O_5$	B	164
Galactose	$C_6H_{12}O_6$	B	180
Glucose	$C_6H_{12}O_6$	B	180
Mannose	$C_6H_{12}O_6$	B	180
Sucrose	$C_{12}H_{22}O_{11}$	B	342
Glucosamine	$C_6H_{13}NO_5$	B	179
Sulfides/Related			
Dimethyl sulfide	C_2H_6S		62
Diethyl sulfide	$C_4H_{10}S$		90
Carbon disulfide	CS_2		76
Sulfur dioxide	SO_2	A	64
Thio/Thioesters/Sulfonyls			
Thiomethane	CH_4S		48
Thioethane	C_2H_6S		62
Thioaceticacid	C_2H_4OS		76

Table 5-1 Continued

Compound	Formula	Remarks	r_M
Thio/Thioesters/Sulfonyls (continued)			
Taurine	C_2H_7NOS	B	125
Ethane sulfonyl chloride	C_2H_5OSCl		128
Urea/Related			
Urea	CH_4N_2O		60
Methylurea	$C_2H_6N_2O$		74
Acetylurea	$C_3H_6N_2O_2$		102
Thiourea	CH_4N_2S		76
Uric acid	$C_5H_4N_4O_3$		168
Vitamins/Related			
Thiamine	$C_{12}H_{16}N_4OS$	B	264
Riboflavin	$C_{17}H_{20}N_4O_6$	B	376
Folic acid	$C_{19}H_{19}N_7O_6$	B	441
Dehydroascorbic acid	$C_6H_6O_6$	B	174
Miscellaneous			
Carbon monoxide	CO	A	28
Carbon dioxide	CO_2	A	44
Methyl thiocyanate	C_2H_3NS		73
Methyl isothiocyanate	C_2H_3NS		73
Epinephrine	$C_9H_{13}NO_3$		183
Phenolphthalein	$C_{20}H_{14}O_4$		318
Dehydrobilirubin	$C_{33}H_{34}N_4O_6$	B	582
Bilirubin	$C_{33}H_{36}N_4O_6$	B	584

Table 5-1 Continued

Explanation of remarks:

A) Low r_M and/or highly volatile compound not suspected to be amenable to identification by cryo-focused methods employed in this chapter.

B) Involatile compound, salt, or compound which decomposes in the temperature range of the analyses. This compound is not expected to be amenable to GC.

C) A gap in the class series exists; however, the presence of the missing compound in the series is implicit in one or more of the literature sources.

D) This compound is suspected to be present, but unconfirmed in the literature.

E) This compound exists in solution only and is not expected to be detected by GC.

possible, as well as the order within each group, for additional tables in this chapter which report qualitative identification of components.

A total of at least 23 methods, including GC/MS, were used in the literature sources to identify compounds listed in this table. The low r_M compounds listed in this table may be difficult to confirm by the GC/MS methods employed here. There are compounds in this table for which the volatility is extremely high; these compounds are not expected to be effectively collected on glass beads, nor are they likely to remain on the glass beads until desorption in the GC. Compounds which fall under this category are noted by an (A) in the remarks column of the table.

The majority of compounds listed were determined using separation methods other than GC. Some compounds in the table were separated by, for example, liquid chromatography (LC). These compounds are involatile and well chromatographed by LC but may not be amenable to GC. Compounds which fall under this category, such as involatiles, salts, or compounds which thermally decompose in the temperature range of analyses, are not amenable to GC analysis; therefore they are noted by the remark code (B) in the Table 5-1.

There is an implicit comment made in one of the literature sources that the presence of the complete series of saturated carboxylic acids from acetic acid up to octadecanoic acid is observed in human perspiration, without specifically providing the data to confirm this [30]. Therefore, completion of the series is noted by the presence of (C) in the remarks indicating the compound(s) of lower carbon number

previous to this compound are present. However, if a compound was only suspected as being present in the literature sources, then the compound is noted by a (D) in the remarks column. The final remark code (E) is used to denote species which are present in solution only. Since GC involves separation in the gas phase, compounds so noted are not expected to be observed in the analyses of this chapter.

In summary, this first table provides a general basis from which to proceed. It should be noted that the analyses which follow (in the remainder of this chapter) are specifically designed to provide information on volatiles from the skin. More specifically, these analyses will only consist of volatiles which transfer to glass (beads) and can be thermally desorbed back off of glass to be detected by either cryo-focused GC/MS or purge and trap GC/MS.

Cryo-focusing GC/MS

A single stage of cryo-focusing combined with GC/MS was the primary method used for identification of volatiles in this work. Most of the analyses involve the identification of volatiles from the hands, arms, and forehead of the author of this dissertation. Additional identification of volatiles and repeated confirmation of compound identification came from the case studies presented later in this chapter. Therefore, the data found in this section are compilations of emanations observed from four different subjects. Studies involved the acquisition of PPINCI and EI mass spectral data. Typical RIC traces from a set of PCI, NCI, and EI analyses of the same subject appear in figure 5-1.

Figure 5-1 Comparison of RIC traces for NCI, PCI, and EI modes of ionization in a typical subject analysis. The sample was 3 glass beads handled for 15 minutes by Mr. Dan Smith of the USDA. Separation was effected on a 25 m x 0.20 mm i.d. FSOT HP5 column. Additional parameters are found in the experimental section.

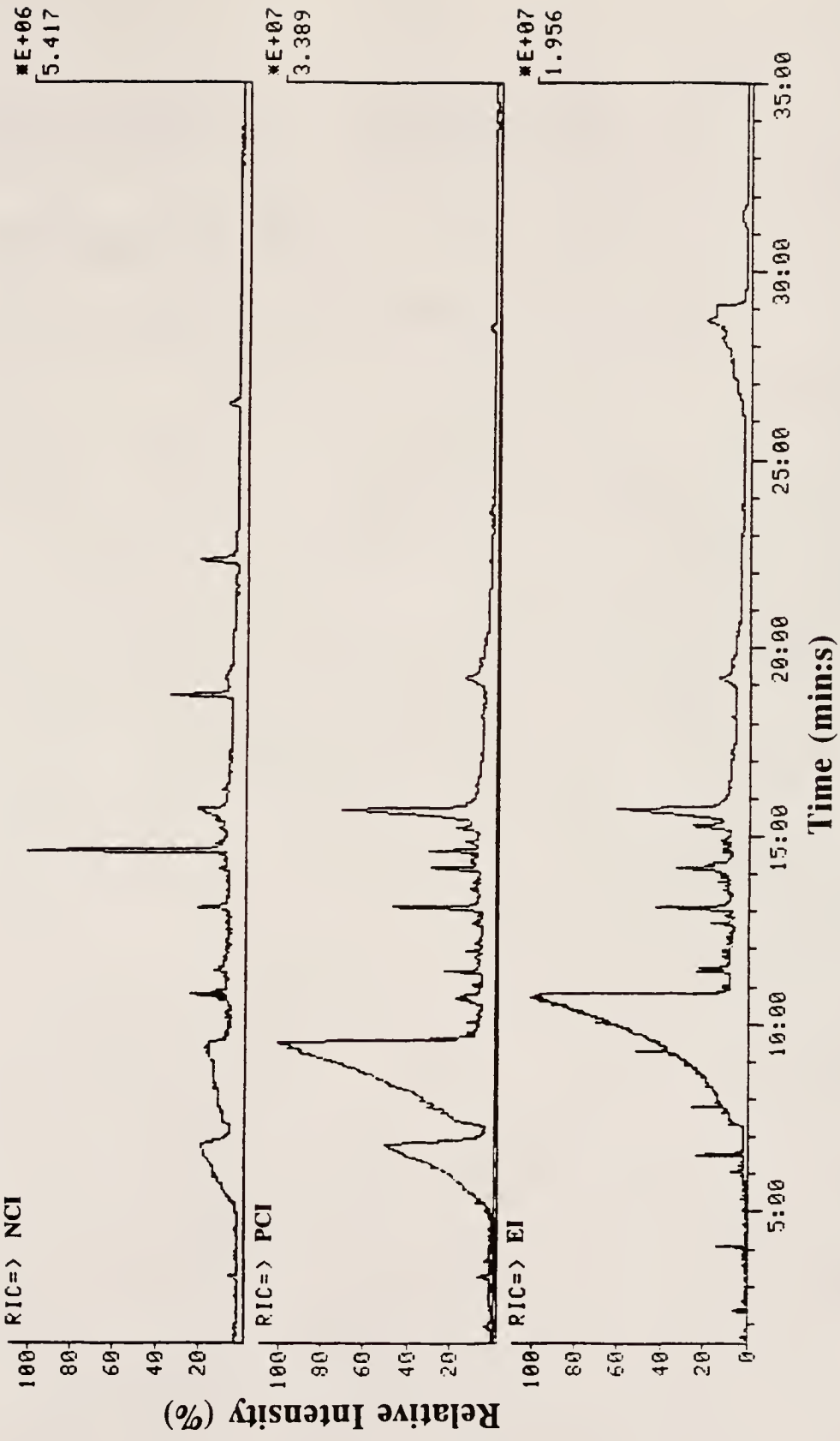
RIC=> NCI
*E+06
5.417
RIC=> PCI
*E+07
3.389
RIC=> EI
*E+07
1.956
Relative Intensity (%)
Time (min:s)
5:00
10:00
15:00
20:00
25:00
30:00
35:00

This figure is included for several reasons. Upon first inspection, the sample may not appear to contain more than 100 discernible peaks; however, the typical analysis by the methods employed here contains over 300 peaks, and may contain up to 350 distinct components. Contained within the RIC trace are many low intensity peaks obscured by the intensity scale use to display the acid peaks. It is evident from this figure that most readily seen components provide observable peaks in CI and EI. There are many components in these analyses that provided interesting problems in terms of identification; however, at this time, only two chromatographic peaks in this figure will be addressed.

The first component of interest is poorly chromatographed and located at a retention time of 6 min. This peak is noticeably abundant in the sample, and it is clearly seen that information in EI is scarce by the absence of significant peak. Upon examination in NCI mode, this peak was identified by its relative molecular mass and characteristic fragment ions of lactic acid (see chapter 3). The second abundant component, located at a retention time between 8 and 10 min, eluded identification for some time, despite being one of the most abundant peaks in analyses conducted with this subject. Due to the absence of a molecular ion in the EI mass spectrum for this compound, the shape of the peak as well as relative molecular mass information from PCI and NCI were employed to aid in identification. The shape of this peak is similar to that of lactic acid; therefore, it was expected that this compound may also be a hydroxy acid, or possibly similar in

structure. Visual inspection of PCI data revealed that a r_M of 92 was plausible due to the abundance of the apparent $[M+H]^+$ ion at m/z 93. However, NCI mass spectra did not contain an abundant $[M-H]^-$ ion at m/z 91. The NCI spectra did contain an ion at m/z 183 which was postulated to be the $[M_2-H]^-$ ion of this compound. When the library searching was restricted to compounds with a r_M of 92, this compound, 1,2,3-propanetriol (glycerol), was still not correctly identified. Final confirmation was achieved by comparing the EI mass spectra to that of a standard of glycerol. Glycerol was delivered into the mass spectrometer ion source via the use of the direct insertion probe. When the ion source was saturated under these conditions, it was revealed that self-CI had occurred upon elution of glycerol during previous sample analyses. The presence of CI-produced fragments in the EI mass spectrum did not permit successful library searching. One final note merits mentioning with respect to the importance of identifying this component in the sample. The glycerol peak from all other subjects was miniscule in comparison to the abundance found in this subject. It was later determined that this high level of glycerol is attributable to the Sta-Sof-Fro™ hair and scalp spray used by this subject; glycerol is one of the primary ingredients in the product.

These two components are two of approximately 310 components observed in these analyses; components identified and components suspected are listed in table 5-2. In general, the subjects studied are similar with respect to composition of emanations. There are some exceptions; further studies may reveal whether these

Table 5-2 Compounds present and compounds suspected of being present which emanate from human skin. This list was derived from cryo-focused GC/MS analyses of four human subjects. Listed with the compounds are the corresponding molecular formula and relative molecular mass (r_M). Explanation of remarks follows this table.

Compound	Formula	Remarks	r_M
Carboxylic acids			
2-propenoic acid	$C_3H_4O_2$	G	72
Propanoic acid	$C_3H_6O_2$	G	74
2-butenoic acid	$C_4H_6O_2$		86
2-methyl-2-butenoic acid	$C_5H_8O_2$	B,C	98
3-methyl-2-pentenoic acid	$C_6H_{10}O_2$	C	114
3-methyl-pentanoic acid	$C_6H_{12}O_2$	C	116
Hexanoic acid	$C_6H_{12}O_2$	A,G	116
Heptanoic acid	$C_7H_{14}O_2$	G	130
Octanoic acid	$C_8H_{16}O_2$	A,G	144
Nonanoic acid	$C_9H_{18}O_2$	G	158
Decanoic acid	$C_{10}H_{20}O_2$	G	172
Undecanoic acid	$C_{11}H_{22}O_2$	A,G	186
Dodecanoic acid	$C_{12}H_{24}O_2$	G	200
Methyldodecanoic acid	$C_{13}H_{26}O_2$	C	214
Tridecanoic acid	$C_{13}H_{26}O_2$	G	214
Tetradecenoic acid	$C_{14}H_{26}O_2$	C	226
Methyltridecanoic acid	$C_{14}H_{28}O_2$	C	228
Tetradecanoic acid	$C_{14}H_{28}O_2$	G	228
14-pentadecenoic acid	$C_{15}H_{28}O_2$		240
12-methyltetradecanoic acid	$C_{15}H_{30}O_2$		242
Methyltetradecanoic acid	$C_{15}H_{30}O_2$	C	242
Methyltetradecanoic acid	$C_{15}H_{30}O_2$	C	242
Pentadecanoic acid	$C_{15}H_{30}O_2$	G	242
9-hexadecenoic acid	$C_{16}H_{30}O_2$		254
Methylpentadecanoic acid	$C_{16}H_{32}O_2$	C	256
Hexadecanoic acid	$C_{16}H_{32}O_2$	G	256
Heptadecenoic acid	$C_{17}H_{32}O_2$	C	268
Heptadecanoic acid	$C_{17}H_{34}O_2$	C,G	270
11-phenoxyundecanoic acid	$C_{17}H_{26}O_3$	A,E	278
9,12-octadienoic acid	$C_{18}H_{32}O_2$		280

Table 5-2 Continued

Compound	Formula	Remarks	r_M
Carboxylic acids (continued)			
9-octadecenoic acid	$C_{18}H_{34}O_2$		282
Methylheptadecanoic acid	$C_{18}H_{36}O_2$	C	284
Octadecanoic acid	$C_{18}H_{36}O_2$	G	284
Docosanoic acid	$C_{22}H_{44}O_2$		340
Lactic acid	$C_6H_6O_3$	G	90
Hexanedioic acid	$C_6H_{10}O_4$	A,E	146
Heptanedioic acid	$C_7H_{12}O_4$	A,E	160
Benzoic acid	$C_7H_6O_2$	G	122
4-hydroxybenzoic acid	$C_7H_6O_3$		138
4-hydroxy-3-methoxybenzoic acid	$C_8H_8O_4$		168
Alcohols			
2-butanol	$C_4H_{10}O$	C	74
3-methyl-4-penten-2-ol	$C_6H_{12}O$	B,C	100
2-hexen-1-ol	$C_6H_{12}O$	C	100
4-hexen-1-ol	$C_6H_{12}O$		100
1-hexen-3-ol	$C_6H_{12}O$		100
2-methyl-3-pentanol	$C_6H_{14}O$	B,C	102
1-hepten-3-ol	$C_7H_{14}O$		114
1-octen-3-ol	$C_8H_{16}O$	A,D	128
2-octen-1-ol	$C_8H_{16}O$		128
2-methyl-3-octenol	$C_9H_{18}O$	C	142
Nonenol	$C_9H_{18}O$	B,C	142
3,7-dimethyl-6-octen-1-ol	$C_{10}H_{20}O$	C	156
Decenol, substituted	$C_{10}H_{20}O$	B,D	156
2-decanol	$C_{10}H_{22}O$		158
Dodecenol	$C_{12}H_{24}O$	A,B	184
Tridecanol	$C_{13}H_{28}O$	A	200
1-tetradecanol	$C_{14}H_{30}O$		214
2-hexadecanol	$C_{16}H_{34}O$	B	242
2-heptadecanol	$C_{17}H_{36}O$	A,B	256
Cholest-5-en-3-ol	$C_{27}H_{46}O$	G	386
Phenol	C_6H_6O	G	94
Benzyl alcohol	C_7H_8O	G	108

Table 5-2 Continued

Compound	Formula	Remarks	r_M
Alcohols (continued)			
Phenylethyl alcohol	$C_8H_{10}O$	A,E	122
2,4-bis(1,1-dimethylethyl)phenol	$C_{14}H_{22}O$	C	206
2,5-bis(1,1-dimethylethyl)phenol	$C_{14}H_{22}O$		206
2,4-bis(1,1-methylpropyl)phenol	$C_{14}H_{22}O$		206
4,6-di(1,1-dimethylethyl)-2-methylphenol	$C_{15}H_{24}O$		220
2-(2H-benzotriazol-2-yl)-4-methylphenol	$C_{13}H_{11}N_3O$	A,D	225
Ethylene glycol	$C_2H_6O_2$	G	62
1,9-nonanediol	$C_9H_{20}O_2$	A,E	160
Glycerol	$C_3H_8O_3$	G	92
2-(hydroxymethyl)-2-methyl-1,3-propanediol	$C_5H_{12}O_3$	A,E	120
Aldehydes			
Propanal	C_3H_6O	G	58
2-methylpropanal	C_4H_8O	G	72
2-methyl-2-butenal	C_4H_6O	B,C	84
2-methylbutanal	$C_5H_{10}O$	C,G	86
3-methylpentanal	$C_6H_{12}O$		100
Heptanal	$C_7H_{14}O$		114
2,2-dimethylhexanal	$C_8H_{16}O$		128
Octanal	$C_8H_{16}O$	B,C	128
2,4-nonadienal	$C_9H_{14}O$		138
Nonanal	$C_9H_{18}O$		142
3,7-dimethyl-2,6-octadienal	$C_{10}H_{16}O$	B,C	152
Decanal	$C_{10}H_{20}O$	B,C	156
Dodecanal	$C_{12}H_{24}O$	B,C	184
2-methylhexadecanal	$C_{17}H_{34}O$	A,B	254
Benzaldehyde	C_7H_6O		106
3-hydroxy-4-methylbenzaldehyde	$C_8H_8O_2$		136
4-phenylmethoxybenzaldehyde	$C_{14}H_{12}O_2$		212

Table 5-2 Continued

Compound	Formula	Remarks	r_M
Aliphatics/Aromatics			
Pentene	C_5H_{10}	B	70
4-methyl-2-pentene	C_6H_{12}		84
Hexane	C_6H_{14}	C	86
Dimethylpentadiene	C_7H_{12}	B,C	96
2-methyl-1-hexene	C_7H_{14}		98
Heptane	C_7H_{16}	C	100
3-ethyl-1,4-hexadiene	C_8H_{14}	A,B	110
5-methyl-1-heptene	C_8H_{16}	C,F	112
2-octene	C_8H_{16}	F	112
3-octene	C_8H_{16}	C,F	112
4-octene	C_8H_{16}	C,F	112
2,4-dimethylhexane	C_8H_{18}	C	114
Octane	C_8H_{18}	C	114
3,4-nonadiene	C_9H_{16}		124
2,6-dimethyl-1-heptene	C_9H_{18}		126
4-ethyl-3-heptene	C_9H_{18}	C	126
4-nonene	C_9H_{18}		126
Nonane	C_9H_{20}		128
N-menth-6-ene	$C_{10}H_{18}$		138
Menthane	$C_{10}H_{20}$	A	140
3,3,6-trimethyl-1,5-heptadiene	$C_{10}H_{18}$	D,E	138
2,7-dimethyl-1-octene	$C_{10}H_{20}$	A,E	140
5-decene	$C_{10}H_{20}$		140
Decane	$C_{10}H_{22}$	C,G	142
Undecadiene	$C_{11}H_{20}$	B	152
2-methyl-2-undecene	$C_{12}H_{24}$	D,E	168
3-methyl-5-undecene	$C_{12}H_{24}$	D,E	168
4-methyl-4-undecene	$C_{12}H_{24}$	B,C	168
2-methyl-2-dodecene	$C_{13}H_{26}$		182
Methyldodecene	$C_{13}H_{26}$	C	182
5-tetradecene	$C_{14}H_{28}$		196
Cyclotetradecane	$C_{14}H_{28}$		196
Tetradecane	$C_{14}H_{30}$	B,C	198
Pentadecane	$C_{15}H_{32}$		212
7-hexadecene	$C_{16}H_{32}$	D,E	224

Table 5-2 Continued

Compound	Formula	Remarks	r_M
Aliphatics/Aromatics (continued)			
Cyclohexadecane	$C_{16}H_{32}$		224
Hexadecane	$C_{16}H_{34}$		226
Heptadecane	$C_{17}H_{36}$	C	240
9-octadecene	$C_{18}H_{36}$		252
Octadecane	$C_{18}H_{38}$	C	254
7,11,15-trimethyl-3-methylene hexadecane	$C_{20}H_{32}$	C	272
Heneicosane	$C_{21}H_{34}$		296
Docosane	$C_{22}H_{46}$		310
Tricosane	$C_{23}H_{48}$		324
Tetracosane	$C_{24}H_{50}$	A,E	338
Pentacosane	$C_{25}H_{52}$		352
Cholesta-3,5-diene	$C_{27}H_{44}$	A,B	392
Triacontene, branched	$C_{30}H_{50}$	C	410
Squalene	$C_{30}H_{50}$	G	410
Benzene	C_6H_6	G	78
Toluene	C_7H_8	G	92
Styrene	C_8H_8		104
1,4-dimethylbenzene	C_8H_{10}	C	106
Ethylbenzene	C_8H_{10}		106
Propylbenzene	C_9H_{12}		120
4,4′-dimethyl-1,1′-biphenyl	$C_{14}H_{14}$	C	182
Amides/Amines/Related			
Propanamide	C_3H_7NO		73
N,N-diethyl-3-methylbenzamide	$C_{12}H_{17}NO$		191
N,N-bis(2-hydroxyethyl)dodecanamide	$C_{13}H_{33}NO_3$	A,E	287
N,N-didodecyl formamide	$C_{25}H_{51}NO$	B	381
1,3-butanediamine	$C_4H_{12}N_2$	A	84
N,N-dimethyl-1,2-ethanediamine	$C_6H_6N_2$	D,E	116
N-ethylcyclopentamine	$C_7H_{15}N$	A	113
N,N-dimethyl-3-butoxypropylamine	$C_9H_{21}NO$	A	159
N,N-dimethyl-3-benzyloxypropylamine	$C_{12}H_{19}NO$		193
N-methyl-N-nitroso-1-dodecanamine	$C_{13}H_{28}N_2O$	A	228

Table 5-2 Continued

Compound	Formula	Remarks	r_M
Amides/Amines/Related (continued)			
N,N-dimethyl-1-dodecanamine	$C_{14}H_{31}N$	F	213
N,N-dimethyl-1-tridecanamine	$C_{15}H_{33}N$	F	227
N,N-dimethyl-1-tetradecanamine	$C_{16}H_{35}N$	F	241
N,N-dimethyl-1-pentadecanamine	$C_{17}H_{37}N$	F	255
N,N-dimethyl-1-hexadecanamine	$C_{18}H_{39}N$	F	269
N,N-dimethyl-1-heptadecanamine	$C_{19}H_{41}N$	F	283
N,N-dimethyl-1-octadecanamine	$C_{20}H_{43}N$	F	297
Esters			
2-butenoic acid, butyl ester	$C_8H_{16}O_2$	A	128
Butanoic acid, Methyl ester	$C_5H_{10}O_2$	A,B	102
Nonanoic acid, methyl ester	$C_{10}H_{20}O_2$		172
Tridecanoic acid, methyl ester	$C_{14}H_{28}O_2$	A	228
13-methylpentadecanoic acid, methyl ester	$C_{17}H_{34}O_2$		270
14-methylpentadecanoic acid, methyl ester	$C_{17}H_{34}O_2$		270
2-methylhexadecanoic acid, methyl ester	$C_{18}H_{36}O_2$		284
Heptadecanoic acid, methyl ester	$C_{18}H_{36}O_2$		284
6-octadecenoic acid, methyl ester	$C_{19}H_{36}O_2$	C	296
Hexadecanoic acid, methyl ester	$C_{19}H_{38}O_2$		298
16-methylheptadecanoic acid, methyl ester	$C_{19}H_{38}O_2$	C	298
Octadecanoic acid, methyl ester	$C_{19}H_{38}O_2$	B	298
Hexadecanoic acid, butyl ester	$C_{20}H_{40}O_2$		312
Octadecanoic acid, phenyl ester	$C_{24}H_{40}O_2$		360
Tetradecanoic acid, undecyl ester	$C_{25}H_{50}O_2$	A,B	382
Tetracosanoic acid, methyl ester	$C_{25}H_{50}O_2$	A,B	382
Pentanedioic acid, ester		D,E	>144
Pentanedioic acid, mono(2-ethylhexyl)ester	$C_{13}H_{24}O_4$		244
Hexanedioic acid, ester		D,E	>160
Hexanedioic acid, ester branched		D,E	>160

Table 5-2 Continued

Compound	Formula	Remarks	r_M
Esters (continued)			
Hexanedioic acid, Mono(2-ethylhexyl)ester	$C_{14}H_{26}O_4$		258
Hexanedioic acid, Octyl ester	$C_{14}H_{26}O_4$	B	258
Heptanedioic acid, Dibutyl ester	$C_{15}H_{28}O_4$	B	272
Hydroxybutanedioic acid, Ethyl ester	$C_8H_{14}O_5$	A	190
3-hydroxybenzoic acid, Ethyl ester	$C_8H_8O_3$		152
4-hydroxybenzoic acid, Propyl ester	$C_{10}H_{12}O_3$		180
2-hydroxybenzoic acid, Phenylmethyl ester	$C_{14}H_{12}O_3$		228
2,4-dihydroxy-3,6-dimethylbenzoic acid, Methyl ester	$C_{10}H_{12}O_4$		196
Halides/Related			
Methyl iodide	CH_3I	G	142
1-chlorohexane	$C_6H_{13}Cl$		120
1-chloroheptane	$C_7H_{15}Cl$		134
1-chlorononane	$C_9H_{19}Cl$		162
1-chlorododecane	$C_{12}H_{25}Cl$		204
1-chlorotetradecane	$C_{14}H_{29}Cl$		232
1-chloropentadecane	$C_{15}H_{31}Cl$	B	246
1-chlorohexadecane	$C_{16}H_{33}Cl$	B	260
1,6-dichloro-1,5-cyclooctadiene	$C_8H_{10}Cl_2$	B,D	176
Benzylchloride	C_7H_7Cl	G	126
3-chlorobenzeneamine	C_6H_6NCl		127
2-chloro-1-methylethylbenzene	$C_9H_{11}Cl$	D	154
1-chloro-4-(4-methyl-4-pentyl) benzene	$C_{12}H_{15}Cl$	D	194
2,3-dichlorobenzeneamine	$C_6H_5NCl_2$	C	161
Heterocyclics			
2-methyl-1H-pyrrole	C_5H_7N		81
3-methyl-1H-pyrrole	C_5H_7N		81

Table 5-2 Continued

Compound	Formula	Remarks	r_M
Heterocyclics (continued)			
Pyridine	C_5H_5N	G	79
2-pyridinamine	$C_5H_6N_2$		94
4-pyridinamine	$C_5H_6N_2$		94
4-methyl-2-pyridinamine	$C_6H_8N_2$		108
2-methylpyridine	C_6H_7N		93
4(1H)-pyridinone	C_5H_5NO		95
6-amino-3-pyridine carboxylic acid	$C_6H_6N_2O_2$	B,F	138
3(1-methyl-2-pyrrolidinyl)pyridine	$C_{10}H_{14}N_2$	F	162
1,2,3-4-tetrahydroquinoline	$C_9H_{11}N$		133
2,3,4-trimethylquinoline	$C_{12}H_{13}N$	A	171
2-ethylpiperidine	$C_7H_{15}N$		113
1-piperidineethanol	$C_7H_{15}NO$	D,E	129
4-piperidinemethanamine	$C_6H_{14}N_2$	A	114
1-phenyl-3-(1-piperidinyl) 2-buten-1-one	$C_{15}H_{19}NO$		229
1H-indole	C_8H_7N	G	117
Indole, substituted		D	>117
4,5-dihydro-2-methyl-1H-imidazole	$C_4H_8N_2$		84
1,5-dimethyl-1H-pyrazole	$C_5H_8N_2$	C	96
Pyrazine	$C_4H_4N_2$		80
2,6-dimethylpyrazine	$C_6H_8N_2$	B	108
Trimethylpyrazine	$C_7H_{10}N_2$	A	122
3-ethyl-2,5-dimethylpyrazine	$C_8H_{12}N_2$	C	136
5-methyl-2-methylthio-4(1H)-pyrimidinone	$C_6H_8N_2OS$	A	156
1-methylpiperazine	$C_5H_{12}N_2$	B	100
2,5-dimethylpiperazine	$C_6H_{14}N_2$	B	114
Oxazole	C_3H_3NO		69
2-methylfuran	C_5H_6O		82
3-methylfuran	C_5H_6O		82
2,3-dihydro-4-methylfuran	C_5H_8O	B	84
2-furanmethanol	$C_5H_6O_2$		98
Benzofuran	C_8H_6O		118
Dihydro-5-tetradecyl-2(3H)furanone	$C_{18}H_{34}O_2$	B	282

Table 5-2 Continued

Compound	Formula	Remarks	r_M
Heterocyclics (continued)			
2,3-dihydro-3,5-dihydroxy-6-methyl-4H-pyran-4-one	$C_6H_8O_4$		144
2-methoxy-6-methyl-4H-pyran-4-one	$C_7H_8O_3$	B	140
2H-1-benzopyran-2-one	$C_9H_6O_2$		146
3-acetyl-6-methyl-2H-pyran-2,4(3H)dione	$C_8H_8O_4$	A	168
Thiazolidine	C_3H_7NS		89
2-methylisothiazole	C_4H_5NS	A	99
5-methyl-2(5H)thiophenone	C_5H_6OS		114
2-methoxy-5-methylthiophene	C_6H_8OS		128
Ketones			
2-butanone	C_4H_8O	G	72
2-pentanone	$C_5H_{10}O$		86
3-pentanone	$C_5H_{10}O$	G	86
2-hexanone	$C_6H_{12}O$	C	100
6-methyl-3,5-heptadien-2-one	$C_8H_{12}O$	C	124
6-methyl-5-hepten-2-one	$C_8H_{14}O$		126
2-nonen-4-one	$C_9H_{16}O$	B	140
2-decanone	$C_{10}H_{20}O$		156
2-methoxy-2-octen-4-one	$C_9H_{16}O_2$		162
6,10-dimethyl-5,9-undecadien-2-one	$C_{13}H_{22}O$	A	194
3-hydroxy-androstan-11,17-dione	$C_{19}H_{28}O_3$		304
Sulfides			
Carbon disulfide	CS_2	G	76
Dimethyl disulfide	$C_2H_6S_2$		94

Table 5-2 Continued

Compound	Formula	Remarks	r_M
Thio/Thioesters/Sulfonyls			
Thiomethane	CH_4S	G	48
2-thiopropane	C_3H_8S	A	76
1-methyl thiobutane	$C_5H_{12}S$		104
1-thiododecane	$C_{12}H_{26}S$	D	202
3-methylthietane	C_4H_8S	A	88
3(methylthio)-1,2-propanediol	$C_4H_{10}O_2S$	D	122
o-(2-butenylthio)phenol	$C_{10}H_{12}OS$		180
Thiocarbamic acid, Butyl ester	$C_5H_{11}NOS$	A,E	127
Acetylthiocarbamic acid, Methyl ester	$C_4H_7NO_2$	B	130
Methanesulfonylchloride	CH_3OSCl		114
1,1′-sulfonylbis[4-chlorobenzene]	$C_{12}H_8O_2SCl_2$		286
Urea/Related			
Urea	CH_4N_2O	G	60
Methylurea	$C_2H_6N_2O$	G	74
Thiourea	CH_4N_2S	G	76
N,N-dimethylthiourea	$C_3H_8N_2S$		104
Miscellaneous			
1-isocyanato-3-methylbenzene	C_8H_7NO	B	133
1,3-dimethoxybutane	$C_6H_{14}O_2$	A,E	118
1,2,3-trimethoxypropane	$C_6H_{14}O_3$	A	134
1,4-benzenedicarbonitrile	$C_8H_{14}N_2$	A	128
Compounds present in background/Blank analyses			
Methylchloride	CH_3Cl	G	50
Tetrachloroethene	C_2Cl_4		164
1,1-difluroethane	$C_2H_4F_2$	F	66
Fluoroethene	C_2H_3F		46
1,1,2-trichloro-1,2,2-trifluoroethene	$C_2Cl_3F_2$		167
1-silacyclo-3-pentene	C_4H_8Si		84
Silacyclopentane	$C_4H_{10}Si$		86

Table 5-2 Continued

Compound	Formula	Remarks	r_M
Compounds present in background/Blank analyses (continued)			
Trimethylsilanol	$C_3H_{10}OSi$		90
Hexamethylcyclotrisiloxane	$C_6H_{18}O_3Si_3$		222
Octamethylcyclotetrasiloxane	$C_8H_{24}O_4Si_4$		296
Decamethylcyclopentasiloxane	$C_{10}H_{30}O_5Si_5$		370
Dodecamethylcyclohexasiloxane	$C_{12}H_{36}O_6Si_6$		444
Tetradecamethylhexasilioxane	$C_{14}H_{42}O_5Si_6$		458
Hexadecamethylcycloheptasiloxane	$C_{16}H_{48}O_6Si_7$		532
3-isopropoxy-1,1,1,7,7-hexamethyl-3,5,5-tris(trimethylsiloxy) Tetrasiloxane	$C_{18}H_{52}O_7Si_7$		576
1,2-benzenedicarboxylic acid, Diethyl ester	$C_{12}H_{14}O_4$		222
1,2-benzenedicarboxylic acid, Butylphenylmethyl ester	$C_{19}H_{20}O_4$		312
1,2-benzenedicarboxylic acid Diheptyl ester	$C_{22}H_{34}O_4$		362
1,2-benzenedicarboxylic acid, Diisooctyl ester	$C_{24}H_{38}O_4$		390
1,2-benzenedicarboxylic acid, Bis(2-ethylhexyl ester)	$C_{24}H_{38}O_4$		390
1,2-benznedicarboxylic acid, Diisononyl ester	$C_{26}H_{42}O_4$		418
1,2-benzenedicarboxylic acid, Undeterminded		D,E	>415

Explanation of remarks:

A) Identity of the compound is questionnable. This denotes a compound for which the most reasonable identity is listed; however, the EI library search purity value is low owing to either the absence of characteristic masses in the sample mass spectrum or the presence of additional masses in the sample spectrum versus the library spectrum.

Table 5-2 Continued

Explanation of remarks (continued):

B) The r_M of this compound is known from CI analysis. The actual structure given is questionnable.

C) The structure is known to a reasonable degree of certainty. Uncertainty exists in the location of the substituted functional group and/or in the double bond location.

D) The class or base structure of this compound is characterized by a specific EI fragmentation pattern. The information from CI may or may not be available to assist in determining the identity of this compound.

E) The r_M from CI analysis for this compound is questionnable.

F) Refer to the text for further explanation about this compound.

G) This compound was previously reported in the literature as one having dermal origin.

originate naturally from the body, or are due to deposition on the skin from an external source. There are approximately 40 component peaks found present in each sample for which the identity could not be determined. These are included in this table.

The remark codes used for this table appear at the end of the table. Absence of remark codes A-E indicates that this compound was identified with a relatively high purity (greater than approximately 800 of 1000 maximum possible score) in some cases. The purity value is generated by the library search program and reflects a weighted average of the forward fit and reverse fit values. The forward fit value is decreased when the sample mass spectrum contains additional masses not found in the reference library mass spectrum. The reverse fit value is decreased when the sample mass spectrum does not contain masses found in the reference library mass spectrum. If the compound had a lower purity, but was confirmed in numerous samples as well as a high reverse fit value, then the compound is reasonably certain to be that which is listed. In most complex analyses, additional masses will be present from background which will reduce the forward fit value but not affect the reverse fit as greatly.

A remark code of (A) denotes those compounds for which the identity is questionnable; these compounds may even belong to a different class. If the molecular weight is known, but the structure given is still questionnable, the compound will be denoted with a (B) code. In some cases the r_M is known and the

EI fragmentation pattern is consistent with the structure. However, due to similarity between isomers, the exact structure can't be postulated with reasonable certainty. Compounds fitting this category are noted by a (C) code. If the EI pattern is consistent with a particular class, but the substitution identity is not known, a code of (D) is used. A code of (E) is given when the CI analysis for the compound did not yield information about the (r_M). A code of F listed in the table refers the reader to the text following this explanation of codes for additional discussion about specific compounds. The final code (G) denotes compounds previously identified in the literature, which are listed in table 5-1.

There are four points of interest to be addressed concerning the compounds listed in this table. The first concerns the four octene isomers listed in the table and denoted by the remark code (F). These are listed in this fashion because in one or more analyses, there were in fact four peaks attributable to octene. This holds true for all multiple listings of isomers of the same compound. Any uncertainty as to the possible structure is treated by listing the best reverse fit structure from the library and using the remark code (C) to denote that this compound may in fact be an isomer of the compound listed. Substituted benzenes, for which two isomeric peaks are often detected, will include the meta- isomer, and either the ortho- or para- listed with a (C) code. This is due to the similarity in the fragmentation of two or more of these isomers which cannot be distinguished by visual inspection or by library search of the mass spectra.

The tertiary amines running from N,N-dimethyl-1-dodecanamine to N,N-dimethyl-1-octadecanamine were not identified until relatively late in the work of this dissertation. Some of these amines elute at almost identical retention times as the carboxylic acids, and their peaks are sometimes hidden under more abundant sample components. When EI mass spectra were examined, there are only two significant ions present, that of the base beak at m/z 58 (due to β-cleavage of the chain) and that of the corresponding odd-mass molecular ion. Library identification typically fails to identify these compounds correctly. Upon manual inspection of library mass spectra for suspected amines, it was determined that in addition to the 12 carbon or greater chain, substitutions of anything larger than but methyl groups would result in additional characteristic ions in the spectra. Once the proper restrictions were imposed upon the library search, the identification of these amines were achieved readily provided they were contained within the library.

The final component of interest to be discussed in the text is one which was introduced unintentionally into the system but later used to aid in comparisons. The compound 1,1-difluoroethene is found in Dust-Off. Dust-Off was employed to cool down the glass injection port liner between runs prior to introducing a sample. When the glass injection port liner was reinserted and the analysis conducted, latent difluoroethene was cryo-focused with the sample. Normally, this was the first peak which eluted off of the column. This retention time of this component was later used in correlating analyses acquired with the same GC and MS parameters.

Purge and trap GC/MS

Limited studies microscale purge and trap were some of the last experiments conducted for this dissertation. Although replicate analyses were conducted, the results are somewhat preliminary. The results from these analyses are reported in table 5-3. Complementary CI analysis was not conducted in these experiments. The compounds listed in the table were derived from EI analyses only. Due to the absence of information on compound r_M by CI, the identification process relied more heavily upon EI library search purity values. The remark codes used in the table reflect this.

A remark code of (A) denotes a questionnable identity of a compound. If the mass spectrum displayed a characteristic EI fragmentation pattern attributable to a specific class, or if there was uncertainty in the structure due to isomers, a code of (B) was used. If the compound was previously identified in the literature (reported in table 5-1), the code (C) appears in the remark column. If the compound identified is also reported as observed in cryo-focused analyses (table 5-2), a code of (D) is present. Finally, a code of (E) in the table indicates that this compound will be addressed further in the following text.

The first designated component to be discussed is ethanol. This was only identified to be present one time in the analyses of emanations from the author of this dissertation. The particular analysis was conducted approximately 15 hours after consumption of two glasses of wine for dinner the previous evening. This may have

Table 5-3 Compounds present and compounds suspected of being present which emanate from human skin. This list was derived from microscale purge and trap GC/MS analyses of two human subjects. Listed with the compounds are the corresponding molecular formula and relative molecular mass (r_M). Explanation of remarks follows this table.

Compound	Formula	Remarks	r_M
Alcohols			
Ethanol	C_2H_6O	C,E	46
Isopropyl alcohol	C_3H_8O	C	60
Butenol	C_4H_8O	B	72
2-methyl-2-propanol	$C_4H_{10}O$		74
2-butanol	$C_4H_{10}O$	D	74
2-methylbutenol	$C_5H_{10}O$	B	86
Pentanol	$C_5H_{12}O$	C	88
Hexanol	$C_6H_{14}O$	D	102
3-methylcyclohexanol	C_7H_{14}	A	114
Heptanol, branched	$C_7H_{16}O$	B,D	116
1-heptanol	$C_7H_{16}O$		116
Octenol	$C_8H_{16}O$	A,D	128
2-propyl-1-pentanol	$C_8H_{18}O$	A	130
2-methyl-1-heptanol	$C_8H_{18}O$		130
Octanol	$C_8H_{18}O$		130
2-nonen-1-ol	$C_9H_{18}O$	B,D	142
2-decen-1-ol	$C_{10}H_{20}O$	D	156
2-propyl-1-heptanol	$C_{10}H_{22}O$	B	158
2-undecen-1-ol	$C_{11}H_{22}O$	A	170
2-tridecen-1-ol	$C_{13}H_{26}$	B,D	198
Eucalyptol	$C_{10}H_{18}O$	A	154
2-methyl-1,5-heptadien-3,4-diol	$C_8H_{14}O_2$	A	142
Phenol	C_6H_6O	C,D	94
3,5-dimethylphenol	$C_8H_{10}O$		122
2-ethyl-5-propylphenol	$C_{11}H_{16}O$	A	164
Aldehydes			
2-methyl-2-propenal	C_4H_6O		70
2-methylpropanal	C_4H_8O	C,D	72
Butanal	C_4H_8O	C	72

Table 5-3 Continued

Compound	Formula	Remarks	r_M
Aldehydes (continued)			
2-ethyl-2-propenal	C_5H_8O		84
2-pentenal	C_5H_8O		84
2,2-dimethylpropanal	$C_5H_{10}O$	B	86
2-methylbutanal	$C_5H_{10}O$	D	86
3-methylbutanal	$C_5H_{10}O$	C	86
Pentanal	$C_5H_{10}O$		86
2-hexadienal	C_6H_8O		96
4-methyl-3-pentanal	$C_6H_{10}O$		98
2-hexenal	$C_6H_{10}O$		98
2-ethylbutanal	$C_6H_{12}O$	A	100
3-methylpentanal	$C_6H_{12}O$	D	100
Hexanal	$C_6H_{12}O$		100
2,4-heptadienal	$C_7H_{10}O$	A	110
2-heptenal	$C_7H_{12}O$		112
Heptanal	$C_7H_{14}O$	D	114
2-octenal	$C_8H_{14}O$	B	126
3,3-dimethylhexanal	$C_8H_{16}O$	A,D	128
Octanal	$C_8H_{16}O$	D	128
2-nonenal	$C_9H_{16}O$		140
Nonenal	$C_9H_{16}O$	B	140
Nonanal	$C_9H_{18}O$	D	142
2-decenal	$C_{10}H_{18}O$	B	154
Decanal	$C_{10}H_{20}O$	D	156
Undecanal	$C_{11}H_{22}O$		170
2-dodecenal	$C_{12}H_{22}O$	B	182
Benzaldehyde	C_7H_6O	D	106
Methylbenzaldehyde	C_8H_8O	B	120
Benzeneacetaldehyde	C_8H_8O		120
Aliphatics/Aromatics			
Propene	C_3H_6	A,C	42
Propane	C_3H_8		44
2-butene	C_4H_8		56
2-methylpropane	C_4H_{10}	A	58

Table 5-3 Continued

Compound	Formula	Remarks	r_M
Aliphatics/Aromatics (continued)			
2-methyl-1,3-butadiene	C_5H_8	C	68
1,3-pentadiene	C_5H_8		68
3-methyl-1-butene	C_5H_{10}		70
1-pentene	C_5H_{10}	D	70
2-methylbutane	C_5H_{12}		72
Pentane	C_5H_{12}		72
2-methyl-1,3-pentadiene	C_6H_{10}		82
2-methylpentene	C_6H_{12}		84
4-methyl-2-pentene	C_6H_{12}	D	84
1-hexene	C_6H_{12}		84
2,3-dimethylbutane	C_6H_{14}	B	86
2-methylpentane	C_6H_{14}		86
Hexane	C_6H_{14}	D	86
1,6-heptadiene	C_7H_{12}		96
1-heptene	C_7H_{14}		98
1-methylcyclohexane	C_7H_{14}		98
2-methylhexane	C_7H_{16}	B	100
3-methyhexane	C_7H_{16}	B	100
Heptane	C_7H_{16}	D	100
1,3-octadiene	C_8H_{14}		110
5,5-dimethyl-1-hexene	C_8H_{16}	B	112
1-octene	C_8H_{16}	D	112
2-methylheptane	C_8H_{18}		114
Octane	C_8H_{18}	D	114
3-ethyl-2-methyl-1,6-hexadiene	C_9H_{16}	B	124
3,6-dimethyl-1,5-heptadiene	C_9H_{16}	B	124
1-nonene	C_9H_{18}		126
2,2,4,4-tetramethylpentane	C_9H_{20}	B	128
2,3,5-trimethylhexane	C_9H_{20}	B	128
Nonane	C_9H_{20}	D	128
Menthene	$C_{10}H_{18}$	A,D	138
2,7-dimethyl-3,5-octadiene	$C_{10}H_{18}$	B	138
3-methylenenonane	$C_{10}H_{20}$	B	140
3,5-dimethyloctane	$C_{10}H_{22}$	B	142
3-ethyloctane	$C_{10}H_{22}$	B	142

Table 5-3 Continued

Compound	Formula	Remarks	r_M
Aliphatics/Aromatics (continued)			
3-methylnonane	$C_{10}H_{22}$	B,C	142
Decane	$C_{10}H_{22}$	D	142
2,8-dimethyl-1,8-nonadiene	$C_{11}H_{20}$	A,D	152
3-undecane	$C_{11}H_{22}$	B	154
Undecane	$C_{11}H_{24}$		156
1,8,10-dodecatriene	$C_{12}H_{20}$	A	164
4-dodecene	$C_{12}H_{24}$	B	168
2,2,7,7-tetramethyloctane	$C_{12}H_{26}$		170
Dodecane	$C_{12}H_{26}$	B	170
2,2,6-trimethyldecane	$C_{13}H_{28}$	B	184
2,6,7-trimethyldecane	$C_{13}H_{28}$	B	184
2,5-dimethylundecane	$C_{13}H_{28}$	B	184
3-methyldodecane	$C_{13}H_{28}$	B	184
4-methyldodecane	$C_{13}H_{28}$	B	184
Tridecane	$C_{13}H_{28}$		184
Tetradecane	$C_{14}H_{30}$	A,D	198
2,7,10-trimethyldodecane	$C_{15}H_{32}$	A	212
Benzene	C_6H_6	C,D	78
Toluene	C_7H_8	C,D	92
Styrene	C_8H_8	D	104
1,2-dimethylbenzene	C_8H_{10}	B,D	106
1,3-dimethylbenzene	C_8H_{10}		106
Ethylbenzene	C_8H_{10}	D	106
Trimethylbenzne	C_9H_{12}	B	120
1-ethyl-2-methylbenzene	C_9H_{12}		120
1-ethyl-3-methylbenzene	C_9H_{12}		120
1-ethyl-4-methylbenzene	C_9H_{12}		120
1-methylethylbenzene	C_9H_{12}		120
Propylbenzene	C_9H_{12}	D	120
1,2,3,4-tetramethylbenzene	$C_{10}H_{14}$		134
1-ethyl-3,5-dimethylbenzene	$C_{10}H_{14}$	B	134
2-ethyl-1,4-dimethylbenzene	$C_{10}H_{14}$		134

Table 5-3 Continued

Compound	Formula	Remarks	r_M
Aliphatics/Aromatics (continued)			
4-ethyl-1,2-dimethylbenzene	$C_{10}H_{14}$		134
2,3-dihydro-5-methylindene	$C_{10}H_{12}$	A	132
Octahydro-2,2,4,4,7,7-hexamethyl-1H-indene	$C_{15}H_{28}$	A	208
Esters			
Formic acid, Propyl ester	$C_4H_8O_2$	C	88
Formic acid, Butyl ester	$C_5H_{10}O_2$	C	102
Formic acid, Octyl ester	$C_9H_{18}O_2$	A	158
Acetic acid, ethyl ester	$C_4H_8O_2$	C	88
Acetic acid, phenylmethyl ester	$C_9H_{10}O_2$		150
Butanoic acid, ethyl ester	$C_6H_{12}O_2$	C	116
3-methylbutanoic acid, ethyl ester	$C_7H_{14}O_2$		130
Halides			
Ethylchloride	C_2H_5Cl	C	64
1-chloropentane	$C_5H_{11}Cl$		106
1-chlorohexane	$C_6H_{13}Cl$	D	120
1-chlorooctane	$C_8H_{17}Cl$	B	148
1-chlorodecane	$C_{10}H_{21}Cl$		176
Heterocyclics			
Pyrrole	C_4H_5N	C	67
2-methyl-1H-pyrrole	C_5H_7N	D	81
3-methyl-1H-pyrrole	C_5H_7N	D	81
2,3,6-dimethylpyridine	$C_8H_{11}N$	B	121
1,2,3,4-tetrahydroquinoline	$C_9H_{11}N$	C	133
2,3-dihydro-1H-indole	C_8H_9N		119
1-methyl-3-nitropyrazole	$C_4H_5N_3O_2$	A	127
2,3-dihydrofuran	C_4H_6O		70
2-methylfuran	C_5H_6O	D	82
3-methylfuran	C_5H_6O	D	82

Table 5-3 Continued

Compound	Formula	Remarks	r_M
Heterocyclics (continued)			
2,3-dihydro-5-methylfuran	C_5H_8O	D	84
2-pentylfuran	$C_9H_{14}O$		138
2-octylfuran	$C_{12}H_{20}O$	A	180
3-furaldehyde	$C_5H_4O_2$		96
4-(5-methyl-2-furanyl)-2-butanone	$C_9H_{12}O_2$	B	152
Ketones			
Acetone	C_3H_6O	C	58
2-butanone	C_4H_8O	C,D	72
Butanone	C_4H_8O	B	72
2-pentanone	$C_5H_{10}O$	C,D	86
3-methyl-2-cyclopenten-1-one	C_6H_8O		96
2-methyl-1-penten-3-one	$C_6H_{10}O$	B	98
4-methyl-2-pentanone	$C_6H_{12}O$	B	100
2-hexanone	$C_6H_{12}O$	D	100
3-methyl-2-hexanone	$C_7H_{14}O$	B	114
2-heptanone	$C_7H_{14}O$		114
6-methyl-3,5-heptadien-2-one	$C_8H_{12}O$	D	124
6-methyl-5-hepten-2-one	$C_8H_{14}O$	D	126
6-methyl-5-hepten-3-one	$C_8H_{14}O$		126
4-methyl-2-heptanone	$C_8H_{16}O$		128
6-methyl-2-heptanone	$C_8H_{16}O$		128
2-octanone	$C_8H_{16}O$		128
4-isopropyl-2-cyclohexen-1-one	$C_9H_{14}O$	A	138
2-nonanone	$C_9H_{18}O$		142
2-decanone	$C_{10}H_{20}O$	D	156
Acetophenone	C_8H_8O	C	120
2,3-dihydro-1H-inden-1-one	C_9H_8O	B	132
Octahydro-2H-inden-2-one	$C_9H_{14}O$	A	138
2,3-butanedione	$C_4H_6O_2$	C	86
2,3-dimethylquinone	$C_8H_{10}O_2$	A	138

Table 5-3 Continued

Compound	Formula	Remarks	r_M
Sulfides			
Carbondisulfide	CS_2	C,D	76
Dimethylsulfide	C_2H_6S	C	62
Dimethyldisulfide	$C_2H_6S_2$	D	94
Thio/Thioesters/Sulfonyls			
Thiomethane	CH_4S	C,D	48
3-methylthiopropanal	C_4H_8OS	B	104
Ureas/Related			
Urea	CH_4N_2O	C,D	60
Miscellaneous			
2-methoxy-1-propene	C_4H_8O	B	72
1-methoxy-4(1-propenyl)benzene	$C_{10}H_{12}O$	A,E	148
Compounds present in background/Blank analyses			
Methylsilane	CH_3Si		46
Hexamethylcyclotrisiloxane	$C_6H_{18}O_3Si_3$	D	222
Octamethylcyclotetrasiloxane	$C_8H_{24}O_4Si_4$	D	296
Decamethylcyclopentasiloxane	$C_{10}H_{30}O_5Si_5$	D	370
Methylchloride	CH_3Cl	C,D	50
Methylenechloride	CH_2Cl_2	C	84
Chloroform	$CHCl_3$		118
Carbontetrachloride	CCl_4		152
Trichloroethylene	C_2HCl_3		130
1,1,1-trichloroethane	$C_2H_3Cl_3$		132
Tetrachloroethylene	C_2Cl_4	D	164
1,2-dichlorobenzene	$C_6H_4Cl_2$		146
1,4-dichlorobenzne-D4	$C_6Cl_2D_4$		150

Table 5-3 Continued

Compound	Formula	Remarks	r_M
Compounds present in background/Blank analyses (continued)			
1-chloro-4-(1-chloroethenyl) cyclohexene	$C_8H_{10}Cl_2$		176
1-chloro-5-(1-chloroethenyl) cyclohexene	$C_8H_{10}Cl_2$		176
1,6-dichloro-1,5-cyclooctadiene	$C_8H_{10}Cl_2$		176
Dichlorofluoromethane	$CHCl_2F$		102
Chlorodifluoromethane	$CHClF_2$		86
Dichlorodifluoromethane	CCl_2F_2		120
Trichlorofluoromethane	CCl_3F		136
1,1,2-trichloro-1,2,2-trifluoroethane	$C_2Cl_3F_3$	D	186
Difluorobenzene	$C_6H_4F_2$	B	114
Bromodichloromethane	$CHCl_2Br$		162
Dibromochloromethane	$CHClBr_2$		206
Bromochlorodifluoromethane	$CClBrF_2$		164
Naphthalene	$C_{10}H_8$		128
Carene	$C_{10}H_{16}$	A	136
3-carene	$C_{10}H_{16}$	B	136
4-carene	$C_{10}H_{16}$	B	136
Limonene	$C_{10}H_{16}$		136
α-pinene	$C_{10}H_{16}$		136
β-pinene	$C_{10}H_{16}$		136
α-phellandrene	$C_{10}H_{16}$		136
β-phellandrene	$C_{10}H_{16}$		136

Explanation of remarks:

A) Exact identification of this compound is questionnable due to low purity value.

B) The class or base structure of this compound is characterized by a specific EI fragmentation pattern. Location of bonds and/or substitution may be uncertain.

Table 5-3 Continued

Explanation of remarks (continued):

C) Compound was previously reported in the literature as a compound having dermal origin (table 5-1).

D) Reported as being observed in the cryo-focused GC/MS analyses (table 5-2).

E) See text for further explanation.

further implications with respect to diet and mosquito attraction, where the consumption of foods enhancing mosquito attraction may increase potential attractants on the skin. Further studies involving alcohol or food consumption and emanation from the skin were not conducted for this dissertation.

The second component of interest is 1-methoxy-4(1-propenyl)benzene (anethole). The reason this compound was noted is due to previous field studies in which methoxybenzene (anisole) gave favorable response to the *Culex nigripalpus* species of mosquito. Should the chemosensilla of this mosquito be compound specific with some class dependency, then it would be beneficial to test similar structures which are present on the skin. Anisole was not observed in emanations analyzed for this work; however, anethole is similar in base structure.

Case Study Comparison of Emanations between Subjects

The comparison studies between subjects were performed not only for comparative purposes; the data were also examined for compounds which decreased in relative abundance over a period of time, typically 6-8 hours. This was accomplished by placing handled beads in a tube open to air. The subjects were chosen based upon their relative attraction of *Ae. aegypti* in an olfactometer bio-assays. The subjects were Mr. Dan Smith, who has been found to be at the high extreme with respect to attraction percentage (c. 70%), and Mr. Carl Schreck, who has been found to be at the low end (c. 20%). The RIC traces for one such

comparative study are presented in figure 5-2. The top trace, produced from beads handled by Mr. Schreck contains, for the most part, the same peaks as that of Mr. Smith (bottom trace). The glycerol peak, located at a retention time of approximately 18.8 min, is not only chromatographed better on the FFAP column employed here (versus the HP5 column used in figure 5-1), but it is present in much greater amount in Mr. Smith's sample. As mentioned earlier, this discrepancy is due to residual glycerol on the hands from the Sta-Sof-Fro™ hair and scalp spray.

Peak heights were measured and normalized to the peak height of tetradecane. The relative peak height ratios of component peaks were then compared to determine specific components which were increased in one subject compared to the other. Sample analyses were also compared with respect to amounts of components present on the glass beads analyzed immediately and on glass beads which were analyzed 6-8 hours later. The results of these comparative studies are presented in table 5-4.

This table contains only two remark codes. A code of (A) denotes compounds for which the exact structure is not known versus other isomers of the same compound. A remark code of (B) denotes that discussion of this compound is found in the following text.

The designation of significantly or slightly combined with increased or decreased employed in the table merits some explanation. It was found that the relative abundances of present components in each sample vary between analyses.

Figure 5-2 Comparison of RIC traces, in EI mode, for two human subjects who differ markedly in attraction of mosquitoes. The top trace is from Mr. Carl Schreck, employed in these studies as the subject with lesser attraction to mosquitoes. The bottom trace is from Mr. Dan Smith, employed in these studies as the subject with greater attraction to mosquitoes. Separation was effected on a 25 m x 0.20 mm i.d. HP-FFAP column. Additional parameters are found in the experimental section.

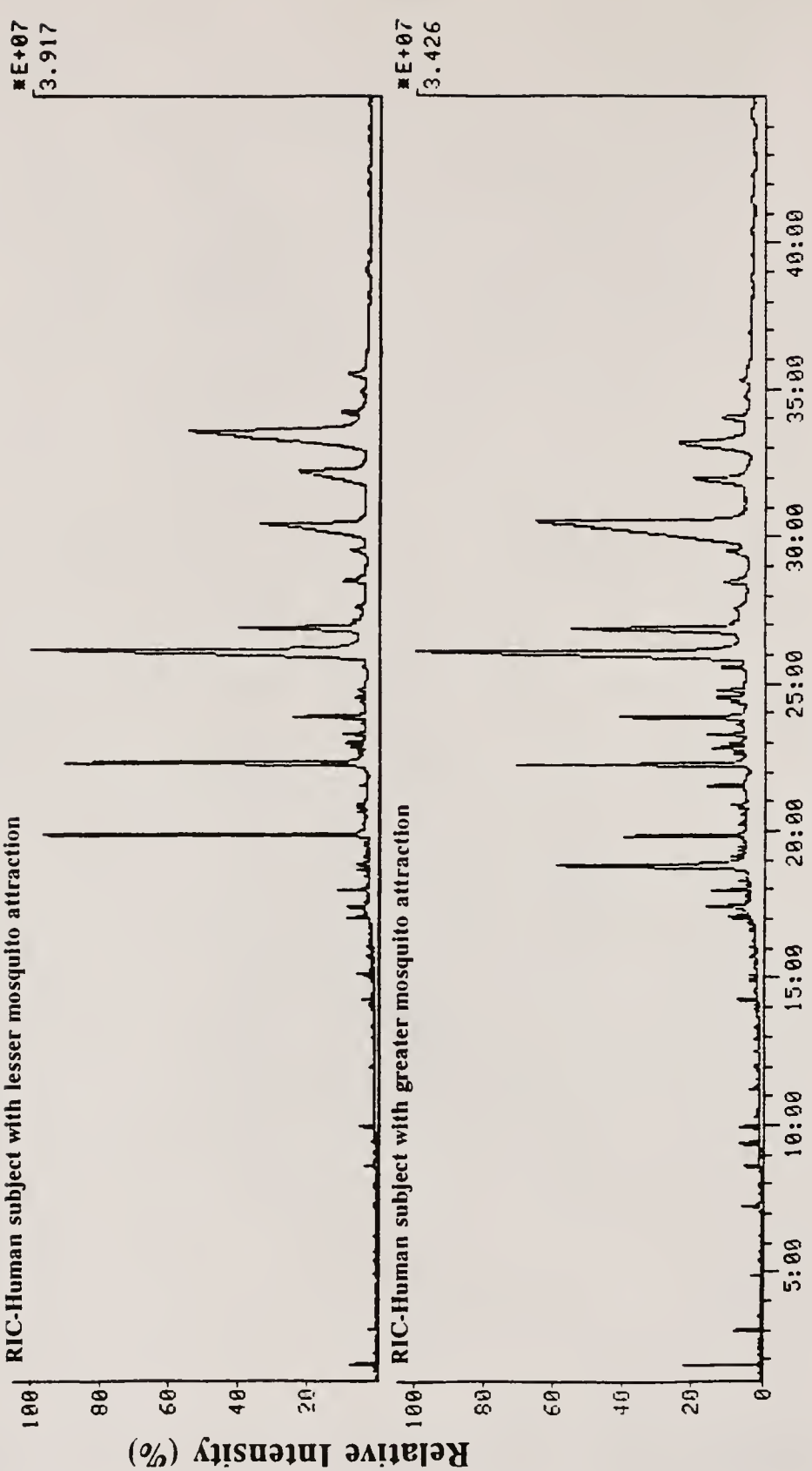
RIC-Human subject with lesser mosquito attraction
RIC-Human subject with greater mosquito attraction
Relative Intensity (%)
Time (min:s)
E+07
3.917
E+07
3.426
100
80
60
40
20
0
5:00
10:00
15:00
20:00
25:00
30:00
35:00
40:00

Table 5-4 Comparison of compounds present on the skin which are observed to be relatively increased from one host with respect to the other. Compounds which decrease markedly after an eight hour period from the more attractive host are also reported. This table is categorically divided into five sections. A significant change reflects a relative difference or change by a factor of 5 or greater between hosts, or between host emanations and emanations detected after 8 hours. A slight change refers to compounds with a relative difference of a factor range of 2-5.

Compound	Remarks
Compounds significantly increased in more attractive host:	
Lactic acid	
Methyltridecanoic acid	A
Pentadecanoic acid	
9-hexadecenoic acid	
Octadecanoic acid	
4-hydroxy-3-methoxybenzoic acid	
1-hepten-3-ol	B
Glycerol	
Squalene	
Toluene	
N,N-dimethyl-1-dodecanamine	B
N,N-dimethyl-1-tridecanamine	B
N,N-dimethyl-1-tetradecanamine	B
N,N-dimethyl-1-hexadecanamine	B
N,N-dimethyl-1-octadecanamine	B
14-methylhexadecanoic acid, methyl ester	
6-Octadecenoic acid, methyl ester	
2-hydroxybenzoic acid, phenylmethyl ester	
Pentanedioic acid, ester	A
Hexanedioic acid, mono(2-ethylhexyl ester)	
Pyridine	
3-(1-methyl-2-pyrrolidinyl)pyridine	B
Oxazole	
2,3-dihydro-3,5-methoxy-6-methyl-4H-pyran-4-one	
2-methylisothiazole	
2-butanone	
2-pentanone	
3-pentanone	
2-decanone	

Table 5-4 Continued

Compound	Remarks
Compounds slightly increased in the more attractive host	
12-methyltetradecanoic acid	
Methylpentadecanoic acid	A
Heptadecanoic acid	
4-hexen-1-ol	B
2,5-bis(1,1-dimethylethyl)phenol	
2-methylpropanal	
7,11,15-trimethyl-3-methylene hexadecane	
Docosane	
2-butenoic acid, Butyl ester	
4-hydroxybenzoic acid, Propyl ester	
2-hydroxybenzoic acid, Phenylmethyl ester	
1-chlorotetradecane	
4-pyridinamine	
2,3-dihydro-4-methylfuran	A
4H-pyran-4-one, substituted	A
6-methyl-5-hepten-2-one	
Urea	
Compounds significantly increased in the less attractive host	
Dodecanoic acid	
Cholesterol	
3-methylpentanol	
Heptane	
Methyliodide	
1,3-butanediamine	A
14-methylpentadecanoic acid, Methyl ester	
Compounds slightly increased in the less attractive host	
Decanoic acid	
Methyltetradecanoic acid	
Heptanal	
Nonanal	
2,4-nonadienal	

Table 5-4 Continued

Compound	Remarks
Compounds slightly increased in the less attractive host (continued)	
4-nonene	
Nonane	
3-dodecene	
Hexacosane	
Compounds significantly decreased after 8 hours (in the more attractive host)	
Hexanedioic acid, Mono(2-ethylhexyl ester)	
2-methylpropanal	
3-methylpentanal	
N,N-dimethyl-1-dodecanamine	B
N,N-dimethyl-1-tridecanamine	B
N,N-dimethyl-1-tetradecanamine	B
N,N-dimethyl-1-hexadecanamine	B
N,N-dimethyl-1-octadecanamine	B
2-octene	
4-nonene	
Benzene	
Toluene	
Styrene	
Pyridine	
Oxazole	
1H-indole	
2-butanone	
2-Pentanone	

Explanation of remarks:

A) Location of substitution or double bond position is uncertain.

B) See text for discussion.

Examples of this follow. Lactic acid was found to vary from 5 times greater in the more attractive host to 1.3 times greater in the lesser attractive host. In the same analyses, 12-methyltetradecanoic acid was found to remain fairly consistent at 1.9-2.2 times greater relative abundance in the more attractive host. Therefore, the tables reflect not necessarily an average value; they reflect what is found in most of the analyses. However, the variation of components from the same host should be kept in mind when examining the results presented here. These compounds may not necessarily yield the answer to what components are attractants. These compounds are still the more likely candidates for the attractants and should be examined by olfactometer and field studies.

The presence of 4-hexen-1-ol and 1-hepten-3-ol are of particular interest. The use of 1-octen-3-ol, as stated in Chapter 1, has been found to attract various species of mosquito. These similar, but lower molecular weight alcohols (and their isomers) may provide better attraction than 1-octen-3-ol, again treating mosquito detection as class/structure dependent. The other components of interest were the tertiary amines previously discussed in the section corresponding to table 5-2. These amines were found to be significantly increased in the more attractive host and found to decrease significantly after 8 hours. These two findings fit the profile of attractants sought after. That is, compounds present in greater abundance in the more attractive host and decreased markedly after 6 hours (as noted in olfactometer tests). Care should be taken with this class of compounds; it is unknown whether or not these

compounds originate from humans or may are deposited on the skin by external sources. The final compound to be addressed from this table is 3-(1-methyl-2-pyrrolidinyl)pyridine (nicotine). This compound was found in much greater abundance on the skin for subjects who use tobacco products.

Case Study Comparison of Bio-assay to GC/MS Assay

The final study of this chapter involves the analysis of emanations from a single host, collected once per day for GC/MS and bio-assay, over a five-day period. The advantage to this comparison is thought to be that a single host provides a more stable and consistent matrix on the skin, with less chance of markedly different trace emanations. The drawback is that the subject variation in attraction to mosquitoes will not vary as much as it would for persons chosen at the extremes of attraction (as in the previous case study).

The range of attraction in the olfactometer, for the five-day period, fell between 12 and 27%. The actual comparison employed only the first two days. The RIC traces from samples analyzed on these two days are shown in Figure 5-3. The results from these analyses are reported in table 5-5. The remark codes used in this table are identical to those for table 5-4.

The two compounds of interest from this table are the unsaturated alcohols identified as 4-hexen-1-ol and 1-hepten-3-ol. Both of these compounds were present at increased relative abundance on the day the human subject was more attractive

Figure 5-3 Comparison of RIC traces in EI mode for Mr. Ken Posey. Samples were either three handled glass beads for GC/MS or a petri dish for olfactometer studies. The beads or dish were handled for 15 minutes prior to analysis. Samples were analyzed each day, approximately one hour apart, on consecutive days.

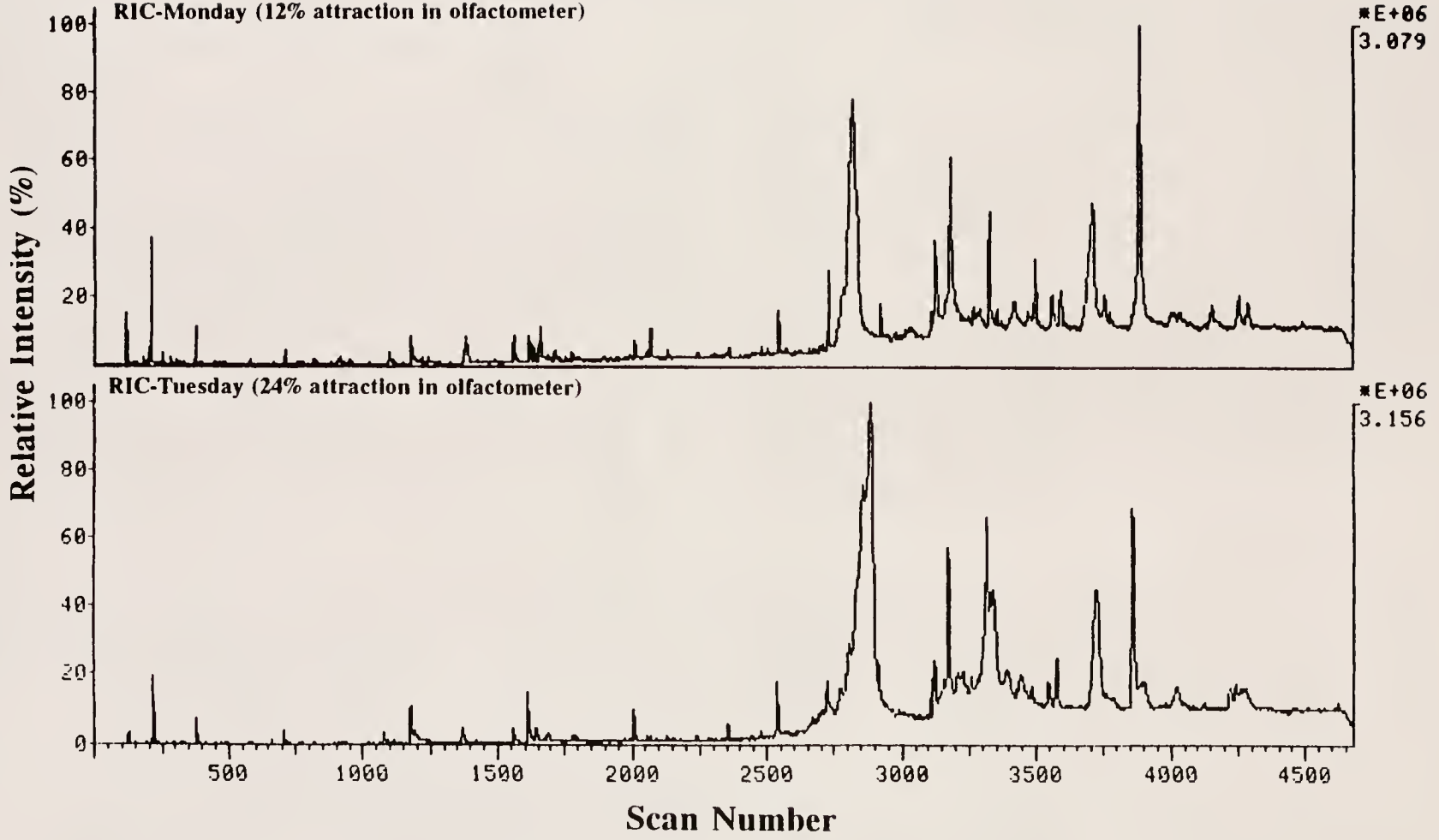
RIC-Monday (12% attraction in olfactometer)
*E+06
3.079
RIC-Tuesday (24% attraction in olfactometer)
*E+06
3.156
Relative Intensity (%)
100
80
60
40
20
0
500
1000
1500
2000
2500
3000
3500
4000
4500
Scan Number

Table 5-5 Comparison of emanations present on the skin on consecutive days from a single human subject. Bio-assays conducted on those days showed 12% and 24% attraction of mosquitoes in an olfactometer. An increase in the table reflects a compound found to be present in a greater relative amount on the second day (24% attraction) with respect to the previous day (12% attraction). A significant change reflects a relative difference by a factor of 5 or greater between days. A slight change refers to compounds with a relative difference of a factor range of 2-5.

Compound	Remarks
Compounds significantly increased on more attractive day:	
Pentadecanoic acid	
Methylpentadecanoic acid	A
Hexadecanoic acid	
1-hepten-3-ol	B
Compounds slightly increased on more attractive day	
9-octadecenoic acid	
4-hexen-1-ol	B
2,4-nonadienal	
Butanamine	A
Nonene	
Menthane	A
Tricosane	
13-methylpentadecanoic acid, Methyl ester	
Methylhexadecanoic acid, Methyl ester	A
Compounds significantly decreased on more attractive day	
Benzoic acid, substituted	A
Heptadienal	A
2-methyl-1-heptene	
Nonane, branched	A
1-chlorohexane	A
1-chlorononane	
Pyridine	
Urea	

Table 5-5 Continued

Compound	Remarks
Compounds slightly decreased on more attractive day	
3-hexadecanol	A
Nonanal	
Benzaldehyde	
Dodecene	A
2-methyl-2-dodecene	
5-tetradecene	
Methyltridecanoic acid, ethyl ester	A
Octenone, branched	A
3-methylthietane	

Explanation of remarks:

A) Location of substitution or double bond position is uncertain.

B) Discussed in text.

to mosquitoes. Again these compounds, as well as other compounds should be referred to as good candidates for attractants. In general, the comparison study conducted here, involving the same subject on consecutive days, showed less overall variation (compared to the previous study with different subjects) in relative abundances of sample components present.

Conclusions

Identified Emanations

Approximately 310 compounds were detected in cryo-focused GC/MS analyses and 200 compounds from purge and trap GC/MS experiments. The components present on the skin were found to be very similar among subjects; however, relative abundances of components vary whether comparing two different subjects, or the same subject at different times. Cryo-focused GC/MS analysis allowed for identification of a wide range of classes whereas microscale purge and trap discriminated against polar compounds, giving slightly different information as a result.

GC/MS Assay of Subjects with Different Attraction Levels

There were 46 compounds which were increased in relative abundance in the more attractive host to mosquitoes. Only 9 compounds were found (with reasonable certainty) to be relatively more abundant in the lesser attractive of the hosts. Among

the 46 compounds are lactic acid, unsaturated alcohols, and tertiary amines. Lactic acid is a known attractant, and was observed present in greater abundance (in most cases) for the more attractive host. This may partially explain the attraction of *Aedes aegypti* to this host as well as fluctuations in mosquito attraction. The unsaturated alcohols are of interest due to the similarity in structure to 1-octen-3-ol, a compound which has been found to attract various species of mosquitoes. The tertiary amines were not only found in increased abundance on the more attractive host; they also decreased significantly in abundance when analyzed for 8 hours later. This profile is similar to observations concerning attraction to handled glass in an olfactometer.

Bio-assay versus GC/MS Assay

The most difficult and potentially most informative study involved comparison of the same subject on consecutive days. The reason for this difficulty stems from the similarity of the skin matrix for the same host, only minor variations in relative abundances of most components were observed. Thirteen compounds, including the unsaturated alcohols mentioned above, were found to increase on the more attractive day; seventeen were found to decrease. This discrepancy may simply be due to normal variations in abundances from day to day, as was seen throughout many of the analyses conducted for the previous case study. Additionally, imprecision exists in bio-assays such that the attraction percentage may not exactly reflect differences between days reported in this study.

CHAPTER 6
CONCLUSIONS AND FUTURE WORK

Conclusions

This dissertation has covered various facets of applying mass spectrometry to elucidating the chemical basis for mosquito attraction to human hosts. The initial concern was the utilization of a sampling method which minimally biased the compounds to be detected while providing some discrimination against compounds which are not of interest, i.e. non-volatile components. This was accomplished by desorbing volatiles off handled glass beads. Host attraction is known to be transferrable to glass and it is believed that the glass actually concentrates the attractant(s), as well as many other compounds.

The sampling method chosen for the majority of work was cryo-focusing, with some studies employing microscale purge and trap. Simple cryo-focusing provides the benefit of narrowing sample bands on the GC column and the detection of gas-phase emanations with minimal sample discrimination. The additional step of employing Tenax and cryo-focusing traps (in microscale purge and trap) provided benefits with respect to the removal of the abundant carboxylic acids (as well as other highly polar compounds) by the metal in the system; however, it is not known at this time if this also removes potential attractants as well. The data from

microscale purge and trap GC/MS applied to skin emanations for this project are preliminary; microscale purge and trap experiments have shown that the composition of components desorbed from beads is similar to that from the enclosed hand in a Tedlar bag. The difference between these two sample introduction methods lies mainly in the markedly different relative intensities of some components. Further studies involving quantitation will be required to confidently report the differences.

The negative ion fragmentations, attachments, and oligomerization (polymerization) of lactic acid, the only previously known attractant for *Ae. aegypti*, were examined in Chapter 3. Negative ions are typically not employed for structural information; however, lactic acid can be readily identified via NCI. Oligomerization reactions, as well as chloride ion attachment, provide easily detectable ions in the NCI mass spectrum of lactic acid. Although lactic acid is one of the major components found emanating from the skin, the determination of its presence by EI is not achievable due to the absence of the $M^{+\bullet}$ ion and the resultant low mass fragments.

Altering the matrix conditions by adding acid or base to lactic acid affected the attraction of *Ae. aegypti*. The observed effects have been rationalized to result from simple acid-base dissociation equilibria. The addition of acid enhanced the attraction of mosquitoes to the sample; the addition of base decreased the attraction. The addition of acid to various lactic acid esters and methyl isovalerate

was also examined. Increased attraction of mosquitoes occurred in all cases for the sample containing acid relative to the unmodified sample.

Skin emanations collected on three 2.9 mm glass beads were found to contain a greater amount of sample than is present from the dissolution of 0.15 mL perspiration in 1 mL methanol. Due to the absence of components in the aqueous phase, it is suspected that lactic acid (and other attractants) preferentially reside in the oily/waxy phase which emanates from the sebaceous glands. Decreased attraction to mosquitoes has been observed in cases of heavy perspiration. If attractants preferentially reside closer to the skin, below the evaporating aqueous phase, then the reduced attraction which is observed can be explained by a masking effect from heavy perspiration.

Tandem mass spectrometry was employed in initial experiments of this dissertation project to compensate for short-column chromatography. The detailed fragmentation studies of lactic acid also necessitated the use of MS/MS modes. A daughter library of characteristic fragmentations was compiled and used to rapidly assess the compound classes present. The results from the rapid screening yielded a conservative estimate number of compound classes as well as number of components present within each class (or similar classes).

Over 350 GC peaks are observed in the work of Chapter 5. There are 310 components identified in the cryo-focused GC/MS analyses; approximately 20 of these have been attributed to background. Human subjects observed throughout this

work appear, for the most part, to be similar with respect to composition of emanations present on the skin. The components present vary in relative abundance among subjects. This was the basis for the comparison studies conducted in this chapter. Components found increased or deceased between hosts are reported in this dissertation. Additional studies involved the comparison of GC/MS results to bio-assay results; compounds observed to increase or decrease between days were reported. The findings from these case comparison studies may not provide the ultimate answer to solving the problem of mosquito attraction; however, the work contained herein should bring the solution closer.

Future Work

Continued use of a single-stage cryo-focusing or single cryo-focusing trap may be beneficial when combined with the use of Tedlar bags described for purge and trap analyses. Although the preferential discrimination of samples which do not transfer and subsequently volatilize from glass is lost, preliminary work comparing the observed components from glass beads and from the hand enclosed in a Tedlar bag show that the presence of components is very similar. Additional studies need to be conducted to verify this. Continued use of a cryo-focusing GC/MS could be conducted with less steep ramp programs and longer columns. This would effect better separation of components which co-eluted during analyses in this work. The

real problem to be overcome will be the high concentration of acids present when analyzing for additional trace components.

Continued use of microscale purge and trap with direct sampling of the hand in a Tedlar bag will most likely provide, in the near future, a useful method of removing acids. Though this method is subject to compound discrimination of polar compounds, concentration of sampled air is a desirable attribute. Air trapped in the bag was used for the experiments contained in this dissertation; however, it is not necessary that air be used. Once the hand is enclosed in the bag, the air could be purged from the bag by an inert gas, such as helium. Purge and trap analyses allowed for concentration of highly volatile materials and for removal of the high concentrations of carboxylic acids which interfere with determination of trace components present.

Quantitation is a dilemma with respect to the bead sampling methods. The actual quantitation by mass spectrometry is not the problem; however, sampling in a consistent manner is. The concentration and presence of components on the skin is not constant and is affected by many variables that have been observed to vary from day to day. One possibility for quantitating known emanations from the skin with direct sampling employing a Tedlar bag might be to coat an area of the skin with a known non-toxic volatile to semi-volatile compound. This may yield some insight about collection efficiency of emanations. Attempts could be made to spike the beads with known concentrations of, for example, lactic acid and additional

carboxylic acids. In particular, since preliminary attempts to measure quantitatively (by weight) sample deposition onto beads were not successful, a study could be conducted to attempt to do this. The protocol may consist of using a steep temperature ramp to cut down on analysis time and focus only upon the carboxylic acids. Beads could be quantitatively analyzed after handling by comparing peak areas of target compounds from one bead, two beads, three beads, etc.

The results from Chapter 3 demonstrated an enhancement in attraction of mosquitoes to samples which had been spiked with acidic solution. An experiment of interest is to spray a fine mist of acidic solution or basic solution onto handled petri dishes. Various comparisons could be made between the attraction of mosquitoes to the untreated handled dish, the dish sprayed with acidic solution, and the dish sprayed with basic solution. An enhancement in attraction towards acidified dishes for one or more species of mosquito may implicate an acid or acids as the potential attractants. This knowledge could then be applicable to GC/MS assays.

The dietary intake of a host influences compounds on the skin. It is believed by some that certain foods enhance attraction. This matter should be examined by comparison studies involving both bio-assay and GC/MS assay. Combining any extraneous knowledge with the knowledge of what is present on the skin should assist in targeting potential attractants. If a connection is observed between dietary intake and mosquito attraction, then the cryo-focused GC/MS or purge and trap GC/MS procedures described in Chapter 5 could be applied to this difference. If specific

components are found to increase (or decrease), these should be targeted for testing by bio-assay.

Another case study related to that described above involves exercise. Attraction of mosquitoes is enhanced (up to a point) during physical exertion and perspiration. Sampling at the proper time interval may yield samples with increased attractant(s) relative to other components in the matrix on the skin. This is speculative; however, should attractants be found in greater concentration on the skin, glass beads could be handled at that time. The bead method would then allow for greater concentration of the attractant(s) while keeping to a minimum the water (from perspiration) adsorbed to the glass, which in turn minimizes water subsequently introduced into the system.

The case studies examined and discussed thus far have focused on human subjects. Humans are not the sole hosts of mosquitoes. Many species of mosquito feed on multiple hosts. Examining emanations from humans and animals known to attract the same mosquito species may aid in determining the attractants by reducing the components of interest to those present in both sets of emanations. This again is somewhat speculative in that there is no guarantee that specific mosquitoes have only a few types of chemosensilla. There is a possibility that the mosquito may detect different volatile components for each host.

Tandem mass spectrometry was used only briefly in this work. The studies for chapter 5 yielded many identified components from PPINICI and EI analyses

alone. There were, however, components that failed to give useful fragmentation patterns in one or more of these modes, preventing confirmation of presence of a compound or in some cases (at least 37) prevented even a speculative estimate of compound identity. There were also cases where compounds were identifiable by PPINICI and/or by EI analysis; however, upon background subtraction, valuable fragmentation information was lost due to coelution of sample components. Tandem mass spectrometry could be employed to obtain daughter spectra of the selected molecular ion, protonated molecular species or deprotonated molecular species to assist in the identification process. There were cases where both the molecular ion (EI) and protonated or deprotonated species (CI) were absent; the use of a reagent gas with lower proton affinity is recommended for PCI to obtain "softer" ionization. Attempts at employing CO_2 as a reagent gas were not successful in this case; however, should this be of interest in the future as a potential reagent gas, the background is covered in the appendix to this dissertation.

The final two studies to be discussed involve the most complex and intricate arrangements. On-line monitoring by mass spectrometry and olfactometer would be advantageous (analogous to organoleptic evaluations used in the fragrance industry). This application was discussed briefly in Chapter 1. The problems to overcome with respect to analyses of this type would be location of both the mass spectrometer and olfactomer, and more importantly, the ability of mosquitoes to respond to successive stimuli should that occur. Mosquitoes may be desensitized by certain compounds,

or high concentrations of compounds in general. In addition, the response of mosquitoes to a stimuli is not an immediate process, such as the detection of column eluents by a mass spectrometer. One way to achieve immediate mosquito response would be to conduct on-line tests with mosquito antennae. This requires a knowledge of mosquito antennae such that specific receptors can be correlated to give responses to specific stimuli. On-line mass spectrometry, with for example, a column split, could be used to identify the compound eliciting a response.

In summary, work conducted in the future in any of the aforementioned areas will provide knowledge that may identify the attractant(s) that have eluded identification thus far; at the least, this information will move humankind one step closer to the answer. Care should be taken with respect to the sampling method such that it answers the question that is being asked. Knowledge of discriminatory effects of the sampling and detection method is of importance. One final issue, applicable to all analyses conducted, is washing of the skin prior to handling beads of sampling of the hand in a Tedlar bag. This methodology should be examined with respect to solvents and time required to allow the skin to dry and additional emanations to concentrate on the skin. Handling of objects should be restricted after washings and until the sample collection procedure is completed.

APPENDIX
CARBON DIOXIDE AS A CI REAGENT GAS

Introduction

This appendix is a compilation of background information and preliminary experiments involving carbon dioxide as a reagent gas for CI. Coverage in this appendix is mainly directed towards the use of CO_2 for production of thermal electrons for electron capture negative ion chemical ionization (ECNCI); however, discussion of charge exchange (CE) for positive ions is also included due to the predominant use of CO_2 as a charge exchange reagent gas.

The examples included in this appendix pertain to optimization of CO_2/ECNCI on the TSQ70, background ions present in positive CO_2/CE and negative CO_2/ECNCI mass spectra, and illustrations of difficulties encountered in these experiments. Due to time constraints, it was not possible to conduct a complete exploration of CO_2 as an electron moderator for ECNCI experiments related to the analysis of volatile skin emanations. Attempts to replace CH_4 with CO_2 as the reagent gas were not successful with the sampling method and detection scheme used for analyses in Chapter 5. The abundance of acid eluents in the ion source led to self-CI reactions. Removal of acids by the purge and trap system described in Chapters 2 and 5 would be beneficial for subsequent attempts at

employing this novel reagent gas. This appendix provides the fundamental background for future work of this nature with optimization related to that on the TSQ70 triple quadrupole mass spectrometer.

High Pressure Charge Exchange Mass Spectrometry

The main use of CO_2 as a reagent gas has been in the analysis of positive ions [33,74]. This reagent gas functions in positive ion mode as a medium for charge exchange. Unlike reagent gases employed for work in this dissertation (i.e. methane and isobutane), carbon dioxide does not contain a hydrogen for proton transfer reactions. Therefore, only hydride (or heavier ion) transfer, electron transfer, or adduct formation are viable routes for the production of positively charged sample ions [33,74,112]. Charge exchange (see Chapter 5 for additional information) occurs by electron ionization of the reagent gas, with subsequent transfer of the positive charge from reagent gas to sample molecules via collisions. The resultant deposition of internal energy (E_i) from these collisions is given by:

$$E_i = RE(X^{+\bullet}) - IE(M) \qquad \text{A-1}$$

where RE ($X^{+\bullet}$) is the recombination energy of the reagent gas ion, $X^{+\bullet}$, and IE (M) is the ionization energy of the sample molecule, M. The recombination energy for $CO_2^{+\bullet}$ is 13.8 eV [74,113]. Extensive fragmentation occurs for a high value of E_i. If RE ($X^{+\bullet}$) is only slightly greater than IE (M), then the mass spectrum is expected to contain predominantly the $M^{+\bullet}$ ion.

Charge exchange reagent gases provide a means for controlling the extent of fragmentation. The mass spectra produced are similar to EI spectra; however, due to the average energy deposition being lower for CE than for EI, the abundance of $M^{+\bullet}$ will be greater. In the case of carbon dioxide, there are several species which can interact with sample molecules. The $CO_2^{+\bullet}$ ion at m/z 44 is the most obvious charge exchange ion. The $(CO_2)_2^{+\bullet}$ cluster ion (RE unlisted) at m/z 88 and the $O_2^{+\bullet}$ ion (RE of 9.7-17.0 eV) at m/z 32 may also react. These species, however, will only have a minor impact on the overall fragmentation pattern due to the low abundance of these ions with respect to $CO_2^{+\bullet}$.

One concern involved with the choice of a charge exchange gas is the production of secondary ion species which may also be involved in the charge exchange process. There is also a greater variation, compared to conventional CI, in major ion abundances of CE reagent gases as a function of ion source pressure. Therefore, optimization and more precise control of the pressure is necessary such that the predominant charge exchange ion is the reagent ion of interest [112]. Water is one of the most detrimental impurities. The presence of $[M+H]^+$ ions from a reagent gas incapable of proton transfer may be due to self-CI or from reaction with ions produced from water, e.g. $(H_3O)^+$ at m/z 19, $(CHO)^+$ at m/z 29, and $(CO \bullet H_2O)^+$ at m/z 46.

Electron Capture Negative Ion Chemical Ionization

Electron capture NCI was addressed in Chapter 5; a brief overview is included here to provide continuity of this appendix. Negative ions are produced from electron capture by three processes [33,72,74,108]. The least common process is that of ion-pair production, whereby the electron is captured, exciting the sample molecule, and then re-ejected at a lower kinetic energy, leaving the molecule dissociated into a positive ion and a negative ion. The more common processes are those of associative resonance electron capture (equation A-2) and dissociative resonance electron capture (equation A-3) of thermal electrons (e_{th}^-):

$$e_{th}^- + MX \rightarrow MX^{-\cdot} \qquad \text{A-2}$$

$$e_{th}^- + MX \rightarrow M + X^{-\cdot} \qquad \text{A-3}$$

In order for a molecule to capture an electron, the electron affinity (EA) of the molecule must be positive. Additionally, the electron attached species must be long-lived enough for collisional quenching (MX^-) or dissociation ($M+X^-$) to occur [72,74,108,114-116].

The appeal of ECNCI, for compounds amenable to this process, is due to the higher efficiency of electron/molecule reactions compared to conventional CI ion/molecule reactions [72,74,108,117]. Unfortunately, ECNCI is not applicable to a majority of compounds; however, this selectivity is generally considered an advantage rather than a disadvantage. Although the electron capture processes are fairly straightforward, mass spectra obtained by ECNCI are not always simple to

interpret. Halogenated species are excellent candidates for ECNCI; however, adduct formation (e.g. $[M+Cl]^-$) may occur [72,81,107,108,114,118-120]. Ion source surface or wall reactions may take place, ultimately complicating mass spectra [114,119,121]. Tetracyanoethylene (TCNE), having a relatively high (positive) EA, readily undergoes EC reactions. It is also particularly susceptible to unexpected ion formation from electron capture [119,121,122]. This compound, when examined by ECNCI with methane and with carbon dioxide reagent gases revealed the absence of unexpected ions for CO_2/ECNCI [121].

ECNCI with Carbon Dioxide

Carbon dioxide has been examined previously as a moderator for thermal electron production for ECNCI of TCNE [121]. It has been shown that when mixed with argon for NCI work, it will enhance the production of the $[M-H]^-$ ion [123]. The allure of CO_2 to work contained in this dissertation is from the potentially simplistic mass spectra for the determination of volatile skin emanations which can undergo electron capture.

Carbon dioxide is efficient at relaxing electron energy distributions, i.e. forming thermal electrons [124,125]. The physical reason for this is the ability of the CO_2 molecule to form a short-lived ion (CO_2^-), which autodetaches a lower energy electron, leaving CO_2 in a vibrationally excited state [126]. By virtue of the size of a CO_2 molecule, it is also efficient at collisional quenching (compared to other inert

and relatively inert gases) [115]. One additional feature of this reagent gas merits mentioning. Due to the absence of hydrogen in the system and the low proton affinity of CO_2 (548 kJ/mol), formation of the $[M-H]^-$ ion from samples would be a rare occurrence with this reagent gas. As with CO_2/CE, impurities present in the ion source need to be minimized to prevent unexpected or unwanted reaction pathways. Production of an $[M-H]^-$ ion from this reagent gas is a likely indication that an impurity is present, or that self-CI is occurring. Self-CI reactions were found to be the most significant cause, in the work for this dissertation, for the inability to perform electron capture. The elution of high concentrations of acids into the ion source, as stated previously, generated mass spectra comparable to that of methane NCI.

Instrument Optimization and Background Ions

The optimization for negative ion analysis was carried out by examining characteristic PFTBA negative ions at m/z 264 and m/z 414, as well as the m/z 127 ion (I^-) found in the background on the TSQ70. The optimization plot is presented in figure A-1. Formation of ions requires indicated pressures greater than 500 mtorr CO_2 in the ion source. Examination of the profiles demonstrates the need for precise control over the ion source pressure to maximize sample ion generation efficiency. The optimum indicated pressure of 1200 mtorr is most likely a combined

Figure A-1 Intensity of selected negative ions as a function of CO_2 reagent gas pressure.

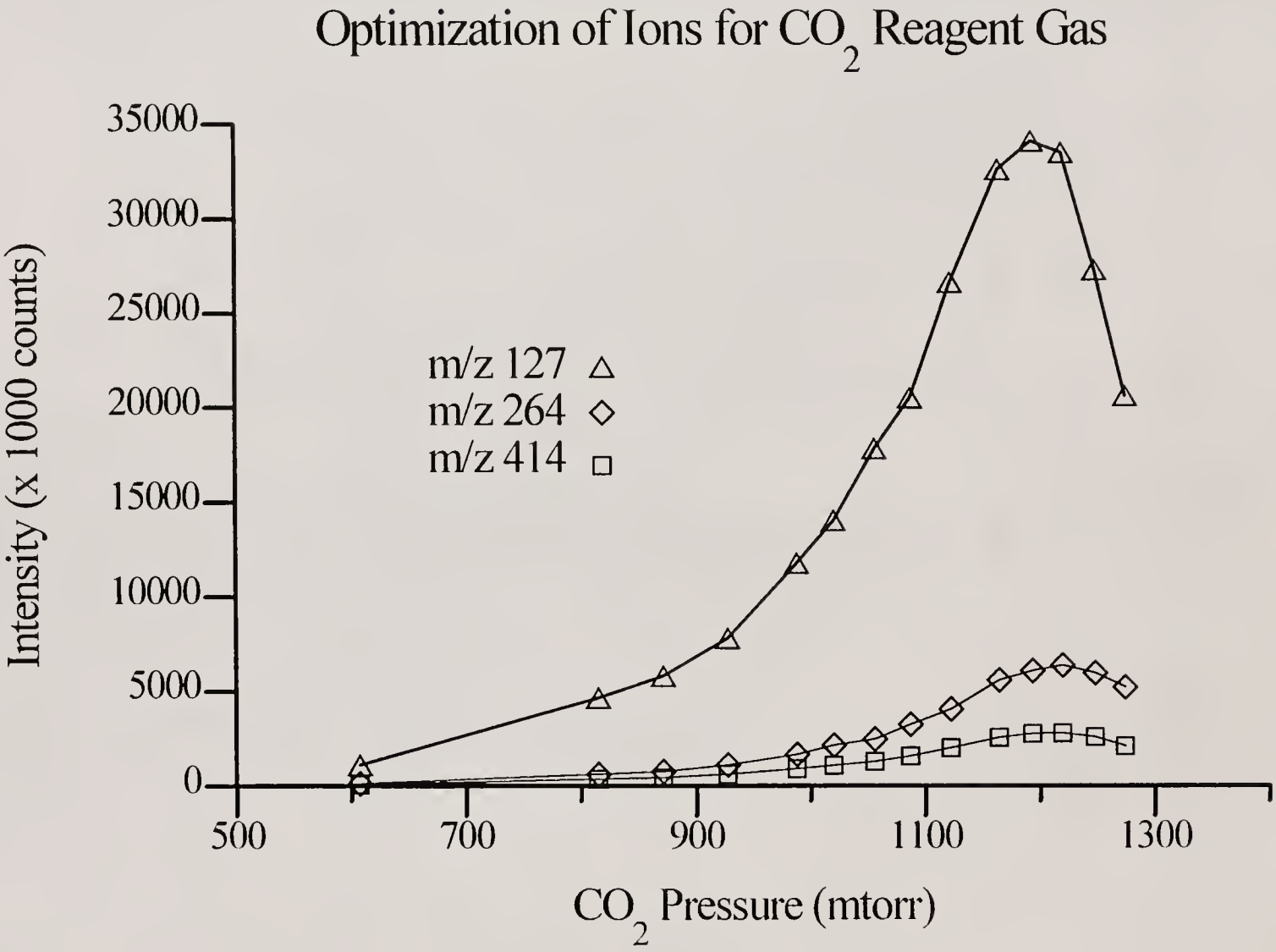
Optimization of Ions for CO_2 Reagent Gas
Intensity (x 1000 counts)
35000
30000
25000
20000
15000
10000
5000
0
m/z 127
m/z 264
m/z 414
500
700
900
1100
1300
CO_2 Pressure (mtorr)

tradeoff between CO_2 efficiency of electron thermalization and collisional quenching of sample ions by this gas.

The negative ion mass spectrum of PFTBA, acquired at an indicated pressure of 1200 mtorr CO_2 reagent gas, is shown in figure A-2. All ions found in the mass spectrum, with the exception of m/z 60, are characteristic ions seen with this instrument when methane is employed as the electron moderating gas for NCI. The m/z 60 ion is presumed to be $CO_3^{-\bullet}$. This ion has been examined previously due to concerns with modeling the ionized atmosphere above the earth, and for instability problems with CO_2 lasers [127]. Based on this literature source, it was proposed that the $CO_3^{-\bullet}$ ion is formed via collisions of CO_2 with $O^{-\bullet}$. Later studies support the attachment of an electron to clusters of $(CO_2)_n$, whereby stepwise elimination of neutral CO_2 or CO occurs from the solvated ion to eventually yield $CO_3^{-\bullet}$ [128]. Additional negative ion clusters are absent from the background spectra shown here due to the low pressures employed in this study; the optimization for EC reactions occurred at a low pressure, i.e. 1200 mtorr. At pressures below 2000 mtorr, the $CO_3^{-\bullet}$ and $O^{-\bullet}$ ions predominate. The appearance of $(CO_2)_2^{-\bullet}$ at m/z 88, or higher cluster ions, will not occur until pressures of 2000 mtorr or greater are reached [128].

Ions produced from cluster reactions in the positive ion mode are more abundant in the pressure regime of these studies (figure A-3). Major ions present in the positive ion background are at m/z 32 ($O_2^{+\bullet}$), m/z 44 ($CO_2^{+\bullet}$), and m/z 88, the $(CO_2)_2^{+\bullet}$ ion. Additionally, ions at m/z 45 and m/z 46 are visible in the mass

Figure A-2 Negative ion mass spectrum of PFTBA acquired at an indicated ion source pressure of 1200 mtorr CO_2.

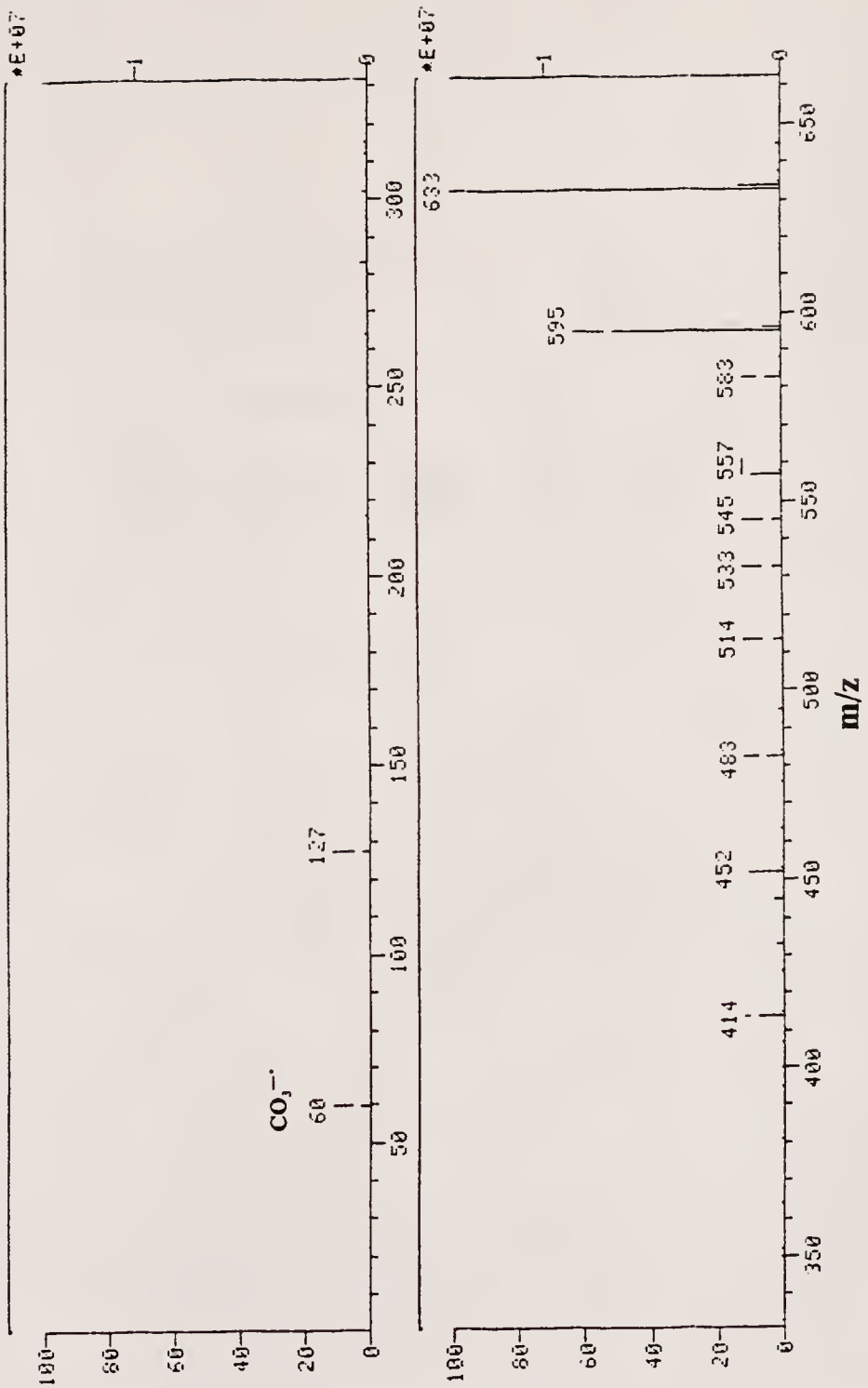
Relative Intensity (%)
m/z
$CO_3^{-\bullet}$
60
127
414
452
483
514
533
545
557
583
595
633

Figure A-3 Positive ion mass spectrum of background ions produced from 1200 mtorr (indicated) CO_2 reagent gas.

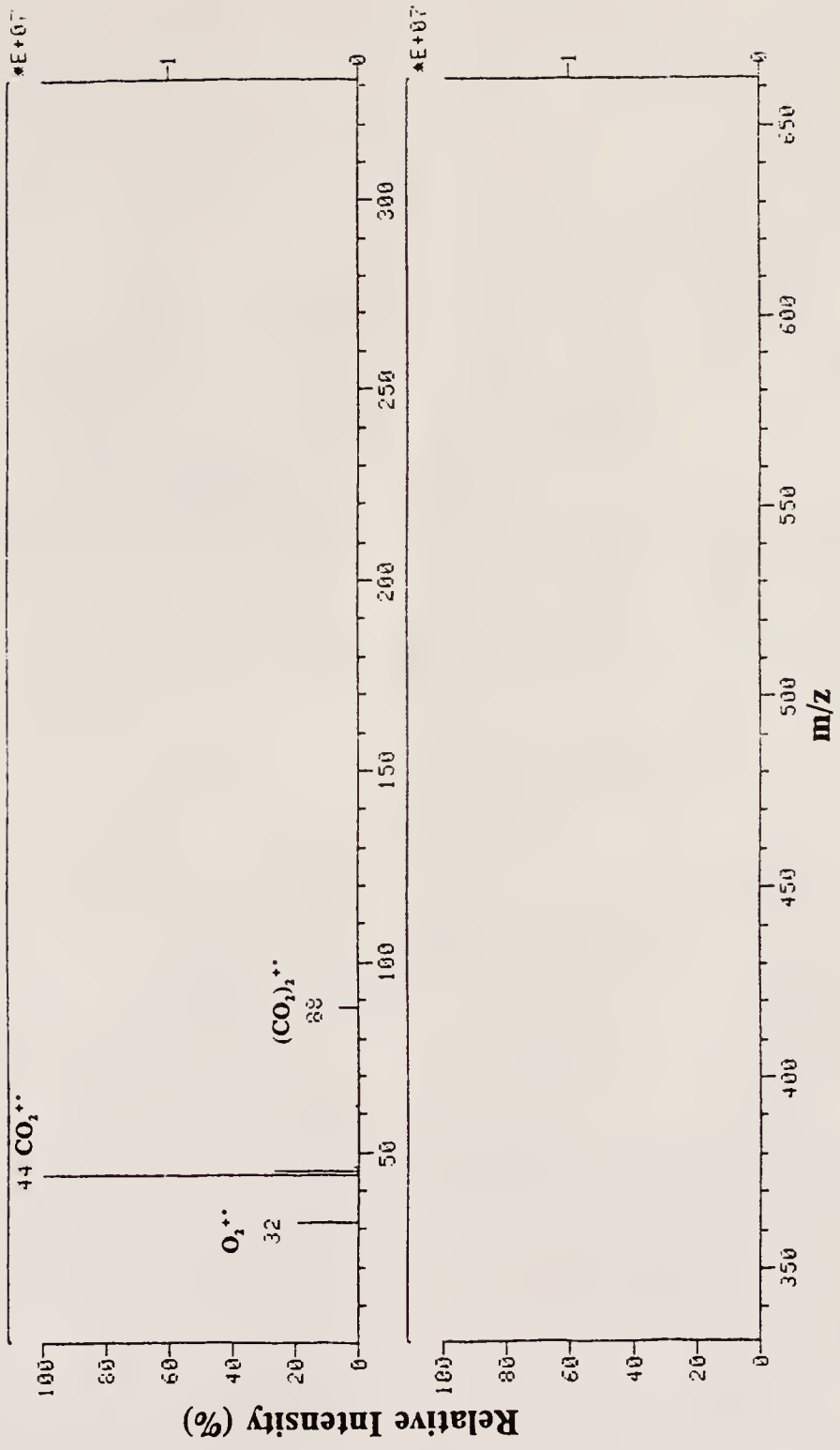
Relative Intensity (%)
m/z
44 $CO_2^{+\cdot}$
32 $O_2^{+\cdot}$
88 $(CO_2)_2^{+\cdot}$

spectrum. These are presumed to originate from either wall reactions, or the presence of an impurity such as water. A closer inspection of the low mass range (figure A-4) reveals the presence of $H_2O^{+\bullet}$ and H_3O^+, at m/z 18 and m/z 19, respectively. The ions at m/z 56, 60, 72, and 76 are generated by CO_2 cluster ions of $(CO_2)C^{+\bullet}$, $(CO_2)O^{+\bullet}$, $(CO_2)CO^{+\bullet}$, and $(CO_2)O_2^{+\bullet}$, respectively [128]. The ions at m/z 30, 34, 45, 46, 47, 63, 89, and 90 are presumed to result from impurities adding hydrogen to the system, either from water, or from surface-bound radicals on the ion source walls [121].

Experiments were conducted involving the addition of water to the system in both positive and negative ion modes. The mass spectra were acquired in the absence of calibration gas. The direct insertion probe was inserted with an empty vial as the blank; the second series contained water in the probe vial. The mass spectrum of the blank in positive ion mode is shown in figure A-5. The relative intensities of the water ions at m/z 18 and m/z 19 should be noted, as well as the ratio of m/z 32 ($O_2^{-\bullet}$) to m/z 28 ($CO^{-\bullet}$). Additionally, the intensity of the m/z 45 ion is approximately 30% of the m/z 44 base peak. The m/z 88 ion is at about 5% RA, with an ion at m/z 89 not observed in this spectrum.

This experiment was repeated with water introduced via the direct insertion probe vial. The mass spectrum in figure A-6 clearly shows the presence of water in the system (compared to figure A-5). The intensity of m/z 18 and m/z 19 are increased to almost the intensity of the base peak. There is also an increase in the

Figure A-4 Positive ion mass spectrum of background ions (enhanced by a factor of 100) from 1200 mtorr (indicated) CO_2 reagent gas.

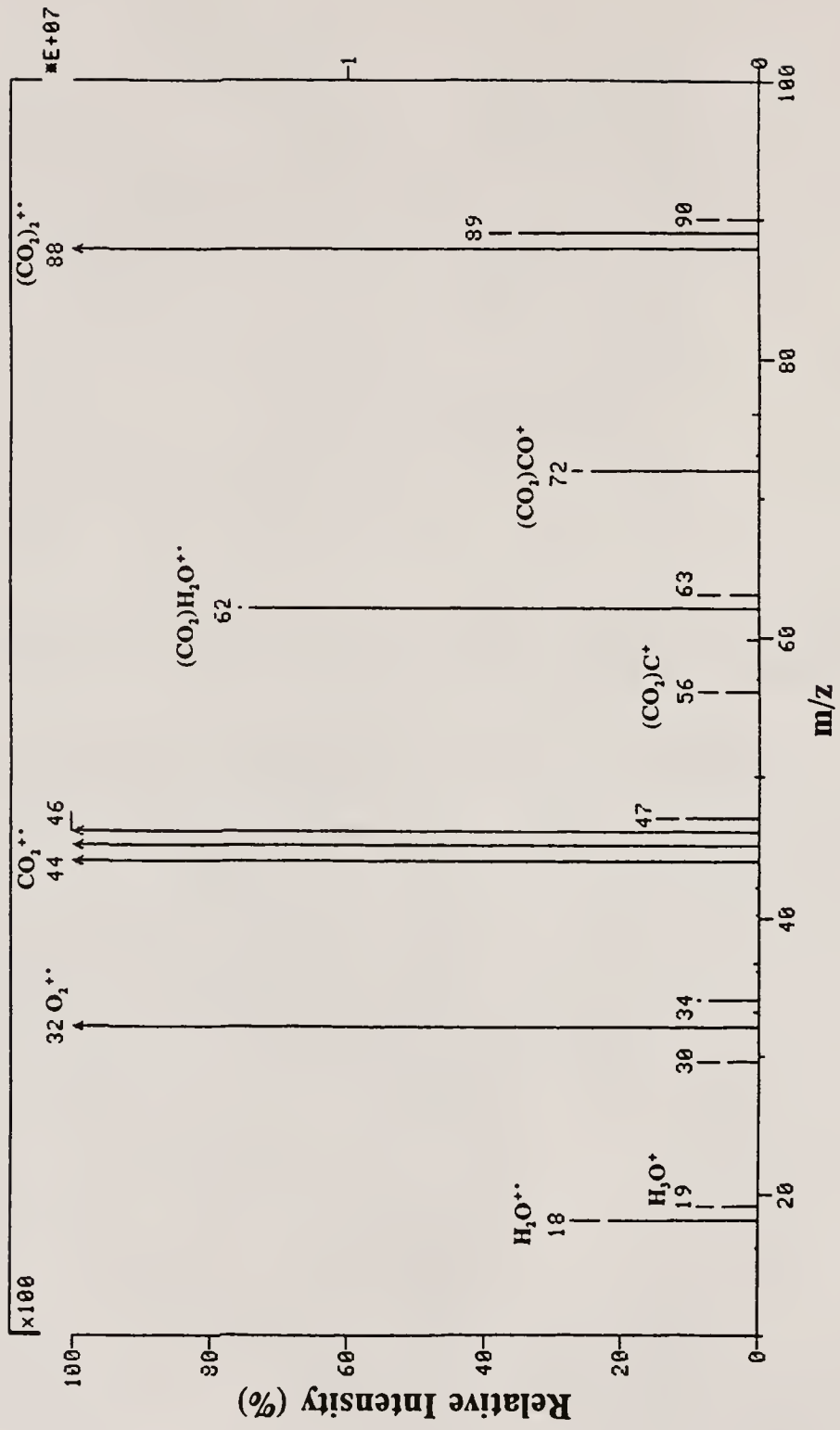
Relative Intensity (%)
m/z
×100
E+07
$H_2O^{+\cdot}$ 18
H_3O^+ 19
30
$32\ O_2^{+\cdot}$
34
$CO_2^{+\cdot}$ 44
46
47
$(CO_2)C^+$ 56
$(CO_2)H_2O^{+\cdot}$ 62
63
$(CO_2)CO^+$ 72
$(CO_2)_2^{+\cdot}$ 88
89
90

Figure A-5 Positive ion mass spectrum of background ions from 1200 mtorr (indicated) CO_2 prior to introduction of water into the system.

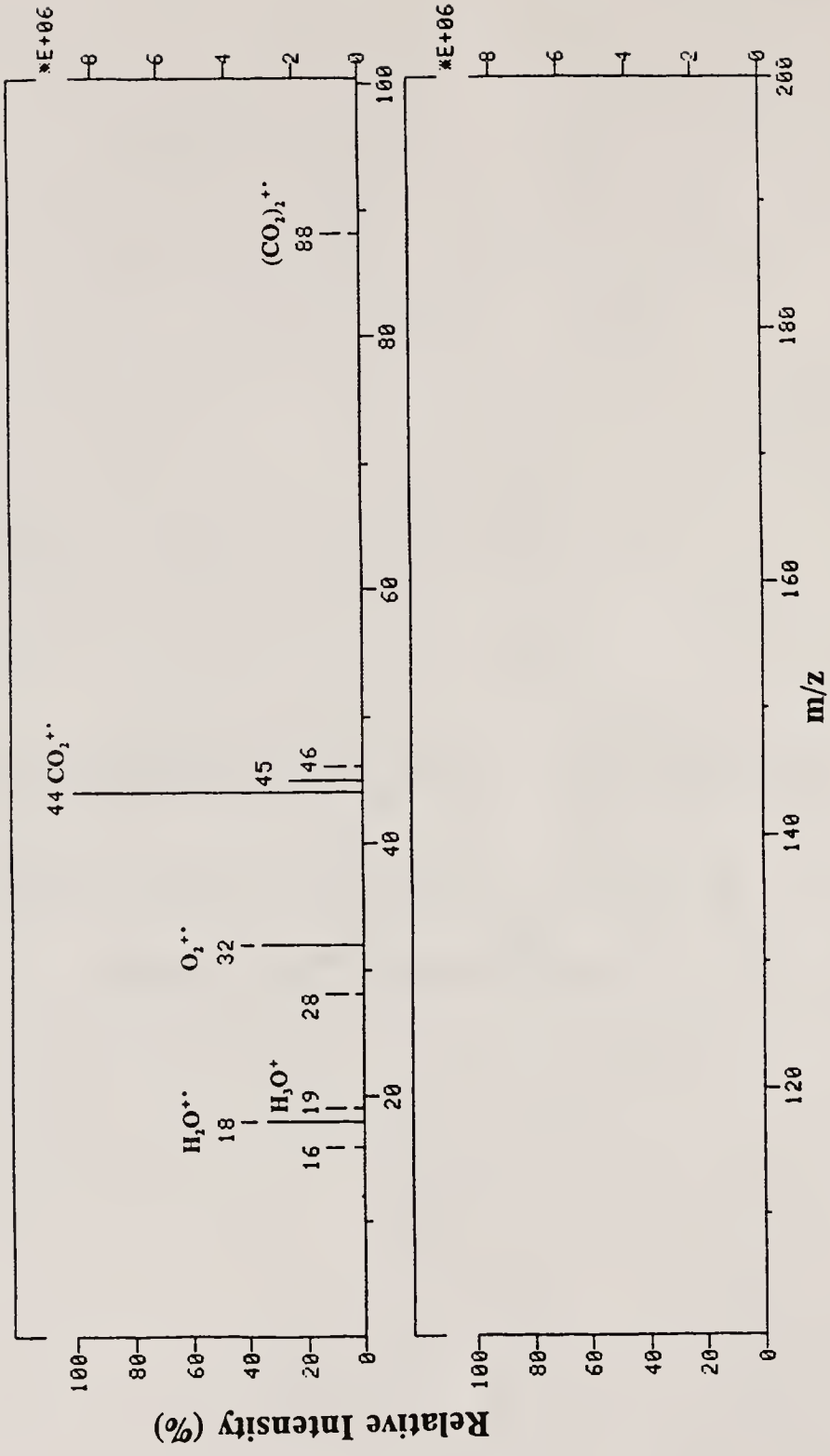
Relative Intensity (%)
m/z
*E+06
*E+06
44 $CO_2^{+\cdot}$
$(CO_2)_2^{+\cdot}$
88
$O_2^{+\cdot}$
32
$H_2O^{+\cdot}$
18
H_3O^+
19
16
28
45
46

Figure A-6 Positive ion mass spectrum of background ions from 1200 mtorr (indicated) CO_2 with additional water introduced into the system via the direct insertion probe.

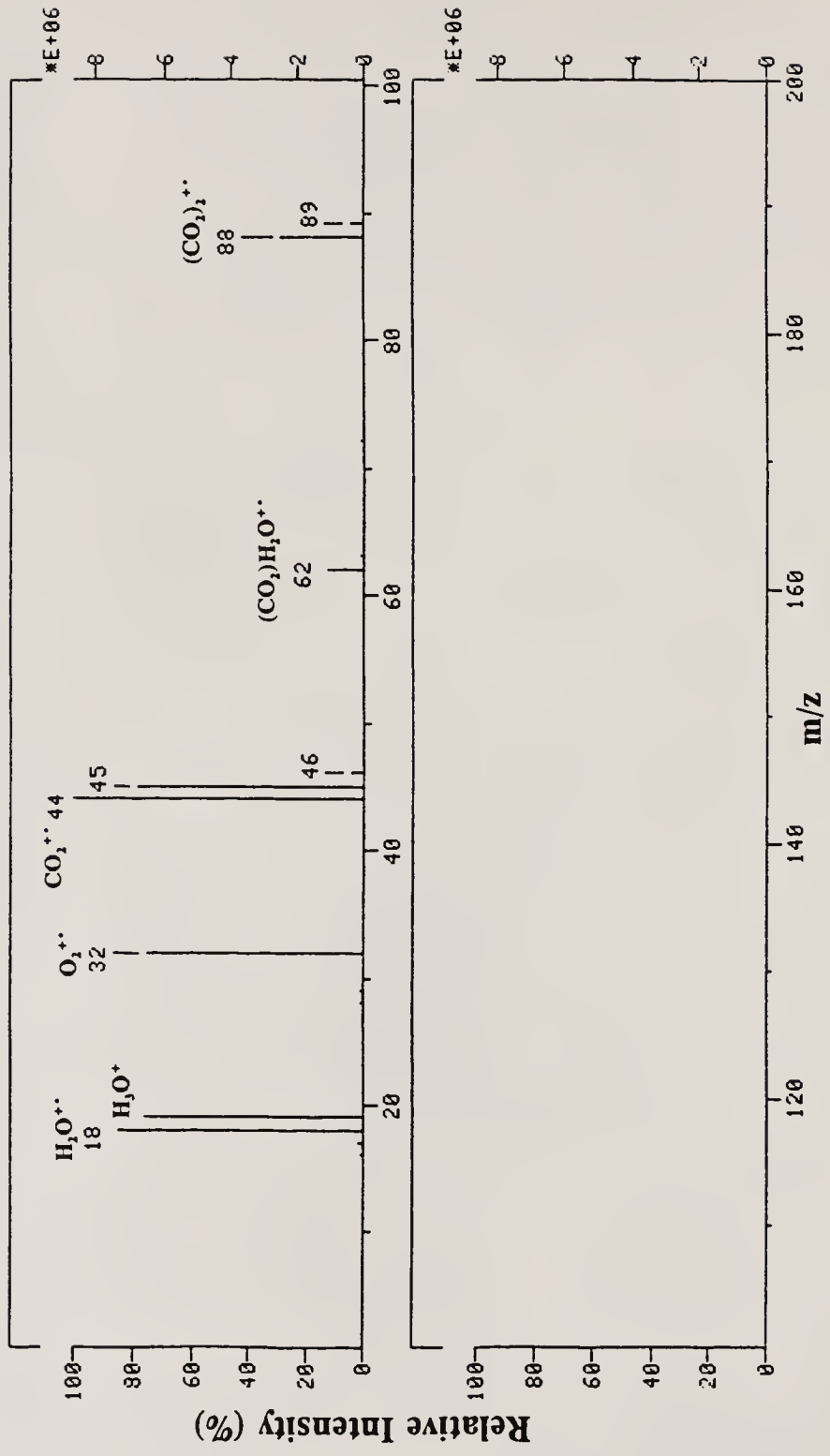
Relative Intensity (%)
m/z
*E+06
$H_2O^{+\cdot}$ 18
H_3O^+
$O_2^{+\cdot}$ 32
$CO_2^{+\cdot}$ 44
45
46
$(CO_2)H_2O^{+\cdot}$ 62
$(CO_2)_2^{+\cdot}$ 88
89

m/z 19 ion relative to m/z 18 indicating increased CI-like high-pressure proton transfer reactions. There is a significant increase in the production of m/z 32 ($O_2^{+\bullet}$) as well as m/z 45 and m/z 62, the $(CO_2)H^+$ and $(CO_2)H_2O^{+\bullet}$ ions, respectively. The presence of an ion at m/z 89 from $(CO_2)_2H^+$ is also noticeable in this mass spectrum. The mass spectra for equivalent experiments with negative ions are in figures A-7 (normal background) and A-8 (with water added). The addition of water to the system does not seem to generate an appreciable difference, except for the increased abundance of the m/z 16 ($O^{-\bullet}$) and m/z 17 (OH^-) ions. Although water may not affect the background ions of CO_2 significantly, the $O^{-\bullet}$ and OH^- ions present may lead to conventional CI proton transfer reactions, generating unexpected fragment ions [129,130].

Selected Examples

Impurities such as water, as stated previously, are not the only cause for unexpected results in a negative ion CI mass spectrum. An example of the presence of both wall reactions and self-CI from high ion source pressure can be seen (in figure A-9) for lactic acid. The predominant ions at m/z 179 and m/z 251 are characteristic ions found in mass spectra of lactic acid under saturated ion source conditions (see Chapter 3). These ions are attributable to self-CI reactions. The region of interest pertaining to suspected wall reactions is in the m/z 87 to m/z 90

Figure A-7 Negative ion mass spectrum of background ions from 1200 mtorr (indicated) CO_2 prior to introduction of water into the system.

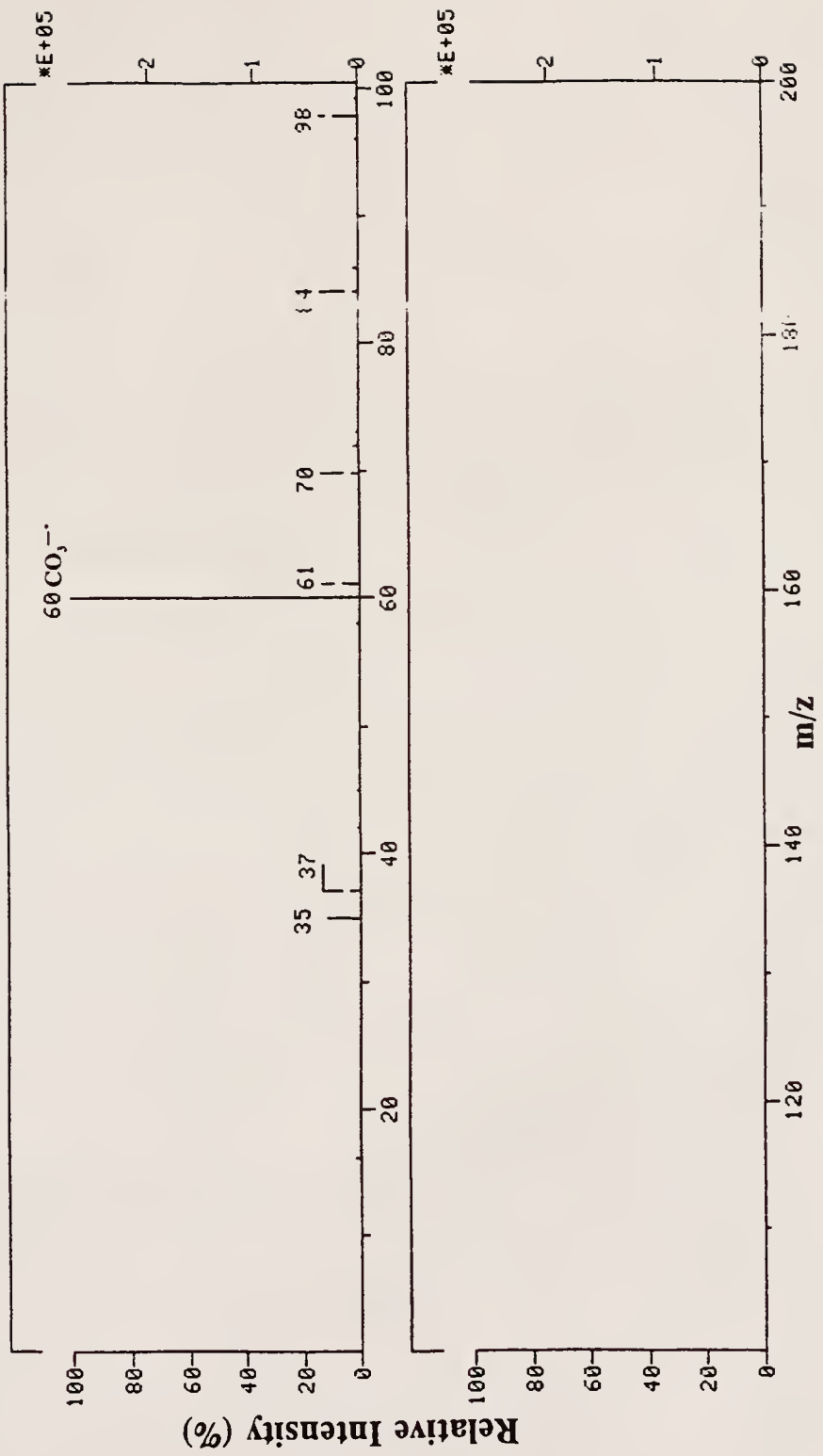

Relative Intensity (%)
m/z
*E+05
60 $CO_3^{-\cdot}$
35
37
61
70
98

Figure A-8 Negative ion mass spectrum of background ions from 1200 mtorr (indicated) CO_2 with additional water introduced into the system via the direct insertion probe.

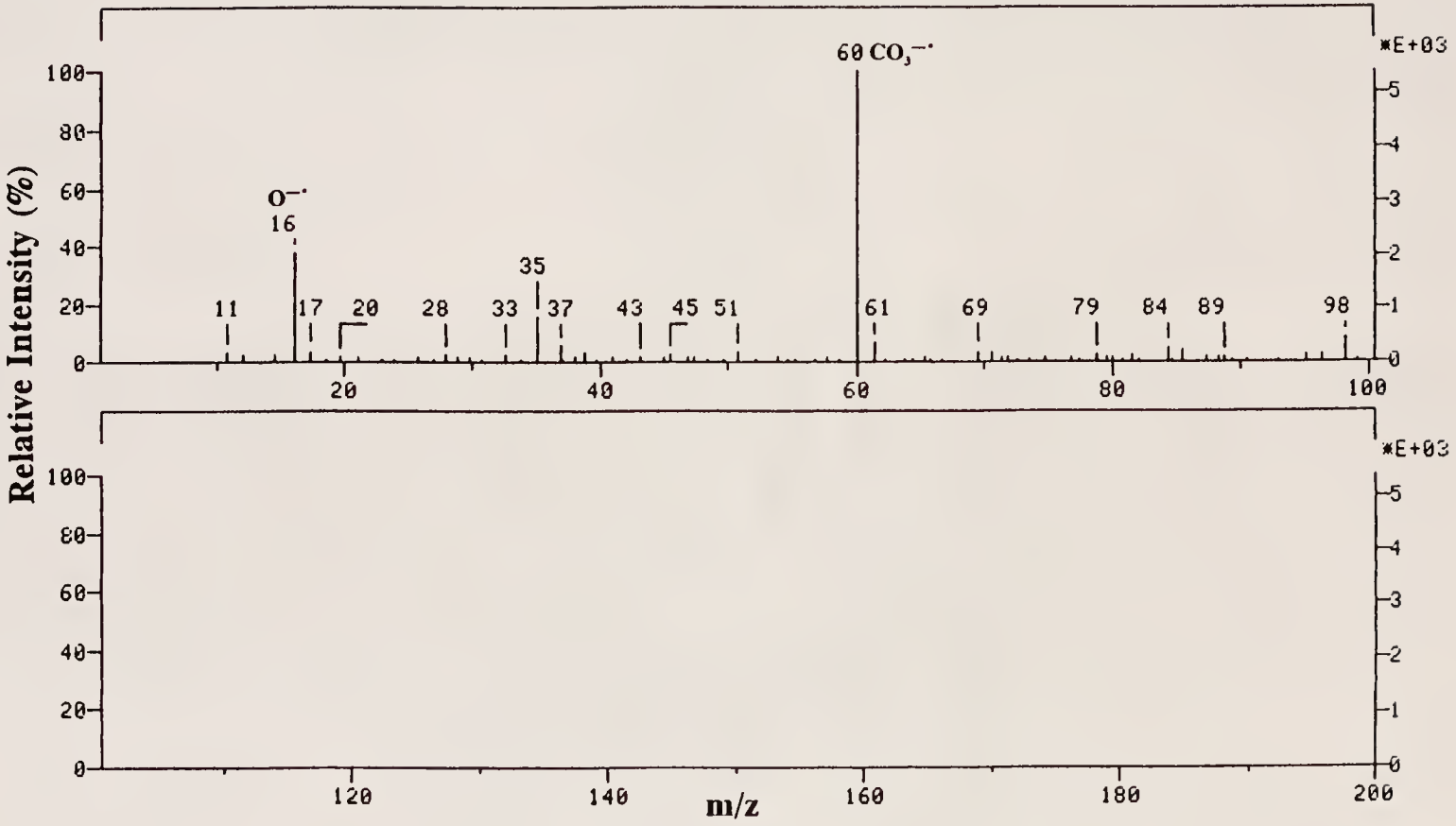
Relative Intensity (%)
100
80
60
40
20
0
O⁻·
16
35
60 CO₃⁻·
11
17
20
28
33
37
43
45
51
61
69
79
84
89
98
*E+03
5
4
3
2
1
0
20
40
60
80
100
120
140
160
180
200
m/z

Figure A-9 Negative ion mass spectrum of lactic acid from 8 handled glass beads, employing 1200 mtorr CO_2 reagent gas at 1200 mtorr (indicated) pressure.

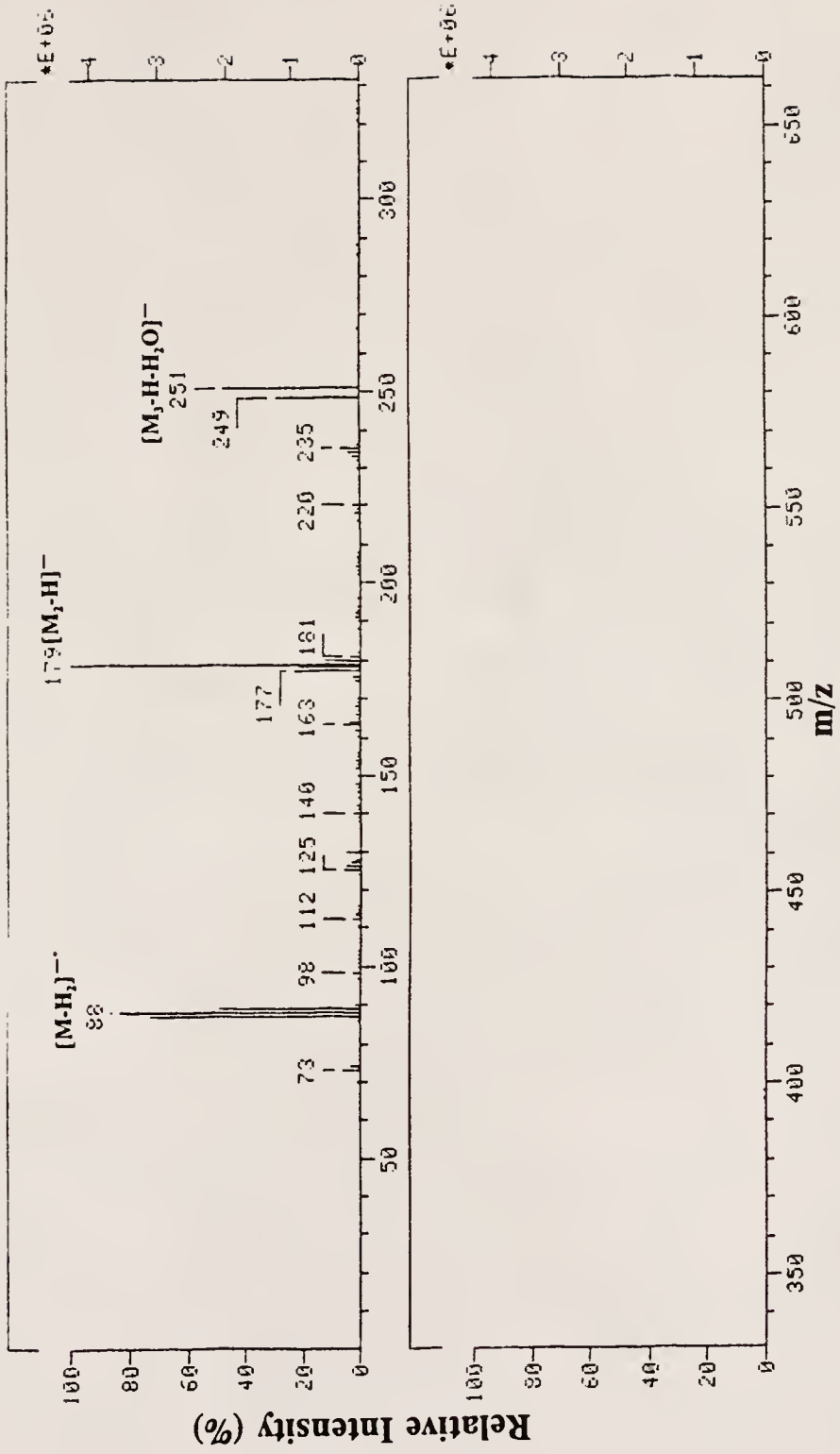
[M-H2]-·
88
179[M1-H]-
177
[M1-H-H2O]-
251
249
m/z
Relative Intensity (%)

range. Saturated conditions with methane as the reagent gas produces the m/z 89 $[M-H]^-$ ion as the base peak and an intense ion at m/z 87 due to the elimination of H_2 from m/z 89, in the gas phase. For conditions below saturation, the m/z 87 ion may be slightly lower in intensity; however, in all cases, the m/z 88 is present but in very low abundance (less than 3% RA).

The intensity of the m/z 88 ion, at greater intensity than seen throughout this work, suggests that there is an alternative mechanism of ion formation occurring with CO_2 as the reagent gas. This alternative route did not occur to the extent seen here for methane CI studies conducted previously. The best explanation for this is the elimination of H_2 prior to electron capture in the gas phase, presumably by a wall reaction, followed by electron attachment to the neutral species forming the m/z 88 $[M-H_2]^{-\bullet}$ ion.

The most common detriment to this work involving CO_2 for CE or ECNCI was high ion source pressures resulting from the presence of the sample in the ion source. An example mass spectrum of standard palmitic (hexadecanoic) acid subjected to CE with 1200 mtorr CO_2 is shown in figure A-10. Although the $M^{+\bullet}$ ion is present at m/z 256, the base peak is the $[M+H]^+$ ion of hexadecanoic acid at m/z 257. The only route for production of this ion is via self-CI. An additional interesting feature of this mass spectrum is the adduct ions present at m/z 271 and m/z 285. The latter ion at m/z 285 is the typical $[M+29]^+$ ion seen in methane CI mass spectra. The $[M+15]^+$ adduct ion at m/z 271 is fairly uncommon in methane

Figure A-10 Positive ion mass spectrum of palmitic acid, introduced via the direct insertion probe. Reagent gas was CO_2 at an indicated ion source pressure of 1200 mtorr.

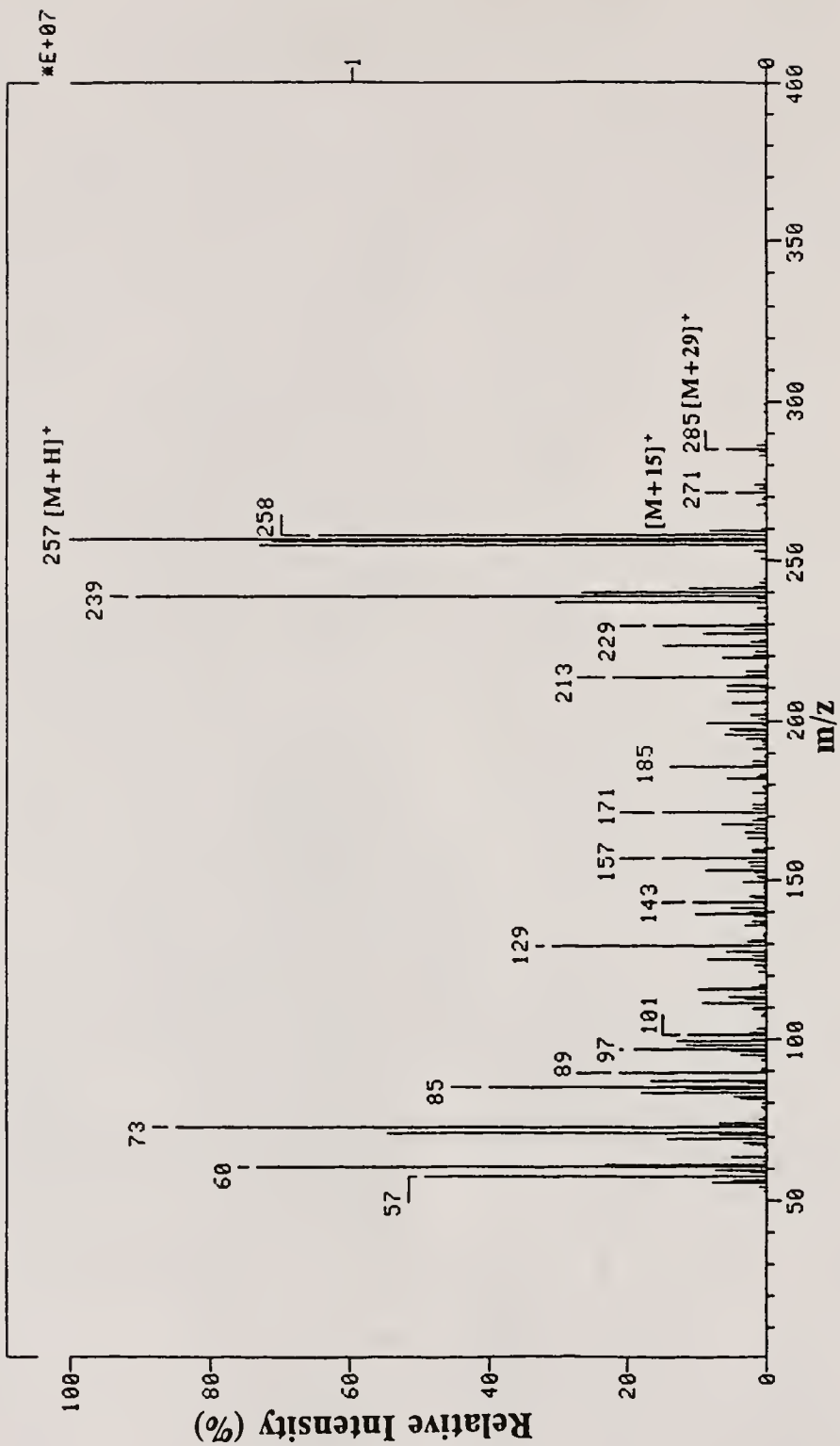
Relative Intensity (%)
m/z
*E+07
257 [M+H]+
[M+15]+
285 [M+29]+
73
60
57
85
89
97
101
129
143
157
171
185
213
229
239
258
271

CI, and ultimately must be formed from reactions of hexadecanoic acid with fragments of itself.

Summary

The use of ECNCI with CO_2 is potentially an asset for continued work involving the identification of trace levels of skin emanations. The fundamentals of using CO_2 as a reagent gas, as well as the problems encountered during preliminary experiments, have been covered herein. Reducing impurities is a necessary step to successful use of this reagent gas. Purification and cold-trapping of CO_2 gas prior to introduction in the ion source may be necessary to reduce or eliminate water. Prolonged pretreatment of the ion source with CO_2 prior to analysis would also be beneficial for the reduction of surface bound radicals. Finally, reduction of sample size would eliminate self-CI reactions due to saturated conditions. The proposed avenue for this is the use of a purge and trap system similar to that used for studies in Chapter 5. This would remove water and acids, which dominate the analyses, leaving trace components to be readily identified. With these suggestions, the technique of CO_2/ECNCI may provide information not previously accessible.

REFERENCE LIST

1. James, A.J., Science, **1992**, 257, 37-38.

2. Gillett, J.D., Mosq. News, **1979**, 39(2), 221-229.

3. Hoelterhoff, M., SmartMoney, **1994**, 3(8), 128-132.

4. McIver, S.B., J. Med. Entomol., **1982**, 19(5), 489-535.

5. Takken, W., Insect Sci. Applic., **1991**, 12, 287-295.

6. Sutcliffe, J.F., J. Am. Mosq. Control Assoc., **1994**, 10(2), 309-315.

7. Gillies, M.T., Bull. Ent. Res., **1980**, 70, 525-532.

8. Belton, P., J. Am. Mosq. Control Assoc., **1994**, 10(2), 297-301.

9. Bidlingmayer, W.L., J. Am. Mosq. Control Assoc., **1994**, 10(2), 272-279.

10. Allan, S.A., J. Am. Mosq. Control Assoc., **1994**, 10(2), 266-271.

11. Kline, D.L., J. Am. Mosq. Control Assoc., **1994**, 10(2), 280-287.

12. Davis, E.E., & Bowen, M.F., J. Am. Mosq. Control Assoc., **1994**, 10(2), 316-325.

13. Foster, W.A., & Hancock, R.G., J. Am. Mosq. Control Assoc., **1994**, 10(2), 288-296.

14. Browne, S.M., & Bennett, G.F., J. Med. Entomol., **1981**, 18(6), 505-521.

15. Schreck, C.E., Gouck, H.K., & Posey, K.H., Mosq. News, **1972**, 32(4), 496-501.

16. Price, G.D., Smith, N., & Carlson, D.A., J. Chem. Ecol., **1979**, 5(3), 383-395.

17. Schreck, C.E., & James, J., Mosq. News, **1968**, 28(1), 33-38.

18. Schreck, C.E., Gouck, H.K., & Posey, K.H., Mosq. News, **1970**, 30(4), 641-645.

19. Carlson, D.A., Smith, N., Gouck, H.K., & Godwin, D.R., J. Econ. Entomol., **1973**, 66(2), 329-331.

20. Takken, W., & Kline, D.L., J. Am. Mosq. Control Assoc., **1989**, 5(3), 311-316.

21. Kline, D.L., Takken, W., Wood, J.R., & Carlson, D.A., Med. Vet. Entomol., **1990**, 4, 383-391.

22. Kline, D.L., Wood, J.R., & Cornell, J.A., J. Med. Entomol., **1991**, 28(2), 254-258.

23. Kline, D.L., Dame, D.A., & Meisch, M.V., J. Am. Mosq. Control Assoc., **1991**, 7(2), 165-169.

24. Kemme, J.A., van Essen, P.H.A., Ritchie, S.A., & Kay, B.H., J. Am. Mosq. Control Assoc., **1993**, 9(4), 431-435.

25. Kline, D.L., J. Am. Mosq. Control Assoc., **1994**, 10(2), 253-257.

26. Rathburn, C.B., Wing Beats, **1990**, 1(2), 12-13.

27. Mankin, R.W., J. Am. Mosq. Control Assoc., **1994**, 10(2), 302-308.

28. Acree, F., Turner, R.B., Gouck, H.K., Beroza, M., & Smith, N., Science, **1968**, 161, 1346-1347.

29. Yokoyama, Y., Aragaki, M., Sato, H., & Tsuchiya, M., Anal. Chim. Acta, **1991**, 246, 405-411.

30. Zeng, X.-N., Leyden, J.J., Lawley, H.J., Sawano, K., Nohara, I., & Preti, G., J. Chem. Ecol., **1991**, 17(7), 1469-1491.

31. Zeng, X.-N., Leyden, J.J., Brand, J.G., Spielman, A.I., McGinley, K.J., & Preti, G., J. Chem. Ecol., **1992**, 18(7), 1039-1055.

32. Nier, A.O., J. Am. Soc. Mass Spectrom., **1991**, 2, 447-452.

33. Chapman, J.R., Practical Organic Mass Spectrometry, 2nd Ed., John Wiley & Sons: Chichester, England, **1993**.

34. Field, F.H., Franklin, J.L., & Lampe, F.W., J. Am. Chem. Soc., **1956**, 78, 5697-5698.

35. Lampe, F.W., J. Am. Chem. Soc., **1957**, 79, 1055-1058.

36. Field, F.H., Franklin, J.L., & Lampe, F.W., J. Am. Chem. Soc., **1957**, 79, 2419-2429.

37. Field, F.H., Franklin, J.L., & Lampe, F.W., J. Am. Chem. Soc., **1957**, 79, 2665-2669.

38. Lampe, F.W., & Field, F.H., J. Am. Chem. Soc., **1957**, 79, 4244-4245.

39. Lampe, F.W., Franklin, J.L., & Field, F.H., J. Am. Chem. Soc., **1957**, 79, 6129-6132.

40. Lampe, F.W., Franklin, J.L., & Field, F.H., J. Am. Chem. Soc., **1957**, 79, 6132-6135.

41. Lampe, F.W., & Field, F.H., J. Am. Chem. Soc., **1959**, 81, 3238-3241.

42. Lampe, F.W., & Field, F.H., J. Am. Chem. Soc., **1959**, 81, 3242-3244.

43. Lampe, F.W., J. Am. Chem. Soc., **1960**, 82, 1551-1555.

44. Field, F.H., J. Am. Chem. Soc., **1961**, 83, 1523-1534.

45. Franklin, J.L., & Field, F.H., J. Am. Chem. Soc., **1961**, 83, 3555-3559.

46. Field, F.H., & Franklin, J.L., J. Am. Chem. Soc., **1961**, 83, 4509-4515.

47. Field, F.H., Head, H.N., & Franklin, J.L., J. Am. Chem. Soc., **1962**, 84, 1118-1122.

48. Field, F.H., Franklin, J.L., & Munson, M.S.B., J. Am. Chem. Soc., **1963**, 85, 3575-3583.

49. Munson, M.S.B., Field, F.H., & Franklin, J.L., J. Am. Chem. Soc., **1963**, 85, 3584-3588.

50. Field, F.H., & Munson, M.S.B., J. Am. Chem. Soc., **1965**, 87, 3289-3293.

51. Munson, M.S.B., & Field, F.H., J. Am. Chem. Soc., **1965**, 87, 3294-3299.

52. Munson, M.S.B., & Field, F.H., J. Am. Chem. Soc., **1965**, 87, 4242-4247.

53. Munson, M.S.B., & Field, F.H., J. Am. Chem. Soc., **1966**, 88, 2621-2630.

54. Yost, R.A., & Enke, C.G., J. Am. Chem. Soc., **1978**, 100, 2274-2275.

55. Dawson, P.H., French, J.B., Buckley, J.A., Douglas, D.J., & Simmons, D., Org. Mass Spectrom., **1982**, 17(5), 205-211.

56. Busch, K.L., Glish, G.L., & McLuckey, S.A., Mass Spectrometry/Mass Spectrometry, VCH Publishers: New York, **1988**.

57. Levsen, K., Org. Mass Spectrom., **1988**, 23, 406-415.

58. Shiraishi, H., Otsuki, A., & Fuwa, K., Biomed. Mass Spectrom., **1985**, 12(2), 86-94.

59. Betkowski, L.D., Webb, H.M., & Sauter, A.D., Biomed. Mass Spectrom., **1983**, 10(6), 369-376.

60. Issachar, D., & Yinon, J., Biomed. Mass Spectrom., **1979**, 6, 47-55.

61. Jellum, E., Phil. Trans. R. Soc. Lond. A, **1979**, 293, 13-19.

62. Issachar, D., Holland, J.F., & Sweeley, C.C., Anal. Chem., **1982**, 54, 29-32.

63. Horning, E.C., & Horning, M.G., Clin. Chem., **1971**, 17(8), 802-809.

64. Stach, J., Zimmer, D., Moder, M., & Herzschuch, R., Org. Mass Spectrom., **1989**, 24, 946-952.

65. Rossi, S.-A., Johnson, J.V., & Yost, R.A., Biol. Mass Spectrom., **1994**, 23, 131-139.

66. Lee, M.S., & Yost, R.A., Biomed. Mass Spectrom., **1988**, 15, 193-204.

67. Schreck, C.E., Gouck, H.K., & Smith, N., J. Econ. Entomol., **1967**, 60, 1188-1190.

68. Ellin, R.I., Farrand, R.L., Oberst, F.W., Crouse, C.L., Billups, N.B., Koon, W.S., Musselman, N.P., & Sidell, F.R., J. Chromatogr., **1974**, 100, 137-152.

69. Nitz, S., Kollmannsberger, H., Albrecht, M., & Friedrich, D., J. Chromatogr., **1991**, 547, 516-522.

70. Hunt, D.F., Stafford, G.C., Crow, F.W., & Russell, J.W., Anal. Chem., **1976**, 48(14), 2098-2105.

71. Bayer, C.W., & Black, M.S., Biomed. Mass Spectrom., **1987**, 14, 363-367.

72. Budzikiewicz, H., Angew. Chem. Int. Ed. Engl., **1981**, 20, 624-637.

73. Wood, K.V., McLuckey, S.A., & Cooks, R.G., Org. Mass Spectrom., **1986**, 21, 11-14.

74. Harrison, A.G., Chemical Ionization Mass Spectrometry, 2nd Ed., CRC Press: Boca Raton, Florida, **1992**.

75. McAdoo, D.J., Org. Mass Spectrom., **1988**, 23, 350-354.

76. Bowie, J.H., Mass Spectrom. Rev., **1984**, 3, 161-207.

77. Sweeney, C.W., & Wellington, C.A., Int. J. Mass Spectrom. Ion Proc., **1984**, 62, 167-185.

78. Budzikiewicz, H., Org. Mass Spectrom., **1988**, 23, 561-565.

79. McLafferty, F.W., & Tureček, F., Interpretation of Mass Spectra, 4th Ed., University Science Books: Berkley, California, **1993**.

80. Streitweiser, A., & Heathcock, C.H., Introduction to Organic Chemistry, 3rd Ed., Macmillan Publishing Company: New York, **1985**, 856-861.

81. Tannenbaum, H.P., Roberts, J.D., & Dougherty, R.C., Anal. Chem., **1975**, 47(1), 49-54.

82. Ballantine, J.A., Barton, J.D., Carter, J.F., & Fussell, B., Org. Mass Spectrom., **1987**, 22, 564-566.

83. McLuckey, S.A., J. Am. Soc. Mass Spectrom., **1992**, 3, 599-614.

84. Löfstedt, C., & Odham, G., Biomed. Mass Spectrom., **1984**, 11(3), 106-113.

85. Lauritsen, F.R., Bohatka, S., & Degn, H., Rapid Commun. Mass Spectrom., **1990**, 4(10), 401-403.

86. Kiplinger, J.P., & Bursey, M.M., Org. Mass Spectrom., **1988**, 23, 342-349.

87. Fetterolf, D.D., & Yost, R.A., Int. J. Mass Spectrom. Ion Phys., **1982**, 44, 37-50.

88. Nacson, S., Harrison, A.G., & Davidson, W.R., Org. Mass Spectrom., **1986**, 21, 317-319.

89. Martinez, R.I., & Ganguli, B., J. Am. Soc. Mass Spectrom., **1992**, 3, 427-444.

90. Eichmann, E.S., Alvarez, E., & Brodbelt, J.S., J. Am. Soc. Mass Spectrom., **1992**, 3, 535-542.

91. Glosik, J., Jordan, A., Shalsky, V., & Lindinger, W., Int. J. Mass Spectrom. Ion Proc., **1993**, 129, 109-116.

92. Brumley, W.C., Andrzejewski, D., & Sphon, J.A., Org. Mass Spectrom., **1988**, 23, 204-212.

93. Gillespie, T.A., & Yost, R.A., J. Am. Soc. Mass Spectrom., **1990**, 1, 389-396.

94. Hunt, D.F., Shabanowitz, J., Harvey, T.M., & Coates, M., Anal. Chem., **1985**, 57, 525-537.

95. Bambagiotti A., M., Coran, S.A., Vincieri, F.F., Petrucciani, T., & Traldi, P., Org. Mass Spectrom., **1986**, 21, 485-488.

96. Russell, D.H., Experimental Mass Spectrometry, Plenum Press: New York, **1994**.

97. Horiike, M., & Hirano, C., Biomed. Mass Spectrom., **1984**, 11(3), 145-148.

98. Guilhaus, M., Kingston, R.G., Brenton, A.G., & Beynon, J.H., Org. Mass Spectrom., **1985**, 20(6), 424-425.

99. Horiike, M., Oomae, S., & Hirano, C., Biomed. Environ. Mass Spectrom., **1986**, 13, 117-120.

100. Yu, Q.-T., Zhang, J.-Y., & Huang, Z.-H, Biomed. Environ. Mass Spectrom., **1986**, 13, 211-216.

101. Fellenberg, A.J., Johnson, D.W., Poulos, A., & Sharp, P., Biomed. Environ. Mass Spectrom., **1987**, 14, 127-129.

102. Noble, D., Anal. Chem., **1995**, 67(13), 435A-438A.

103. Kingston, E.E., Shannon, J.S., & Lacey, M.J., Org. Mass Spectrom., **1983**, 18(5), 183-192.

104. Zollinger, M. & Seibl, J., Org. Mass Spectrom., **1985**, 20(11), 649-661.

105. Hunt, D.F., & Crow, F.W., Anal. Chem., **1978**, 50(13), 1781-1784.

106. Christophorou, L.G., Chem. Rev., **1976**, 76(4), 409-423.

107. Dougherty, R.C., Anal. Chem., **1981**, 53(4), 625A-636A.

108. Dillard, J.G., Chem. Rev., **1973**, 73(6), 589-643.

109. Davis, R., & Frearson, M., Mass Spectrometry, John Wiley & Sons: New York, **1987**.

110. Maccoll, A., Org. Mass Spectrom., **1988**, 23, 381-387.

111. Orlowski, R., & Poyer, J., Scientific and Technological Application Forecast for Chemical Detection of Personnel by Gaseous and Particulate Matter, **1966**, Army Research Report, Contract No. DA-49-092-ARO-103.

112. Einolf, N., & Munson, B., Int. J. Mass Spectrom. Ion Phys., **1972**, 9, 141-160.

113. Lias, S.G., Bartmess, J.E., Liebman, J.F., Holmes, J.L., Levin, R.D., & Mallard, W.G., J. Phys. Chem. Ref. Data, ed. Lide, D.R., Jr., **1988**, 17, Supplement No. 1

114. Sears, L.J., Campbell, J.A., & Grimsrud, E.P., Biomed. Environ. Mass Spectrom., **1987**, 14, 401-415.

115. Gregor, I.K., & Guilhaus, M., Int. J. Mass Spectrom. Ion Proc., **1984**, 56, 167-176.

116. Ahmed, M.S., & Dunbar, R.C., J. Am. Chem. Soc., **1987**, 109, 3215-3219.

117. Stemmler, E.A., & Hites, R.A., Electron Capture Negative Ion Mass Spectra of Environmental Contaminants and Related Compounds, VCH Publishers: New York, **1988**.

118. Caldwell, G.W., Masucci, J.A., & Ikonomou, M.G., Org. Mass Spectrom., **1989**, 24, 8-14.

119. Culbertson, J.A., Sears, L.J., Knighton, W.B., & Grimsrud, E.P., Org. Mass Spectrom., **1992**, 27, 277-283.

120. Kassel, D.B., Kayganich, K.A., Watson, J.T., & Allison, J., Anal. Chem., **1988**, 60, 911-917.

121. Sears, L.J., & Grimsrud, E.P., Anal. Chem., **1989**, 61, 2523-2528.

122. Stöckl, D., & Budzikiewicz, H., Org. Mass Spectrom., **1982**, 17(8), 376-381.

123. Lauber, R., & Schlunegger, U.P., Org. Mass Spectrom., **1986**, 21, 401-405.

124. Woodin, R.L., Foster, M.S., & Beauchamp, J.L., J. Chem. Phys., **1980**, 72(7), 4223-4227.

125. Warman, J.M., & Sauer, M.C., Jr., J. Chem. Phys., **1975**, 62(5), 1971-1981.

126. George, P.M., & Beauchamp, J.L., J. Chem. Phys., **1982**, 76(6), 2959-2964.

127. Hong, S.P., Woo, S.B., & Helmy, E.M., Phys. Rev. A, **1977**, 15(4), 1563-1569.

128. Stamatovic, A., Stephan, K., & Märk, T.D., Int. J. Mass Spectrom. Ion Proc., **1985**, 63, 37-47.

129. Marshall, A., Tkaczyk, M., & Harrison, A.G., J. Am. Mass Spectrom., **1991**, 2, 292-298.

130. Roy, T.A., Field, F.H., Lin, Y.Y., & Smith, L.L., Anal. Chem., **1979**, 51(2), 272-278.

BIOGRAPHICAL SKETCH

Ulrich R. Bernier, son of Joseph J. Bernier and Rita I. Bernier, was born November 16, 1966, at Travis A.F.B. in Fairfield, California. He and his family moved to Indian Harbour Beach, Florida, in 1969. Ulrich graduated from Satellite High School in June, 1984. In August, 1984, he began his studies at the Florida State University in Tallahassee, Florida. In May, 1985, after one year of study, he received the Outstanding General Chemistry Student Award from the Department of Chemistry. In January, 1986, Ulrich was initiated into Alpha Chi Sigma, a national (chemistry) fraternity. He received an A.C.S. certified B.S. in Chemistry from the Florida State University in August, 1987.

Upon graduation, Ulrich began his graduate work in analytical chemistry at the University of Florida under the direction of Dr. Richard A. Yost. In August, 1992, he received his M.S. degree for "Short-Column Gas Chromatography with Flame Ionization Detection Under Vacuum-Outlet Conditions." Ulrich continued working under the supervision of Dr. Yost. He received his Ph.D. in December, 1995 for "Mass Spectrometric Investigations of Mosquito Attraction to Human Skin Emanations." Upon graduation, Ulrich will be employed by the USDA (Gainesville, FL). His work will continue in the field of mass spectrometry, under the supervision of Dr. David A. Carlson, on projects related to insect research.

I certify that I have read this study and that in my opinion it conforms to acceptable standards of scholarly presentation and is fully adequate, in scope and quality, as a dissertation for the degree of Doctor of Philosophy.

Richard A. Yost, Chair
Professor of Chemistry

I certify that I have read this study and that in my opinion it conforms to acceptable standards of scholarly presentation and is fully adequate, in scope and quality, as a dissertation for the degree of Doctor of Philosophy.

James D. Winefordner
Graduate Research Professor
of Chemistry

I certify that I have read this study and that in my opinion it conforms to acceptable standards of scholarly presentation and is fully adequate, in scope and quality, as a dissertation for the degree of Doctor of Philosophy.

David H. Powell
Associate Scientist of Chemistry

I certify that I have read this study and that in my opinion it conforms to acceptable standards of scholarly presentation and is fully adequate, in scope and quality, as a dissertation for the degree of Doctor of Philosophy.

J. Eric Enholm
Associate Professor of Chemistry

I certify that I have read this study and that in my opinion it conforms to acceptable standards of scholarly presentation and is fully adequate, in scope and quality, as a dissertation for the degree of Doctor of Philosophy.

Daniel L. Kline
Assistant Professor of Entomology
and Nematology

This dissertation was submitted to the Graduate Faculty of the Department of Chemistry in the College of Liberal Arts and Sciences and to the Graduate School and was accepted as partial fulfillment of the requirements for the degree of Doctor of Philosophy.

December, 1995

_____

Dean, Graduate School

LD
1761
1995
.B482

UNIVERSITY OF FLORIDA
3 1262 08557 0629